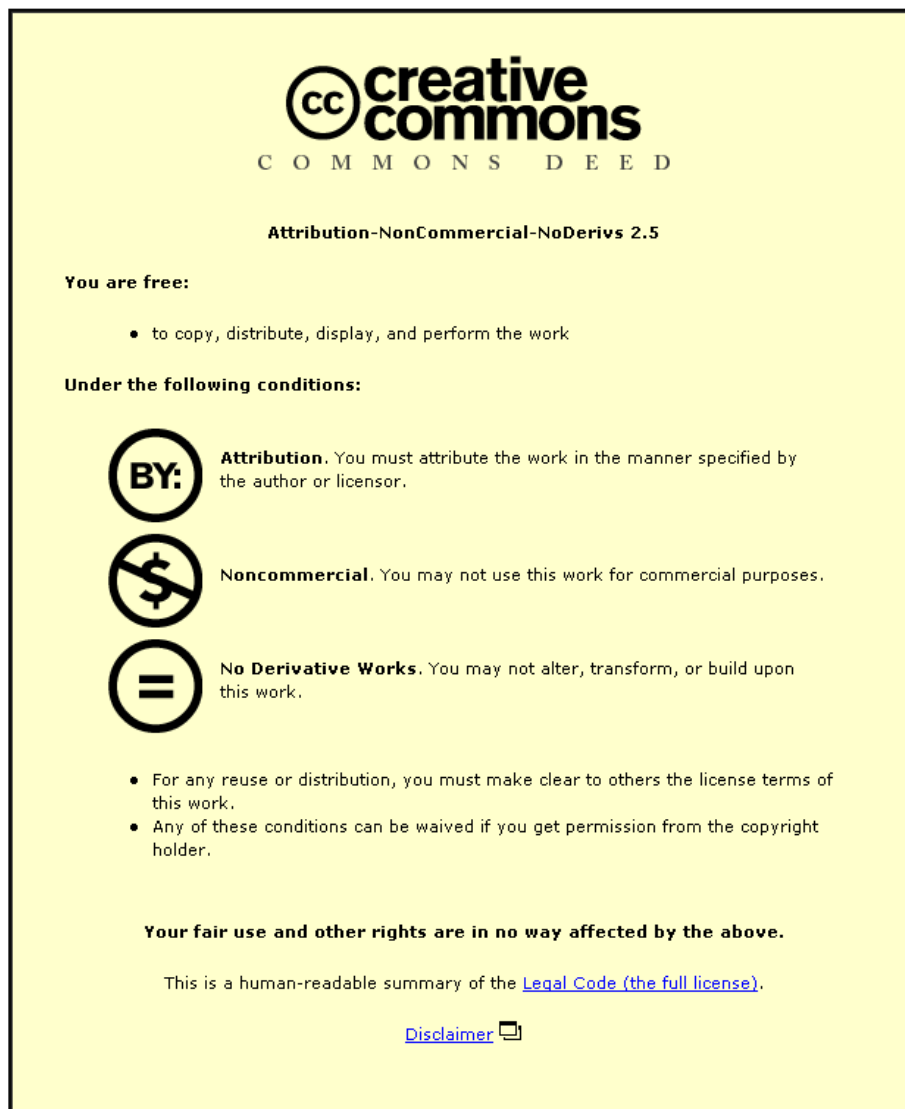




This item was submitted to Loughborough University as a PhD thesis by the author and is made available in the Institutional Repository (<https://dspace.lboro.ac.uk/>) under the following Creative Commons Licence conditions.



CC creative commons
COMMONS DEED

Attribution-NonCommercial-NoDerivs 2.5

You are free:

- to copy, distribute, display, and perform the work

Under the following conditions:

BY: **Attribution.** You must attribute the work in the manner specified by the author or licensor.

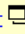
Noncommercial. You may not use this work for commercial purposes.

No Derivative Works. You may not alter, transform, or build upon this work.

- For any reuse or distribution, you must make clear to others the license terms of this work.
- Any of these conditions can be waived if you get permission from the copyright holder.

Your fair use and other rights are in no way affected by the above.

This is a human-readable summary of the [Legal Code \(the full license\)](#).

[Disclaimer](#) 

For the full text of this licence, please go to:
<http://creativecommons.org/licenses/by-nc-nd/2.5/>

Rate Enhancement and Multi-Relay Selection Schemes for Application in Wireless Cooperative Networks

by

Gaojie Chen

A Doctoral Thesis submitted in partial fulfilment of the requirements
for the award of the degree of Doctor of Philosophy (PhD)

October 2012



Advanced Signal Processing Group,
School of Electronic, Electrical and Systems Engineering,
Loughborough University, Loughborough,
Leicestershire, UK, LE11 3TU

© by Gaojie Chen, 2012

CERTIFICATE OF ORIGINALITY

This is to certify that I am responsible for the work submitted in this thesis, that the original work is my own except as specified in acknowledgements or in footnotes, and that neither the thesis nor the original work contained therein has been submitted to this or any other institution for a degree.

..... (Signed)

.....GAOJIE..CHEN..... (candidate)

I dedicate this thesis to my parents, E Gao and Jianjun Chen, my grandmothers, my late grandfathers and my girl friend, Lan.

Abstract

In this thesis new methods are presented to achieve performance enhancement in wireless cooperative networks. In particular, techniques to improve transmission rate, mitigate asynchronous transmission and maximise end-to-end signal-to-noise ratio are described.

An offset transmission scheme with full interference cancellation for a two-hop synchronous network with frequency flat links and four relays is introduced. This approach can asymptotically, as the symbol block size increases, achieve maximum transmission rate together with full cooperative diversity provided the destination node has multiple antennas. A novel full inter-relay interference cancellation method that also achieves asymptotically maximum rate and full cooperative diversity is then designed which only requires a single antenna at the destination node. Extension to asynchronous networks is then considered through the use of orthogonal frequency division multiplexing (OFDM) type transmission with a cyclic prefix, and interference cancellation techniques are designed for situations when synchronization errors are present in only the second hop or both the first and second hop. End-to-end bit error rate evaluations, with and without outer coding, are used to assess the performance of the various offset transmission schemes.

Multi-relay selection methods for cooperative amplify and forward type networks are then studied in order to overcome the degradation of end-to-end bit error rate performance in single-relay selection networks when there are feedback errors in the destination to relay node links. Outage probability analysis for two and four relay selection is performed to show the advantage of multi-relay selection when no interference occurs and when adjacent cell

interference is present both at the relay nodes and the destination node. Simulation studies are included which support the theoretical expressions.

Finally, outage probability analysis of a cognitive amplify and forward type relay network with cooperation between certain secondary users, chosen by single and multi-relay (two and four) selection is presented. The cognitive relays are assumed to exploit an underlay approach, which requires adherence to an interference constraint on the primary user. The relay selection is performed either with a max-min strategy or one based on maximising exact end-to-end signal-to-noise ratio. The analyses are again confirmed by numerical evaluations.

Contents

1	INTRODUCTION	1
1.1	Multi-Input Multi-Output	2
1.2	Wireless Cooperative Networks	5
1.3	Relay Selection in Cooperative Networks	9
1.4	Cognitive Relay Networks	10
1.5	Challenges and Thesis Contributions	13
1.6	Structure of Thesis	15
2	BACKGROUND OF WIRELESS COOPERATIVE NETWORKS	18
2.1	Introduction	18
2.2	Overview of Distributed Space-Time Coding Schemes	20
2.2.1	Distributed Transmission Technology	21
2.2.2	Orthogonal and Quasi-Orthogonal Codes	23
2.3	Distributed Differential Space-Time Coding	26
2.4	Performance Analysis of Wireless Cooperative Networks	28
2.4.1	Pairwise Error Probability Analysis	29
2.4.2	Outage Probability Analysis	33
2.5	Uncoded Versus Coded Transmission	39
2.5.1	Coding Gain	39
2.5.2	Convolution Coding	39
2.5.3	Turbo Coding and Iteration Decoding	40

2.6	Summary	45
3	FIC AND FSIC SCHEMES FOR SYNCHRONOUS SYSTEMS	46
3.1	Introduction	46
3.2	FIC with DSTC and DDSTC Schemes in Synchronous Systems	47
3.2.1	FIC with DSTC	48
3.2.2	FIC with DDSTC	55
3.3	FSIC with DSTC Schemes in Synchronous Systems	62
3.3.1	System Model	63
3.3.2	Four-Path Relaying with Inter-Relay Interference Cancellation at the Relay	64
3.3.3	Pairwise Error Probability and Diversity Analysis	70
3.3.4	Simulation Studies	75
3.4	Summary	77
4	FIC SCHEMES FOR ASYNCHRONOUS COOPERATIVE NETWORKS	78
4.1	Introduction	78
4.2	FIC Scheme for Cooperative Networks with Asynchronism in the Second Stage	79
4.2.1	OFDM Type Transmission with CP Scheme for A Cooperative Four Relay Network with Asynchronism in the Second Stage	79
4.2.2	Interference Cancellation Scheme	83
4.2.3	Simulation Studies	87
4.3	FIC Scheme for Cooperative Networks with Asynchronism in the Both Stages	90

4.3.1	OFDM Type Transmission with CP Scheme for A Co-operative Four Relay Network with Asynchronism in Both Stages	90
4.3.2	Interference Cancellation Scheme	94
4.3.3	Simulation Studies	98
4.4	Summary	101
5	OUTAGE PROBABILITY OF MULTI-RELAY SELECTION WITHOUT INTERFERENCE	102
5.1	Introduction	103
5.2	The Best Relay Pair Selection Without Interference	104
5.2.1	System Model	104
5.2.2	Outage Probability Analysis	106
5.2.3	Simulation Results	115
5.2.4	Analysis of The Impact of Feedback Errors	119
5.3	The Best Four Relays Selection Without Interference	120
5.3.1	System Model	120
5.3.2	Outage Probability Analysis	124
5.3.3	Analysis of The Impact of Feedback Errors	126
5.3.4	Outage Probability Analysis Verification	127
5.4	Summary	128
6	OUTAGE PROBABILITY OF MULTI-RELAY SELECTION WITH INTERFERENCE	129
6.1	Introduction	130
6.2	Multi-Relay Selection with Interference at the Relay	131
6.2.1	System Model	131
6.2.2	Two or four Relay Selection with Outage Probability Analysis	134

6.2.3	Simulation results for outage probability analysis and impact of relay selection feedback errors	142
6.3	Relay Selection with Interference at Both the Relay and Destination	146
6.3.1	System Model	146
6.3.2	Relay Selection Scheme with Outage Probability Analysis	149
6.3.3	Outage Probability Analysis Verification	150
6.4	Summary	152
7	OUTAGE PROBABILITY OF MULTI-RELAY SELECTION IN COGNITIVE RELAY NETWORKS	153
7.1	Introduction	154
7.2	System Model	156
7.3	Relay Selection Scheme with Outage Probability Analysis	159
7.3.1	The CDF and PDF of Lower Bound SNR	159
7.3.2	The CDF and PDF of Upper Bound SNR	160
7.3.3	The CDF and PDF of Exact SNR	160
7.3.4	Outage Probability Analysis	161
7.4	Outage Probability Analysis Verification	166
7.5	Summary	169
8	SUMMARY, CONCLUSION AND FUTURE WORK	170
8.1	Summary and Conclusions	170
8.2	Future Work	173

Statement of Originality

The contributions of this thesis are mainly on the improvement of transmission rate with the cancellation of interference and the outage probability analysis in the context of multi-relay selection. The novelty of the contributions is supported by the following international journal and conference papers:

In Chapter 3, full interference cancellation and full inter-relay self interference cancellation schemes for synchronous cooperative networks are presented to improve the end-to-end transmission rate and mitigate the interference between the relays. The results have been published in:

1. G. Chen and J. A. Chambers, “Full interference cancellation for an asymptotically full rate cooperative four relay network”, in Proc. IEEE ICITIS, Beijing, China, Dec. 2010.
2. G. Chen, O. Alnatouh, L. Ge and J. A. Chambers, “A Distributed Differential Space-Time Coding With Full Interference Cancellation Scheme for A Cooperative Four Relay Network”, In Proc. IET MIC-CSC, Istanbul, Turkey, Oct. 2012.
3. G. Chen, O. Alnatouh, and J. A. Chambers, “Full inter-relay self interference cancellation for a four relay cooperative network”, In Proc. UKIWCWS, New Delhi, India, Dec. 2010.

The contribution of Chapter 4 is a full interference cancellation scheme with orthogonal frequency-division multiplexing type transmission for use in a two-hop cooperative four relay network with asynchronism. These works have been presented in:

4. G. Chen and J. A. Chambers, “Full interference cancellation for an asymptotically full rate asynchronous cooperative four relay network”, In Proc. IEEE ISWCS, York, UK, Sep. 2010.

5. G. Chen, L. Ge and J. A. Chambers, “Offset transmission scheme with full interference cancellation for an asynchronous cooperative four relay network”, In Proc. IEEE WiAd, London, UK, June 2011.

In Chapter 5, outage probability analysis in the multi-relay selection application without interference is presented. The novelty of this work is supported by the following publications:

6. G. Chen, and J. A. Chambers, “Outage Probability in Distributed Transmission Based on Best Relay Pair Selection”, IET Communications, vol. 6, no. 12, pp. 1829-1836, Aug. 2012.
7. G. Chen, O. Alnatouh, L. Ge and J. A. Chambers, “Performance Analysis of Four Relays Selection Scheme for Cooperative Networks”, In Proc. ISSPA, Montreal, Canada, July 2012.

In Chapter 6, outage probability analysis in the multi-relay selection context with interference is presented. The novelty of this work is reinforced by the following works:

8. G. Chen and J. A. Chambers, “Two and Four Relay Selection Schemes for Application in Interference Limited Legacy Networks”, accepted for publication in EURASIP J. Wire. Commun. and Networking, June 2012.
9. G. Chen and J. A. Chambers, “Outage probability analysis for a cooperative AF relay network with relay selection in the presence of inter-cell interference”, IET Electronics Lett., vol. 48, no. 21, pp. 1346-1347, Oct. 2012.

In Chapter 7, outage probability analysis for a cognitive amplify-and-forward relay network with single and multi-relay selection is presented. The novelty of this work is supported by the following works:

-
10. G. Chen, O. Alnatouh and J. A. Chambers, “Outage Probability Analysis for A Cognitive Amplify-and-Forward Relay Network with Single and Multi-relay Selection”, submitted to IEEE Trans. on Vehicular Technology, July 2012.
 11. G. Chen, V. Dwyer, I. Krikidis, J. S. Thompson, S. McLaughlin and J. A. Chambers, “Comment on “Relay Selection for Secure Cooperative Networks with Jamming””, IEEE Trans. Wireless Commun., vol. 11, no. 6, pp. 2351, June 2012.

Acknowledgements

I AM DEEPLY INDEBTED to my supervisor Professor Jonathon A. Chambers for his kind interest, generous support and constant advice throughout the past three years. I have benefitted tremendously from his rare insight, his ample intuition and his exceptional knowledge. This thesis would never have been written without his tireless and patient mentoring. It is my very great privilege to have been one of his research students. I wish that I will have more opportunities to work with him in the future.

I am extremely thankful to Professor Sangarapillai Lambotharan, Dr. Yu Gong, Dr Des McLernon, Dr. Vincent Dwyer, Dr. Mohsen and June for their support and encouragement.

I am also grateful to all my colleagues Miao, Yanfeng, Jie Tang, Abdulla, Adel, Mustafa, Lu Ge, Ziming, Yu Wu, Juncheng, Ousma and Tian Zhao in the Advanced Signal Processing Group for providing a stable and cooperative environment within the Advanced Signal Processing Group.

Last, but most importantly, I really can not find appropriate words or suitable phrases to express my deepest and sincere heartfelt thanks, appreciations and gratefulness to my parents, my grandmothers, my brothers, my sisters and my girl friend for their constant encouragement, attention, prayers and their support in innumerable ways throughout my PhD and before. I would like to dedicate this thesis to my late grandfathers.

Gaojie Chen

September, 2012

List of Acronyms

3G	Third Generation
3GPP	3rd Generation Partnership Project
4G	Fourth Generation
AF	Amplify-and-Forward
AWGN	Additive White Gaussian Noise
BER	Bit Error Rate
BPSK	Binary Phase Shift Keying
CCI	Co-Channel Interference
CDF	Cumulative Distribution Function
CP	Cyclic Prefix
CRN	Cognitive Relay Network
CSI	Channel State Information
DDSTC	Distributed Differential Space-Time Coding
DF	Decode-and-Forward
DFT	Discrete Fourier Transform
FCC	Federal Communications Commission

FIC	Full Interference Cancellation
FSA	Fixed Spectrum Access
FSIC	Full Inter-Relay Self Interference Cancellation
IEEE	Institute of Electrical and Electronics Engineers
IDFT	Inverse Discrete Fourier Transform
i.i.d.	Independent and Identically Distributed
INR	Interference-to-Noise Ratio
IIR	Infinite Impulse Response
IRI	Inter-Relay Interference
ISI	Inter-Symbol Interference
LTE	Long Term Evolution
MAP	Maximum A Posteriori
MGF	Moment Generating Function
MIMO	Multiple-Input-Multiple-Output
ML	Maximum Likelihood
MRC	Maximum Ratio Combiner
ODSTC	Orthogonal Distributed Space-Time Code
OFDM	Orthogonal Frequency Division Multiplexing
PDF	Probability Density Function
PEP	Pairwise Error Probability
PU	Primary User

QPSK	Quadrature Phase Shift Keying
QoS	Quality of Service
RSC	Recursive Systematic Convolutional
SIMO	Single-Input-Multiple-Output
SINR	Signal-to-Noise plus Interference Ratio
SISO	Single-Input-Single-Output
SNR	Signal-to-Noise Ratio
SOVA	Soft Output Viterbi Algorithm
SU	Secondary User
WiFi	Wireless Fidelity
WiMax	Worldwide Interoperability for Microwave Access

List of Symbols

Scalar variables are denoted by plain lower-case letters, (e.g., x), vectors by bold-face lower-case letters, (e.g., \mathbf{x}), and matrices by upper-case bold-face letters, (e.g., \mathbf{X}). Some frequently used notations are as follows:

$E(\cdot)$	Statistical expectation
$\text{Var}(\cdot)$	Variance
$\text{Covar}(\cdot)$	Covariance
$(\cdot)^T$	Transpose
$(\cdot)^H$	Hermitian transpose
$(\cdot)^*$	Complex conjugate
$ \cdot $	Modulus of a complex number
$\ \cdot\ $	Euclidean norm
\mathbf{I}	Identity matrix
$\mathbf{0}_M$	$M \times M$ matrix of zeros
\mathbf{I}_M	$M \times M$ unity diagonal matrix
$\text{Re}(\cdot)$	Real part
$\text{Im}(\cdot)$	Imaginary part
$\text{DFT}(\cdot)$	Discrete Fourier transform

$\text{IDFT}(\cdot)$	Inverse discrete Fourier transform
$\text{Tr}(\cdot)$	Trace
$\text{diag}(\cdot)$	Diagonal matrix
$\det(\cdot)$	Matrix determinant
\cap	OR operation
\cup	AND operation
\circ	Hadamard product
$\max(\cdot)$	Maximum value
$\min(\cdot)$	Minimum value
$\zeta(\cdot)$	Time reversal operator
$D(\cdot)$	Cyclic delay operator
argmax	The argument which maximizes the expression
argmin	The argument which minimizes the expression
$F_{2,1}(\cdot)$	First hypergeometric function
$F_1(\cdot)$	Appell hypergeometric function
$\Gamma(\cdot)$	Gamma function
$\text{Ei}(\cdot)$	Exponential integral

List of Figures

- 1.1 A functional block diagram illustrating various forms of wireless communication system: SISO: single-input single-output; SIMO: single-input multiple-output; MISO: multiple-input single-output and MIMO: multiple-input multiple-output. 3
- 1.2 Ergodic capacity for different MIMO sizes. 4
- 1.3 A cooperative network with a relay selection scheme, where only the second relay is employed in the second stage of the transmission. 9
- 1.4 Underlay spectrum paradigm. Green and red represent the spectrum occupied by the primary users and the secondary users respectively. 11
- 1.5 Interweave spectrum scheme. Green and red represent the spectrum occupied by the primary users and secondary users respectively. 12
- 2.1 The block diagram of a two-hop wireless cooperative relay network over which distributed linear space time codes can be transmitted. The network consists of a source, four relay and one destination nodes; the frequency flat links are labeled with a scalar coefficient. 20

2.2	A basic wireless cooperative network with a direct link and single relay node.	33
2.3	The difference in the effects of coding gain and diversity gain on bit error rate.	39
2.4	An example convolution encoder structure.	40
2.5	Parallel Turbo recursive systematic convolution (RSC) encoder structure.	41
2.6	A 4-state, half rate RSC structure with generator polynomial (5,7).	42
2.7	Turbo decoder structure.	43
2.8	End-to-end BER comparison between coded and uncoded BPSK modulation cooperative networks with increasing cooperative diversity.	43
2.9	End-to-end BER comparison between coded and uncoded for QPSK modulation cooperative networks with increasing cooperative diversity.	44
3.1	A cooperative four relay network model with offset transmission scheme.	47
3.2	End-to-end BER performance.	54
3.3	End-to-end BER performance of the DSTC with FIC and varying uncertainty Assumption 1.	54
3.4	End-to-end BER performance.	60
3.5	End-to-end coded and uncoded BER performance of the differential STBC with FIC and varying uncertainty in Assumption 1.	61
3.6	The end-to-end data rate performance.	62

3.7	AF four-path relaying scheme.	63
3.8	Comparison of average rate between the different channel coefficients.	76
3.9	Comparison of BER performance for different levels of IRI.	76
4.1	A two hop wireless communication network with offset transmission scheme showing asynchronous transmission due to timing error.	80
4.2	BER performance for no FIC and FIC approaches.	88
4.3	BER performance of the FIC relay network as compared to a half rate Alamouti relay network.	89
4.4	BER performance for FIC approaches with coded and uncoded transmission.	89
4.5	An offset transmission model for a four relay network with asynchronism.	91
4.6	Architecture of the offset transmission relay network.	91
4.7	BER performance for no FIC and FIC approaches.	99
4.8	End-to-end transmission rate.	100
4.9	BER performance of the four relay with offset transmission and FIC and varying uncertainty in Assumption 1.	101
5.1	(a) shows the best relay pair selection from different clusters; (b) illustrates the best relay pair selection from the same cluster.	104
5.2	Comparison of the outage probability of the best relay pair selection from same cluster versus SNR, the theoretical results are shown in line style and the simulation results as points, where the threshold value α is 6 dB.	115

-
- 5.3 The outage probability of the best relay pair selection from different clusters based on the same SNR, the theoretical results are shown in line style and the simulation results as points. 116
- 5.4 The outage probability of the best relay pair selection from different clusters based on different SNRs, the theoretical results are shown in line style and the simulation results as points. 117
- 5.5 The outage probability of the best relay pair selection from the same cluster, the theoretical results are shown in line style and the simulation results as points. 117
- 5.6 Comparison of the outage probability of different relay selection schemes. 118
- 5.7 BER performance comparison of the best relay pair selection (solid line) from the same cluster with the best single relay selection (dashed line), with varying error in the feedback relay selection information from the destination. 120
- 5.8 A half-duplex dual-hop best four relay selection system. 120
- 5.9 BER performance comparison of the best four relays selection (solid line) with the best single relay selection (dashed line), with varying error in the feedback relay selection information from the destination. 126
- 5.10 Comparison of the outage probability of the single relay selection and the best four relays selection schemes, the theoretical results are shown in line style and the simulation results as points. 127

-
- 6.1 The system model. C1: cluster of interest, which contains a cooperative network which uses best two relay selection. S: source; D: Destination; R_n: potential relay group. C2: neighboring cluster, S': source; D': Destination. INF_i: interference signal for the i^{th} relay (S' → R_n). 131
- 6.2 Comparison of the outage probability of the best two relay selection schemes, the theoretical results are shown in line style and the simulation results as points. 142
- 6.3 Comparison of the outage probability of the best four relay selection schemes, the theoretical results are shown in line style and the simulation results as points. 143
- 6.4 Comparison of the outage probability of the single relay selection and the best two and four relay selection schemes. 144
- 6.5 BER performance comparison of different best two relay selection schemes (blue line) with the different best single relay selection schemes (red line), with varying error in the feedback relay selection information from the destination. 145
- 6.6 The cooperative transmission system model wherein the dashed lines denote the interference links and solid lines denote the selected transmission links, i.e. R_2 is selected for relaying to the destination. 147
- 6.7 Comparison of the outage probability of the best relay selection schemes, the theoretical results are shown in line style and the simulation results as points. 151

-
- 7.1 The cognitive relay network model wherein the dashed lines denote the interference links and the solid lines denote the selected transmission links, i.e., only SR_2 and SR_n are used for relaying to the secondary destination. 156
- 7.2 Comparison of the theoretical and simulated three types of outage probability analysis schemes for the best two relays selection ($\phi_0 = 5$, $\phi_1 = 10$ and $I_{th} = 2$). 166
- 7.3 Comparison of the exact theoretical outage probability for the best relay selection and the best multi-relay selection ($\phi_0 = 5$, $\phi_1 = 10$ and $I_{th} = 2$). 167
- 7.4 Comparison of the exact outage probability for a best single and best two relays selection for different thresholds I_{th} and mean channel gain ratios, ϕ_0 and ϕ_1 , $N = 8$. 168

INTRODUCTION

Signal propagation through a wireless channel faces more difficulties than through a guided wire, including greater additive noise, fading, multi-path spread, co-channel interference, and adjacent channel interference [1], whereas fiber and coaxial cables can be almost free of interference. However, wireless transmission has become the favorable platform to transfer information nowadays, due to the associated support for user freedom from being physically connected and providing, flexibility and portability [2]. The design of a reliable wireless system is difficult due to the random nature of the wireless channel, and the diversity of environments in which they are likely to be deployed. The next generation of wireless systems needs to have higher voice quality as compared to current cellular mobile radio standards and provide higher bit rate data services with greater coverage [3]. Wireless communications also has additional challenges, for example, limited bandwidth and security [4]. Recently, long-term evolution (LTE) and fourth generation (4G) have been vigorously developed in order to provide a high-data-rate, low-latency and packet-optimized radio-access technology supporting flexible bandwidth deployments [5].

1.1 Multi-Input Multi-Output

The demands for high data rate wireless communication systems have been increasing dramatically over the last decade. However, the performance of wireless communication systems at the link level is limited by multipath propagation effects, which lead to inter-symbol interference (ISI), path loss, and interference from other users in the form of co-channel interference (CCI) [5]. These limitations provide a number of technical challenges for reliable wireless communication systems. One approach to address these challenges is to use multiple antenna wireless communication systems, which have received a great deal of attention recently due to the potential gains in capacity and quality of service [3]. By using multiple antennas at both ends of a point-to-point communication link a multi-input multi-output (MIMO) system can be formed, which is included in Fig. 1.1, which can potentially combat multipath fading propagation effects and increase the channel capacity as compared with a conventional single-input single-output (SISO) system. This is already happening in 802.11x systems wireless fidelity (WiFi), 802.16x worldwide interoperability for microwave access (WiMax) and is a major focus for LTE and fourth generation (4G) cellular systems [6].

MIMO is an important technology for wireless links. It theoretically offers significant increases in data throughput and link range without additional bandwidth or transmit power. In particular, some significant advantages will be presented, such as array gain, diversity gain and spatial multiplexing.

To begin with, array gain, is a key parameter in MIMO communication systems, which means a power gain of the transmitted signals can be achieved by using multiple-antennas at the transmitter and/or receiver. Through an antenna array, as well as a correlative combination technique, the average signal-to-noise ratio (SNR) at the receiver can be improved significantly.

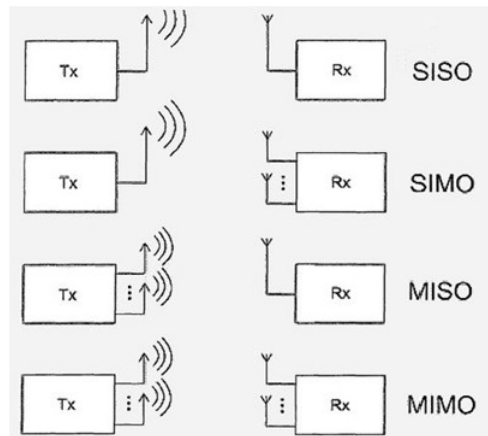


Figure 1.1. A functional block diagram illustrating various forms of wireless communication system: SISO: single-input single-output; SIMO: single-input multiple-output; MISO: multiple-input single-output and MIMO: multiple-input multiple-output.

MIMO can also achieve a linear growth of the capacity of the channel with the maximum spatial multiplexing order $\min(N_s, N_d)$ without increasing the power of the transmitter and the bandwidth, where N_s and N_d are the number of antennas at the source and destination node.

Finally, diversity is an important method to be used in wireless channels to combat fading. Furthermore, diversity gain is the increase in signal-to-interference ratio and is usually expressed in decibels, and sometimes given as a power ratio. The spatial diversity order for frequency flat channels is equal to the product of the number of antennas at the source and destination node ($N_s \times N_d$), if the channel between each transmit-receive antenna pair fades independently from the others.

Recent research on MIMO systems shows that theoretically the channel capacity can significantly increase by using multiple transmit and/or receive antennas assuming independent channels between transmit and receive antennas [7]. The channel capacity is a measure of the maximum amount of information that can be transmitted over a channel and received with a low probability of error at the receiver. The ergodic capacity of a SISO channel

is the ensemble average of the information rate over the distribution of the channel h_{sd} [3], which is given by

$$C_{SISO} = E(\log_2(1 + \rho|h_{sd}|^2)), \quad (1.1.1)$$

where h_{sd} is a complex Gaussian random channel coefficient, and ρ is the average SNR ratio at the receiver branch and $E(\cdot)$ denotes the statistical expectation over all channel realizations. And the ergodic capacity of a MIMO system is given by [7]

$$C_{MIMO} = E(\log_2(\det(\mathbf{I}_{N_d} + \frac{\rho}{N_s} \mathbf{H}\mathbf{H}^H))), \quad (1.1.2)$$

where \mathbf{I}_{N_d} is the $N_d \times N_d$ identity matrix, \mathbf{H} is the $N_d \times N_s$ normalized channel response matrix and $\det(\cdot)$ denotes the matrix determinant.

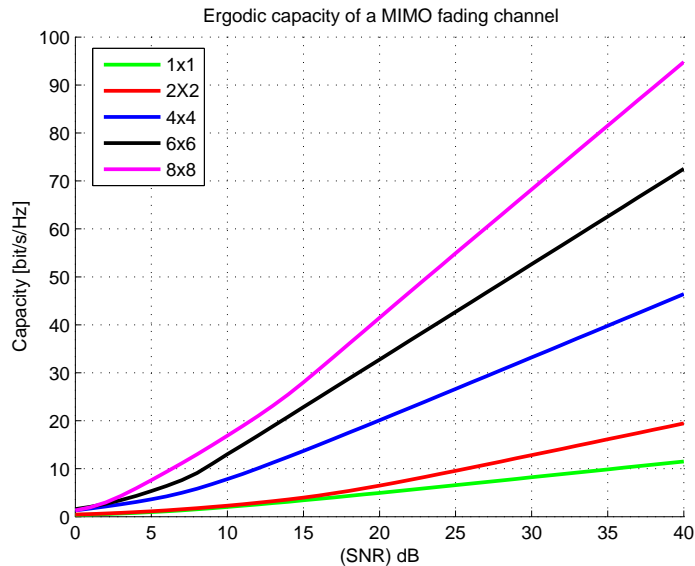


Figure 1.2. Ergodic capacity for different MIMO sizes.

Fig. 1.2 illustrates the ergodic capacity of a MIMO flat fading wireless link with an equal number of N_s and N_d antennas at the source and destination node. It can be seen that the ergodic capacity increases with SNR and with

the number of antennas at the transmitter and the receiver. For example at $\text{SNR} = 20$ dB the capacity increases approximately eight-fold when the SISO link is replaced by an 8×8 MIMO link. Therefore, when the channels between all antennas are uncorrelated, MIMO can offer major increase in capacity proportional to $\min(N_s, N_d)$.

Therefore, a MIMO point-to-point system can effectively provide ergodic capacity gain, array gain, diversity gain and spatial multiplexing. However, the requirements of multiple-antenna terminals increases the system complexity and the separation between the antennas increases the terminal size. Furthermore, MIMO systems suffer from the effect of path loss and shadowing, where path loss is the signal attenuation between the source and destination nodes due to propagation distance, while the shadowing is the signal fading due to objects obstructing the propagation path between the source and destination nodes [8]. Wireless cooperative networks can provide some solutions to deal with the aforementioned problems.

1.2 Wireless Cooperative Networks

Compared with conventional point-to-point MIMO systems, a cooperative network has different nodes which can share antennas, and thereby generate a virtual multiple antenna array (virtual MIMO) based on cooperation protocols [9] and [10]. Such cooperative relay networks have become a useful technique that can achieve the same advantage as MIMO systems whilst avoiding some of their disadvantages. Therefore, they have recently been adopted for different new wireless systems such as 3GPP LTE-Advanced [11]. Also, they have been considered in different wireless system standards such as WiMAX standards (IEEE 802.16j and IEEE 802.16m) [12] and WiFi standards (IEEE 802.11s and IEEE 802.11n) [13].

Cooperative relay networks can potentially yield several gains, i.e., co-

operative diversity gain, cooperative multiplexing gain and pathloss gain. Cooperative diversity gain can efficiently combat the detrimental effects of severe fading in the wireless channel [9]. Copies of the same information can be forward to the destination node by intermediate relays between the source and destination over independent channels. Therefore, cooperative diversity gain can be obtained in proportion to the number of independent channels in the cooperative relay network, which depends on the number of relay nodes and the environment [16]. For example, in a frequency-flat channel, the maximum cooperative diversity gain $G_d = N_s \times N_r \times N_d$, where N_r is the number of single-antenna relay nodes. Increased cooperative diversity gain leads to improvements in the system performance such as the probability of error P_e or the outage probability P_{out} . The cooperative diversity gain is related to how fast the probability of error decreases with an increase in the signal strength typically measured by SNR [3]. The cooperative diversity gain or diversity order, G_d , in terms of end-to-end error probability and outage probability are given by [8] and [14]

$$G_d = - \lim_{SNR \rightarrow \infty} \frac{\log(P_e(SNR))}{\log(SNR)} \quad \text{and} \quad G_d = - \lim_{SNR \rightarrow \infty} \frac{\log(P_{out}(R))}{\log(SNR)},$$

where $P_{out}(R)$ denotes the probability that the instantaneous system capacity R is lower than a particular transmission rate threshold R_{th} , such that

$$P_{out} = Pr\{G_m \log_2(1 + SNR) \leq R_{th}\},$$

where G_m is the cooperative spatial multiplexing gain effectively equals the number of independent channels over which different information can be transmitted, which can improve capacity or transmission data rates. The cooperative multiplexing gain as a function of SNR is given by

$$G_m = \lim_{SNR \rightarrow \infty} \frac{R(SNR)}{\log_2(SNR)}.$$

Finally, using intermediate relay nodes helps in avoiding the pathloss problem because dividing the propagation path between the source and destination nodes into at least two parts yields transmit power gains because the total resultant pathloss of part of the whole path is less than the pathloss of the whole path [14]. This advantage of the cooperative relay network can be referred to as pathloss gain. It is known theoretically that SNR is inversely proportional to the signal propagation distance, d , [14].

$$SNR \propto \frac{1}{d^n},$$

where d is the distance between the source and destination node and n is the pathloss exponent which typically fluctuates between 2 (light-of-sight) and 6 (highly cluttered environment) based on the type of the propagation environment [14]. According to this relation, a cooperative relay network where the intermediate relay is in the middle between the source and destination and the power is divided equally between the source and the relay will result in the following gain as compared to the conventional point-to-point system, therefore, pathloss gain can be obtained as

$$G_p = \frac{\frac{1/2}{(d/2)^n} + \frac{1/2}{(d/2)^n}}{1/d^n} = 2^n,$$

which means the cooperative relay network can achieve a transmit power saving of $(10\log_{10}2^n)$ dB.

This thesis is focused upon exploiting spatial cooperative diversity gain rather than cooperative multiplexing and pathloss gain. In summary, cooperative relay systems potentially offer several advantages and disadvantages for wireless communications [14] and [15] as follows:

1. Main advantages

a. Performance Gains: large system-wide performance gains can be achieved due to pathloss, diversity and multiplexing gains. These gains can

decrease transmission powers and provide higher capacity and transmission rate.

b. Coverage Extension: the coverage of the cell is impacted because of the limit in transmission power. For example, a user at the cell edge may experience insufficient power levels to communicate due to the weak signal of interest from the base station [14]. However, a cooperative relay system can effectively expand the network coverage through the relaying capability, and therefore the transmitted signal can service more range as compared to point-to-point systems.

c. Quality of service: a cooperative relay system can be extremely effective to combat the effects of channel fading by cooperative diversity [15]. Also, it can effectively enhance the transmission robustness by guaranteeing the transmission between the source and destination even if the direct link is in fade or several of the system relays are off or lost.

2. Main disadvantages

a. Increased interference: the use of relays will certainly generate extra intra- and inter-cell interference, which potentially causes the system performance to deteriorate [14]. In this thesis, interference cancellation schemes are proposed to mitigate this problem.

b. Strict synchronization: a tight synchronization generally needs to be maintained to facilitate cooperation, which is difficult to achieve, due to the nodes being in different locations and the varying timing delays between nodes. This thesis also considers asynchronous cooperative relay networks, and provides effective solutions to deal with asynchronism.

In the next subsection, another important method will be presented to improve performance and reduce system complexity, which is the relay selection scheme.

1.3 Relay Selection in Cooperative Networks

Recently, relay selection has been proposed as an attractive solution to improve the performance of conventional cooperative networks. For example, in cooperative wireless networks, the relay nodes have different locations so each transmitted signal from the source node to the destination node must pass through different paths causing different attenuations within the signals received at the destination which results in reducing the overall system performance. Therefore, to minimize this effect and benefit from cooperative communication, high quality paths should be chosen by using relay selection techniques. Furthermore, some works [16–18] have shown that full cooperative diversity order can be achieved with the relay selection scheme.

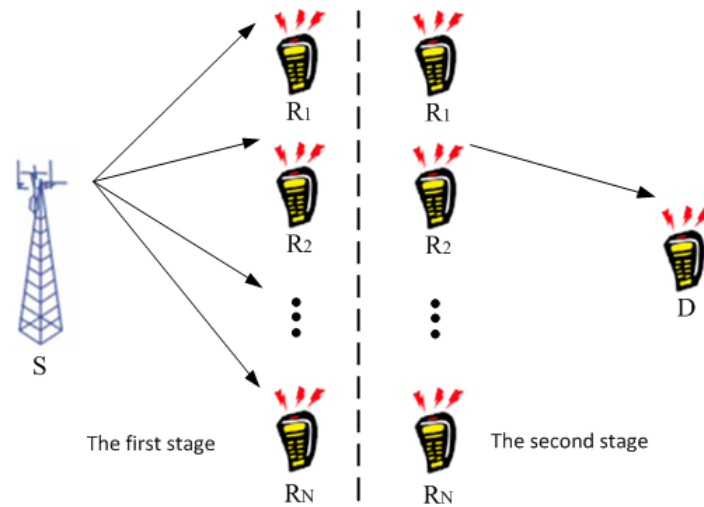


Figure 1.3. A cooperative network with a relay selection scheme, where only the second relay is employed in the second stage of the transmission.

In Fig. 1.3, a transmitter broadcasts its signal toward all the relay nodes at the first stage; the best relay can then be selected, by using local measurements of the instantaneous channel conditions between the source-relay and the relay-destination, and then used to transmit its received signal to the destination node during the second stage. No direct link between the source and destination is assumed due to path loss and shadowing. A relay

selection scheme can be exploited in both decode and forward (DF) (regenerative) and amplify and forward (AF) (nonregenerative) relaying schemes. In the literature, the DF relay selection scheme has been investigated in [19,20] over Rayleigh fading channels. The performance of a DF relay network has been provided in [21] over a Nakagami-m fading channel.

Two selection policies for AF networks can generally be used to choose the best relay node to help the source to transmit its signal to the destination node, which are the max-min and max-harmonic mean schemes as below [16]

$$R_{best} = \arg \max_i (\min(|h_{sr_i}|^2, |h_{r_i d}|^2)) \quad \text{Policy I}$$

$$R_{best} = \arg \max_i \left(\frac{2|h_{sr_i}|^2|h_{r_i d}|^2}{|h_{sr_i}|^2 + |h_{r_i d}|^2} \right) \quad \text{Policy II,}$$

where h_{sr_i} and $h_{r_i d}$ are channel links between the source-relay and relay-destination. On the basis of these two policies, some works in [22–24] have been considered to select the best relay from a cooperative AF network. In this thesis, an exact selection policy will be provided to obtain an accurate outage probability in cooperative AF networks. In the next section, a brief introduction to cognitive relay networks will be presented.

1.4 Cognitive Relay Networks

The radio spectrum and its use are strictly managed by governments in most countries, and spectrum allocation is a legacy command-and-control regulation enforced by regulatory bodies, such as the federal communications commission (FCC) in the United States [25] and Ofcom [26] in the United Kingdom. Most of the existing wireless networks and devices follow fixed spectrum access (FSA) policies to use radio spectrum, which means that radio spectral bands are licensed to dedicated users and services, such as TV, 3G networks, and vehicular ad hoc networks. Licensed users are referred to as the primary users (PUs), and a network consisting of PUs is referred

to as a primary network. In this context, only the PUs have the right to use the assigned spectrum, and others are not allowed to use it, even when the licensed spectral bands are idle. Although interference among different networks and devices can be efficiently coordinated by using FSA, this policy causes significant spectral under-utilization [26].

Therefore, cognitive radio is an emerging paradigm of wireless communication in which an intelligent wireless system utilizes information about the radio environment to adapt its operating characteristics in order to ensure reliable communication and efficient spectrum utilization [27]. Recently, several IEEE 802 standards for wireless systems have considered cognitive radio systems such as IEEE 802.22 standard [28] and IEEE 802.18 standard [29].

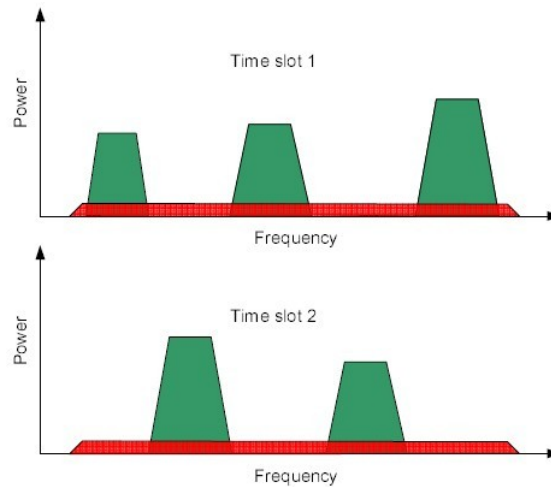


Figure 1.4. Underlay spectrum paradigm. Green and red represent the spectrum occupied by the primary users and the secondary users respectively.

Moreover, there are three main spectrum sharing approaches which are overlay, underlay and interweave cognitive approaches [30]. In the overlay approach, the secondary users coexist with primary users and use part of the transmission power to relay the primary users' signals to the primary receiver. This assistance will offset the interference caused by the secondary

user transmissions at the primary users' receiver. Hence, there is no loss in primary users' signal-to-noise ratio by secondary users spectrum access.

In the underlay approach, the secondary users access the licensed spectrum without causing harmful interference to primary users' communications. In this method, the secondary users ensure that interference leakage to the primary users is below an acceptable level as shown in Fig. 1.4.

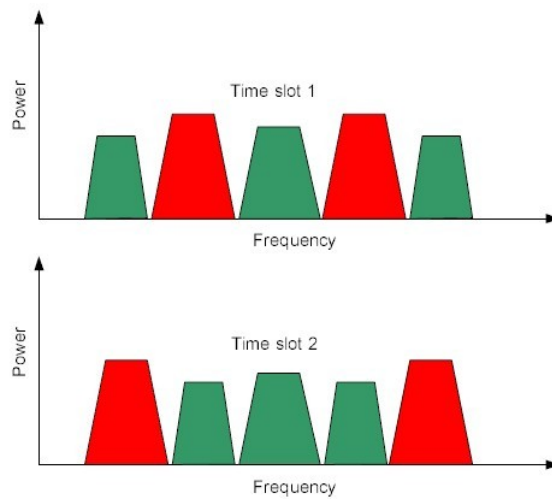


Figure 1.5. Interweave spectrum scheme. Green and red represent the spectrum occupied by the primary users and secondary users respectively.

In the interweave approach as shown in Fig. 1.5, identifying spectrum holes in the absence of cooperation between primary and secondary networks is very challenging [31]. For example, a secondary transmitter could be in the shadow region of the primary transmitter which will falsely indicate (to the secondary transmitter) availability of spectrum. The secondary transmission based on this false indication may harm the primary receivers. This hidden terminal problem is deemed to be very challenging and a limiting factor for the employment of interweave cognitive radio networks. On the other hand, the overlay cognitive radio is very interesting in terms of its theoretical advantages, however, there are even more challenges in terms of

practical implementation as this requires the secondary transmitter to have prior knowledge of the primary user transmitted signal. Therefore, the underlay scheme seems more realistic and easy to implement compared to the other schemes. Therefore the underlay cognitive radio is considered in this thesis.

1.5 Challenges and Thesis Contributions

Although, cooperative relaying has been considered as an effective method to combat fading by exploiting spatial diversity [32]; compared with traditional systems, relaying can additionally provide high quality of service for users at the cell edge or in shadowed areas; moreover, the relaying capability of this cooperative relay system can cope with the effects of path loss and shadowing, but there are two main challenging problems related to cooperative systems. Firstly, end-to-end transmission rate can be decreased due to the requirement of increasing the number of transmission stages (hops). Therefore, some researchers provide two way transmission schemes to increase the end-to-end transmission rate [33–35]. However, some redundant information has to be transmitted between two destination nodes and relay nodes, which can decrease the efficiency of the system. This thesis addresses the aforementioned challenging problems by exploiting offset transmission with full interference cancellation and full inter-relay self interference cancellation schemes.

The second challenge in designing high-performance cooperative networks is symbol-level synchronization among the relay nodes, due to the nodes being in different locations and mismatch between their individual oscillators. Therefore, in this thesis, this issue will be considered and an effective solution that can combat the timing error problem in two transmission stages will be provided by exploiting orthogonal frequency division

multiplexing with cyclic prefix type transmission.

Moreover, due to the random nature of the wireless environment the channel gains between the source, via relay nodes, and destination node are different which results in some relays providing a poor channel quality. This issue can affect the transmission quality to a certain extent. Therefore, in this thesis, the utilizing of multi-relay selection schemes is considered to overcome this problem and decrease the outage probability of cooperative networks. Finally, a cognitive relay network with multi-relay selection will be provided to decrease the outage probability and also improve the spectrum efficiency.

In summary, the contributions of this thesis can be summarized into five main parts:

1. Full interference cancellation and full inter-relay self interference cancellation schemes for synchronous cooperative networks are presented to obtain asymptotically unity end-to-end transmission rate and mitigate the interference between the relays.

2. A full interference cancellation scheme with orthogonal frequency-division multiplexing is used in a two-hop cooperative four relay network with asynchronism in both stages. This approach can achieve asymptotically full rate and completely cancel the timing error.

3. A multi-relay selection scheme is proposed based on the local measurements of the instantaneous channel conditions to improve the diversity and decrease the outage probability. And the best multi-relay selection scheme is also shown to have robustness against feedback error and to outperform a scheme based on selecting only the best single relay.

4. An outage probability analysis for two different multi-relay selection policies to select the best multi-relays from a group of available relays by using local measurements of the instantaneous channel conditions is examined when inter-cluster interference is present.

5. Three types of outage probability analysis are presented for a cognitive AF network with single or multi-relay selection from the potential cooperative secondary relays based on the underlay approach, while adhering to an interference constraint on the primary user.

1.6 Structure of Thesis

To simplify the understanding of this thesis and its contributions, its structure is summarized as follows:

In Chapter 1, a general introduction to wireless communication systems was presented. Furthermore, a brief introduction to cooperative networks including system features and pros and cons of the performance were presented. Then, a brief introduction to the relay selection scheme was presented. In addition, because a cognitive relay network has been used as an application for the proposed multi-relay selection, a brief introduction to cognitive radio systems was provided highlighting the main functions of cognitive radio and the features of cooperative cognitive networks.

In Chapter 2, a brief introduction to distributed space-time block coding schemes with orthogonal and quasi-orthogonal codes is presented. A differential distributed space-time code is briefly introduced, which does not need channel state information at the receiver for decoding. Two important performance measures, which are the pairwise error probability analysis and outage probability analysis, are described. Finally, two outer coding methods are introduced to achieve coding gain. A simulation study is included to confirm the performance advantage of distributed transmission with and without outer coding.

In Chapter 3, an offset transmission with full interference cancellation scheme is used to improve end-to-end transmission rate. Using offset transmission, the source can serially transmit signal to the destination node. How-

ever, the one group of relays scheme may suffer from inter-relay interference which is caused by the simultaneous transmission of the source and another group of relays. Therefore, the full interference cancellation scheme can be used to remove fully these inter-relay interference terms. Moreover, a full inter-relay self interference cancellation scheme at the relay nodes within a four relay network is provided and the pairwise error probability approach has been used to analyze distributed diversity.

In Chapter 4, an offset transmission with full interference cancellation scheme and orthogonal frequency-division multiplexing is applied in a cooperative network with asynchronism in the second stage to mitigate the timing error from the relays and from the relays to the destination. Furthermore, a new method is provided to avoid the cyclic prefix removal at the relays and cancel completely timing error at both stages.

In Chapter 5, outage probability analysis of the multi-relay selection scheme in a cooperative amplify and forward network without inter-cluster interference is provided. And the best multi-relay selection scheme is shown to have robustness to feedback error and to outperform a scheme based on selecting only the best single relay.

In Chapter 6, two different selection schemes are proposed to select the best multi-relays from a group of available relays in the same cluster by using local measurements of the instantaneous channel conditions in the context of legacy systems, when inter-cluster interference is present only at the relay nodes. Then the best relay selection is extended to maximize end-to-end signal-to-noise plus interference ratio, when inter-cluster interference is considered both at the relay nodes and the destination node. Moreover, a new exact closed form expression for outage probability in the high signal-to-noise ratio region is provided.

In Chapter 7, three types of outage probability analysis strategies for a cognitive amplify and forward network with single or multi-relay (two

and four) selection from the potential cooperative secondary relays based on the underlay approach, while adhering to an interference constraint on the primary user, is examined. New analytical expressions for the probability density function, and cumulative distribution function of end-to-end signal-to-noise ratio are derived together with near closed form expressions for outage probability over Rayleigh fading channels. Moreover, the theoretical values for the new exact outage probability are shown to match the simulated results.

Finally, in the last chapter which is Chapter 8, this thesis is concluded by summarizing its contributions and suggestions are given for some future possible research directions.

BACKGROUND OF WIRELESS COOPERATIVE NETWORKS

2.1 Introduction

It is well known that due to the fading effect, transmission over wireless channels can potentially suffer from severe attenuation in signal strength. Performance of wireless communication is generally much worse than that of wired communication. For a point-to-point wireless system, this problem was theoretically solved by using multiple antennas at the transmitter and/or the receiver, and spatial diversity was exploited by using space-time coding [36], [37]. However, due to physical constraints, when applying multiple antennas at the transmitter and/or the receiver it is difficult to obtain independent spatial paths between the transmitter and receiver. Therefore, recently, with increasing interest in wireless cooperative networks, researchers have been looking for methods to exploit spatial diversity provided by antennas of different users to improve the reliability of transmission [38] [39]. This improvement is called cooperative diversity since it is achieved by having different users in the network cooperate in some way.

Recently, therefore, cooperative relaying has been considered as an effec-

tive method to combat fading by exploiting spatial diversity [9], and as a way for two users with no or weak direct connection to attain a robust link. One or more relay nodes are generally used in such relaying to forward signals transmitted from the source node to the destination node. In a cooperative communication system, there are two main cooperative methods: decode and forward (DF) (regenerative relaying protocol) and amplify and forward (AF) (transparent relaying protocol) [14]. In the DF method, relay nodes decode the source information and then re-encode and re-transmit it to the destination. In the AF method, relay nodes only amplify and retransmit their received signals, including noise, to the destination. Therefore, compared with DF, AF type schemes have the advantage of simple implementation and low complexity in practical scenarios. In addition to complexity benefits, it has been shown in [40] that an AF scheme asymptotically, in terms of appropriate power control, approaches a DF one with respect to diversity. Therefore, in this thesis, AF type methods will be considered.

In this chapter, a brief overview of wireless cooperative networks concepts relevant to this thesis is presented. The chapter begins with an introduction to distributed space-time coding schemes and overviews two important codes, namely orthogonal and quasi-orthogonal codes. Then a coding scheme which avoids the need for channel state information in decoding is represented which is the differential space-time code. This is followed by a description of the performance analysis for such AF cooperative networks. Finally, outer coding methods are introduced to achieve additional coding gain based upon convolutional and Turbo coding.

2.2 Overview of Distributed Space-Time Coding Schemes

In a general wireless relay network, different relays receive different noisy copies of the same information symbols. The relays process these received signals and forward them to the destination. The distributed processing at the different relay nodes thus forms a virtual antenna array [14]. Therefore, conventional space-time block coding schemes can be applied to relay networks to achieve cooperative diversity. In this section, the focus is the design of distributed space-time block codes based on an AF type relay protocol. There is much literature on AF type space-time block codes, i.e. [41], [42], [43] and [44]. Next, the fundamental designs proposed in [44] are considered in detail.

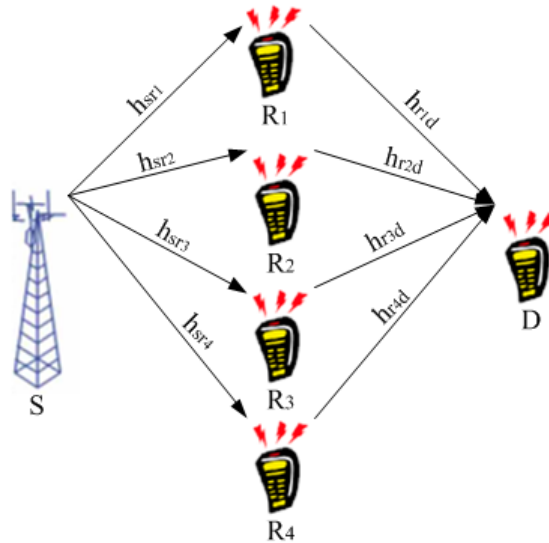


Figure 2.1. The block diagram of a two-hop wireless cooperative relay network over which distributed linear space time codes can be transmitted. The network consists of a source, four relay and one destination nodes; the frequency flat links are labeled with a scalar coefficient.

2.2.1 Distributed Transmission Technology

A wireless cooperative relay network is represented in Fig. 2.1, it consists of one transmitter node S with one antenna (only one of the antennas in the diagram for the source is being used), one destination node D with one antenna and R relay nodes, four in the figure. Each relay node (R) has a half duplex antenna for reception and transmission. It is assumed that the communication channels are quasi-static independent Rayleigh flat fading and the receiver has perfect channel information h_{sr_i} and $h_{r_i d}$, where h_{sr_i} and $h_{r_i d}$ denote respectively the channels from the transmitter to the i^{th} relay and from the i^{th} relay to the receiver. And there is no direct link between the source and the destination as path loss or shadowing is expected to render it unusable.

It is assumed that the transmitter sends the signal $\mathbf{s} = [s_1, \dots, s_M]^T$, which is normalized so that $E[\mathbf{s}^H \mathbf{s}] = 1$ where M is the time slot, $(\cdot)^T$, $(\cdot)^H$ and $E[\cdot]$ denote the transpose, Hermitian transpose and the expectation of a random variable, respectively [45]. The transmission operation has two steps, in step one the transmitter sends signals $\sqrt{P_1 M} \mathbf{s}$ to each relay where P_1 is the average power used at the transmitter for every transmission, whereas in step two, the i^{th} relay sends a signal vector to the receiver. The noise terms at the i^{th} relay within the vectors \mathbf{v}_i and at the receiver \mathbf{w}_i are independent complex Gaussian random variables with zero-mean and unit-variance. The received signal vector at the relays is given by

$$\mathbf{r}_i = \sqrt{P_1 M} h_{sr_i} \mathbf{s} + \mathbf{v}_i. \quad (2.2.1)$$

The i^{th} relay transmits the signal vector \mathbf{t}_i which corresponds to the received signal vector \mathbf{r}_i multiplied by a scaled unitary matrix, as such this approach has more complexity than an AF scheme and therefore is termed AF-type.

The transmitted signal vector from the i^{th} relay node can be generated from

$$\begin{aligned} \mathbf{t}_i &= \sqrt{\frac{P_2}{P_1 + 1}} (\mathbf{A}_i \mathbf{r}_i + \mathbf{B}_i \mathbf{r}_i^*) \\ &= \sqrt{\frac{P_1 P_2 M}{P_1 + 1}} (h_{sr_i} \mathbf{A}_i \mathbf{s} + h_{sr_i}^* \mathbf{B}_i \mathbf{s}^*) + \sqrt{\frac{P_2}{P_1 + 1}} (\mathbf{A}_i \mathbf{v}_i + \mathbf{B}_i \mathbf{v}_i^*), \end{aligned} \quad (2.2.2)$$

where \mathbf{A}_i and \mathbf{B}_i are $M \times M$ complex matrices, which depend on the distributed space time code, the 1 in the denominator scaling terms is the unity noise power, $(\cdot)^*$ denotes the complex conjugate and P_2 is the average transmission power at every relay node. The received signal vector \mathbf{y} at the receiver, assuming perfect synchronization between all the relays and the destination node, is given by

$$\mathbf{y} = \sum_{i=1}^R h_{r_i d} \mathbf{t}_i + \mathbf{w}. \quad (2.2.3)$$

The special cases that either $\mathbf{A}_i = \mathbf{0}_M$, \mathbf{B}_i is unitary or $\mathbf{B}_i = \mathbf{0}_M$ and \mathbf{A}_i is unitary are considered, where $\mathbf{0}_M$ represents the $M \times M$ zero matrix. $\mathbf{A}_i = \mathbf{0}_M$ means that the i^{th} relay column of the code matrix only contains the conjugates s_1^*, \dots, s_M^* and $\mathbf{B}_i = \mathbf{0}_M$ means that the i^{th} relay column contains only the information symbols s_1, \dots, s_M . Thus the following variables are defined as [45]

$$\hat{\mathbf{A}}_i = \mathbf{A}_i, \quad \hat{h}_{sr_i} = h_{sr_i}, \quad \hat{\mathbf{v}}_i = \mathbf{v}_i, \quad \mathbf{s}^{(i)} = \mathbf{s}, \quad \text{if } \mathbf{B}_i = \mathbf{0}_M$$

$$\hat{\mathbf{A}}_i = \mathbf{B}_i, \quad \hat{h}_{sr_i} = h_{sr_i}^*, \quad \hat{\mathbf{v}}_i = \mathbf{v}_i^*, \quad \mathbf{s}^{(i)} = \mathbf{s}^*, \quad \text{if } \mathbf{A}_i = \mathbf{0}_M.$$

From (2.2.2),

$$\mathbf{t}_i = \sqrt{\frac{P_1 P_2 M}{P_1 + 1}} \hat{h}_{sr_i} \hat{\mathbf{A}}_i \mathbf{s}^{(i)} + \sqrt{\frac{P_2}{P_1 + 1}} \hat{\mathbf{A}}_i \hat{\mathbf{v}}_i.$$

The signal vector at the receiver can be calculated from equations (2.2.1)

and (2.2.3) to be

$$\mathbf{y} = \sqrt{\frac{P_1 P_2 M}{P_1 + 1}} \mathbf{S} \mathbf{h} + \mathbf{w}'_d, \quad (2.2.4)$$

where

$$\mathbf{S} = [\hat{\mathbf{A}}_1 \mathbf{s}^{(1)} \hat{\mathbf{A}}_2 \mathbf{s}^{(2)} \dots \hat{\mathbf{A}}_R \mathbf{s}^{(R)}], \quad \mathbf{h} = [\hat{h}_{sr_1} h_{r_1 d} \hat{h}_{sr_2} h_{r_2 d} \dots \hat{h}_{sr_n} h_{r_n d}]^T \quad (2.2.5)$$

and

$$\mathbf{w}'_d = \sqrt{\frac{P_2}{P_1 + 1}} \sum_{i=1}^R h_{sr_i} \hat{\mathbf{A}}_i \hat{\mathbf{v}}_i + \mathbf{w}. \quad (2.2.6)$$

Therefore, without decoding, the relays generate a space-time codeword S distributively at the receiver. The vector \mathbf{h} is the equivalent channel and \mathbf{w}'_d is the equivalent noise. The optimum power allocation [44] is when the transmitter uses half the total power and the relays share the other half. If the total power is P and the number of relays is N , the average powers used at the source and relays are

$$P_1 = \frac{P}{2} \quad \text{and} \quad P_2 = \frac{P}{2N}. \quad (2.2.7)$$

If the channel vector \mathbf{h} is known at the receiver, the maximum-likelihood (ML) decoding is

$$\hat{\mathbf{S}} = \arg \min_{\mathbf{S}} \|\mathbf{y} - \sqrt{\frac{P_1 P_2 M}{P_1 + 1}} \mathbf{S} \mathbf{h}\|, \quad (2.2.8)$$

where $\|\cdot\|$ denotes the Euclidean norm, and $\arg \min$ represents finding the smallest Euclidean norm from all possible \mathbf{S} formed as in (2.2.5) from the source signal vectors \mathbf{s} defined by the chosen source constellation.

2.2.2 Orthogonal and Quasi-Orthogonal Codes

A) Real Orthogonal Designs

For a real orthogonal distributed space-time code (ODSTC), because every

entry of the code matrix is a linear combination of the information symbols, then $\mathbf{B}_i = \mathbf{0}_M$. Actually, from the definition of a real ODSTC, [37] proves that \mathbf{A}_i satisfies

$$\begin{cases} \mathbf{A}_i^T \mathbf{A}_i = k\mathbf{I}_M \\ \mathbf{A}_i^T \mathbf{A}_j = -\mathbf{A}_j^T \mathbf{A}_i, \end{cases} \quad (2.2.9)$$

where \mathbf{I}_M represents an $M \times M$ unity diagonal matrix. For the case that every symbol appears once only in each column, which is true for most real ODSTCs, \mathbf{A}_i has the structure of a permutation matrix whose entries can be 1, 0, or -1. For example, the application of the 2×2 real ODSTC is

$$\mathbf{S} = \begin{bmatrix} s_1 & s_2 \\ -s_2 & s_1 \end{bmatrix}. \quad (2.2.10)$$

It can be applied in two relays schemes, and the matrices used at the relays are

$$\mathbf{A}_1 = \begin{bmatrix} 1 & 0 \\ 0 & -1 \end{bmatrix} \quad \text{and} \quad \mathbf{A}_2 = \begin{bmatrix} 0 & 1 \\ 1 & 0 \end{bmatrix}. \quad (2.2.11)$$

B) Complex Orthogonal Designs

Similarly, in a complex ODSTC, \mathbf{A}_i needs to satisfy

$$\begin{cases} \mathbf{A}_i^H \mathbf{A}_i = k\mathbf{I}_M \\ \mathbf{A}_i^H \mathbf{A}_j = -\mathbf{A}_j^H \mathbf{A}_i. \end{cases} \quad (2.2.12)$$

Taking the application of the 2×2 Alamouti ODSTC in [46] as an example, the matrices \mathbf{A}_i and \mathbf{B}_i which are used at the two relays become

$$\mathbf{A}_1 = \mathbf{I}_2, \quad \mathbf{A}_2 = \mathbf{B}_1 = \mathbf{0}_2, \quad \mathbf{B}_2 = \begin{bmatrix} 0 & -1 \\ 1 & 0 \end{bmatrix}.$$

The space-time code word formed at the two relays has the following form:

$$\mathbf{S} = \begin{bmatrix} s_1 & -s_2^* \\ s_2 & s_1^* \end{bmatrix}. \quad (2.2.13)$$

It is clear that the space-time code in (2.2.13) is the transpose of the Alamouti structure. By defining $\mathbf{s} = [s_1 \ -s_2^*]^T$, the Alamouti code is obtained which has the structure

$$\mathbf{S} = \begin{bmatrix} s_1 & s_2 \\ -s_2^* & s_1^* \end{bmatrix}. \quad (2.2.14)$$

C) Quasi-Orthogonal Designs

For quasi-orthogonal designs in [47] and [48], the matrices \mathbf{A}_i and \mathbf{B}_i which are used at the four relays become

$$\mathbf{A}_1 = \mathbf{I}_4, \mathbf{A}_2 = \mathbf{A}_3 = \mathbf{B}_1 = \mathbf{B}_1 = \mathbf{0}_4, \mathbf{A}_4 = \begin{bmatrix} 0 & 0 & 0 & 1 \\ 0 & 0 & -1 & 0 \\ 0 & -1 & 0 & 0 \\ 1 & 0 & 0 & 0 \end{bmatrix}$$

$$\mathbf{B}_2 = \begin{bmatrix} 0 & -1 & 0 & 0 \\ 1 & 0 & 0 & 0 \\ 0 & 0 & 0 & -1 \\ 0 & 0 & 1 & 0 \end{bmatrix} \quad \text{and} \quad \mathbf{B}_3 = \begin{bmatrix} 0 & 0 & -1 & 0 \\ 0 & 0 & 0 & -1 \\ 1 & 0 & 0 & 0 \\ 0 & 1 & 0 & 0 \end{bmatrix}.$$

It is straightforward to see $\hat{\mathbf{A}}_i$ for $i = 1, 2, \dots, 4$ are unitary, but they do not satisfy the second equation in (2.2.12), therefore the code is quasi-orthogonal.

The space-time codeword formed at the four relays has the following form:

$$\mathbf{S} = \begin{bmatrix} s_1 & -s_2^* & -s_3^* & s_4 \\ s_2 & s_1^* & -s_4^* & -s_3 \\ s_3 & -s_4^* & s_1^* & -s_2 \\ s_4 & s_3^* & s_2^* & s_1 \end{bmatrix}.$$

Again, it is the transpose of the originally proposed quasi-orthogonal code, and by using $\mathbf{s} = [s_1 \ -s_2^* \ -s_3^* \ s_4]^T$ the original form can be obtained. In the next section, distributed differential space-time coding will be represented.

2.3 Distributed Differential Space-Time Coding

In Section 2.2, decoding the DSTC does require full channel information; both the channels from the source node to relay nodes and from the relay nodes to destination node, at the destination node. Therefore, the source node and the relay nodes have to send training symbols. However, in some situations, because of the cost on time and power and the complexity of channel estimation, using training symbols is not desired [49]. Therefore, the distributed differential space-time coding (DDSTC) in [50] is a useful scheme to solve this problem, because the relay and destination nodes do not require such channel knowledge, however there is a performance loss in bit error rate of 3 dB in the decoding process.

The scheme is based on the coherent distributed space-time coding in Section 2.2. The differential scheme uses two blocks that overlap by one block. The first is a reference block for the next. For generality, the $(n-1)^{th}$ and the n^{th} block are considered. According to (2.2.4) and (2.2.6), the

received signal vector at the $(n-1)^{th}$ block can be written as

$$\mathbf{y}_d(n-1) = \sqrt{\frac{P_1 P_2 M}{P_1 + 1}} \left[\hat{\mathbf{A}}_1 \hat{\mathbf{s}}_1(n-1) \quad \hat{\mathbf{A}}_2 \hat{\mathbf{s}}_2(n-1) \right] \mathbf{h}(n-1) + \mathbf{w}'(n-1), \quad (2.3.1)$$

where $\hat{\mathbf{s}}_1(n-1)$ and $\hat{\mathbf{s}}_2(n-1)$ are reference signals. The set of possible information is encoded as a set of unitary matrices \mathbf{U} , which for the Alamouti code [49], take the form

$$\mathbf{U} = \frac{1}{\sqrt{|s_1|^2 + |s_2|^2}} \begin{bmatrix} s_1 & -s_2^* \\ s_2 & s_1^* \end{bmatrix}, \quad (2.3.2)$$

where $|\cdot|$ denotes the modulus of a complex number. During block n , the signal vector sent by the transmitter is encoded differentially as

$$\mathbf{s}(n) = \mathbf{U}(n)\mathbf{s}(n-1). \quad (2.3.3)$$

For the first block, $\mathbf{s}(1) = [1 \ 0]^T$ is a reference signal. Therefore, the received signal vector at the n^{th} block can be written as

$$\mathbf{y}_d(n) = \sqrt{\frac{P_1 P_2 M}{P_1 + 1}} \left[\hat{\mathbf{A}}_1 \hat{\mathbf{U}}(n) \hat{\mathbf{s}}_1(n-1) \quad \hat{\mathbf{A}}_2 \hat{\mathbf{U}}(n) \hat{\mathbf{s}}_2(n-1) \right] \mathbf{h}(n) + \mathbf{w}'(n), \quad (2.3.4)$$

where $\hat{\mathbf{U}}(n) = \mathbf{U}(n)$ if $\mathbf{B}_i = \mathbf{0}_2$ and $\hat{\mathbf{U}}(n) = \mathbf{U}^*(n)$ if $\mathbf{A}_i = \mathbf{0}_2$. If $\mathbf{U}(n)\hat{\mathbf{A}}_i = \hat{\mathbf{A}}_i\hat{\mathbf{U}}(n)$, or equivalently,

$$\mathbf{U}(n)\mathbf{A}_i = \mathbf{A}_i\mathbf{U}(n) \quad \text{and} \quad \mathbf{U}(n)\mathbf{B}_i = \mathbf{B}_i\mathbf{U}^*(n), \quad (2.3.5)$$

therefore,

$$\mathbf{y}_d(n) = \sqrt{\frac{P_1 P_2 M}{P_1 + 1}} \mathbf{U}(n) \left[\hat{\mathbf{A}}_1 \hat{\mathbf{s}}_1(n-1) \quad \hat{\mathbf{A}}_2 \hat{\mathbf{s}}_2(n-1) \right] \mathbf{h}(n) + \mathbf{w}'(n).$$

The channel coefficients h_{sr_i} and h_{r_id} are assumed to be constant over at least two blocks, i.e., $\mathbf{h}(n) = \mathbf{h}(n - 1)$, therefore,

$$\mathbf{y}_d(n) = \mathbf{U}(n)\mathbf{y}_d(n - 1) + \mathbf{w}''(n),$$

where

$$\mathbf{w}''(n) = \mathbf{w}'(n) - \mathbf{U}(n)\mathbf{w}'(n - 1).$$

The ML decoding can be applied as

$$\arg \max_{\mathbf{U}(n)} \|\mathbf{y}_d(n) - \mathbf{U}(n)\mathbf{y}_d(n - 1)\|, \quad (2.3.6)$$

which needs no channel information. In the next section, methods to analyze the performance of cooperative networks are presented.

2.4 Performance Analysis of Wireless Cooperative Networks

In wireless cooperative networks, signal fading arising from multipath propagation is a particularly severe channel impairment that can be mitigated through the application of diversity [51]. Compared with the more conventional forms of single-user space diversity with physical arrays, this section sets up the classical relay channel model and examines the problem of creating and exploiting space diversity using a collection of distributed antennas belonging to multiple terminals, each with its own information to transmit. This form of space diversity is defined as cooperative diversity, because the terminals share their antennas and other resources to create a virtual antenna array through distributed transmission and signal processing [17]. Therefore, pairwise error probability (PEP) analysis is an important method to analyze the cooperative diversity and will be described in this section. Moreover, performance characterization in terms of outage events is also an important evaluation of robustness of transmission to fading, typically performed as

outage probability analysis. Therefore, the outage probability analysis will be presented after the PEP analysis in this section.

2.4.1 Pairwise Error Probability Analysis

Chernoff Bound of General Communication System

The analysis of the Chernoff bound for a general communication network is briefly described. A random variable z is assumed together with function $f(z)$, which satisfies

$$f(z) \geq \begin{cases} 1 & z \geq 0 \\ 0 & z < 0. \end{cases} \quad (2.4.1)$$

If the mean of z always exist [52], the Chernoff bound implies that the following inequality always exists:

$$P(z > 0) \leq E(f(z)), \quad (2.4.2)$$

where $E(\cdot)$ represents the statistical expectation operation. Let $f(z) = \exp(\lambda z)$, then the Chernoff bound becomes:

$$P(z > 0) \leq E(\exp(\lambda z)), \quad (2.4.3)$$

where $\lambda > 0$. Then, a general point-to-point single antenna communication system is considered. The received signal is obtained as $y = hs + n$, where s is the transmission signal, h is the fading coefficient and n is a Gaussian random noise with the spectrum density of N_0 per dimension. And the maximum likelihood (ML) decoding is used as

$$\hat{s} = \arg \max_s P(y|s) = \arg \min_s |y - hs|^2. \quad (2.4.4)$$

For ML decoding, the decoder selects the symbol that has the minimum distance to the received signal. Therefore, the probability that the decoder chooses that an erroneous symbol s_e is transmitted, denoted by $P(s \rightarrow s_e|y, h)$, is given by:

$$P(s \rightarrow s_e|y, h) = P(|y - hs|^2 > |y - hs_e|^2) = P(|y - hs|^2 - |y - hs_e|^2 > 0). \quad (2.4.5)$$

Substituting (2.4.5) into the Chernoff bound of (2.4.3), yields:

$$P(s \rightarrow s_e|y, h) \leq E(\exp(\lambda(|y - hs|^2 - |y - hs_e|^2))). \quad (2.4.6)$$

After some algebraic manipulation, (2.4.6) can be obtained as:

$$P(s \rightarrow s_e|y, h) \leq \exp(-\lambda h^2(1 - N_0\lambda)|s - s_e|^2), \quad (2.4.7)$$

where $\lambda = 1/2N_0$, then

$$P(s \rightarrow s_e|y, h) \leq \exp\left(-\frac{1}{4N_0}h^2|s - s_e|^2\right). \quad (2.4.8)$$

Similarly, for a multiple antenna space-time coded system, the transmitted codeword, channel and noise terms become matrices, namely \mathbf{S} , \mathbf{H} and \mathbf{N} , respectively. And the received signal matrix can be represented as:

$$\mathbf{Y} = \mathbf{H}\mathbf{S} + \mathbf{N}. \quad (2.4.9)$$

Therefore, the upper bounded PEP of the decoding error can be calculated by using the same method as [44]:

$$P(\mathbf{S} \rightarrow \mathbf{S}_e|\mathbf{Y}, \mathbf{H}) \leq \exp\left(-\frac{1}{4N_0}\mathbf{H}^H(\mathbf{S} - \mathbf{S}_e)^H(\mathbf{S} - \mathbf{S}_e)\mathbf{H}\right). \quad (2.4.10)$$

In the next subsequent sections, the PEP upper bound of distributed space-time coding will be described.

PEP Upper Bound for a Distributed Space-Time Code

This section employs the Chernoff bound to derive the PEP upper bound for an AF type DSTC network. Since in (2.2.6) $\hat{\mathbf{A}}_i$ are unitary and ω_j , ν_i the elements of \mathbf{w} and $\hat{\mathbf{v}}_i$ are independent Gaussian random variables, \mathbf{w}'_d is a Gaussian random vector when the $h_{s,ri}$ are known. It is clear that $E(\mathbf{w}'_d) = 0_{M,1}$ and $Covar(\mathbf{w}'_d) = \left(1 + \frac{P_2}{P_1+1} \sum_{i=1}^R |h_{r_i d}|^2\right) \mathbf{I}_M$. Thus, \mathbf{w}'_d is both spatially and temporally white. Define $\mathbf{S} = [\hat{\mathbf{A}}_1 \mathbf{s}^{(1)} \dots \hat{\mathbf{A}}_R \mathbf{s}^{(R)}]$ as in (2.2.5). Therefore, \mathbf{S} is an element matrix in the distributed space-time code set. When both $\hat{h}_{s,ri}$ and $h_{r_i d}$ are known, $\mathbf{x}|\mathbf{s}^{(i)}$ is also a Gaussian random vector with a covariance matrix $\left(1 + \frac{P_2}{P_1+1} \sum_{i=1}^R |h_{r_i d}|^2\right) \mathbf{I}_M$ and mean $\sqrt{\frac{P_1 P_2 M}{P_1+1}} \mathbf{S} \mathbf{h}$. Then,

$$p(\mathbf{x}|\mathbf{s}^{(i)}) = \frac{e^{-\frac{\left(x - \sqrt{\frac{P_1 P_2 M}{P_1+1}} \mathbf{S} \mathbf{h}\right)^H \left(x - \sqrt{\frac{P_1 P_2 M}{P_1+1}} \mathbf{S} \mathbf{h}\right)}{1 + \frac{P_2}{P_1+1} \sum_{i=1}^R |h_{r_i d}|^2}}}{\pi^M \left(1 + \frac{P_2}{P_1+1} \sum_{i=1}^R |h_{r_i d}|^2\right)^M}. \quad (2.4.11)$$

The ML decoding of the system can be easily seen to be

$$\hat{\mathbf{s}} = \arg \max_{\mathbf{s}} P(\mathbf{x}|\mathbf{s}^{(i)}) = \arg \min_{\mathbf{s}} \|\mathbf{y} - \sqrt{\frac{P_1 P_2 M}{P_1+1}} \mathbf{S} \mathbf{h}\|. \quad (2.4.12)$$

Since \mathbf{S} is linear in $\mathbf{s}^{(i)}$, by splitting the real and imaginary parts, the decoding is equivalent to the decoding of a real linear system. Therefore, sphere decoding can be used [53] and [54].

According to the Chernoff bound, with the ML decoding in (2.4.12), the PEP, averaged over the channel coefficients, of mistaking $\mathbf{s}^{(i)}$ by $\mathbf{s}^{(e)}$ has the

bound [44]:

$$P(\mathbf{S} \rightarrow \mathbf{S}_e | \mathbf{Y}, \mathbf{h}) \leq \exp \left(\frac{-P_1 P_2 M}{4(1 + P_1 + P_2 \sum_{i=1}^R |h_{r_i,d}|^2)} \mathbf{h}^H (\mathbf{S} - \mathbf{S}_e)^H (\mathbf{S} - \mathbf{S}_e) \mathbf{h} \right). \quad (2.4.13)$$

Integrating over \hat{h}_{sr_i} , yields

$$P(\mathbf{S} \rightarrow \mathbf{S}_e | \mathbf{Y}, h_{r_i,d}, i = 1, \dots, N) \leq \det^{-1} \left[\mathbf{I}_R + \frac{P_1 P_2 M}{4(1 + P_1 + P_2 g)} \mathbf{C} \mathbf{G} \right], \quad (2.4.14)$$

where $\mathbf{C} = (\mathbf{S} - \mathbf{S}_e)^H (\mathbf{S} - \mathbf{S}_e)$, $\mathbf{G} = \text{diag}\{|h_{r_1,d}|^2, \dots, |h_{r_n,d}|^2\}$ and $g = \sum_{i=1}^R |h_{r_i,d}|^2$, and $\det(\cdot)$ and $\text{diag}(\cdot)$ denote the matrix determinant and diagonal matrix, respectively. In order to derive the final PEP upper bound, average (2.4.14) over $h_{r_i,d}, i = 1, \dots, N$. Unfortunately, the expectations over all $h_{r_i,d}$ are difficult to calculate in a closed form, therefore, some approximation has to be considered. Note that $g = \sum_{i=1}^R |h_{r_i,d}|^2$ is Gamma distributed [55]:

$$f(g) = \frac{g^{N-1} e^{-g}}{(N-1)!}, \quad (2.4.15)$$

whose mean and variance are both N . For large N , g can be approximated by its mean, that is $g \approx N$ [44]. Therefore, (2.4.14) becomes

$$P(\mathbf{S} \rightarrow \mathbf{S}_e | \mathbf{Y}, h_{r_i,d}, i = 1, \dots, N) \leq \det^{-1} \left[\mathbf{I}_R + \frac{P_1 P_2 M}{4(1 + P_1 + P_2 N)} \mathbf{C} \mathbf{G} \right], \quad (2.4.16)$$

which is minimized when $\frac{P_1 P_2 M}{4(1 + P_1 + P_2 N)}$ is maximized. Assume $P = P_1 + N P_2$ is the total power in the whole network. Therefore,

$$\frac{P_1 P_2 M}{4(1 + P_1 + P_2 N)} = \frac{P_1 (P - P_1) M}{4N(1 + P)} \leq \frac{P^2 M}{16N(1 + P)},$$

with equality when

$$P_1 = \frac{P}{2} \quad \text{and} \quad P_2 = \frac{P}{2N}. \quad (2.4.17)$$

Thus, the optimal power allocation strategy allocates half of the total power

to the source and the relays share the other half. Finally, substituting (2.4.17) into (2.4.16), gives

$$P(\mathbf{S} \rightarrow \mathbf{S}_e | \mathbf{Y}, h_{r_i d}, i = 1, \dots, N) \leq \det^{-1} \left[\mathbf{I}_R + \frac{PM}{16N} \mathbf{C} \mathbf{G} \right]. \quad (2.4.18)$$

Then, integrating the above equation with respect to $|h_{r_i d}|^2$ and assuming that \mathbf{C} is a full rank matrix and $M \geq N$, the average PEP of the distributed space-time coding can be approximated as:

$$P(\mathbf{S} \rightarrow \mathbf{S}_e | \mathbf{Y}) \leq \det^{-1}[\mathbf{C}] \left(\frac{8N}{M} \right)^N P^{-N(1 - \frac{\log \log P}{\log P})}. \quad (2.4.19)$$

Therefore, the diversity order of DSTC is $N(1 - \frac{\log \log P}{\log P})$ when \mathbf{C} is a full rank matrix and $M \geq N$. When P is very large, $\frac{\log \log P}{\log P} \rightarrow 0$, and the asymptotic diversity order is N . However, $M \geq N$ is assumed, for the general case, the rank of \mathbf{C} will be $\min(M, N)$ instead of N , therefore, the diversity order achieved by the DSTC is $\min(M, N)(1 - \frac{\log \log P}{\log P})$. Next, the outage probability analysis for certain cooperative networks is considered.

2.4.2 Outage Probability Analysis

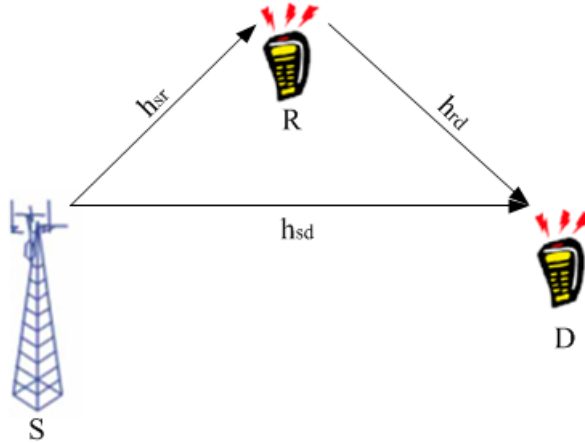


Figure 2.2. A basic wireless cooperative network with a direct link and single relay node.

In this section, outage events and outage probabilities are shown to characterize performance of the system in Fig. 2.2, which denotes the basic cooperative network including a direct link. According to different types of processing by the relay node and different types of combining at the destination node, the outage probability analysis of the direct link, fixed, selection and incremental relaying will be discussed, respectively; I denotes the mutual information, and for a target rate R , $I < R$ and $P(I < R)$ denote the outage event and outage probability, respectively.

A. Direct transmission

For the direct transmission case, the source transmits directly the signal to the destination node, the relay node is not working at the same time, therefore, the maximum average mutual information between input and output is given by

$$I_D = \log_2(1 + SNR|h_{sd}|^2). \quad (2.4.20)$$

The outage event for spectral efficiency R is given by $I_D < R$ and is equivalent to the event

$$|h_{sd}|^2 < \frac{2^R - 1}{SNR}. \quad (2.4.21)$$

For Rayleigh fading, i.e., $|h_{sd}|^2$ is exponentially distributed with parameter σ_{sd}^{-2} , the outage probability satisfies

$$\begin{aligned} P_D^{out}(SNR, R) &= P(I_D < R) = P(|h_{sd}|^2 < \frac{2^R - 1}{SNR}) \\ &= 1 - \exp(-\frac{2^R - 1}{SNR\sigma_{sd}^2}) \approx \frac{1}{\sigma_{sd}^2} \cdot \frac{2^R - 1}{SNR}, \end{aligned} \quad (2.4.22)$$

where σ_{sd}^2 is the channel variance from the source to the destination. Obviously, the outage probability is inversely proportional both to SNR and to channel variance σ_{sd}^2 .

B. Fixed relaying

For fixed relaying, the relay can either amplify its received signals subject to its power constraint, or to decode, re-encode, and retransmit the messages.

1) Amplify and forward: the AF scheme with a direct link and transmission over two time slots produces an equivalent one-input, two-output complex Gaussian noise channel with different noise levels in the outputs, and the maximum average mutual information between input and output is given by

$$I_{AF} = \frac{1}{2} \log_2(1 + SNR|h_{sd}|^2 + f(SNR|h_{sr}|^2, SNR|h_{rd}|^2)), \quad (2.4.23)$$

where $f(x, y) = \frac{xy}{x+y+1}$. The outage event for spectral efficiency R is given by $I_D < R$ and is equivalent to the event

$$|h_{sd}|^2 + \frac{1}{SNR} f(SNR|h_{sr}|^2, SNR|h_{rd}|^2) < \frac{2^{2R} - 1}{SNR}. \quad (2.4.24)$$

For Rayleigh fading, i.e., $|h_{ij}|^2$ is exponentially distributed with parameter σ_{ij}^{-2} , the outage probability satisfies [17]

$$P_{AF}^{out}(SNR, R) = P(I_{AF} < R) \approx \left(\frac{\sigma_{sr}^2 + \sigma_{rd}^2}{2\sigma_{sd}^2\sigma_{sr}^2\sigma_{rd}^2} \right) \left(\frac{2^{2R} - 1}{SNR} \right)^2, \quad (2.4.25)$$

where σ_{ij}^2 , $i \in (s, r)$ and $i \in (r, d)$, are the channel variances.

2) Decode and forward: A particular decoding structure is applied at the relay in order to analyze DF transmission. In [17], the maximum average mutual information for repetition-coded DF can be shown to be

$$I_{DF} = \frac{1}{2} \min\{\log_2(1 + SNR|h_{sr}|^2), \log_2(1 + SNR|h_{sd}|^2 + SNR|h_{rd}|^2)\}, \quad (2.4.26)$$

where the first term of (2.4.26) denotes the maximum rate at which the relay can reliably decode the source message, and the second term of (2.4.26) represents the maximum rate at which the destination can reliably decode the

source message given repeated transmissions from the source and relay. The outage event for spectral efficiency R is given by $I_{DF} < R$ and is equivalent to the event

$$\min\{|h_{sr}|^2, |h_{sd}|^2 + |h_{rd}|^2\} < \frac{2^{2R} - 1}{SNR}. \quad (2.4.27)$$

For Rayleigh fading, the outage probability for repetition-coded DF can be computed as [17]

$$\begin{aligned} P_{DF}^{out}(SNR, R) &= P(I_{DF} < R) = P(|h_{sr}|^2 < \frac{2^{2R} - 1}{SNR}) \\ &+ P(|h_{sr}|^2 \geq \frac{2^{2R} - 1}{SNR}) P(|h_{sd}|^2 + |h_{rd}|^2 < \frac{2^{2R} - 1}{SNR}), \end{aligned} \quad (2.4.28)$$

when $SNR \rightarrow \infty$, this becomes

$$P_{DF}^{out}(SNR, R) \approx \frac{2^{2R} - 1}{\sigma_{sr}^2 SNR}, \quad (2.4.29)$$

where σ_{sr}^2 is channel variance from the source to the relay. Clearly, the outage probability is inversely proportional both to SNR and to channel variance σ_{sr}^2 .

C. Selection relaying

Selection relaying builds upon fixed relaying by allowing transmitting nodes to choose a suitable cooperative or noncooperative action according to the measured SNR. Selection relaying can be applied to overcome the weakness of the DF transmission in [17], i.e. when the relay cannot decode, direct transmission is implemented. As an example analysis, considering the performance of selection DF, its mutual information is somewhat involved to write down in general; however, in the case of repetition coding at the relay,

using (2.4.20) and (2.4.26), it can be shown [17] to be

$$I_{SDF} = \begin{cases} \frac{1}{2} \log_2(1 + 2SNR|h_{sd}|^2), & |h_{sr}|^2 < \frac{2^{2R}-1}{SNR} \\ \frac{1}{2} \log_2(1 + SNR|h_{sd}|^2 + SNR|h_{rd}|^2), & |h_{sr}|^2 \geq \frac{2^{2R}-1}{SNR}. \end{cases} \quad (2.4.30)$$

In the first case in (2.4.30), the relay can not decode and the source must repeat its transmission. Therefore, the mutual information is that of repetition coding from the source to the destination, hence the extra factor of two in the SNR. Similarly, for the second case in (2.4.30), the mutual information is that of repetition coding from the source and relay to the destination. The outage event for spectral efficiency R is given by $I_{SDF} < R$ and is equivalent to the event

$$\begin{aligned} & (\{|h_{sr}|^2 < \frac{2^{2R}-1}{SNR}\} \cap \{(2|h_{sd}|^2 < \frac{2^{2R}-1}{SNR})\}) \cup \\ & (\{|h_{sr}|^2 \geq \frac{2^{2R}-1}{SNR}\} \cap \{|h_{sd}|^2 + |h_{rd}|^2 < \frac{2^{2R}-1}{SNR}\}), \end{aligned} \quad (2.4.31)$$

where \cap and \cup denote “OR” and “AND” operations. Because the events in the union of (2.4.31) are mutually exclusive, the outage probability becomes a sum

$$\begin{aligned} P_{SDF}^{out}(SNR, R) &= P(I_{SDF} < R) = P(|h_{sr}|^2 < \frac{2^{2R}-1}{SNR})P(2|h_{sd}|^2 \\ &< \frac{2^{2R}-1}{SNR}) + P(|h_{sr}|^2 \geq \frac{2^{2R}-1}{SNR})P(|h_{sd}|^2 + |h_{rd}|^2 < \frac{2^{2R}-1}{SNR}), \end{aligned} \quad (2.4.32)$$

when $SNR \rightarrow \infty$, it becomes approximately

$$P_{SDF}^{out}(SNR, R) \approx \left(\frac{\sigma_{sr}^2 + \sigma_{rd}^2}{2\sigma_{sd}^2\sigma_{sr}^2\sigma_{rd}^2} \right) \left(\frac{2^{2R}-1}{SNR} \right)^2. \quad (2.4.33)$$

where σ_{ij}^2 , $i \in (s, r)$ and $i \in (r, d)$, are the channel variances. Clearly, for large SNR , the performance of selection DF is identical to that of fixed AF.

D. Incremental relaying

Incremental relaying improves upon the spectral efficiency of both fixed and selection relaying by exploiting limited feedback from the destination and relaying only when necessary. Outage analysis of incremental relaying is complicated by its variable-rate nature [9]. Specifically, the protocols operate at spectral efficiency R when the source-destination transmission is successful, and spectral efficiency $R/2$ when the relay repeats the source transmission. The outage probability is a function of SNR and the expected spectral efficiency \bar{R} . Taking incremental AF as an example, the outage probability as a function of SNR and R is given by

$$\begin{aligned} P_{IAF}^{out}(SNR, R) &= P(I_D < R)P(I_{AF} < R/2|I_D < R) = P(I_{AF} < R/2) \\ &= P(|h_{sr}|^2 + \frac{1}{SNR}f(SNR|h_{sr}|^2, SNR|h_{rd}|^2) < \frac{2^R - 1}{SNR}). \end{aligned} \quad (2.4.34)$$

Furthermore, the expected spectral efficiency can be computed as

$$\begin{aligned} \bar{R} &= RP(|h_{sd}|^2 \geq \frac{2^R - 1}{SNR}) + \frac{R}{2}P(|h_{sd}|^2 < \frac{2^R - 1}{SNR}) = R\exp(-\frac{2^R - 1}{SNR}) \\ &\quad + \frac{R}{2}(1 - \exp(-\frac{2^R - 1}{SNR})) = \frac{R}{2}(1 + \exp(-\frac{2^R - 1}{SNR})) = h_{SNR}(R). \end{aligned} \quad (2.4.35)$$

Therefore, when the value of SNR is given, a fixed value of \bar{R} can arise from several possible R , namely, the pre-image $h_{SNR}^{-1}(\bar{R})$ contains several possible R . Thus, the optimal pre-image value $\tilde{h}_{SNR}^{-1}(\bar{R})$ is $\min(h_{SNR}^{-1}(\bar{R}))$ which can capture an optimal mapping from \bar{R} to R . For fair comparison to protocols without feedback, a modified outage expression in the large-SNR regime is considered. Then compared with outage of fixed and selection relaying protocols, for large SNR, the outage probability is

$$P_{IAF}^{out}(SNR, \tilde{h}_{SNR}^{-1}(\bar{R})) \approx (\frac{\sigma_{sr}^2 + \sigma_{rd}^2}{2\sigma_{sd}^2\sigma_{sr}^2\sigma_{rd}^2})(\frac{2^{\bar{R}} - 1}{SNR})^2, \quad (2.4.36)$$

where σ_{ij}^2 , $i \in (s, r)$ and $i \in (r, d)$, are the channel variances. In the next section uncoded and coded transmission schemes will be introduced.

2.5 Uncoded Versus Coded Transmission

2.5.1 Coding Gain

Coding gain is the measure in the difference between the SNR levels between the uncoded system and coded system required to reach the same BER levels. It also can reduce error rate to improve system performance, however, compared with diversity gain, the nature of coding gain is different. Diversity gain attests itself by rising the magnitude of the slope of the BER curve, whereas coding gain generally just shifts the error rate curve to the left [3], see Fig. 2.3. In the following section, convolution coding will be briefly introduced.

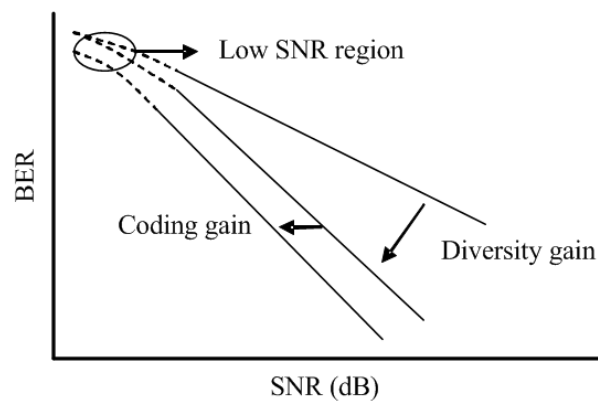


Figure 2.3. The difference in the effects of coding gain and diversity gain on bit error rate.

2.5.2 Convolution Coding

Convolutional codes are used extensively in practical applications in order to achieve reliable data transfer, i.e. third generation (3G) cellular communication system. A convolution code generates coded symbols by passing

the information bits through a linear finite-state shift register as shown in Fig. 2.4. The shift register consists of K stages with k bits per stage. There are n binary addition operations with input taken from all K stages: these operators produce a codeword of length n for each k bit input sequence. Moreover, the rate of the code is k/n , because the binary input data is shifted into each stage of the shift register k bits at a time, and each of these shifts produces a coded sequence of length n . The number of shift register stages K is called the constraint length. In Section 4.2.3, a half rate ($n = 2, k = 1, K = 3$) convolution coding will be used to improve the BER performance. A well known scheme can be employed to decode the convolution coding, which is the Viterbi algorithm, full details of which can be found in [56]. To obtain increased coding gain iterative decoding can be employed, a review of which is given in the next section.

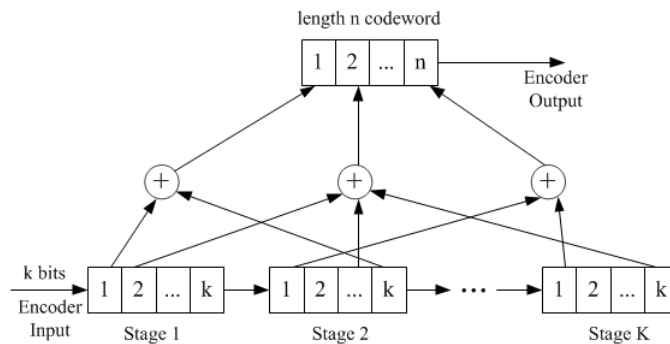


Figure 2.4. An example convolution encoder structure.

2.5.3 Turbo Coding and Iteration Decoding

Turbo codes are parallel concatenated convolutional codes which have demonstrated near-capacity performance through the use of simple constituent encoders and an iterative, soft-decoding algorithm. The true power of these codes is in their ability to create very powerful code structures while retaining the ability to perform soft-decoding without dramatically increased

complexity.

The Turbo Encoder

The turbo encoder can be constructed from two constituent encoders which are separated by an interleaver in Fig. 2.5. Through the interleaver, the second constituent encoder operates on a permuted version of the input frame. Puncturing of the parity streams from the constituent encoders may be done to achieve desired code rates. In generally, for large blocks, randomly generated interleavers have been shown to perform best [57]. However, for small blocks, other interleaver design is feasible and advantageous, i.e. the helical interleaver [58].

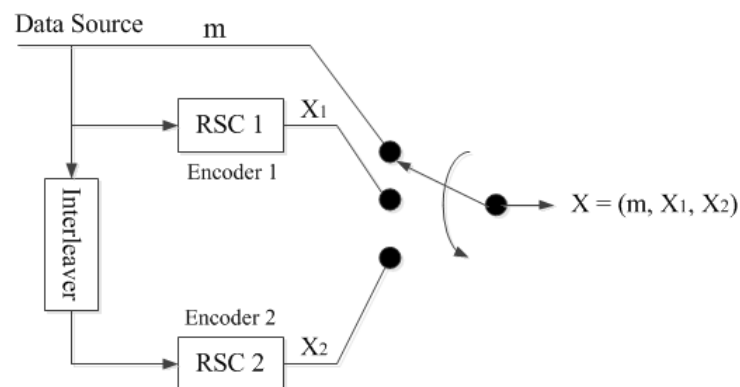


Figure 2.5. Parallel Turbo recursive systematic convolution (RSC) encoder structure.

Constituent Encoders

In general, any systematic block or trellis encoder maybe used in the constituent encoder of a turbo scheme [59]. However, due to the operation of the decoder, convolutional codes are most advantageous due to the existence of maximum a posteriori (MAP) soft decoding algorithms. While all block codes can be described with a trellis, the number of states in this trellis could be large. For convolutional codes, the trellis descriptions are known and the

number of states is fixed by the memory order of the encoder. Throughout the literature, recursive systematic convolutional (RSC) encoders have been primarily used in the turbo schemes. Moreover, the infinite impulse response (IIR) nature of these encoders allows for interleaver designs which obtain large global Hamming distances for the turbo code [60]. For example, consider the four-state RSC with generator (5,7) shown in Fig. 2.6. This encoder has a feedback polynomial and parity polynomial which are $g_b = 1 + D^2$ and $g_a = 1 + D + D^2$, where D represents time delay. And this encoder will also be used in Section 3.2.2 (B) in Chapter 3.

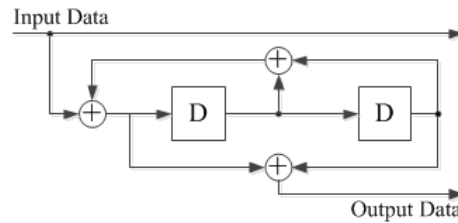


Figure 2.6. A 4-state, half rate RSC structure with generator polynomial (5,7).

The Turbo Decoders

Iterative (turbo) decoding exploits the component-code substructure of the turbo encoder by associating a component decoder with each of the component encoders [61]. More specifically, each decoder performs soft input/output decoding, as shown in Fig. 2.7 which is an example decoder of Fig. 2.5. Firstly, a soft decision in the form of a probability measure $P(m_1)$ on the transmitted information bits based on the received codeword (m, X_1) can be generated by Decoder 1. The probability measure is generated by either a MAP probability algorithm or a soft output Viterbi algorithm (SOVA). In Section 3.2.2 (B), the MAP scheme will be used for decoding. This reliability information is passed to Decoder 2, which generates its own probability measure $P(m_2)$ from its received codeword (m, X_2)

and the probability measure $P(m_1)$. This reliability information is input to Decoder 1, which revises its measure $P(m_1)$ based on this information and the original received codeword. Then the new reliability information is sent by Decoder 1 to Decoder 2, which revises its measure using this new information. Turbo decoding proceeds in an iterative manner, with the two component decoders alternately updating their probability measures. Ideally, the decoders eventually agree on probability measures that reduce to hard decisions $m = m_1 = m_2$.

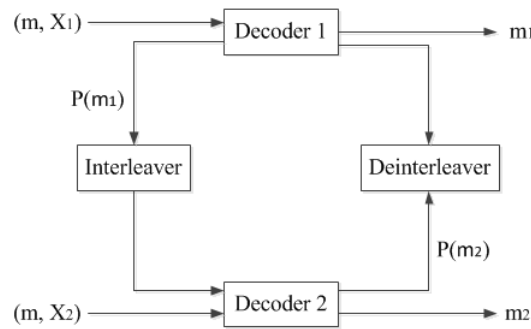


Figure 2.7. Turbo decoder structure.

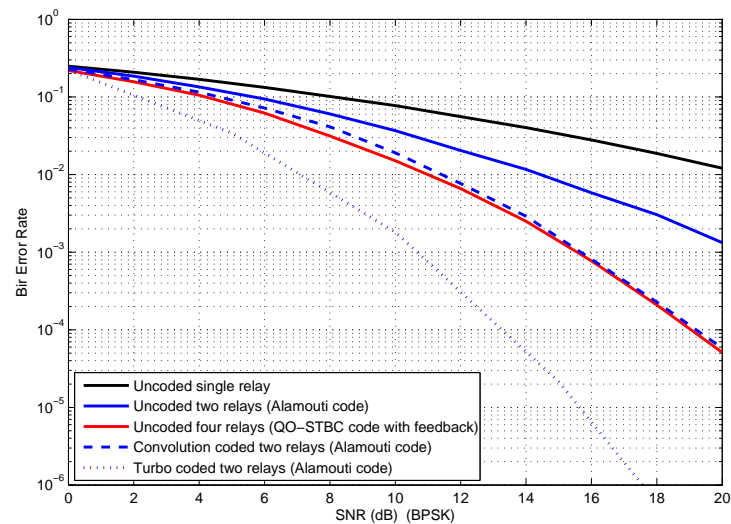


Figure 2.8. End-to-end BER comparison between coded and uncoded BPSK modulation cooperative networks with increasing cooperative diversity.

Finally, Fig. 2.8 and Fig. 2.9 present the end-to-end BER comparisons for cooperative networks with binary phase shift keying (BPSK) and quadrature phase shift keying (QPSK) modulation. Firstly, it can be seen that with increasing number of relays, the BER is decreased, i.e., in Fig. 2.8, when the SNR is 20dB, the BER of single relay, two relay and four relay networks are approximately 1.2×10^{-2} , 1.3×10^{-3} and 5×10^{-5} , respectively. Therefore, the end-to-end BER performance is an important parameter for cooperative networks, and Fig. 2.8 and Fig. 2.9 confirm the advantage of distributed transmission schemes which exploit cooperative diversity. Secondly, the additional outer coding scheme can also improve the BER performance. For example, in Fig. 2.9, when the SNR is 15 dB, the BER of Turbo coded transmission with two relays, convolution coded for two relay and uncoded for two relay networks are almost 2×10^{-5} , 1.3×10^{-3} and 9×10^{-3} , respectively. Therefore, in this thesis, BPSK and/or QPSK transmission with or without outer coding is used in BER evaluations.

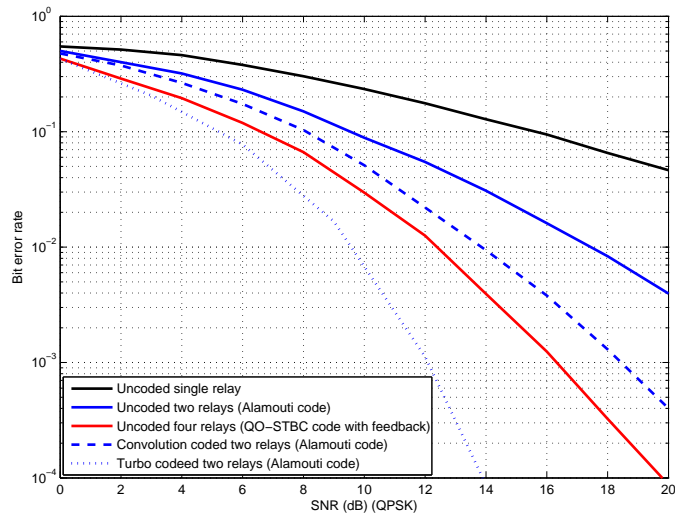


Figure 2.9. End-to-end BER comparison between coded and uncoded for QPSK modulation cooperative networks with increasing cooperative diversity.

2.6 Summary

This chapter presented an overview of the various methodologies in cooperative networks that are of interest in the thesis. A brief introduction to distributed space-time coding schemes with orthogonal and quasi-orthogonal codes was given. An important method for distributed space-time coding, which does not need channel state information (CSI) at the receiver for decoding, which is differential space-time code, was discussed. This was followed by the performance analysis of cooperative networks. One approach was the pairwise error probability analysis, and the other was outage probability analysis. Finally, methods to achieve coding gain in transmission were considered. A simulation study was included to confirm the performance advantage of distributed transmission with and without outer coding. In the next chapter, in order to improve transmission rate in distributed space-time coding techniques, full interference cancellation and full self-interference cancellation schemes for synchronous systems will be described.

FIC AND FSIC SCHEMES FOR SYNCHRONOUS SYSTEMS

In this chapter, the full interference cancellation (FIC) and full inter-relay self interference cancellation (FSIC) schemes for synchronous cooperative networks are presented to improve the end-to-end transmission rate and mitigate the interference between the relays. The chapter begins with the introduction of the other work in the literature which has addressed the transmission rate and interference between the relays issue in cooperative networks. This is followed by the description of FIC with offset transmission scheme for synchronous cooperative networks. Then the diversity analysis method is discussed for using the FSIC scheme in synchronous cooperative networks. Finally, simulation results to demonstrate the behaviours of the algorithms are presented.

3.1 Introduction

A cooperative network is one of the most popular approaches to exploit spatial diversity in wireless systems, in particular, through distributed space-time block coding [37], [45] and [46]. Relay nodes can not only provide

independent channels between the source and the destination, to leverage space diversity [3], but they also can help two users with no or weak direct connection to attain a robust link. Although these schemes achieve the maximal cooperative diversity, i.e. in [46], the full diversity is two with two relays; the full diversity is four with closed feedback in [45], its end-to-end transmission rate is only a half. Therefore, offset transmission is an efficient method to improve the end-to-end transmission rate from a half to asymptotically unity.

3.2 FIC with DSTC and DDSTC Schemes in Synchronous Systems

In this section, the use of DSTC and DDSTC within a two-hop cooperative wireless four relay network over block quasi-static Rayleigh fading channels is proposed, which can achieve full cooperative diversity and improve the transmission rate.

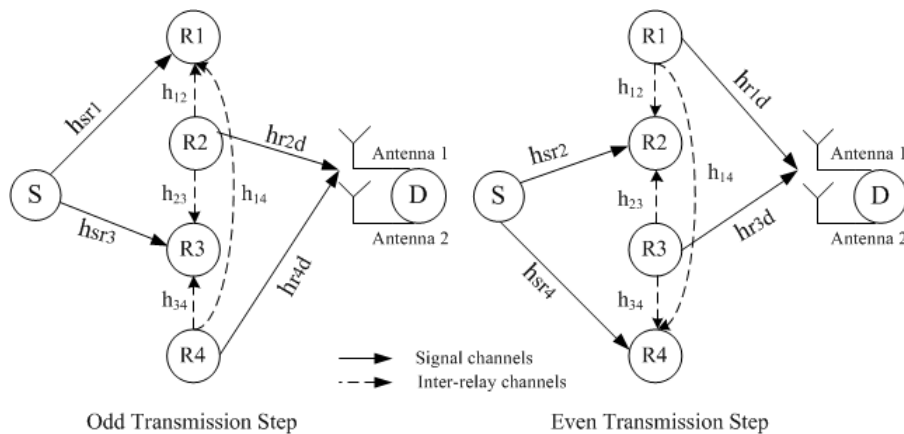


Figure 3.1. A cooperative four relay network model with offset transmission scheme.

In Fig. 3.1, the relay model for the offset transmission scheduling method is illustrated. The four relay nodes are arranged as two groups of two relay

nodes, both of which employ DSTC or DDSTC design, but with offset transmission scheduling, i.e., at the odd time slot, relay one and three receive the signal from the source, at the same time, relay two and four send the received signal which was received from the source at the previous time slot to the destination node. Therefore, the source can serially transmit data to the destination and the overall rate can be improved. However, the four-path relay scheme may suffer from inter-relay interference (IRI) which is caused by the simultaneous transmission of the source and another group of relays. An FIC approach is therefore used to remove the inter-relay interference at the destination node.

In Fig. 3.1, h_{sr_i} ($i = 1, \dots, 4$) denote the channels from the transmitter to the four relays and h_{r_id} ($i = 1, \dots, 4$) denote the channels from the four relays to the destination. There is no direct link between the source and the destination as path loss or shadowing is assumed to render it unusable. The inter-relay channels are assumed to be reciprocal, i.e. the gains from R1 and R3 to R2 and R4 are the same as those from R2 and R4 to R1 and R3, which are denoted h_{12} , h_{23} , h_{34} and h_{14} . The channels are assumed to be block quasi-static Rayleigh flat-fading: h_{sr_i} and h_{r_id} are independent and identically distributed (i.i.d.) zero-mean and unit-variance complex Gaussian random variables. The usual requirement for space-time block coding is that the channel is constant for at least M time instants (channel uses). And all of the channel information is assumed known by the receiver. The FIC with DSTC scheme is next introduced to achieve asymptotically full rate and to completely remove IRI.

3.2.1 FIC with DSTC

A) Interference Cancellation Scheme.

In this section, a full interference cancellation scheme is proposed to completely remove the inter-relay interference from the other relays. Similarly

to that in [62], it is assumed that the relay nodes R2 and R4 receive at time slot $n-1$, at the same time, the relay nodes R1 and R3 send their signals to the destination nodes. All of the channel information is assumed known by the receiver.

Therefore, the received signal vector at the destination at the time slot $n-1$ is obtained as:

$$\mathbf{y}_d(n-1) = \mathbf{t}_1(n-2)h_{r_1d}(n-1) + \mathbf{t}_3(n-2)h_{r_3d}(n-1) + \mathbf{w}_d(n-1), \quad (3.2.1)$$

where \mathbf{w}_d is the Gaussian noise vector at the destination, and $\mathbf{t}_1(n-2)$ and $\mathbf{t}_3(n-2)$ are formed from the received signal vectors at R1 and R3 at the time slot $n-2$, which are given by:

$$\mathbf{t}_1(n-2) = N\mathbf{A}_1\mathbf{r}_1(n-2) \quad \text{and} \quad \mathbf{t}_3(n-2) = N\mathbf{B}_2\mathbf{r}_3^*(n-2), \quad (3.2.2)$$

where N is $\sqrt{P_2/(P_1+1)}$. The receive vectors $\mathbf{r}_1(n-2)$ and $\mathbf{r}_3(n-2)$ are given by:

$$\begin{aligned} \mathbf{r}_1(n-2) &= \sqrt{P_1M}h_{sr_1}(n-2)\mathbf{s} + \mathbf{t}_2(n-3)h_{12} + \mathbf{t}_4(n-3)h_{14} + \mathbf{v}_1 \\ \mathbf{r}_3(n-2) &= \sqrt{P_1M}h_{sr_3}(n-2)\mathbf{s} + \mathbf{t}_2(n-3)h_{23} + \mathbf{t}_4(n-3)h_{34} + \mathbf{v}_3, \end{aligned} \quad (3.2.3)$$

where \mathbf{v}_i is the Gaussian noise vector at the relay nodes, and M is the time slot. The received signal vector at the destination at time slot $n-2$ can also be obtained as:

$$\mathbf{y}_d(n-2) = \mathbf{t}_2(n-3)h_{r_2d}(n-2) + \mathbf{t}_4(n-3)h_{r_4d}(n-2) + \mathbf{w}_d(n-2). \quad (3.2.4)$$

ASSUMPTION 1: If multiple antennas were available at the destination node, and given that the relays are sufficiently spatially separated, the assumption is made that it is possible to separate out the individual relay

components within $\mathbf{y}_d(n-2)$

$$\mathbf{y}_d(n-2) = \mathbf{y}_{d1}(n-2) + \mathbf{y}_{d2}(n-2) + \mathbf{w}_d(n-2),$$

which are given by

$$\mathbf{y}_{d1}(n-2) = \mathbf{t}_2(n-3)h_{r_2d}(n-2) \quad \text{and} \quad \mathbf{y}_{d2}(n-2) = \mathbf{t}_4(n-3)h_{r_4d}(n-2), \quad (3.2.5)$$

where the noise term is assumed to be insignificant in the current development however this issue and the validity of this assumption is addressed in simulation studies. Next

$$\mathbf{t}_2(n-3) = \frac{\mathbf{y}_{d1}(n-2)}{h_{r_2d}(n-2)} \quad \text{and} \quad \mathbf{t}_4(n-3) = \frac{\mathbf{y}_{d2}(n-2)}{h_{r_4d}(n-2)}, \quad (3.2.6)$$

and finally, substituting (3.2.2), (3.2.3) and (3.2.6) into (3.2.1) gives:

$$\begin{aligned} \mathbf{y}_d(n-1) &= N\sqrt{P_1M}\mathbf{A}_1h_{r_1d}(n-1)h_{sr_1}(n-2)\mathbf{s} + N\mathbf{A}_1h_{r_1d}(n-1) \\ &\quad \left(\frac{\mathbf{y}_{d1}(n-2)}{h_{r_2d}(n-2)}h_{12} + \frac{\mathbf{y}_{d2}(n-2)}{h_{r_4d}(n-2)}h_{14} \right) \\ &\quad + N\sqrt{P_1M}\mathbf{B}_2h_{r_3d}(n-1)h_{sr_3}^*(n-2)\mathbf{s}^* + N\mathbf{B}_2h_{r_3d}(n-1) \\ &\quad \left(\frac{\mathbf{y}_{d1}(n-2)}{h_{r_2d}(n-2)}h_{23} + \frac{\mathbf{y}_{d2}(n-2)}{h_{r_4d}(n-2)}h_{34} \right)^* + \mathbf{w}'_d(n-1), \end{aligned} \quad (3.2.7)$$

where $\mathbf{w}'_d(n-1)$ is the noise vector which is given by:

$$\mathbf{w}'_d(n-1) = NA_1\mathbf{v}_1h_{r_1d}(n-1) + NB_2\mathbf{v}_3^*h_{r_3d}(n-1) + \mathbf{w}_d(n-2). \quad (3.2.8)$$

From (3.2.7), the inter-relay interference is found as a recursive term in the received signal at the destination nodes. For example, (3.2.9) and (3.2.10)

are IRI terms

$$N\mathbf{A}_1 h_{r_1d}(n-1) \left(\frac{\mathbf{y}_{d1}(n-2)}{h_{r_2d}(n-2)} h_{12} + \frac{\mathbf{y}_{d2}(n-2)}{h_{r_4d}(n-2)} h_{14} \right), \quad (3.2.9)$$

$$N\mathbf{B}_2 h_{r_3d}(n-1) \left(\frac{\mathbf{y}_{d1}(n-2)}{h_{r_2d}(n-2)} h_{23} + \frac{\mathbf{y}_{d2}(n-2)}{h_{r_4d}(n-2)} h_{34} \right)^*, \quad (3.2.10)$$

which are functions only of the previous vector output values $\mathbf{y}_{d1}(n-2)$ and $\mathbf{y}_{d2}(n-2)$. Therefore, these terms can be completely removed from (3.2.7) in order to cancel the inter-relay interference at the receiver, which is given by:

$$\begin{aligned} \mathbf{y}'_d(n-1) &= N\sqrt{P_1 M} \mathbf{A}_1 h_{r_1d}(n-1) h_{sr_1}(n-2) \mathbf{s} + N\sqrt{P_1 M} \mathbf{B}_2 \\ &h_{r_3d}(n-1) h_{sr_3}^*(n-2) \mathbf{s}^* + \mathbf{w}'_d(n-1). \end{aligned} \quad (3.2.11)$$

As such, (3.2.11) has no inter-relay interference, only the desired signal and the noise. However, a very useful relationship for the received signal at the destination at the different odd-even time slots can be found. And then the same method is used to obtain the received signal vector at time slot n at the destination node and cancel completely the IRI,

$$\begin{aligned} \mathbf{y}_d(n) &= N\sqrt{P_1 M} \mathbf{A}_1 h_{r_2d}(n) h_{sr_2}(n-1) \mathbf{s} + N\mathbf{A}_1 h_{r_2d}(n) \\ &\left(\frac{\mathbf{y}_{d1}(n-1)}{h_{r_1d}(n-1)} h_{12} + \frac{\mathbf{y}_{d2}(n-1)}{h_{r_3d}(n-1)} h_{23} \right) \\ &+ N\sqrt{P_1 M} \mathbf{B}_2 h_{r_4d}(n) h_{sr_4}^*(n-2) \mathbf{s}^* + N\mathbf{B}_2 h_{r_4d}(n) \\ &\left(\frac{\mathbf{y}_{d1}(n-1)}{h_{r_1d}(n-1)} h_{14} + \frac{\mathbf{y}_{d2}(n-1)}{h_{r_3d}(n-1)} h_{34} \right)^* + \mathbf{w}'_d(n), \end{aligned} \quad (3.2.12)$$

where $\mathbf{w}'_d(n)$ is the noise term which is given by:

$$\mathbf{w}'_d(n) = N\mathbf{A}_1 \mathbf{v}_2 h_{r_2d}(n) + N\mathbf{B}_2 \mathbf{v}_4^* h_{r_4d}(n) + \mathbf{w}_d(n-1). \quad (3.2.13)$$

From (3.2.12), the IRI can be found as a recursive term in the received signal

at the destination node. For example, (3.2.14) and (3.2.15) are IRI terms.

$$N\mathbf{A}_1 h_{r_2d}(n) \left(\frac{\mathbf{y}_{d1}(n-1)}{h_{r_1d}(n-1)} h_{12} + \frac{\mathbf{y}_{d2}(n-1)}{h_{r_3d}(n-1)} h_{23} \right), \quad (3.2.14)$$

$$N\mathbf{B}_2 h_{r_4d}(n) \left(\frac{\mathbf{y}_{d1}(n-1)}{h_{r_1d}(n-1)} h_{14} + \frac{\mathbf{y}_{d2}(n-1)}{h_{r_3d}(n-1)} h_{34} \right)^*. \quad (3.2.15)$$

Therefore, these terms can be completely removed from (3.2.12) by using the same method, which is given by:

$$\begin{aligned} \mathbf{y}'_d(n) = & N\sqrt{P_1 M} \mathbf{A}_1 h_{r_2d}(n) h_{sr_2}(n-1) \mathbf{s} + N\sqrt{P_1 M} \mathbf{B}_2 h_{r_4d}(n) \\ & h_{sr_4}^*(n-1) \mathbf{s}^* + \mathbf{w}'_d(n). \end{aligned} \quad (3.2.16)$$

Compared with (3.2.7) and (3.2.12), the similarity in structure is evident. Therefore, the transmission symbols can be easily detected by the ML decoding. The FIC scheme has the following advantages: firstly, the FIC can completely remove the inter-relay interference. Secondly, the FIC only depends on the previous received signal without error propagation. Finally, only two buffers are required to store the previous received signal vectors, i.e. $\mathbf{y}_{d1}(n-1)$ and $\mathbf{y}_{d2}(n-1)$, in the FIC approach.

B) Simulation studies.

The simulated performance of the orthogonal DSTCs with the FIC approach is now shown. The performance is exhibited by the end-to-end BERs using QPSK symbols. The total power per symbol transmission is fixed as P.

In Fig. 3.2, firstly, the BER performances without full inter-relay interference cancellation and with full inter-relay interference cancellation are shown. These are plotted against total transmit power since signal-to-noise ratio varies in the network, however, for reference the signal-to-interference plus noise in (3.2.7) has the form $\frac{\sqrt{P_1 M} v_f^2 v_g^2}{2N v_g^2 v_h^2 (\sqrt{P_1 M} v_f^2 + \sigma^2) + \sigma^2 v_g^2 + \frac{\sigma^2}{2N}}$, where $E(|h_{12}|^2) = E(|h_{14}|^2) = E(|h_{23}|^2) = E(|h_{34}|^2) = v_h^2$, $E(|h_{sr_i}|^2) = v_f^2$, $E(|h_{r_i d}|^2) = v_g^2$

($i = 1, \dots, 4$), $E(\cdot)$ denotes the statistical expectation operator, and all of the noise variance terms are σ^2 , which takes the values -13.5 dB to -3.85 dB over the range of transmit power in Fig. 3.2. The advantage of using the FIC scheme is clear, the BER performance is significantly better than without the FIC approach. In fact, without using FIC the scheme is unusable. The inter-relay interference considerably corrupts the transmission signal, thereby leading to the performance degradation. Secondly, the performance of distributed Alamouti DSTCs with a two relay network is compared, without inter-relay interference, and that of the FIC Alamouti DSTCs with a four relay network (Assumption 1). For the two hop cooperative four relay network, if the FIC scheme is used to completely remove the inter-relay interference, the performance closely matches Alamouti DSTCs. However, for the Alamouti DSTCs with two relay networks, every transmission time slot is divided into two sub-slots: firstly, the source transmits to the relay nodes; secondly, the relay node sends the data to the destination. Therefore, the rate and bandwidth efficiency of this scheme is a half of the direct transmission. On the contrary, the later proposed method uses the two group relay nodes in order to retain the successive transmission signal from the source node, so the full unity data rate can be approached when the number of symbols is large.

In the next simulation study in Fig. 3.3, the effect of relaxing Assumption 1 is considered. To model the effect that even with multiple antennas at the destination node there will be uncertainties in the values of $\mathbf{y}_{d1}(n-2)$ and $\mathbf{y}_{d2}(n-2)$ in (3.2.5), due for example to estimation errors in beamforming, the noise vectors are added to yield $\mathbf{y}_{d1}(n-2) = \mathbf{t}_2(n-3)h_{r_2d}(n-2) + \mathbf{n}_1$ and $\mathbf{y}_{d2}(n-2) = \mathbf{t}_4(n-3)h_{r_4d}(n-2) + \mathbf{n}_2$, where all the elements of the \mathbf{n}_1 and \mathbf{n}_2 vectors are chosen to have relative noise powers of either -9 or -12 dB, and these two cases are denoted as Assumption 2 and Assumption 3. The degradation in BER is shown in Fig. 3.3, for

example, at $\text{BER} = 10^{-3}$ the required transmit power increases from 26.5 to 28, and to 32.5 dB for the three cases.

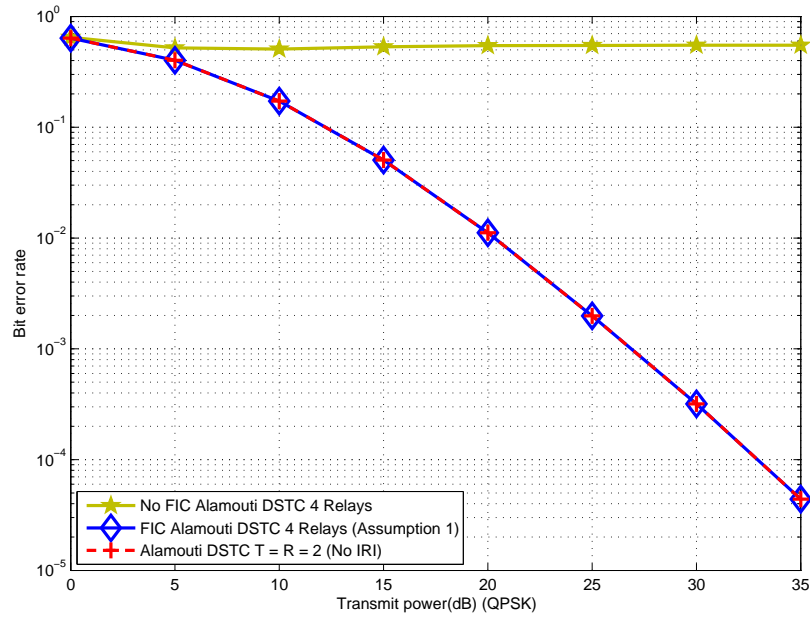


Figure 3.2. End-to-end BER performance.

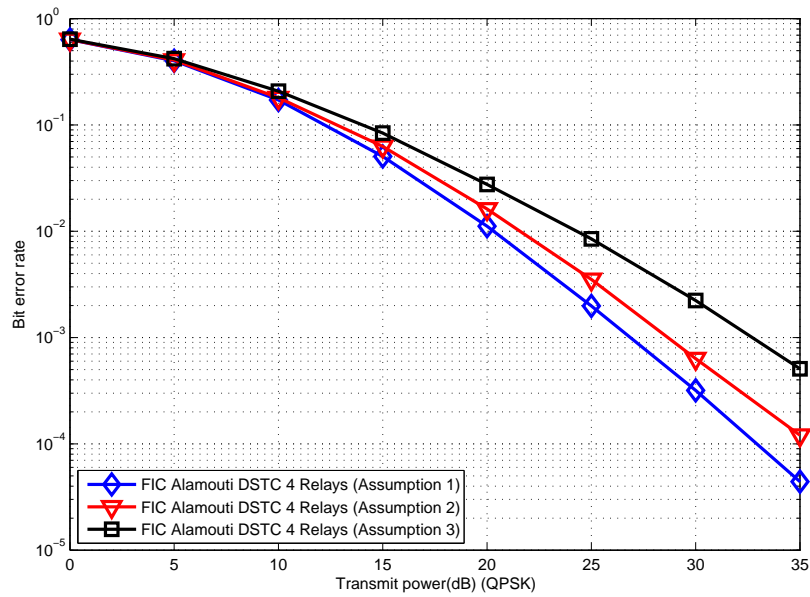


Figure 3.3. End-to-end BER performance of the DSTC with FIC and varying uncertainty Assumption 1.

3.2.2 FIC with DDSTC

In the last subsection, using the DSTC scheme does require full channel information at the destination node, both the channels from the transmitter to relays and the channels from relays to the destination. Therefore, the source and relay nodes have to exchange training symbols. However, in some situations, regular training is not possible, because of the cost on time and power and the complexity of the channel estimation. Therefore, the differential transmission scheme for wireless relay networks with no channel information at either relays or the destination was proposed in [49]. In order to use the FIC scheme, the previous assumption of no channel knowledge at the destination must be relaxed and the relay to destination channels are assumed to be known which are easier to estimate than the other channel values. Moreover, the destination node needs to know the inter-relay channels between the relay nodes.

A) Interference Cancellation Scheme

Building on the approach followed in [62], it is assumed that the relay nodes R2 and R4 receive at time slots $n-1$ and $n-3$, and at the same times, the relay nodes R1 and R3 are transmitting to the destination nodes. It is assumed that the channel g_i information is known by the receiver. Considering the received signal at the destination at time slot $n-3$:

$$\mathbf{y}_d(n-3) = \mathbf{t}_1(n-4)h_{r_1d} + \mathbf{t}_3(n-4)h_{r_3d} + \mathbf{w}_d(n-3), \quad (3.2.17)$$

where \mathbf{w}_d is the Gaussian noise vector at the destination, and $\mathbf{t}_1(n-4)$ and $\mathbf{t}_3(n-4)$ are formed from the received signal vectors at R1 and R3 at time slot $n-4$, which are given by:

$$\mathbf{t}_1(n-4) = N\mathbf{A}_1\mathbf{r}_1(n-4) \quad \text{and} \quad \mathbf{t}_3(n-4) = N\mathbf{B}_2\mathbf{r}_3^*(n-4), \quad (3.2.18)$$

where $N = \sqrt{P_2/(P_1 + 1)}$. The received signal vectors $\mathbf{r}_1(n-4)$ and $\mathbf{r}_3(n-4)$ are given by:

$$\begin{aligned}\mathbf{r}_1(n-4) &= \sqrt{P_1 M} h_{sr_1} \mathbf{U}(n-4) \mathbf{ss}(n-6) + \mathbf{t}_2(n-5) h_{12} + \mathbf{t}_4(n-5) h_{14} \\ &\quad + \mathbf{v}_1(n-4), \\ \mathbf{r}_3(n-4) &= \sqrt{P_1 M} h_{sr_3} \mathbf{U}(n-4) \mathbf{ss}(n-6) + \mathbf{t}_2(n-5) h_{23} + \mathbf{t}_4(n-5) h_{34} \\ &\quad + \mathbf{v}_3(n-4),\end{aligned}\tag{3.2.19}$$

where $\mathbf{U}(n-4)$ can be obtained by (2.3.2) and M is time slot, \mathbf{v}_1 and \mathbf{v}_3 are the Gaussian noise vectors at the relay nodes. The received signal vector can also be obtained at the destination at time slot $n-4$ as:

$$\mathbf{y}_d(n-4) = \mathbf{t}_2(n-5) h_{r_2d} + \mathbf{t}_4(n-5) h_{r_4d} + \mathbf{w}_d(n-4).\tag{3.2.20}$$

ASSUMPTION 1: If multiple antennas were available at the destination node, and given that the relays are sufficiently spatially separated, the assumption that it is possible to separate out the individual relay components within $\mathbf{y}_d(n-4)$ is made

$$\mathbf{y}_d(n-4) = \mathbf{y}_{d1}(n-4) + \mathbf{y}_{d2}(n-4) + \mathbf{w}_d(n-4),$$

as given by

$$\mathbf{y}_{d1}(n-4) = \mathbf{t}_2(n-5) h_{r_2d} \quad \text{and} \quad \mathbf{y}_{d2}(n-4) = \mathbf{t}_4(n-5) h_{r_4d},\tag{3.2.21}$$

where the noise term is assumed to be insignificant in the current development however this issue and the validity of this assumption is addressed

further in the simulation studies. So

$$\mathbf{t}_2(n-5) = \frac{\mathbf{y}_{d1}(n-4)}{h_{r_2d}} \quad \text{and} \quad \mathbf{t}_4(n-5) = \frac{\mathbf{y}_{d2}(n-4)}{h_{r_4d}}. \quad (3.2.22)$$

Finally, substituting (3.2.18), (3.2.19) and (3.2.22) into (3.2.17) gives:

$$\begin{aligned} \mathbf{y}_d(n-3) = & N\sqrt{P_1M}\mathbf{A}_1h_{r_1d}h_{sr_1}\mathbf{U}(n-4)\mathbf{ss}(n-6) + \\ & N\mathbf{A}_1h_{r_1d}\left(\frac{\mathbf{y}_{d1}(n-4)}{h_{r_2d}}h_{12} + \frac{\mathbf{y}_{d2}(n-4)}{h_{r_4d}}h_{14}\right) \\ & + N\sqrt{P_1M}\mathbf{B}_2h_{r_3d}h_{sr_3}^*\mathbf{U}^*(n-4)\mathbf{ss}^*(n-6) + \\ & N\mathbf{B}_2h_{r_3d}\left(\frac{\mathbf{y}_{d1}(n-4)}{h_{r_2d}}h_{23} + \frac{\mathbf{y}_{d2}(n-4)}{h_{r_4d}}h_{34}\right)^* + \mathbf{w}'_d(n-3), \end{aligned} \quad (3.2.23)$$

where $\mathbf{w}'_d(n-3)$ is the noise vector which is given by:

$$\mathbf{w}'_d(n-3) = N\mathbf{A}_1\mathbf{v}_1h_{r_1d} + N\mathbf{B}_2\mathbf{v}_3^*h_{r_3d} + \mathbf{w}_d(n-4). \quad (3.2.24)$$

From (3.2.23), the inter-relay interference is found as a recursive term in the received signal vector at the destination nodes. For example, the IRI terms are

$$N\mathbf{A}_1h_{r_1d}\left(\frac{\mathbf{y}_{d1}(n-4)}{h_{r_2d}}h_{12} + \frac{\mathbf{y}_{d2}(n-4)}{h_{r_4d}}h_{14}\right), \quad (3.2.25)$$

$$N\mathbf{B}_2h_{r_3d}\left(\frac{\mathbf{y}_{d1}(n-4)}{h_{r_2d}}h_{23} + \frac{\mathbf{y}_{d2}(n-4)}{h_{r_4d}}h_{34}\right)^*, \quad (3.2.26)$$

which are functions only of the previous output values $\mathbf{y}_{d1}(n-4)$ and $\mathbf{y}_{d2}(n-4)$. Therefore, these terms can be completely removed from (3.2.23) in order to cancel the inter-relay interference at the receiver, which is given by:

$$\begin{aligned} \mathbf{y}'_d(n-3) = & N\sqrt{P_1M}\mathbf{A}_1h_{r_1d}h_{sr_1}\mathbf{U}(n-4)\mathbf{ss}(n-6) + N\sqrt{P_1M}\mathbf{B}_2h_{r_3d} \\ & h_{sr_3}^*\mathbf{U}^*(n-4)\mathbf{ss}^*(n-6)\mathbf{w}'_d(n-3). \end{aligned} \quad (3.2.27)$$

As such, (3.2.27) has no inter-relay interference, and contains only the desired signal and the noise, and $\mathbf{ss} = \mathbf{U}(n)\mathbf{ss}(n-2)$ and $\mathbf{ss}(n-4) = \mathbf{U}(n-4)\mathbf{ss}(n-6)$, which is a reference signal for the next time slot. Next using the same method to obtain the received signal vector at time slot $n-2$ at the destination node and canceling completely the IRI,

$$\begin{aligned} \mathbf{y}_d(n-2) = & N\sqrt{P_1M}\mathbf{A}_1h_{r_2d}h_{sr_2}\mathbf{U}(n-3)\mathbf{ss}(n-5) + \\ & N\mathbf{A}_1h_{r_2d}\left(\frac{\mathbf{y}_{d1}(n-3)}{h_{r_1d}}h_{12} + \frac{\mathbf{y}_{d2}(n-3)}{h_{r_3d}}h_{23}\right) \\ & + N\sqrt{P_1M}\mathbf{B}_2h_{r_4d}h_{sr_4}^*\mathbf{U}^*(n-3)\mathbf{ss}^*(n-5) + \\ & N\mathbf{B}_2h_{r_4d}\left(\frac{\mathbf{y}_{d1}(n-3)}{h_{r_1d}}h_{14} + \frac{\mathbf{y}_{d2}(n-3)}{h_{r_3d}}h_{34}\right)^* + \mathbf{w}'_d(n-2), \end{aligned} \quad (3.2.28)$$

where $\mathbf{w}'_d(n-2)$ is the noise vector which is given by:

$$\mathbf{w}'_d(n-2) = N\mathbf{A}_1\mathbf{v}_2h_{r_2d} + N\mathbf{B}_2\mathbf{v}_4^*h_{r_4d} + \mathbf{w}_d(n-3). \quad (3.2.29)$$

The second and fourth terms in the right hand side of (3.2.28) are IRI terms which can be removed as in (3.2.25) and (3.2.26). Therefore, (3.2.28) becomes

$$\begin{aligned} \mathbf{y}'_d(n-2) = & N\sqrt{P_1M}\mathbf{A}_1h_{r_2d}h_{sr_2}\mathbf{U}(n-3)\mathbf{ss}(n-5) + N\sqrt{P_1M}\mathbf{B}_2h_{r_4d} \\ & h_{sr_4}^*\mathbf{U}^*(n-3)\mathbf{ss}^*(n-5) + \mathbf{w}'_d(n-2), \end{aligned} \quad (3.2.30)$$

and defining $\mathbf{ss}(n-3) = \mathbf{U}(n-3)\mathbf{ss}(n-5)$, which is a reference signal for the next time slot. Compared with (3.2.27) and (3.2.30), the same structure is evident. However, according to the offset time slots, the alternate channels are switched regularly. And then the same method is used to obtain the received signal at time slots $n-1$ and n at the destination node and cancel

completely the IRI.

$$\begin{aligned} \mathbf{y}'_d(n-1) = & N\sqrt{P_1 M} \mathbf{A}_1 h_{r_1 d} h_{sr_1} \mathbf{U}(n-2) \mathbf{ss}(n-4) + N\sqrt{P_1 M} \mathbf{B}_2 h_{r_3 d} \\ & h_{sr_3}^* \mathbf{U}^*(n-2) \mathbf{ss}^*(n-4) + \mathbf{w}'_d(n-1), \end{aligned} \quad (3.2.31)$$

$$\begin{aligned} \mathbf{y}'_d(n) = & N\sqrt{P_1 M} \mathbf{A}_1 h_{r_2 d} h_{sr_2} \mathbf{U}(n-1) \mathbf{ss}(n-3) + N\sqrt{P_1 M} \mathbf{B}_2 h_{r_4 d} \\ & h_{sr_4}^* \mathbf{U}^*(n-1) \mathbf{ss}^*(n-3) + \mathbf{w}'_d(n). \end{aligned} \quad (3.2.32)$$

Therefore, the transmission symbols can be easily detected by the ML decoding, i.e.

$$\arg \max_{\mathbf{U}(n)} \left\| \mathbf{y}'_d(n) - \mathbf{U}(n) \mathbf{y}'_d(n-2) \right\|$$

and

$$\arg \max_{\mathbf{U}(n-1)} \left\| \mathbf{y}'_d(n-1) - \mathbf{U}(n-1) \mathbf{y}'_d(n-3) \right\|.$$

B) Simulation studies.

In this section, the simulated performance of the distributed differential space-time coding with the FIC approach is shown and compared with the performance of coherent distributed space-time coding. The performance is assessed by the BERs using BPSK symbols. The total power per symbol transmission is fixed as P . The reference signals $\mathbf{s}(1)$ and $\mathbf{s}(2)$ are chosen as $[1 \ 0]^T$. And the length of the block over which the channels are assumed constant N is 8.

In Fig. 3.4, firstly, the BER performance is shown without full inter-relay interference cancellation and with full inter-relay interference cancellation. The advantage of using the FIC scheme is clear, the BER performance is significantly better than without the FIC approach. In fact, without using FIC the scheme is unusable. The inter-relay interference considerably corrupts the transmission signal, thereby leading to the performance degradation.

Secondly, the performance of differential Alamouti DSTCs with a two relay network, without inter-relay interference, and that of the FIC differential Alamouti DSTCs with a four relay network (Assumption 1) is compared. For the two hop cooperative four relay network, if the FIC scheme is used to completely remove the inter-relay interference, the performance closely matches Alamouti DSTCs, whilst essentially doubling the transmission rate. Finally, compared with the performance of coherent distributed space-time coding with FIC, the differential scheme has the expected 3 dB loss in coding [63].

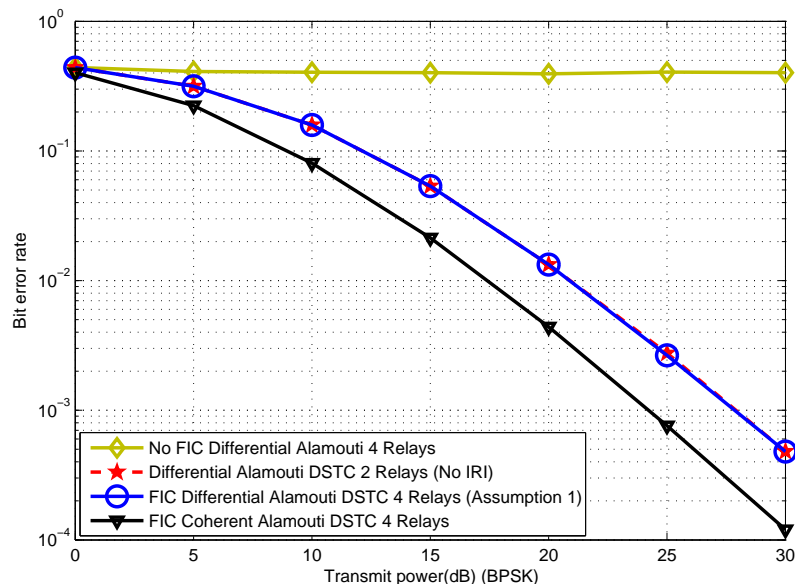


Figure 3.4. End-to-end BER performance.

In the next simulation study, the effect of relaxing Assumption 1 is considered. To model the effect that even with multiple antennas at the destination node there will be uncertainties in the values of $\mathbf{y}_{d1}(n-4)$ and $\mathbf{y}_{d2}(n-4)$ in (3.2.21), due for example to estimation errors in beamforming, the noise vectors are added to yield $\mathbf{y}_{d1}(n-4) = \mathbf{t}_2(n-5)h_{r_2d} + \mathbf{n}_1$ and $\mathbf{y}_{d2}(n-4) = \mathbf{t}_4(n-5)h_{r_4d} + \mathbf{n}_2$, where all the elements of the \mathbf{n}_1 and \mathbf{n}_2 vectors are chosen to have noise powers of either -9 or -12 dB, and these two cases are denoted

Assumption 2 and Assumption 3. The degradation in BER is shown in Fig. 3.5, for example, at $\text{BER} = 10^{-3}$ the required transmit power increases from 27.5 to 33, and to 38 dB for the three cases. Through the use of Turbo Coding, with generating polynomials $g(D) = [1, 1 + D^2 / 1 + D + D^2]$ and four iterations, these powers can be reduced to 19, 21.5 and 22.5 dB. As such, additional outer coding is one method to mitigate the practical difficulties in achieving Assumption 1.

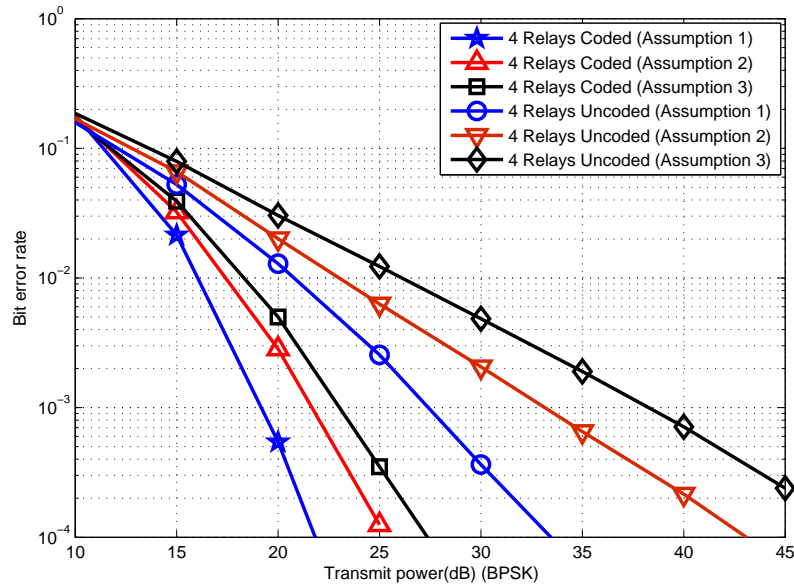


Figure 3.5. End-to-end coded and uncoded BER performance of the differential STBC with FIC and varying uncertainty in Assumption 1.

In Fig. 3.6, the data rate performance of the two relay differential scheme and that of the four relay differential scheme is compared. When the useful block size M is unity, the data rates of two and four relay schemes are the same which is 0.25. When the useful block size M is 10, the two relay scheme data rate is 0.46 whereas the four relay scheme data rate is 0.77. Obviously, when the useful block size M is large, the data rate of the four relay scheme is almost equal to unity, which is twice that of the two relay scheme, which is almost equal to 0.5.

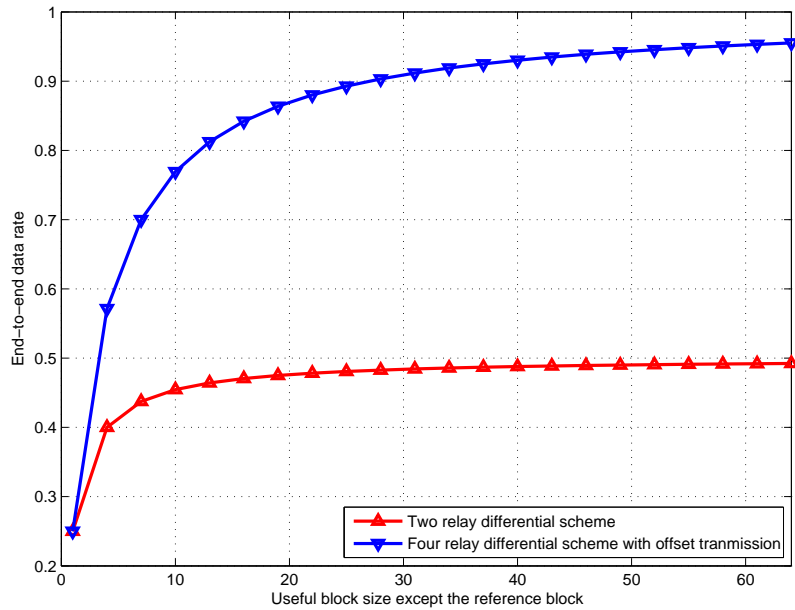


Figure 3.6. The end-to-end data rate performance.

3.3 FSIC with DSTC Schemes in Synchronous Systems

Jing and Hassibi in [44] proposed a new cooperative strategy, distributed space-time coding, which has two steps. However, this model lacks a direct link between the source node and the destination node. In [64] a direct link is considered, but the end-to-end transmission rate is only a half. In order to improve the transmission rate, an offset transmission scheme and full inter-relay interference cancellation has been applied in [65]. However, the interference cancellation is performed at the destination node, and so multiple antennas have to be used which maybe infeasible to achieve in practice. This problem is solved in [66] by using full inter-relay self interference cancellation at the relay nodes. However, in [66], the diversity order is only two without using an additional precoder scheme. In this work, therefore, an FSIC scheme at the relay nodes so that the IRI terms can be removed totally and diversity order 3.5 can be achieved without a precoder together

with asymptotically full rate.

3.3.1 System Model

The relay model for the four-path relay scheme is illustrated in Fig. 3.7, where $h_{sr_i} \sim CN(0, \gamma_{sr_i}^2)$ ($i = 1, \dots, 4$) denote the channels from the transmitter to the four relays and $h_{r_i d} \sim CN(0, \gamma_{r_i d}^2)$ ($i = 1, \dots, 4$) denote the channels from the four relays to the destination. It is assumed that only the inter-relay channels $h_{r_1} \sim CN(0, \gamma_{r_1}^2)$ and $h_{r_2} \sim CN(0, \gamma_{r_2}^2)$ are considered between R1 and R2 and between R3 and R4, respectively. This can be achieved in practice by constraining the locality of the relay pairs. And the inter-relay channels are assumed reciprocal. There is a direct link $h_{sd} \sim CN(0, \gamma_{sd}^2)$ between the source and the destination. The channels are quasi-static flat-fading: hence h_{sr_i} , $h_{r_i d}$ and h_{sd} are i.i.d zero-mean and unit-variance complex Gaussian random variables. The destination node is assumed to know perfectly all the channel coefficients. The relaying protocol is next defined.

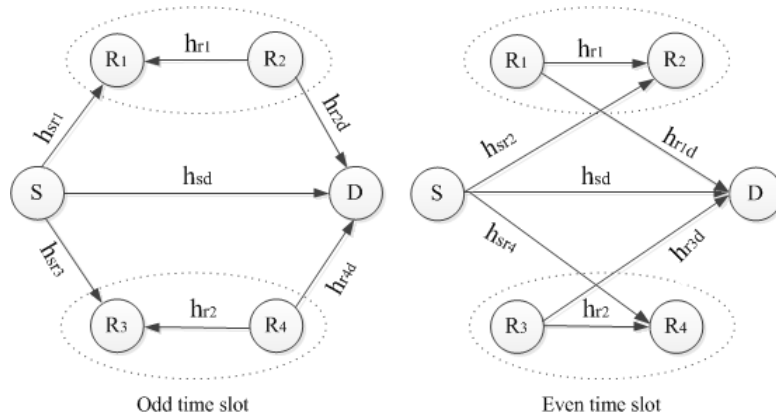


Figure 3.7. AF four-path relaying scheme.

3.3.2 Four-Path Relaying with Inter-Relay Interference Cancellation at the Relay

A) Transmission Protocol

At the source node, the source transmission is divided into frames, each containing L data vectors of the form

$$\mathbf{x}(l) = \begin{bmatrix} x_{1,R}(l) + jx_{1,I}(l) \\ x_{2,R}(l) + jx_{2,I}(l) \end{bmatrix} \text{ where } l = 1, 2, \dots, L.$$

At the time slot 1, $\mathbf{x}(1)$ is sent from S to R1, R3 and D so that

$$\begin{aligned} \mathbf{y}_{r1}(1) &= \sqrt{\rho}\mathbf{x}(1)h_{sr_1} + \mathbf{n}_{r1}(1) \\ \mathbf{y}_{r3}(1) &= \sqrt{\rho}\mathbf{x}(1)h_{sr_3} + \mathbf{n}_{r3}(1) \\ \mathbf{y}_d(1) &= \sqrt{\rho}\mathbf{x}(1)h_{sd} + \mathbf{n}_d(1), \end{aligned}$$

where $\mathbf{n}_{rj}(1) \sim CN(\mathbf{0}, \sigma^2 I)$ and $\mathbf{n}_d(1) \sim CN(\mathbf{0}, \sigma^2 I)$ are the additive white Gaussian noise (AWGN) vectors at the i^{th} relay and D respectively for the 1^{st} time slot, and these noise terms take the same form for the later time slots. Notice that $\mathbf{y}_d(1)$ contains only $\mathbf{x}(1)$ because R2 and R4 do not send in the first time slot.

Then for time slot 2, $\mathbf{x}(2)$ is transmitted from S to D, R2 and R4; at the same time, the transmitted signal at R1 is sent to R2, the transmitted signal at R3 is sent to R4, which are respectively the inter-relay interferences.

$$\begin{aligned} \mathbf{y}_{r2}(2) &= \sqrt{\rho}\mathbf{x}(2)h_{sr_2} + h_{r1} \mathbf{x}_{r1}(2) + \mathbf{n}_{r2}(2) \\ \mathbf{y}_{r4}(2) &= \sqrt{\rho}\mathbf{x}(2)h_{sr_4} + h_{r2} \mathbf{x}_{r3}(2) + \mathbf{n}_{r4}(2) \\ \mathbf{y}_d(2) &= \sqrt{\rho}\mathbf{x}(2)h_{sd} + h_{r1d} \mathbf{x}_{r1}(2) + h_{r3d} \mathbf{x}_{r3}(2) + \mathbf{n}_d(2), \end{aligned}$$

where $\mathbf{x}_{r1}(2) = \mathbf{A}g_{r1}(2)\mathbf{y}_{r1}(1)$ and $\mathbf{x}_{r3}(2) = \mathbf{B}g_{r3}(2)\mathbf{y}_{r3}^*(1)$. And matrices \mathbf{A}

and \mathbf{B} are used to encode the signals at the relay nodes, which are

$$\mathbf{A} = \begin{bmatrix} 1 & 0 \\ 0 & 1 \end{bmatrix} \quad \mathbf{B} = \begin{bmatrix} 0 & -1 \\ 1 & 0 \end{bmatrix}$$

and $g_{ri}(l)$ is the power scaling factor at the i^{th} relay, which will be defined later.

At time slot 3, $\mathbf{x}(3)$ is sent from S to D, R1 and R3, while $\mathbf{x}_{r2}(3)$ and $\mathbf{x}_{r4}(3)$ are sent from R2 to R1 and from R4 to R3, respectively, so that

$$\begin{aligned} \mathbf{y}_{r1}(3) &= \sqrt{\rho}\mathbf{x}(3)h_{sr1} + h_{r1}\mathbf{x}_{r2}(3) + \mathbf{n}_{r1}(3) = \sqrt{\rho}\mathbf{x}(3)h_{sr1} + \mathbf{A}h_{r1}g_{r2}(3) \\ &\quad [\sqrt{\rho}\mathbf{x}(2)h_{sr2} + h_{r1}\mathbf{x}_{r1}(2) + \mathbf{n}_{r2}(2)] + \mathbf{n}_{r1}(3), \end{aligned}$$

$$\begin{aligned} \mathbf{y}_{r3}(3) &= \sqrt{\rho}\mathbf{x}(3)h_{sr3} + h_{r2}\mathbf{x}_{r4}(3) + \mathbf{n}_{r3}(3) = \sqrt{\rho}\mathbf{x}(3)h_{sr3} + \mathbf{B}h_{r2}g_{r4}(3) \\ &\quad [\sqrt{\rho}\mathbf{x}(2)h_{sr4} + h_{r2}\mathbf{x}_{r3}(2) + \mathbf{n}_{r4}(2)]^* + \mathbf{n}_{r3}(3) \end{aligned}$$

$$\mathbf{y}_d(3) = \sqrt{\rho}\mathbf{x}(3)h_{sd} + h_{r2d}\mathbf{x}_{r2}(3) + h_{r4d}\mathbf{x}_{r4}(3) + \mathbf{n}_d(3),$$

where $\mathbf{x}_{r2}(3) = \mathbf{A}g_{r2}(3)\mathbf{y}_{r2}(2)$ and $\mathbf{x}_{r4}(3) = \mathbf{B}g_{r4}(3)\mathbf{y}_{r4}^*(2)$. Notice that $\mathbf{y}_{r1}(3)$ and $\mathbf{y}_{r3}(3)$ contain the inter-relay self interference terms, $\mathbf{A}h_{r1}g_{r2}(3)h_{r1}\mathbf{x}_{r1}(2)$ and $\mathbf{B}h_{r2}g_{r4}(3)h_{r2}\mathbf{x}_{r3}^*(2)$, respectively, which are known perfectly at R1 and R3, and thus can be removed. Therefore, the transmit signals at slot 4 from R1 and R3 will be

$$\begin{aligned} \mathbf{x}_{r1}(4) &= \mathbf{A}g_{r1}(4)[\mathbf{y}_{r1}(3) - \mathbf{A}h_{r1}g_{r2}(3)h_{r1}\mathbf{x}_{r1}(2)] = \mathbf{A}g_{r1}(4)\{\sqrt{\rho}\mathbf{x}(3)h_{sr1} \\ &\quad + \mathbf{A}h_{r1}g_{r2}(3)[\sqrt{\rho}\mathbf{x}(2)h_{sr2} + \mathbf{n}_{r2}(2)] + \mathbf{n}_{r1}(3)\}, \end{aligned} \tag{3.3.1}$$

$$\begin{aligned} \mathbf{x}_{r3}(4) &= \mathbf{B}g_{r3}(4)[\mathbf{y}_{r3}^*(3) - \mathbf{B}h_{r2}^*g_{r4}^*(3)h_{r2}\mathbf{x}_{r3}(2)] = \mathbf{B}g_{r3}(4)\{\sqrt{\rho}\mathbf{x}^*(3)h_{sr3}^* \\ &\quad + \mathbf{B}h_{r2}^*g_{r4}^*(3)[\sqrt{\rho}\mathbf{x}(2)h_{sr4} + \mathbf{n}_{r4}(2)] + \mathbf{n}_{r3}^*(3)\}. \end{aligned} \tag{3.3.2}$$

At time slot 4, $\mathbf{x}(4)$ is sent from S to D, R2 and R4, while $\mathbf{x}_{r1}(4)$ and $\mathbf{x}_{r3}(4)$ are sent from R1 and R3. Therefore, at R2, R4 and D,

$$\begin{aligned}\mathbf{y}_{r2}(4) &= \sqrt{\rho}\mathbf{x}(4)h_{sr_2} + h_{r1}\mathbf{x}_{r1}(4) + \mathbf{n}_{r2}(4) \\ \mathbf{y}_{r4}(4) &= \sqrt{\rho}\mathbf{x}(4)h_{sr_4} + h_{r2}\mathbf{x}_{r3}(4) + \mathbf{n}_{r4}(4) \\ \mathbf{y}_d(4) &= \sqrt{\rho}\mathbf{x}(4)h_{sd} + h_{r1d}\mathbf{x}_{r1}(4) + h_{r3d}\mathbf{x}_{r3}(4) + \mathbf{n}_d(4).\end{aligned}$$

The transmit signals at time slot 5 from R2 and R4 are $\mathbf{x}_{r2}(5) = \mathbf{A}g_{r2}(5)\mathbf{y}_{r2}(4)$ and $\mathbf{x}_{r4}(5) = \mathbf{B}g_{r4}(5)\mathbf{y}_{r4}^*(4)$, respectively. There is not inter-relay interference at R2 and R4 because $\mathbf{x}_{r2}(3)$ and $\mathbf{x}_{r4}(3)$ do not exist in the received signals due to the cancellation in R1 and R3 as shown in (3.3.1) and (3.3.2). Using the same method, L symbols will have been transmitted from the source to the destination.

From the equations above, the transmitted signals at R1, R2, R3 and R4 in the l^{th} time slot can be generalized as

$$\mathbf{x}_{r1}(l) \begin{cases} \mathbf{A}g_{r1}(l)\mathbf{y}_{r1}(l-1) & \text{for } l = 2 \\ \mathbf{A}g_{r1}(l)[\mathbf{y}_{r1}(l-1) - \mathbf{A}h_{r1}g_{r2}(l-1)h_{r1}\mathbf{x}_{r1}(l-2)], \\ & \text{for } l = 4, 6, 8, \dots, L, \end{cases}$$

$$\mathbf{x}_{r3}(l) \begin{cases} \mathbf{B}g_{r3}(l)\mathbf{y}_{r3}^*(l-1) & \text{for } l = 2 \\ \mathbf{B}g_{r3}(l)[\mathbf{y}_{r3}^*(l-1) - \mathbf{B}h_{r2}^*g_{r4}^*(l-1)h_{r2}\mathbf{x}_{r3}(l-2)], \\ & \text{for } l = 4, 6, 8, \dots, L. \end{cases}$$

$$\mathbf{x}_{r2}(l) = \mathbf{A}g_{r2}(l)\mathbf{y}_{r2}(l-1), \quad \mathbf{x}_{r4}(l) = \mathbf{B}g_{r4}(l)\mathbf{y}_{r4}^*(l-1) \quad \text{for } l = 3, 5, 7, \dots, L-1,$$

respectively, where $g_{ri}(l)$ are defined as

$$g_{rm}(l) \begin{cases} \sqrt{\frac{\rho}{\gamma_{sr_m}^2 \rho + \sigma^2}} & \text{for } l = 2 \\ \sqrt{\frac{\rho}{\gamma_{sr_m}^2 \rho + \gamma_{rw}^2 g_{rn}^2(l-1)(\gamma_{sr_n}^2 \rho + \sigma^2) + \sigma^2}} \\ & \text{for } l = 4, 6, 8, \dots, L, \end{cases}$$

$$g_{rn}(l) = \sqrt{\frac{\rho}{\gamma_{sr_n}^2 \rho + \gamma_{rw}^2 \rho + \sigma^2}}, \quad \text{for } l = 3, 5, 7, \dots, L-1,$$

where $m = 1$ or 3 , $n = 2$ or 4 and $w = 1$ or 2 . And ρ is the average transmitted power at the source and the four relays. The gains $g_{r2}(l)$ and $g_{r4}(l)$ are constant for $l = 3, 5, 7, \dots, L-1$. Thus, $g_{r1}(l)$ and $g_{r3}(l)$ which depend on $g_{r2}(l-1)$ and $g_{r4}(l-1)$ are also constant for $l = 4, 6, \dots, L$, respectively. Therefore, the time index l can be removed hereafter.

B) Equivalent MIMO Channel

According to all the equations in Section 3.3.2-A, the received signal at the destination can be rewritten as

$$\mathbf{y}_d = \sqrt{\rho} \mathbf{H} \tilde{\mathbf{x}} + \mathbf{n}_d + \mathbf{C} \mathbf{n}_r \quad (3.3.3)$$

where $\mathbf{y}_d = [y_{d1}(1) \ y_{d2}(1) \ y_{d1}(2) \ y_{d2}(2) \ \dots \ y_{d1}(L) \ y_{d2}(L)]^T$, and in order to analyze the pairwise error probability (PEP) and diversity order, rewrite the real and imaginary parts of the signals and the noise to be vectors, which are $\tilde{\mathbf{x}} = [x_{1,R}(1) \ x_{2,R}(1) \ x_{1,R}(2) \ x_{2,R}(2) \ \dots \ x_{1,R}(L) \ x_{2,R}(L) \ jx_{1,I}(1) \ jx_{2,I}(1) \ jx_{1,I}(2) \ jx_{2,I}(2) \ \dots \ jx_{1,I}(L) \ jx_{2,I}(L)]^T$, $\mathbf{n}_d = [n_{d1,R}(1) \ n_{d2,R}(1) \ n_{d1,R}(2) \ n_{d2,R}(2) \ \dots \ n_{d1,R}(L) \ n_{d2,R}(L) \ jn_{d1,I}(1) \ jn_{d2,I}(1) \ jn_{d1,I}(2) \ jn_{d2,I}(2) \ \dots \ jn_{d1,I}(L) \ jn_{d2,I}(L)]^T$ and $\mathbf{n}_r = [n_{r11,R}(1) \ n_{r12,R}(1) \ n_{r21,R}(2) \ n_{r22,R}(2) \ \dots \ n_{r21,R}(L) \ n_{r22,R}(L) \ jn_{r11,I}(1) \ jn_{r12,I}(1) \ jn_{r21,I}(2) \ jn_{r22,I}(2) \ \dots \ jn_{r21,I}(L) \ jn_{r22,I}(L) \ n_{r31,R}(1) \ n_{r32,R}(1) \ n_{r41,R}(2) \ n_{r42,R}(2) \ \dots \ n_{r41,R}(L) \ n_{r42,R}(L) \ jn_{r31,I}(1) \ jn_{r32,I}(1) \ jn_{r41,I}(2) \ jn_{r42,I}(2) \ \dots \ jn_{r41,I}(L) \ jn_{r42,I}(L)]^T$. Let $H(p, q)$ and $C(p, q)$ denote the elements at the p^{th} row and q^{th} column of \mathbf{H} and \mathbf{C} respectively. Then, the non-zero elements of \mathbf{H} and \mathbf{C} are given as

$$H(m, m) = H(m, m + 12) = h_{sd}, \quad m = 1, 2, \dots, 2L,$$

$$H(m, m-2) = H(m+1, m-1) = H(m+1, m+11) = H(m, m+10) = \begin{cases} h_{r_1d}h_{sr_1}g_{r_1} & \text{for } m = 3, 7, \dots, 2L-1 \\ h_{r_2d}h_{sr_2}g_{r_2} & \text{for } m = 5, 9, \dots, 2L-1, \end{cases}$$

$$H(m, m-1) = -H(m+1, m-2) = -H(m, m+11) = H(m+1, m+10) = \begin{cases} -h_{r_3d}h_{sr_3}^*g_{r_3} & \text{for } m = 3, 7, \dots, 2L-1 \\ h_{r_4d}h_{sr_4}^*g_{r_4} & \text{for } m = 5, 9, \dots, 2L-1, \end{cases}$$

$$H(m, m-4) = H(m+1, m-3) = H(m, m+8) = H(m+1, m+9) = \begin{cases} h_{r_2d}h_{sr_1}g_{r_2}h_{r_1}g_{r_1} - h_{r_4d}h_{sr_3}g_{r_4}h_{r_2}g_{r_3}^* & \text{for } m = 5, 9, \dots, 2L-1 \\ h_{r_1d}h_{sr_2}g_{r_1}h_{r_1}g_{r_2} - h_{r_3d}h_{sr_4}g_{r_3}h_{r_2}g_{r_4}^* & \text{for } m = 7, 11, \dots, 2L-1, \end{cases}$$

$$H(m, m-6) = H(m+1, m-5) = H(m, m+6) = H(m+1, m+7) \\ = g_{r_2}h_{r_2d}h_{r_1}g_{r_1}h_{r_1}g_{r_2}h_{sr_2} \quad \text{for } m = 9, 13, \dots, 2L-1,$$

$$H(m, m-5) = -H(m+1, m-6) = -H(m, m+7) = H(m+1, m+6) \\ = g_{r_4}h_{r_4d}h_{r_2}g_{r_3}h_{r_2}g_{r_4}h_{sr_4}^* \quad \text{for } m = 9, 13, \dots, 2L-1.$$

Furthermore,

$$C(m, m-2) = C(m+1, m-1) = C(m+1, m+11) = C(m, m+10) = \begin{cases} h_{r_1d}g_{r_1} & \text{for } m = 3, 7, \dots, 2L-1 \\ h_{r_2d}g_{r_2} & \text{for } m = 5, 9, \dots, 2L-1, \end{cases}$$

$$C(m, m+23) = -C(m+1, m+22) = C(m+1, m+34) = -C(m, m+35) = \begin{cases} -h_{r_3d}g_{r_3} & \text{for } m = 3, 7, \dots, 2L-1 \\ -h_{r_4d}g_{r_4} & \text{for } m = 5, 9, \dots, 2L-1, \end{cases}$$

$$C(m, m-4) = C(m+1, m-3) = C(m+1, m+9) = C(m, m+8) = \begin{cases} h_{r_2d}g_{r_2}h_{r_1}g_{r_1} & \text{for } m = 5, 9, \dots, 2L-1 \\ h_{r_1d}g_{r_1}h_{r_1}g_{r_2} & \text{for } m = 7, 11, \dots, 2L-1, \end{cases}$$

$$C(m, m+20) = C(m+1, m+21) = C(m+1, m+33) = C(m, m+32) = \begin{cases} -h_{r_4d}g_{r_4}h_{r_2}^*g_{r_3}^* & \text{for } m = 5, 9, \dots, 2L-1 \\ -h_{r_3d}g_{r_3}h_{r_2}^*g_{r_4}^* & \text{for } m = 7, 11, \dots, 2L-1, \end{cases}$$

$$\begin{aligned} C(m, m-6) &= C(m, m+6) = C(m+1, m-5) = C(m+1, m+7) \\ &= g_{r_2}h_{r_2d}h_{r_1}g_{r_1}h_{r_1}g_{r_2} \quad \text{for } m = 9, 13, \dots, 2L-1, \end{aligned}$$

$$\begin{aligned} C(m, m+19) &= -C(m, m+31) = -C(m+1, m+18) = C(m+1, m+30) \\ &= g_{r_4}h_{r_4d}h_{r_2}^*g_{r_3}h_{r_2}g_{r_4} \quad \text{for } m = 9, 13, \dots, 2L-1. \end{aligned}$$

Notice that $\mathbf{C}\mathbf{n}_r$ is the residual noise from the relays and it is in general not white. Rewriting (3.3.3) as

$$\mathbf{y}_d = \sqrt{\rho}\mathbf{H}\tilde{\mathbf{x}} + \mathbf{C}'\mathbf{n}, \quad (3.3.4)$$

where $\mathbf{C}' = [\mathbf{C} \ \mathbf{I}_{12} \ \mathbf{I}_{12}]$, and $\mathbf{n} = [\mathbf{n}_r \ \mathbf{n}_d]$.

Then, the mutual information of the four-path relaying is given as (3.3.5) from the mutual information of the equivalent MIMO system in (3.3.4). Following the derivation in [67],

$$I(\mathbf{x}; \mathbf{y}_d) = \frac{L}{L+2} \log_2 \det(\mathbf{I} + \mathbf{H}\mathbf{R}_x\mathbf{H}^H(\mathbf{C}'\mathbf{R}_n\mathbf{C}'^H)^{-1}), \quad (3.3.5)$$

where $\mathbf{R}_x = E[\tilde{\mathbf{x}}\tilde{\mathbf{x}}^H] = \rho\mathbf{I}$ and $\mathbf{R}_n = E[\mathbf{n}\mathbf{n}^H] = \sigma^2\mathbf{I}$. Since two additional time slots are required at the end as the terminating sequence, the mutual information is decreased by $\frac{L}{L+2}$, however, the slight loss is asymptotical zero for large values of L . Moreover, because $\mathbf{C}'\mathbf{R}_n\mathbf{C}'^H = \sigma^2[\mathbf{C} \ \mathbf{I}_{12} \ \mathbf{I}_{12}][\mathbf{C} \ \mathbf{I}_{12} \ \mathbf{I}_{12}]^H = \sigma^2(\mathbf{C}\mathbf{C}^H + 2\mathbf{I})$, the mutual information can be simplified to

$$I(\mathbf{x}; \mathbf{y}_d) = \frac{L}{L+2} \log_2 \det(\mathbf{I} + \frac{\rho}{\sigma^2}\mathbf{H}\mathbf{H}^H(\mathbf{C}\mathbf{C}^H + 2\mathbf{I})^{-1}). \quad (3.3.6)$$

3.3.3 Pairwise Error Probability and Diversity Analysis

In this section, the PEP of the four-path relaying is derived. First, express the received signal in (3.3.3) as

$$\mathbf{y}_d = \sqrt{\rho} \mathbf{X} \mathbf{h} + \mathbf{w}, \quad (3.3.7)$$

where $\mathbf{X} = [\mathbf{X}_{\text{Re}} \ j\mathbf{X}_{\text{Im}}]$, and $\mathbf{h} = [\mathbf{h}_R \ \mathbf{h}_I]^T$

$\mathbf{X}_{\text{Re}} =$

$$\begin{bmatrix} x_{1,R}(1) & 0 & 0 & 0 & 0 & 0 & 0 & 0 & 0 & 0 & 0 & 0 \\ x_{2,R}(1) & 0 & 0 & 0 & 0 & 0 & 0 & 0 & 0 & 0 & 0 & 0 \\ x_{1,R}(2) & x_{2,R}(1) & x_{1,R}(1) & 0 & 0 & 0 & 0 & 0 & 0 & 0 & 0 & 0 \\ x_{2,R}(2) & 0 & x_{2,R}(1) & x_{1,R}(1) & 0 & 0 & 0 & 0 & 0 & 0 & 0 & 0 \\ x_{1,R}(3) & 0 & 0 & 0 & x_{2,R}(2) & x_{1,R}(2) & x_{1,R}(1) & 0 & 0 & 0 & 0 & 0 \\ x_{2,R}(3) & 0 & 0 & 0 & 0 & x_{2,R}(2) & x_{2,R}(1) & x_{1,R}(2) & 0 & 0 & 0 & 0 \\ x_{1,R}(4) & x_{2,R}(3) & x_{1,R}(3) & 0 & 0 & 0 & 0 & 0 & x_{1,R}(2) & 0 & 0 & 0 \\ x_{2,R}(4) & 0 & x_{2,R}(3) & x_{1,R}(3) & 0 & 0 & 0 & 0 & x_{2,R}(2) & 0 & 0 & 0 \\ x_{1,R}(5) & 0 & 0 & 0 & x_{2,R}(4) & x_{2,R}(3) & x_{1,R}(4) & 0 & 0 & x_{2,R}(2) & x_{1,R}(2) & 0 \\ x_{2,R}(5) & 0 & 0 & 0 & 0 & x_{2,R}(4) & x_{2,R}(3) & x_{1,R}(4) & 0 & 0 & x_{2,R}(2) & x_{1,R}(2) \\ x_{1,R}(6) & x_{2,R}(5) & x_{1,R}(5) & 0 & 0 & 0 & 0 & 0 & x_{1,R}(4) & 0 & 0 & 0 \\ x_{2,R}(6) & 0 & x_{2,R}(5) & x_{1,R}(5) & 0 & 0 & 0 & 0 & x_{2,R}(4) & 0 & 0 & 0 \end{bmatrix}$$

$\mathbf{X}_{\text{Im}} =$

$$\begin{bmatrix} x_{1,I}(1) & 0 & 0 & 0 & 0 & 0 & 0 & 0 & 0 & 0 & 0 & 0 \\ x_{2,I}(1) & 0 & 0 & 0 & 0 & 0 & 0 & 0 & 0 & 0 & 0 & 0 \\ x_{1,I}(2) & x_{2,I}(1) & x_{1,I}(1) & 0 & 0 & 0 & 0 & 0 & 0 & 0 & 0 & 0 \\ x_{2,I}(2) & 0 & x_{2,I}(1) & x_{1,I}(1) & 0 & 0 & 0 & 0 & 0 & 0 & 0 & 0 \\ x_{1,I}(3) & 0 & 0 & 0 & x_{2,I}(2) & x_{1,I}(2) & x_{1,I}(1) & 0 & 0 & 0 & 0 & 0 \\ x_{2,I}(3) & 0 & 0 & 0 & 0 & x_{2,I}(2) & x_{2,I}(1) & x_{1,I}(2) & 0 & 0 & 0 & 0 \\ x_{1,I}(4) & x_{2,I}(3) & x_{1,I}(3) & 0 & 0 & 0 & 0 & 0 & x_{1,I}(2) & 0 & 0 & 0 \\ x_{2,I}(4) & 0 & x_{2,I}(3) & x_{1,I}(3) & 0 & 0 & 0 & 0 & x_{2,I}(2) & 0 & 0 & 0 \\ x_{1,I}(5) & 0 & 0 & 0 & x_{2,I}(4) & x_{1,I}(4) & x_{1,I}(3) & 0 & 0 & x_{2,I}(2) & x_{1,I}(2) & 0 \\ x_{2,I}(5) & 0 & 0 & 0 & 0 & x_{2,I}(4) & x_{2,I}(3) & x_{1,I}(4) & 0 & 0 & x_{2,I}(2) & x_{1,I}(2) \\ x_{1,I}(6) & x_{2,I}(5) & x_{1,I}(5) & 0 & 0 & 0 & 0 & 0 & x_{1,I}(4) & 0 & 0 & 0 \\ x_{2,I}(6) & 0 & x_{2,I}(5) & x_{1,I}(5) & 0 & 0 & 0 & 0 & x_{2,I}(4) & 0 & 0 & 0 \end{bmatrix}$$

$$\mathbf{h}_R = \begin{bmatrix} h_{sd} \\ -g_{r3}h_{r3d}h_{sr3}^* \\ g_{r1}h_{r1d}h_{sr1} \\ g_{r3}h_{r3d}h_{sr3}^* \\ -g_{r4}h_{r4d}h_{sr4}^* \\ g_{r2}h_{r2d}h_{sr2} \\ g_{r2}h_{r2d}h_{r1}g_{r1}h_{sr1} - g_{r4}h_{r4d}h_{r2}^*g_{r3}^*h_{sr3} \\ g_{r4}h_{r4d}h_{sr4}^* \\ g_{r1}h_{r1d}h_{r1}g_{r2}h_{sr2} - g_{r3}h_{r3d}h_{r2}^*g_{r4}^*h_{sr4} \\ g_{r4}h_{r4d}h_{r2}^*g_{r3}h_{r2}g_{r4}h_{sr4}^* \\ g_{r2}h_{r2d}h_{r1}^2g_{r1}g_{r2}h_{sr2} \\ -g_{r4}h_{r4d}h_{r2}^*g_{r3}h_{r2}g_{r4}h_{sr4}^* \end{bmatrix},$$

$$\mathbf{h}_I = \begin{bmatrix} h_{sd} \\ g_{r3}h_{r3d}h_{sr3}^* \\ g_{r1}h_{r1d}h_{sr1} \\ -g_{r3}h_{r3d}h_{sr3}^* \\ g_{r4}h_{r4d}h_{sr4}^* \\ g_{r2}h_{r2d}h_{sr2} \\ g_{r2}h_{r2d}h_{r1}g_{r1}h_{sr1} - g_{r4}h_{r4d}h_{r2}^*g_{r3}^*h_{sr3} \\ -g_{r4}h_{r4d}h_{sr4}^* \\ g_{r1}h_{r1d}h_{r1}g_{r2}h_{sr2} - g_{r3}h_{r3d}h_{r2}^*g_{r4}^*h_{sr4} \\ -g_{r4}h_{r4d}h_{r2}^*g_{r3}h_{r2}g_{r4}h_{sr4}^* \\ g_{r2}h_{r2d}h_{r1}^2g_{r1}g_{r2}h_{sr2} \\ g_{r4}h_{r4d}h_{r2}^*g_{r3}h_{r2}g_{r4}h_{sr4}^* \end{bmatrix}.$$

Here, it is assumed that $L = 6$, \mathbf{X} is a $2L \times 24$ matrix consisting of the transmitted symbols, \mathbf{h} is the equivalent channel vector, and $\mathbf{w} = \mathbf{C}\mathbf{n}_r + \mathbf{n}_d$ conditioned on \mathbf{h} is the correlated Gaussian noise with covariance matrix $\Sigma_{\mathbf{w}} = \sigma^2(\mathbf{C}\mathbf{C}^H + 2\mathbf{I})$. Then, use ML decoding at the receiver. If \mathbf{X} is transmitted, then from [68], the PEP of mistaking \mathbf{X} with \mathbf{X}_e has the

following Chernoff upper bound

$$P(\mathbf{X} \rightarrow \mathbf{X}_e) \leq \mathbf{E}_h \{ e^{-\frac{1}{4} \rho \mathbf{h}^H (\mathbf{X} - \mathbf{X}_e)^H \Sigma_{\mathbf{w}}^{-1} (\mathbf{X} - \mathbf{X}_e) \mathbf{h}} \}. \quad (3.3.8)$$

Since the covariance matrix $\Sigma_{\mathbf{w}}$ is not a diagonal matrix, (3.3.5) cannot be easily analyzed. However, the covariance matrix $\Sigma_{\mathbf{w}}$ is a positive semi-definite matrix, therefore, the PEP can be upperbounded by $\Sigma_{\mathbf{w}} \leq \text{tr}(\Sigma_{\mathbf{w}}) \mathbf{I}$, where $\text{tr}(\Sigma_{\mathbf{w}})$ is the trace of $\Sigma_{\mathbf{w}}$. With this, it follows that

$$P(\mathbf{X} \rightarrow \mathbf{X}_e) \leq \mathbf{E}_h \{ e^{-\frac{\rho}{4 \text{tr}(\Sigma_{\mathbf{w}})} \mathbf{h}^H (\mathbf{X} - \mathbf{X}_e)^H (\mathbf{X} - \mathbf{X}_e) \mathbf{h}} \}. \quad (3.3.9)$$

In order to calculate the expectation in (3.3.9), express $\mathbf{h} = (\mathbf{T}_1 \mathbf{U}_1 + \mathbf{T}_2 \mathbf{U}_2) \mathbf{v}$, where $\mathbf{v} = [h_{sd,R} \ h_{sr1,R}, \dots, h_{sr4,R} \ h_{sd,I} \ h_{sr1,I}, \dots, h_{sr4,I}]^T$, and \mathbf{T}_1 , \mathbf{T}_2 , $\mathbf{U}_1 = [\mathbf{U}_{11}; \mathbf{U}_{11}]$ and $\mathbf{U}_2 = [\mathbf{U}_{21}; \mathbf{U}_{21}]$ are shown as

$$\mathbf{U}_{11} = \begin{bmatrix} 1 & 0 & 0 & 0 & 0 & 1 & 0 & 0 & 0 & 0 \\ 0 & 0 & 0 & 1 & 0 & 0 & 0 & 0 & -1 & 0 \\ 0 & 1 & 0 & 0 & 0 & 0 & 1 & 0 & 0 & 0 \\ 0 & 0 & 0 & 1 & 0 & 0 & 0 & 0 & -1 & 0 \\ 0 & 0 & 0 & 0 & 1 & 0 & 0 & 0 & 0 & -1 \\ 0 & 0 & 1 & 0 & 0 & 0 & 0 & 1 & 0 & 0 \\ 0 & 1 & 0 & 0 & 0 & 0 & 1 & 0 & 0 & 0 \\ 0 & 0 & 0 & 0 & 1 & 0 & 0 & 0 & 0 & -1 \\ 0 & 0 & 1 & 0 & 0 & 0 & 0 & 1 & 0 & 0 \\ 0 & 0 & 0 & 0 & 1 & 0 & 0 & 0 & 0 & -1 \\ 0 & 0 & 1 & 0 & 0 & 0 & 0 & 1 & 0 & 0 \\ 0 & 0 & 0 & 0 & 1 & 0 & 0 & 0 & 0 & -1 \end{bmatrix}$$

$$\mathbf{U}_{21} = \begin{bmatrix} 1 & 0 & 0 & 0 & 0 & 1 & 0 & 0 & 0 & 0 \\ 0 & 0 & 0 & 1 & 0 & 0 & 0 & 0 & -1 & 0 \\ 0 & 1 & 0 & 0 & 0 & 0 & 1 & 0 & 0 & 0 \\ 0 & 0 & 0 & 1 & 0 & 0 & 0 & 0 & -1 & 0 \\ 0 & 0 & 0 & 0 & 1 & 0 & 0 & 0 & 0 & -1 \\ 0 & 0 & 1 & 0 & 0 & 0 & 0 & 1 & 0 & 0 \\ 0 & 0 & 0 & 1 & 0 & 0 & 0 & 0 & 1 & 0 \\ 0 & 0 & 0 & 0 & 1 & 0 & 0 & 0 & 0 & -1 \\ 0 & 0 & 0 & 0 & 1 & 0 & 0 & 0 & 0 & 1 \\ 0 & 0 & 0 & 0 & 1 & 0 & 0 & 0 & 0 & -1 \\ 0 & 0 & 1 & 0 & 0 & 0 & 0 & 1 & 0 & 0 \\ 0 & 0 & 0 & 0 & 1 & 0 & 0 & 0 & 0 & -1 \end{bmatrix}$$

$$\begin{aligned}
\mathbf{T}_1 = & \text{diag} \left(\begin{array}{c} 0.5 \\ -0.5g_r3h_{r3d} \\ 0.5g_r1h_{r1d} \\ 0.5g_r3h_{r3d} \\ -0.5g_r4h_{r4d} \\ 0.5g_r2h_{r2d} \\ 0.5g_r2h_{r2d}h_{r1}g_{r1} \\ 0.5g_r4h_{r4d} \\ 0.5g_r1h_{r1d}h_{r1}g_{r2} \\ 0.5g_r4h_{r4d}h_{r2}^*g_{r3}h_{r2}g_{r4} \\ 0.5g_r2h_{r2d}h_{r1}^2g_{r1}g_{r2} \\ -0.5g_r4h_{r4d}h_{r2}^*g_{r3}h_{r2}g_{r4} \\ 0.5 \\ 0.5g_r3h_{r3d} \\ 0.5g_r1h_{r1d} \\ -0.5g_r3h_{r3d} \\ 0.5g_r4h_{r4d} \\ 0.5g_r2h_{r2d} \\ 0.5g_r2h_{r2d}h_{r1}g_{r1} \\ -0.5g_r4h_{r4d} \\ 0.5g_r1h_{r1d}h_{r1}g_{r2} \\ -0.5g_r4h_{r4d}h_{r2}^*g_{r3}h_{r2}g_{r4} \\ 0.5g_r2h_{r2d}h_{r1}^2g_{r1}g_{r2} \\ 0.5g_r4h_{r4d}h_{r2}^*g_{r3}h_{r2}g_{r4} \end{array} \right) \\
\mathbf{T}_2 = & \text{diag} \left(\begin{array}{c} 0.5 \\ -0.5g_r3h_{r3d} \\ 0.5g_r1h_{r1d} \\ 0.5g_r3h_{r3d} \\ -0.5g_r4h_{r4d} \\ 0.5g_r2h_{r2d} \\ -0.5g_r4h_{r4d}h_{r2}^*g_{r3} \\ 0.5g_r4h_{r4d} \\ -0.5g_r3h_{r3d}h_{r2}^*g_{r4} \\ 0.5g_r4h_{r4d}h_{r2}^*g_{r3}h_{r2}g_{r4} \\ 0.5g_r2h_{r2d}h_{r1}^2g_{r1}g_{r2} \\ -0.5g_r4h_{r4d}h_{r2}^*g_{r3}h_{r2}g_{r4} \\ 0.5 \\ 0.5g_r3h_{r3d} \\ 0.5g_r1h_{r1d} \\ -0.5g_r3h_{r3d} \\ 0.5g_r4h_{r4d} \\ 0.5g_r2h_{r2d} \\ -0.5g_r4h_{r4d}h_{r2}^*g_{r3} \\ -0.5g_r4h_{r4d} \\ -0.5g_r3h_{r3d}h_{r2}^*g_{r4} \\ -0.5g_r4h_{r4d}h_{r2}^*g_{r3}h_{r2}g_{r4} \\ 0.5g_r2h_{r2d}h_{r1}^2g_{r1}g_{r2} \\ 0.5g_r4h_{r4d}h_{r2}^*g_{r3}h_{r2}g_{r4} \end{array} \right)
\end{aligned}$$

Thus, by taking expectation over \mathbf{v} first yields

$$\begin{aligned}
& P(\mathbf{X} \rightarrow \mathbf{X}_e) \\
& \leq \mathbf{E}_T \left\{ \int \frac{1}{\pi^3} e^{-\frac{\rho}{4tr(\sum \mathbf{W})} \mathbf{v}^H (\mathbf{T}_1^H \mathbf{U}_1^H + \mathbf{T}_2^H \mathbf{U}_2^H) (\mathbf{X} - \mathbf{X}_e)^H (\mathbf{X} - \mathbf{X}_e) (\mathbf{T}_1 \mathbf{U}_1 + \mathbf{T}_2 \mathbf{U}_2) \mathbf{v}} e^{-\mathbf{v}^H \mathbf{v}} d\mathbf{v} \right\} \\
& = \mathbf{E}_T \left\{ \det^{-1} \left(\mathbf{I} + \frac{\rho}{4tr(\sum \mathbf{W})} \mathbf{A}^H \mathbf{A} \right) \right\},
\end{aligned}$$

where $\mathbf{A} = (\mathbf{X} - \mathbf{X}_e) (\mathbf{T}_1 \mathbf{U}_1 + \mathbf{T}_2 \mathbf{U}_2)$, $tr(\cdot)$ represents trace of matrix. Using the diversity criterion in [36] the diversity order can be analyzed, which is determined by the rank of \mathbf{A} . It can be observed that \mathbf{T}_1 and \mathbf{T}_2 are full rank. The rank of \mathbf{U}_1 and \mathbf{U}_2 are 5. The rank of \mathbf{A} is determined by the

rank of the product $(\mathbf{X} - \mathbf{X}_e)$ and $(\mathbf{U}_1 + \mathbf{U}_2)$.

Because the real and imaginary parts of $x_j(i)$ have the same effect for the rank of the product $(\mathbf{X} - \mathbf{X}_e)$, consider only the real part $x_{j,R}(i)$, where $i = 1, 2, \dots, L$ and $j = 1$ or 2 . There are three scenarios.

Firstly, only the first symbol at the odd time slots is different between \mathbf{X} and \mathbf{X}_e . If only $x_{1,R}(1)$ is different, there are four independent columns in $(\mathbf{X} - \mathbf{X}_e)$ (1, 3, 4, 7). However, both \mathbf{U}_1 and \mathbf{U}_2 have three and four independent rows in (1, 3, 4, 7), respectively. Using the same method, only the second symbol at the odd time slots is different, such as $x_{2,R}(1)$. There are four independent columns in $(\mathbf{X} - \mathbf{X}_e)$ (1, 2, 3, 7). However, both \mathbf{U}_1 and \mathbf{U}_2 only have three and four independent rows in (1, 2, 3, 7). Therefore, the product terms in \mathbf{A} , i.e. $(\mathbf{X} - \mathbf{X}_e)\mathbf{U}_1$ and $(\mathbf{X} - \mathbf{X}_e)\mathbf{U}_2$, have limited rank of three and four, respectively.

Secondly, only the first symbol at the even time slot is different, in this case there are six independent columns in $(\mathbf{X} - \mathbf{X}_e)$ (1, 6, 8, 9, 11, 12). However, the limited rank of the product terms are three and four, because there are only three and four independent corresponding rows in \mathbf{U}_1 and \mathbf{U}_2 , respectively. If the second symbol at the even time slot is different, there are six independent columns in $(\mathbf{X} - \mathbf{X}_e)$ (1, 5, 6, 9, 10, 11), but both \mathbf{U}_1 and \mathbf{U}_2 only have three and four independent rows in $(\mathbf{X} - \mathbf{X}_e)$ (1, 5, 6, 9, 10, 11). Therefore, the product terms in \mathbf{A} have limited rank of three and four, respectively.

Thirdly, if all of the symbols are different, the matrix $(\mathbf{X} - \mathbf{X}_e)$ is full rank, the rank of the product is equal to five as \mathbf{U}_1 and \mathbf{U}_2 are both rank five matrices. Based on the above three cases, the minimum rank of the product terms are three and four, respectively. Therefore, the overall diversity order is between three and four.

Furthermore, some special situations are discussed in the following:

Firstly, if there is no direct path from the source to destination ($h_{sd} = 0$),

then minimum diversity order of two can be achieved, because the first row of \mathbf{U}_1 and \mathbf{U}_2 are removed.

Secondly, if h_{r1} and h_{r2} do not exist ($h_{r1} = h_{r2} = 0$), then the (7, 9, 10, 11, 12) diagonal elements of \mathbf{T}_1 and \mathbf{T}_2 will be 0. Thus, if one symbol is different between \mathbf{X} and \mathbf{X}_e , there are three independent rows in \mathbf{U}_1 and \mathbf{U}_2 . Therefore, the diversity order of three can still be obtained without the h_{r1} and h_{r2} in the equivalent channel matrix.

Thirdly, if γ_{r1}^2 and γ_{r2}^2 increase, both g_{r2} and g_{r4} will approach 0 and both g_{r1} and g_{r3} will approach to a constant value. And the 5th to 12th diagonal elements of \mathbf{T}_1 and \mathbf{T}_2 will be 0. Therefore, when the γ_{r1}^2 and γ_{r2}^2 increase, the diversity order will be decreased.

3.3.4 Simulation Studies

In this section, the simulated performance of the proposed scheme is shown i.e. four-path relaying with inter-relay self interference cancellation. The performance is shown by the end-to-end BER using QPSK symbols. The length of symbol L is assumed to be six, and all average channel gains are normalized to 0 dB. And the asymptotic achievable rate can be obtained where L is sufficiently large and hence $\frac{L}{L+2} \rightarrow 1$.

Fig. 3.8 compares the average rate as a function of the signal-to-noise ratio. Equation (3.3.6) is used to calculate the average rate. The average rate decreases when γ_{sd}^2 is lower than other channels, i.e. γ_{sd}^2 is -20 dB. However, when γ_{ri}^2 $i \in (1, 2)$ increases to 10 dB, the average rate is slightly decreased, i.e. the average rate decreases from 70 (bit/s/Hz) to 66 (bit/s/Hz) when the SNR is equal to 30 dB.

Fig. 3.9 contrasts the BER performance with different inter-relay channel gains. Obviously, the diversity order decreases with the increase of γ_{ri}^2 , from 3.5 to essentially two. However, when $\gamma_{ri}^2 = 0$, the diversity order is three.

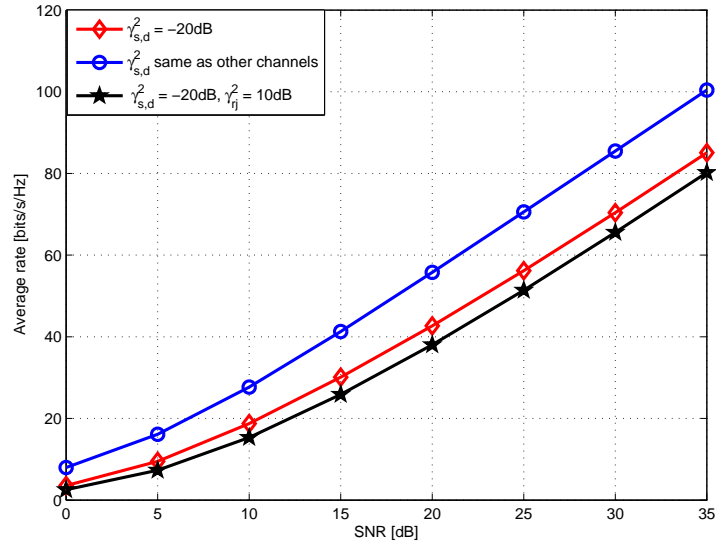


Figure 3.8. Comparison of average rate between the different channel coefficients.

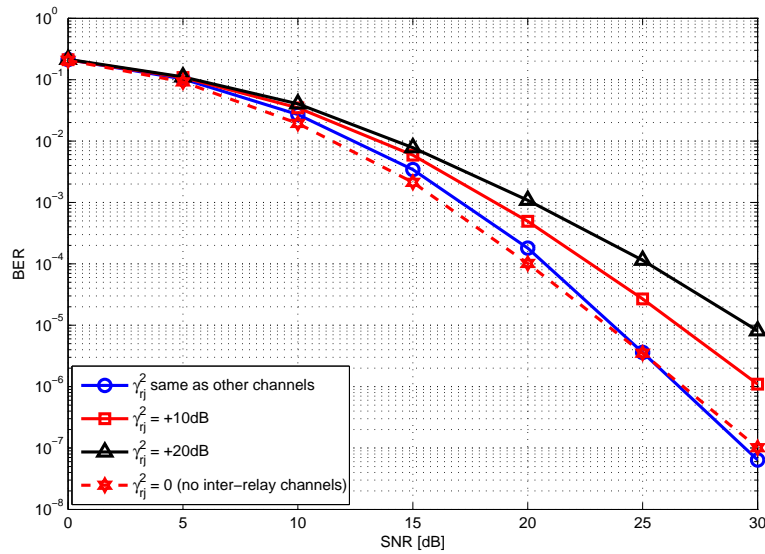


Figure 3.9. Comparison of BER performance for different levels of IRI.

3.4 Summary

In this chapter, full diversity and improved end-to-end transmission rate can be achieved because the offset transmission with FIC scheme was used. Using offset transmission, the source can serially transmit data to the destination. However, the four-path relay scheme may suffer from IRI which is caused by the simultaneous transmission of the source and another group of relays. Therefore, the FIC scheme was used to remove fully these IRI terms. However, the FIC scheme is performed at the destination node, and so multiple antennas have to be used which maybe infeasible to achieve in practice. Therefore, an FSIC scheme at the relay nodes within a four relay network was provided and the pairwise error probability approach has been used to analyze distributed diversity. The four single antenna relay nodes were arranged as two groups of spatially separated two relay groups with offset transmission scheduling. This approach can achieve the full available distributed diversity order 3.5 without precoding and its end-to-end transmission rate can asymptotically approach one when the number of samples is large. However, a synchronous system must be assumed in the above schemes, because the timing error can significantly degrade the end-to-end BER performance. Therefore, in the next chapter, offset transmission with FIC scheme is applied within an asynchronous cooperative four relay network. The transmission efficiency will also be improved.

FIC SCHEMES FOR ASYNCHRONOUS COOPERATIVE NETWORKS

In this chapter, firstly, a simple FIC scheme and orthogonal frequency-division multiplexing (OFDM) are used in a two-hop cooperative four relay network with asynchronism in the second stage. This approach can achieve the full available diversity and asymptotically full rate. This is followed by the description of an FIC with offset transmission scheme for a more practical cooperative network with asynchronism in the both stages. Finally, simulation results to demonstrate the behavior of the algorithm are presented.

4.1 Introduction

One of the key challenges to designing high-performance distributed space-time code systems is symbol-level synchronization among the relay nodes. In conventional point-to-point space time coded MIMO systems, co-located antennas obviate this issue. In cooperative systems, the antennas are separated by wireless links. One way is to use appropriate hardware and higher-layer protocols to ensure that transmissions from every participating relay are syn-

chronized, i.e. [49] and [46]. Unfortunately, it is difficult, and in most cases impossible, to achieve perfect synchronization among distributed transmitters. For example, asynchronism results from the nodes being in different locations and mismatch between their individual oscillators [69]. The scheme in [70] achieves robustness to asynchronism with a simple space-time coding cooperative scheme through the use of OFDM type transmission and a cyclic prefix (CP). However, this scheme has two weaknesses, the first disadvantage is that its end-to-end transmission rate is only one half. Therefore, the offset transmission scheme with FIC is applied in Section 4.2. The second disadvantage which is that this network just considers the timing error from one relay node to the destination node and assumes perfect symbol level synchronization in the transmission from the source to the relays, namely the signals are assumed to arrive at the relays at the same time. However, this assumption may not hold in practice. Therefore, in Section 4.3, two timing errors are considered in the channels, one from the source to a relay and a separate one from a relay to the destination. The timing errors are removed by exploiting the CP, and in order to decrease the complexity of decoding at the relay nodes, the CP removal is only implemented at the destination.

4.2 FIC Scheme for Cooperative Networks with Asynchronism in the Second Stage

4.2.1 OFDM Type Transmission with CP Scheme for A Cooperative Four Relay Network with Asynchronism in the Second Stage

The relay model for the four-path relay scheme is illustrated in Fig. 4.1, and h_{sr_i} ($i = 1, \dots, 4$) denote the channels from the transmitter to the four relays and h_{r_id} ($i = 1, \dots, 4$) denote the channels from the four relays to the

destination. It is assumed that τ_1 and τ_2 are delays from R3 to D and R4 to D, respectively. There is no direct link between the source and the destination as path loss or shadowing renders it unusable. The inter-relay channels are reciprocal, i.e. the gains from R1 and R3 to R2 and R4 are the same as those from R2 and R4 to R1 and R3, which are denoted h_{12} , h_{23} , h_{34} and h_{14} . The channels are assumed quasi-static flat-fading: h_{sri} and h_{rid} are i.i.d. zero-mean and unit-variance complex Gaussian random variables.

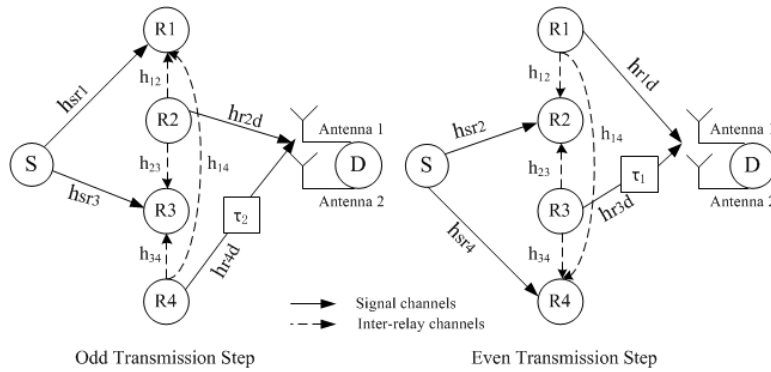


Figure 4.1. A two hop wireless communication network with offset transmission scheme showing asynchronous transmission due to timing error.

Implementation at the source node

To begin with, information bits are modulated into QPSK symbols $x_{i,j}$, and each set of K modulated symbols is fed as a block to an OFDM modulator of subcarriers. Denote two consecutive OFDM blocks as $\mathbf{x}_1 = [x_{0,1}, x_{1,1}, \dots, x_{K-1,1}]^T$ and $\mathbf{x}_2 = [x_{0,2}, x_{1,2}, \dots, x_{K-1,2}]^T$, where $(\cdot)^T$ denotes the vector transpose operator. Moreover, the first block \mathbf{x}_1 is modulated by a K -point inverse discrete fourier transform (IDFT), and the second block \mathbf{x}_2 is modulated by a K -point discrete fourier transform (DFT). Then each block is preceded by a CP with length $l_{CP} = 16$. The parameters τ_1 and τ_2 are assumed to be random integer variables in the range from 0 to 15 with uni-

form distribution, the length of CP is more than τ_1 and τ_2 , which are the maximum timing error of the signal from relay two and three to the destination node. Therefore, each OFDM symbol consists of $K + l_{CP}$ samples. Finally, the OFDM symbols are sent to the two relays. Denote two consecutive time domain OFDM symbols as $\bar{\mathbf{x}}_1$ and $\bar{\mathbf{x}}_2$, where $\bar{\mathbf{x}}_1$ consists of the IDFT(\mathbf{x}_1) and the corresponding CP, and $\bar{\mathbf{x}}_2$ consists of the IDFT(\mathbf{x}_2) and the corresponding CP.

Implementation at the relay nodes

At the relay nodes, assume the channel coefficients are constant during two OFDM symbol intervals. The received signal at relay i ($i = 1, 2$) for two successive OFDM symbol durations can be written as

$$\mathbf{y}_{i1} = \bar{\mathbf{x}}_1 h_{sr_i} + \mathbf{n}_{i1} \quad \text{and} \quad \mathbf{y}_{i2} = \bar{\mathbf{x}}_2 h_{sr_i} + \mathbf{n}_{i2}, \quad (4.2.1)$$

where \mathbf{n}_{i1} and \mathbf{n}_{i2} are the corresponding AWGN at the relay node i with zero-mean and unity-variance elements, in two successive OFDM symbol durations, respectively. Let P_1 be the transmission power at the source node. Because of the presence of AWGN, the mean power of the signal at a relay node is $P_1 + 1$, and P_2 is the average transmission power at every relay node. The relationship between P_1 and P_2 is:

$$P_1 = NP_2 = P/2, \quad (4.2.2)$$

where P is the total transmission power in the whole scheme and N is the number of the used relay nodes ($N = 2$) [44]. The relay nodes will process and transmit the received noisy signal according to the i^{th} column of the

relay encoding matrix \mathbf{S} ,

$$\mathbf{S} = \beta \begin{bmatrix} \mathbf{y}_{11} & -\mathbf{y}_{32}^* \\ \zeta(\mathbf{y}_{12}) & \zeta(\mathbf{y}_{31}^*) \end{bmatrix} \quad \text{or} \quad \beta \begin{bmatrix} \mathbf{y}_{21} & -\mathbf{y}_{42}^* \\ \zeta(\mathbf{y}_{22}) & \zeta(\mathbf{y}_{41}^*) \end{bmatrix} \quad (4.2.3)$$

where $\beta = \sqrt{\frac{P_2}{P_1+1}}$, $(\cdot)^*$ denotes complex conjugation, and $\zeta(\cdot)$ represents the time-reversal of the signal, i.e. $\zeta(\mathbf{y}(n)) \triangleq \mathbf{y}(L_s - n)$, $n = 0, 1, \dots, L_s - 1$, and $\zeta(\mathbf{y}(L_s)) \triangleq \mathbf{y}(0)$, L_s is the length of signal.

Implementation at the destination node

At the destination node, for the OFDM symbol one, the CP is removed first in a successive OFDM system. Then for the OFDM symbol two, the first step is removing the CP. And the second step is to shift the last 16 samples to the first 16 samples. Finally, the received signals are transformed by the N -point DFT. As mentioned before, because of timing errors, the signals from R3 or R4 arrive at the destination node τ_i ($i = 1, 2$) samples later than the signals from R1 or R2, respectively. Since l_{CP} is not less than τ_i , the orthogonality can still be maintained between the subcarriers. The delay in the time domain corresponds to a phase change in the frequency domain,

$$\mathbf{f}^{\tau_i} = [f_0^{\tau_i}, f_1^{\tau_i}, \dots, f_{K-1}^{\tau_i}]^T \quad (4.2.4)$$

where $f_k^{\tau_i} = \exp(-j2\pi k\tau_i/K)$ and $k = 0, 1, \dots, K - 1$. Let $\mathbf{z}_1 = [z_{0,1}, z_{1,1}, \dots, z_{K-1,1}]^T$ and $\mathbf{z}_2 = [z_{0,2}, z_{1,2}, \dots, z_{K-1,2}]^T$ be the received signals for two successive OFDM blocks at the destination node after the CP removal and the DFT transformation. Define $F_1 = DFT(IDFT(\mathbf{x}_1))$, $F_2 = DFT(-(IDFT(\mathbf{x}_2))^*)$, $F_3 = DFT(\zeta(DFT(\mathbf{x}_2)))$ and $F_4 = DFT(\zeta((IDFT(\mathbf{x}_1))^*))$. Taking hop 1 as an example, \mathbf{z}_1 and \mathbf{z}_2 can be written as

$$\mathbf{z}_1 = \beta[F_1 h_{sr1} h_{r1d} + F_2 \circ \mathbf{f}^{\tau_1} h_{sr3}^* h_{r3d} + \check{\mathbf{n}}_{11} h_{r1d} + \check{\mathbf{n}}_{32} \circ \mathbf{f}^{\tau_1} h_{r3d} + \mathbf{w}_1] \quad (4.2.5)$$

$$\mathbf{z}_2 = \beta[F_3 h_{sr_1} h_{r_1d} + F_4 \circ \mathbf{f}^{\tau_1} h_{sr_3}^* h_{r_3d} + \check{\mathbf{n}}_{12} h_{r_1d} + \check{\mathbf{n}}_{31} \circ \mathbf{f}^{\tau_1} h_{r_3d} + \mathbf{w}_2] \quad (4.2.6)$$

where \circ is the Hadamard product, and $\check{\mathbf{n}}_{ij}$ are the DFTs of \mathbf{n}_{ij} and $\mathbf{w}_j = (w_{k,j})$ are AWGN terms at the destination node with zero-mean and unit-variance. Using $(DFT(x))^* = IDFT(x)^*$, $(IDFT(x))^* = DFT(x^*)$ and $DFT(\zeta(DFT(x))) = IDFT(DFT(x))$, (4.2.5) and (4.2.6) can be rewritten as in the following Alamouti code at each subcarrier k , $0 \leq k \leq K - 1$

$$\begin{bmatrix} z_{k,1} \\ z_{k,2} \end{bmatrix} = \beta \begin{bmatrix} x_{k,1} & -x_{k,2}^* \\ x_{k,2} & x_{k,1}^* \end{bmatrix} \begin{bmatrix} h_{sr_1} h_{r_1d} \\ f_k^{\tau_1} h_{sr_3}^* h_{r_3d} \end{bmatrix} + \begin{bmatrix} v_{k,1} \\ v_{k,2} \end{bmatrix} \quad (4.2.7)$$

where $v_{k,j} = \beta(n_{k,1j} h_{r_1d} + n_{k,3j} \circ f_k^{\tau_1} h_{r_3d}) + w_{k,j}$. Then the Alamouti fast symbolwise ML decoding can be used at the destination node.

4.2.2 Interference Cancellation Scheme

In this part, a full interference cancellation scheme is proposed to remove completely the inter-relay inference from the other relays. Similarly to that in [62], assume that the relay nodes R1 and R3 receive at step $n-1$, at the same time, and the relay nodes R2 and R4 send the signal to the destination nodes. And assume all of the channel information is known by the receiver.

Therefore, the receiver signal at the destination can be obtained at the step $n-1$ as:

$$\begin{aligned} \mathbf{z}_{n-1,1} &= \beta \mathbf{y}_{21} h_{r_2d}(n-1) + \beta(-\mathbf{y}_{42}^*) h_{r_4d}(n-1) \mathbf{f}^{\tau_2} + \mathbf{w}_1 \\ \mathbf{z}_{n-1,2} &= \beta \zeta(\mathbf{y}_{22}) h_{r_2d}(n-1) + \beta \zeta(\mathbf{y}_{41}^*) h_{r_4d}(n-1) \mathbf{f}^{\tau_2} + \mathbf{w}_2 \end{aligned} \quad (4.2.8)$$

where \mathbf{w}_1 is the Gaussian noise at the destination, and \mathbf{y}_{21} , \mathbf{y}_{42} , \mathbf{y}_{22} and \mathbf{y}_{41} are the received signals at R2 and R4 at the step $n-2$, respectively, and they

are encoded by using (4.2.3), which are given by:

$$\begin{aligned}
 \mathbf{y}_{21} &= \bar{\mathbf{x}}_1 h_{sr_2}(n-2) + \check{\mathbf{n}}_{21} + \mathbf{y}_{11} h_{12} + (-\mathbf{y}_{32}^*) h_{32} \\
 \mathbf{y}_{41} &= \bar{\mathbf{x}}_1 h_{sr_4}(n-2) + \check{\mathbf{n}}_{41} + \mathbf{y}_{11} h_{14} + (-\mathbf{y}_{32}^*) h_{34} \\
 \mathbf{y}_{22} &= \bar{\mathbf{x}}_2 h_{sr_2}(n-2) + \check{\mathbf{n}}_{22} + \zeta(\mathbf{y}_{12}) h_{12} + \zeta(\mathbf{y}_{31}^*) h_{32} \\
 \mathbf{y}_{42} &= \bar{\mathbf{x}}_2 h_{sr_4}(n-2) + \check{\mathbf{n}}_{42} + \zeta(\mathbf{y}_{12}) h_{14} + \zeta(\mathbf{y}_{31}^*) h_{34}
 \end{aligned} \tag{4.2.9}$$

The received signals at the destination at step $n-2$ are also obtained as:

$$\begin{aligned}
 \mathbf{z}_{n-2,1} &= \beta \mathbf{y}_{11} h_{r_1 d}(n-2) + \beta (-\mathbf{y}_{32}^*) h_{r_3 d}(n-2) \mathbf{f}^{r_1} + \mathbf{w}_1 \\
 \mathbf{z}_{n-2,2} &= \beta \zeta(\mathbf{y}_{12}) h_{r_1 d}(n-2) + \beta \zeta(\mathbf{y}_{31}^*) h_{r_3 d}(n-2) \mathbf{f}^{r_1} + \mathbf{w}_2
 \end{aligned} \tag{4.2.10}$$

Because multiple antennas are available at the destination node, and given that the relays are sufficiently spatially separated, assume that it is possible to separate out the individual relay component within $\mathbf{z}_{n-2,1}$ and $\mathbf{z}_{n-2,2}$

$$\mathbf{z}_{n-2,1} = \mathbf{z}_{n-2,1,1} + \mathbf{z}_{n-2,1,2} \mathbf{f}^{r_1} + \mathbf{w}_1 \quad \text{and} \quad \mathbf{z}_{n-2,2} = \mathbf{z}_{n-2,2,1} + \mathbf{z}_{n-2,2,2} \mathbf{f}^{r_1} + \mathbf{w}_2 \tag{4.2.11}$$

as given by

$$\begin{aligned}
 \mathbf{z}_{n-2,1,1} &= \beta \mathbf{y}_{11} h_{r_1 d}(n-2) \quad \text{and} \quad \mathbf{z}_{n-2,1,2} = \beta (-\mathbf{y}_{32}^*) h_{r_3 d}(n-2) \\
 \mathbf{z}_{n-2,2,1} &= \beta \zeta(\mathbf{y}_{12}) h_{r_1 d}(n-2) \quad \text{and} \quad \mathbf{z}_{n-2,2,2} = \beta \zeta(\mathbf{y}_{31}^*) h_{r_3 d}(n-2)
 \end{aligned}$$

where the noise term is assumed to be insignificant. So

$$\begin{aligned}
 \mathbf{y}_{11} &= \frac{\mathbf{z}_{n-2,1,1}}{\beta h_{r_1 d}(n-2)} \quad \text{and} \quad -\mathbf{y}_{32}^* = \frac{\mathbf{z}_{n-2,1,2}}{\beta h_{r_3 d}(n-2)} \\
 \zeta(\mathbf{y}_{12}) &= \frac{\mathbf{z}_{n-2,2,1}}{\beta h_{r_1 d}(n-2)} \quad \text{and} \quad \zeta(\mathbf{y}_{31}^*) = \frac{\mathbf{z}_{n-2,2,2}}{\beta h_{r_3 d}(n-2)}
 \end{aligned} \tag{4.2.12}$$

Finally, substituting (4.2.12) and (4.2.9) into (4.2.8) gives:

$$\begin{aligned} \mathbf{z}_{n-1,1} = & \beta((\bar{\mathbf{x}}_1 h_{sr_2}(n-2) + \check{\mathbf{n}}_{21})h_{r_2d}(n-1) + h_{r_2d}(n-1))\left(\frac{\mathbf{z}_{n-2,1,1}}{\beta h_{r_1d}(n-2)}h_{12}\right. \\ & + \frac{\mathbf{z}_{n-2,1,2}}{\beta h_{r_3d}(n-2)}h_{32}) - (\bar{\mathbf{x}}_2^* h_{sr_4}^*(n-2) + \check{\mathbf{n}}_{42}^*)h_{r_4d}(n-1)\mathbf{f}^{\tau_2} - h_{r_4d} \\ & (n-1)\mathbf{f}^{\tau_2}\left(\frac{\mathbf{z}_{n-2,2,1}}{\beta h_{r_1d}(n-2)}h_{14} + \frac{\mathbf{z}_{n-2,2,2}}{\beta h_{r_3d}(n-2)}h_{34}\right)^* + \mathbf{w}_1 \end{aligned}$$

$$\begin{aligned} \mathbf{z}_{n-1,2} = & \beta((\zeta(\bar{\mathbf{x}}_2 h_{sr_2}(n-2)) + \zeta(\check{\mathbf{n}}_{22}))h_{r_2d}(n-1) + \zeta\left(\frac{\mathbf{z}_{n-2,2,1}}{\beta h_{r_1d}(n-2)}h_{12} + h_{32}\right. \\ & \left.\frac{\mathbf{z}_{n-2,2,2}}{\beta h_{r_3d}(n-2)}\right)h_{r_2d}(n-1) + (\zeta(\bar{\mathbf{x}}_1^* h_{sr_4}^*(n-2)) + \zeta(\check{\mathbf{n}}_{41}^*))\mathbf{f}^{\tau_2}h_{r_4d}(n-1) \\ & + h_{r_4d}(n-1)\mathbf{f}^{\tau_2}\zeta\left(\frac{\mathbf{z}_{n-2,1,1}}{\beta h_{r_1d}(n-2)}h_{14} + \frac{\mathbf{z}_{n-2,1,2}}{\beta h_{r_3d}(n-2)}h_{34}\right)^* + \mathbf{w}_2 \end{aligned} \quad (4.2.13)$$

From (4.2.13), the inter-relay interference is found as a recursive term in the received signal at the destination nodes. For example, (4.2.14) to (4.2.17) are IRI terms.

$$\beta h_{r_2d}(n-1) \left(\frac{\mathbf{z}_{n-2,1,1}}{\beta h_{r_1d}(n-2)}h_{12} + \frac{\mathbf{z}_{n-2,1,2}}{\beta h_{r_3d}(n-2)}h_{32} \right) \quad (4.2.14)$$

$$\beta h_{r_4d}(n-1)\mathbf{f}^{\tau_2} \left(\frac{\mathbf{z}_{n-2,2,1}}{\beta h_{r_1d}(n-2)}h_{14} + \frac{\mathbf{z}_{n-2,2,2}}{\beta h_{r_3d}(n-2)}h_{34} \right)^* \quad (4.2.15)$$

$$\beta h_{r_2d}(n-1)\zeta \left(\frac{\mathbf{z}_{n-2,2,1}}{\beta h_{r_1d}(n-2)}h_{12} + \frac{\mathbf{z}_{n-2,2,2}}{\beta h_{r_3d}(n-2)}h_{32} \right) \quad (4.2.16)$$

$$\beta h_{r_4d}(n-1)\mathbf{f}^{\tau_2}\zeta \left(\frac{\mathbf{z}_{n-2,1,1}}{\beta h_{r_1d}(n-2)}h_{14} + \frac{\mathbf{z}_{n-2,1,2}}{\beta h_{r_3d}(n-2)}h_{34} \right)^* \quad (4.2.17)$$

Therefore, these terms can be completely removed from (4.2.13) in order to cancel the IRI terms at the receiver, which are given by:

$$\begin{aligned} \mathbf{z}'_{n-1,1} = & \beta((\bar{\mathbf{x}}_1 h_{rs_2}(n-2) + \check{\mathbf{n}}_{21})h_{r_2d}(n-1) - (\bar{\mathbf{x}}_2^* h_{rs_4}^*(n-2) + \check{\mathbf{n}}_{42}^*)\mathbf{f}^{\tau_2} \\ & h_{r_4d}(n-1)) + \mathbf{w}_1 \end{aligned}$$

$$\begin{aligned} \mathbf{z}'_{n-1,2} = & \beta((\zeta(\bar{\mathbf{x}}_2 h_{rs_2}(n-2)) + \zeta(\check{\mathbf{n}}_{22}))h_{r_2d}(n-1) + (\zeta(\bar{\mathbf{x}}_1^* h_{rs_4}^*(n-2)) + \\ & \zeta(\check{\mathbf{n}}_{41}^*))h_{r_4d}(n-1)\mathbf{f}^{r_2}) + \mathbf{w}_2 \end{aligned} \quad (4.2.18)$$

As such, (4.2.18) has no IRI, only the desired signal and the noise. However, a very useful relationship for the received signal at the destination at the different odd-even time steps is found. And then the same method is used to obtain the received signal at step n at the destination node and cancel completely the IRI.

$$\begin{aligned} \mathbf{z}_{n,1} = & \beta((\bar{\mathbf{x}}_1 h_{sr_1}(n-1) + \check{\mathbf{n}}_{11})h_{r_1d}(n) + h_{r_1d}(n)\zeta(\frac{\mathbf{z}_{n-1,1,1}}{\beta h_{r_2d}(n-1)}h_{21} + \\ & \frac{\mathbf{z}_{n-1,1,2}}{\beta h_{r_4d}(n-1)}h_{41}) - (\bar{\mathbf{x}}_2^* h_{sr_3}^*(n-1) + \check{\mathbf{n}}_{32}^*)h_{r_3d}(n)\mathbf{f}^{r_1} - h_{r_3d}(n) \\ & \mathbf{f}^{r_1}(\frac{\mathbf{z}_{n-1,2,1}}{\beta h_{r_2d}(n-1)}h_{23} + \frac{\mathbf{z}_{n-1,2,2}}{\beta h_{r_4d}(n-1)}h_{43})^*) + \mathbf{w}_1 \\ \mathbf{z}_{n,2} = & \beta((\zeta(\bar{\mathbf{x}}_2 h_{sr_1}(n-1)) + \zeta(\check{\mathbf{n}}_{12}))h_{r_1d}(n) + h_{r_1d}(n)\zeta(\frac{\mathbf{z}_{n-1,2,1}}{\beta h_{r_2d}(n-1)}h_{21} + \\ & \frac{\mathbf{z}_{n-1,2,2}}{\beta h_{r_4d}(n-1)}h_{41}) + (\zeta(\bar{\mathbf{x}}_1^* h_{sr_3}^*(n-1)) + \zeta(\check{\mathbf{n}}_{31}^*))h_{r_3d}(n)\mathbf{f}^{r_1} + h_{r_3d}(n)\mathbf{f}^{r_1} \\ & \zeta(\frac{\mathbf{z}_{n-1,1,1}}{\beta h_{r_2d}(n-1)}h_{23} + \frac{\mathbf{z}_{n-1,1,2}}{\beta h_{r_4d}(n-1)}h_{43})^*) + \mathbf{w}_2 \end{aligned} \quad (4.2.19)$$

From (4.2.19), the IRI can easily be found as a recursive term in the received signal at the destination node. For example, (4.2.20) to (4.2.23) are IRI terms.

$$\beta h_{r_1d}(n) \left(\frac{\mathbf{z}_{n-1,1,1}}{\beta h_{r_2d}(n-1)}h_{21} + \frac{\mathbf{z}_{n-1,1,2}}{\beta h_{r_4d}(n-1)}h_{41} \right) \quad (4.2.20)$$

$$\beta h_{r_3d}(n)\mathbf{f}^{r_1} \left(\frac{\mathbf{z}_{n-1,2,1}}{\beta h_{r_2d}(n-1)}h_{23} + \frac{\mathbf{z}_{n-1,2,2}}{\beta h_{r_4d}(n-1)}h_{43} \right)^* \quad (4.2.21)$$

$$\beta h_{r_2d}(n-1)\zeta \left(\frac{\mathbf{z}_{n-2,2,1}}{\beta h_{r_1d}(n-2)}h_{12} + \frac{\mathbf{z}_{n-2,2,2}}{\beta h_{r_3d}(n-2)}h_{32} \right) \quad (4.2.22)$$

$$\beta h_{r_4d}(n-1)\mathbf{f}^{r_2}\zeta \left(\frac{\mathbf{z}_{n-2,1,1}}{\beta h_{r_1d}(n-2)}h_{14} + \frac{\mathbf{z}_{n-2,1,2}}{\beta h_{r_3d}(n-2)}h_{34} \right)^* \quad (4.2.23)$$

Therefore, these terms can be completely removed from (4.2.19) by using the same method, which are given by:

$$\begin{aligned} \mathbf{z}'_{n,1} &= \beta((\bar{\mathbf{x}}_1 h_{sr_1}(n-1) + \check{\mathbf{n}}_{11})h_{r_2d}(n) - (\bar{\mathbf{x}}_2^* h_{sr_3}^*(n-1) + \check{\mathbf{n}}_{32}^*)h_{r_3d}(n)\mathbf{f}^{r_1}) + \mathbf{w}_1 \\ \mathbf{z}'_{n,2} &= \beta((\zeta(\bar{\mathbf{x}}_2 h_{sr_1}(n-1)) + \zeta(\check{\mathbf{n}}_{12}))h_{r_1d}(n) + (\zeta(\bar{\mathbf{x}}_1^* h_{sr_3}^*(n-1)) + \zeta(\check{\mathbf{n}}_{31}^*)) \\ &\quad h_{r_3d}(n)\mathbf{f}^{r_1}) + \mathbf{w}_2 \end{aligned} \tag{4.2.24}$$

Compared with (4.2.18) and (4.2.24), they are found to have the same structure. However, according to the different odd-even steps, the odd-even channels are switched regularly. Therefore, the transmission symbols can be easily detected by the fast symbol-wise ML decoding.

4.2.3 Simulation Studies

In this section, the simulated performance of the asynchronous relay network using the FIC and OFDM approaches is shown. The performance is shown by the end-to-end BER using QPSK symbols. The total power per symbol transmission is fixed as P .

Fig. 4.2 compares the BER performance without FIC and with FIC. The advantage of using the FIC scheme is clear, the BER performance is significantly better than when the FIC approach is not used. The inter-relay interference considerably corrupts the transmission signal, thereby leading to the performance degradation.

Fig. 4.3 contrasts the performance of asynchronous Alamouti with a two relay network, without IRI, and that of the asynchronous FIC Alamouti with a four relay network. For the two hop cooperative four relay network, if the FIC scheme is used to completely remove the inter-relay interference, the performance closely matches the asynchronous Alamouti scheme without IRI. However, for the asynchronous Alamouti with two relay networks,

every transmission time slot is divided into two sub-slots: firstly, the source transmits to the relay nodes; secondly, the relay node sends the data to the destination. Therefore, the rate and bandwidth efficiency of this scheme is a half of the direct transmission. On the contrary, the later proposed method uses the two group relay nodes in order to retain the successive transmission signal from the source node, so full unity data rate can be approached when the number of symbols is large.

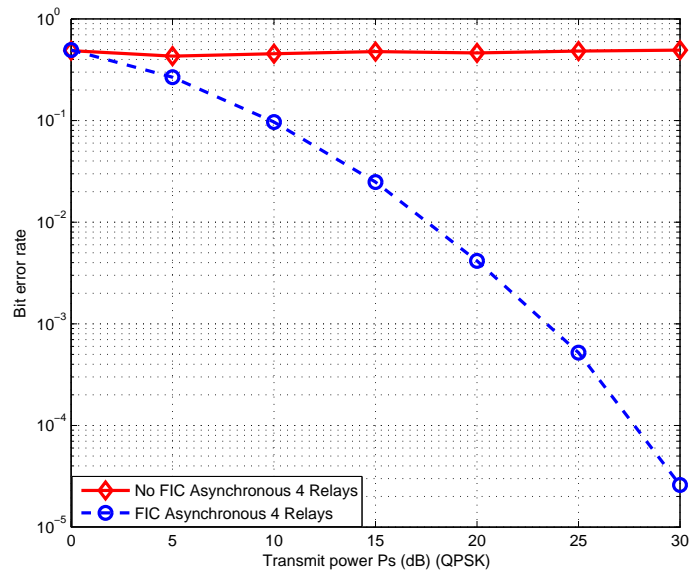


Figure 4.2. BER performance for no FIC and FIC approaches.

Fig. 4.4 compares the performance of asynchronous Alamouti with using 1/2 rate convolution coding and Viterbi decoding and that of the asynchronous FIC Alamouti without using 1/2 rate convolution coding and Viterbi decoding. From the figure, at a BER of 10^{-3} , the coded scheme requires approximately 18 dB while the uncoded scheme requires almost 23 dB. Obviously, the performance of the coded scheme is better than that of uncoded one, which is 5 dB, because of the coding gain. Therefore, using outer coding in the source and destination can improve end-to-end performance of the cooperative communication scheme.

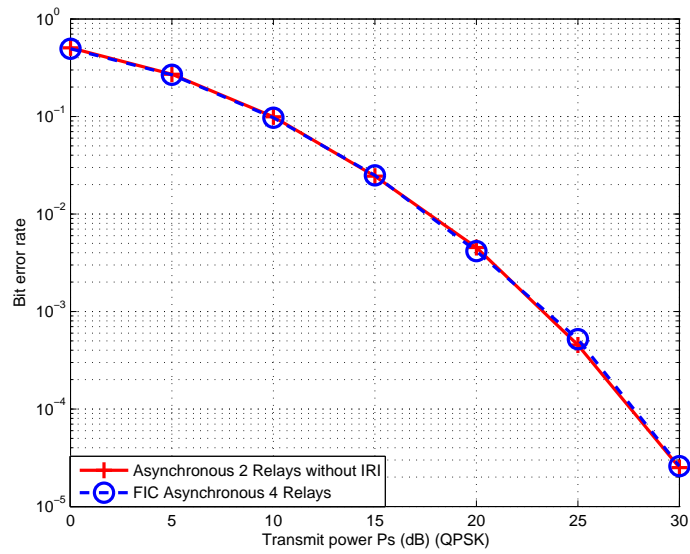


Figure 4.3. BER performance of the FIC relay network as compared to a half rate Alamouti relay network.

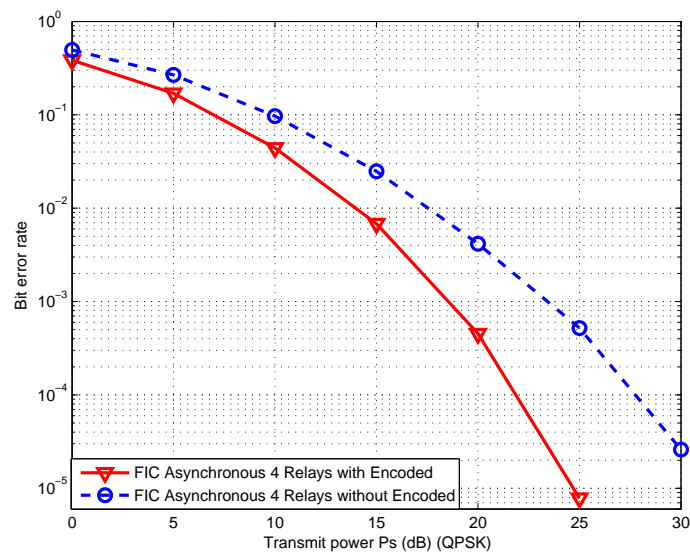


Figure 4.4. BER performance for FIC approaches with coded and uncoded transmission.

In the next section, a more practical asynchronous cooperative networks will be considered.

4.3 FIC Scheme for Cooperative Networks with Asynchronism in the Both Stages

In the last section, an offset transmission scheme with FIC and orthogonal frequency-division multiplexing (OFDM) was used in a cooperative network with asynchronism in the second stage. However, in practice, timing error should be considered at both stages. Therefore, in this section, OFDM type transmission with CP scheme is used at the source to combat timing errors from the source to the destination node. Moreover, through the use of time reversal in the destination node, CP removal is avoided at the relays in order to decrease the complexity of relay decoding.

4.3.1 OFDM Type Transmission with CP Scheme for A Cooperative Four Relay Network with Asynchronism in Both Stages

The relay model for the four-path relay scheme is illustrated in Fig. 4.5. The h_{sr_i} ($i = 1, \dots, 4$) denote the channels from the transmitter to the four relays and h_{r_id} ($i = 1, \dots, 4$) denote the channels from the four relays to the destination. And τ_1 and τ_2 are delays from S to R1 and R2, and τ_3 and τ_4 are delays from R3 and R4 to D, respectively. There is no direct link between the source and the destination as path loss or shadowing renders it unusable. The inter-relay channels are reciprocal, i.e. the gains from R1 and R3 to R2 and R4 are the same as those from R2 and R4 to R1 and R3, which are denoted h_{12} , h_{23} , h_{34} and h_{14} . And the channels are quasi-static flat-fading: h_{rs_i} and h_{r_id} are i.i.d. zero-mean and unit-variance complex Gaussian random variables. Two receive antennas 1 and 2 are assumed to be used to separate the signals from R1 (R2) and R3 (R4), respectively, since a beamforming technique can be applied at the destination node [71]. And Fig. 4.6 shows in block diagram form an architecture for the offset transmission relay network.

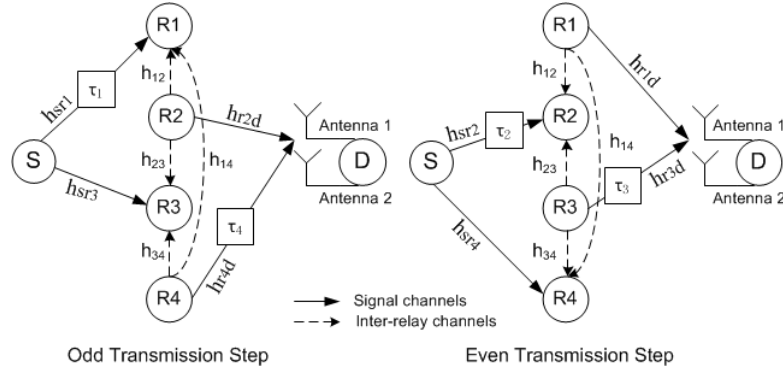


Figure 4.5. An offset transmission model for a four relay network with asynchronism.

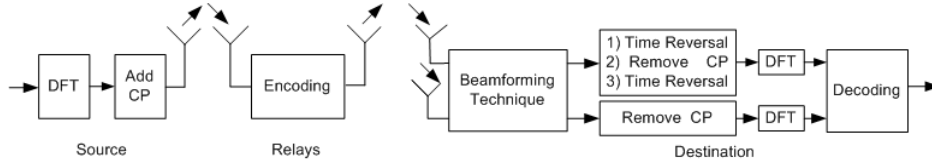


Figure 4.6. Architecture of the offset transmission relay network.

Implementation at the source node

To begin with, two consecutive OFDM blocks $\mathbf{x}_1 = [x_{0,1}, x_{1,1}, \dots, x_{K-1,1}]^T$ and $\mathbf{x}_2 = [x_{0,2}, x_{1,2}, \dots, x_{K-1,2}]^T$ are broadcasted, which are composed of a set of K modulated complex symbols $x_{i,j}$ $j = 1$ or 2 , which are modulated into time domain samples using DFT operations. Then each block is preceded by a CP with length l_{CP} . Thus, each OFDM symbol consists of $L_s = K + l_{CP}$ samples. The length of the CP is not less than the maximum of the possible relative timing errors (τ_{max}) of the signals which arrive at the destination node from the relay nodes is assumed. The two OFDM symbols with their corresponding CPs are denoted as $\bar{\mathbf{x}}_1$ and $\bar{\mathbf{x}}_2$.

Implementation at the relay nodes

At the relay nodes, assume the channel coefficients are constant during two OFDM symbol intervals. The received signal at relay i , $i = 1, 2$ for two

successive OFDM symbol durations can be written as

$$\mathbf{y}_{i1} = \bar{\mathbf{x}}_1 h_{sr_i} + \mathbf{n}_{i1} \quad \text{and} \quad \mathbf{y}_{i2} = \bar{\mathbf{x}}_2 h_{sr_i} + \mathbf{n}_{i2}, \quad (4.3.1)$$

where \mathbf{n}_{i1} and \mathbf{n}_{i2} are the corresponding AWGN at the relay node i with zero-mean and unity-covariance matrix, in two successive OFDM symbol durations, respectively. Let P_1 be the transmission power at the source node. Because of the presence of AWGN, the mean power of the signal at a relay node is $P_1 + 1$. And P_2 is the average transmission power at every relay node. The relationship between P_1 and P_2 is:

$$P_1 = NP_2 = P/2, \quad (4.3.2)$$

where P is the total transmission power in the whole scheme and N is the number of the used relay nodes ($N = 2$) [44]. The relay nodes will process and transmit the received noisy signal according to the i^{th} column of the relay encoding matrix \mathbf{S} ,

$$\mathbf{S} = \beta \begin{bmatrix} \zeta(\mathbf{y}_{11}) & -\mathbf{y}_{32}^* \\ \zeta(\mathbf{y}_{12}) & \mathbf{y}_{31}^* \end{bmatrix} \quad \text{or} \quad \beta \begin{bmatrix} \zeta(\mathbf{y}_{21}) & -\mathbf{y}_{42}^* \\ \zeta(\mathbf{y}_{22}) & \mathbf{y}_{41}^* \end{bmatrix} \quad (4.3.3)$$

where $\beta = \sqrt{\frac{P_2}{P_1+1}}$, $(\cdot)^*$ denotes complex conjugation, and $\zeta(\cdot)$ represents the time-reversal of the signal.

Implementation at the destination node

At the destination node, in order to separate out the individual relay transmitted signals, which arrive at the destination, a perfect beamforming technique is assumed to be used. The effect of errors in this operation are considered in the simulation section. The CP only needs to be removed at the destination node thereby reducing complexity as compared to schemes

which also remove the CP at the relays [72]. The destination processing consists of two paths for both sets of signals received from R1 and R3 and for the received signals from R2 and R4, as represented in Fig. 4.6. The first path consists of i) Time reversal; ii) Remove CP; and iii) Time reversal, and a second path in which only the CP is removed. After that, the two received signals are transformed by the K -point DFT. As mentioned before, because of timing errors, the signals from the source arrive at R1 or R2 τ_i ($i = 1, 2$) samples later than the signals from the source to R3 or R4, respectively. And the signals from R3 or R4 arrive at the destination node τ_i ($i = 3, 4$) samples later than the signals from R1 or R2, respectively. Since l_{CP} is not less than τ_{max} , the orthogonality between the subcarriers can still be maintained. The delay in the time domain corresponds to a phase change in the frequency domain,

$$\mathbf{f}^{\tau_i} = [f_0^{\tau_i}, f_1^{\tau_i}, \dots, f_{K-1}^{\tau_i}]^T \quad (4.3.4)$$

where $f_k^{\tau_i} = \exp(-j2\pi k\tau_i/K)$ and $k = 0, 1, \dots, K-1$. Let $\mathbf{z}_1 = [z_{0,1}, z_{1,1}, \dots, z_{K-1,1}]^T$ and $\mathbf{z}_2 = [z_{0,2}, z_{1,2}, \dots, z_{K-1,2}]^T$ be the received signals for two successive OFDM blocks at the destination node after the DFT transformation. And let $F_1 = \text{DFT}[\zeta(D(\text{DFT}(\mathbf{x}_1)))]$, $F_2 = \text{DFT}[D(-(\text{DFT}(\mathbf{x}_2))^*)]$, $F_3 = \text{DFT}[\zeta(D(\text{DFT}(\mathbf{x}_2)))]$ and $F_4 = \text{DFT}[D((\text{DFT}(\mathbf{x}_1))^*)]$, where $D(\cdot)$ denotes the cyclic delay, the maximum delay is 15. Taking transmission step one as an example, \mathbf{z}_1 and \mathbf{z}_2 can be written as

$$\mathbf{z}_1 = \gamma[F_1 h_{rs1} h_{r1d} + F_2 h_{rs3}^* h_{r3d}] + \mathbf{w}'_1 \quad (4.3.5)$$

$$\mathbf{z}_2 = \gamma[F_3 h_{rs1} h_{r1d} + F_4 h_{rs3}^* h_{r3d}] + \mathbf{w}'_2 \quad (4.3.6)$$

where $\mathbf{w}'_1 = \beta(\check{\mathbf{n}}_{11}g_1 + \check{\mathbf{n}}_{32} \circ \mathbf{f}^{\tau_3} h_{r3d}) + \mathbf{w}_1$ and $\mathbf{w}'_2 = \beta(\check{\mathbf{n}}_{12}h_{r1d} + \check{\mathbf{n}}_{31} \circ \mathbf{f}^{\tau_3} h_{r3d}) + \mathbf{w}_2$, $\gamma = \sqrt{\frac{P_1 P_2}{P_1 + 1}}$, and $\check{\mathbf{n}}_{ij}$ is the DFT of \mathbf{n}_{ij} and \mathbf{w}_j $j \in (1, 2)$ are AWGN vectors at the destination node with zero-mean and unit-covariance elements in

the j time slot. Using $\text{DFT}[\zeta(D(\text{DFT}(\mathbf{x})))] = \mathbf{x} \circ \mathbf{f}^{\tau_i^*}$, $\text{DFT}[D(-(\text{DFT}(\mathbf{x}))^*)] = -\mathbf{x}^* \circ \mathbf{f}^\tau$ and $\text{DFT}[D((\text{DFT}(\mathbf{x}))^*)] = \mathbf{x}^* \circ \mathbf{f}^\tau$, (4.3.5) and (4.3.6) can be rewritten as in the following Alamouti code at each subcarrier k , $0 \leq k \leq K - 1$

$$\begin{bmatrix} z_{k,1} \\ z_{k,2} \end{bmatrix} = \gamma \begin{bmatrix} x_{k,1} & -x_{k,2}^* \\ x_{k,2} & x_{k,1}^* \end{bmatrix} \begin{bmatrix} f_k^{\tau_1^*} h_{rs_1} h_{r_1d} \\ f_k^{\tau_3} h_{rs_3}^* h_{r_3d} \end{bmatrix} + \begin{bmatrix} v_{k,1} \\ v_{k,2} \end{bmatrix}$$

where $v_{k,j} = \beta(\check{n}_{k,1j} h_{r_1d} + \check{n}_{k,3j} \circ f_k^{\tau_3} h_{r_3d}) + w_{k,j}$. Then the Alamouti fast symbolwise ML decoding can be used at the destination node.

4.3.2 Interference Cancellation Scheme

In this part, a full interference cancellation scheme is used to remove completely the inter-relay inference from the other relays. Similarly to that in section 4.2.2, the relay nodes R1 and R3 is assumed to receive at the transmission step $n-1$, which corresponds to two time slots, and the relay nodes R2 and R4 send the signal to the destination node. And all of the channel information is assumed to know by the receiver.

Therefore, the received signals in the two time slots at the destination node at the transmission step $n-1$ as:

$$\begin{aligned} \mathbf{z}_{n-1,1} &= \beta \zeta(\mathbf{y}_{21}) h_{r_2d}(n-1) + \beta D((-\mathbf{y}_{42}^*) h_{r_4d}(n-1)) + \mathbf{w}_1 \\ \mathbf{z}_{n-1,2} &= \beta \zeta(\mathbf{y}_{22}) h_{r_2d}(n-1) + \beta D(\mathbf{y}_{41}^* h_{r_4d}(n-1)) + \mathbf{w}_2 \end{aligned} \quad (4.3.7)$$

where $\beta = \sqrt{\frac{P_2}{P_1+1}}$, and $\mathbf{z}_{i,j}$ denote the received signals in the j^{th} $j \in (1, 2)$ time slot at the i^{th} ($i = 1, 2, \dots, k$) transmission step, \mathbf{y}_{21} and \mathbf{y}_{42} , \mathbf{y}_{22} and \mathbf{y}_{41} are the received signal vectors at R2 and R4 at transmission step $n-2$,

respectively, and they are encoded by using (4.3.3), which are given by:

$$\begin{aligned}
\mathbf{y}_{21} &= \sqrt{P_1}D(\bar{\mathbf{x}}_1 h_{rs_2}(n-2)) + \check{\mathbf{n}}_{21} + \beta(\zeta(\mathbf{y}_{11})h_{12} + (-\mathbf{y}_{32}^*)h_{32}) \\
\mathbf{y}_{41} &= \sqrt{P_1}\bar{\mathbf{x}}_1 h_{rs_4}(n-2) + \check{\mathbf{n}}_{41} + \beta(\zeta(\mathbf{y}_{11})h_{14} + (-\mathbf{y}_{32}^*)h_{34}) \\
\mathbf{y}_{22} &= \sqrt{P_1}D(\bar{\mathbf{x}}_2 h_{rs_2}(n-2)) + \check{\mathbf{n}}_{22} + \beta(\zeta(\mathbf{y}_{12})h_{12} + \mathbf{y}_{31}^*h_{32}) \\
\mathbf{y}_{42} &= \sqrt{P_1}\bar{\mathbf{x}}_2 h_{rs_4}(n-2) + \check{\mathbf{n}}_{42} + \beta(\zeta(\mathbf{y}_{12})h_{14} + \mathbf{y}_{31}^*h_{34})
\end{aligned} \tag{4.3.8}$$

The received signals can be obtained at the destination node at transmission step $n-2$ as:

$$\begin{aligned}
\mathbf{z}_{n-2,1} &= \beta\zeta(\mathbf{y}_{11})h_{r_1d}(n-2) + \beta D((-\mathbf{y}_{32}^*)h_{r_3d}(n-2)) + \mathbf{w}_1 \\
\mathbf{z}_{n-2,2} &= \beta\zeta(\mathbf{y}_{12})h_{r_1d}(n-2) + \beta D((\mathbf{y}_{31}^*)h_{r_3d}(n-2)) + \mathbf{w}_2
\end{aligned} \tag{4.3.9}$$

ASSUMPTION 1: If multiple antennas are available at the destination node, and given that the relays are sufficiently spatially separated by using a perfect beamforming technique, it is assumed that it is possible to separate out the individual relay components within

$$\mathbf{z}_{n-2,1} = \mathbf{z}_{n-2,1,1} + \mathbf{z}_{n-2,1,2} + \mathbf{w}_1$$

$$\mathbf{z}_{n-2,2} = \mathbf{z}_{n-2,2,1} + \mathbf{z}_{n-2,2,2} + \mathbf{w}_2,$$

as given by

$$\begin{aligned}
\mathbf{z}_{n-2,1,1} &= \beta\zeta(\mathbf{y}_{11})h_{r_1d}(n-2) \\
\mathbf{z}_{n-2,1,2} &= \beta D((-\mathbf{y}_{32}^*)h_{r_3d}(n-2)) \\
\mathbf{z}_{n-2,2,1} &= \beta\zeta(\mathbf{y}_{12})h_{r_1d}(n-2) \\
\mathbf{z}_{n-2,2,2} &= \beta D((\mathbf{y}_{31}^*)h_{r_3d}(n-2))
\end{aligned} \tag{4.3.10}$$

where the noise term is assumed to be insignificant in the current development however this issue and the validity of this assumption is addressed

further in Section 4.3.3. Therefore,

$$\begin{aligned}\zeta(\mathbf{y}_{11}) &= \frac{\mathbf{z}_{n-2,1,1}}{\beta h_{r_1 d}(n-2)} & D(-\mathbf{y}_{32}^*) &= \frac{\mathbf{z}_{n-2,1,2}}{\beta D(h_{r_3 d}(n-2))} \\ \zeta(\mathbf{y}_{12}) &= \frac{\mathbf{z}_{n-2,2,1}}{\beta h_{r_1 d}(n-2)} & D(\mathbf{y}_{31}^*) &= \frac{\mathbf{z}_{n-2,2,2}}{\beta D(h_{r_3 d}(n-2))}\end{aligned}\quad (4.3.11)$$

Because the destination node knows the channel information and all of the delays, $-\mathbf{y}_{32}^*$ and \mathbf{y}_{31}^* can be obtained at the destination node by using: i) CP removal; ii) shifting the first length of τ (l_τ) samples as the last samples; and iii) adding a CP. These processes can be denoted by $\psi(\cdot)$. Finally, substituting (4.3.11) and (4.3.8) into (4.3.7) gives:

$$\begin{aligned}\mathbf{z}_{n-1,1} &= \beta h_{r_2 d}(n-1) [\zeta(\sqrt{P_1} D(\bar{\mathbf{x}}_1 h_{sr_2}(n-2)) + \check{\mathbf{n}}_{21} + \frac{\mathbf{z}_{n-2,1,1}}{h_{r_1 d}(n-2)} h_{12} + \\ &\quad \psi(\frac{\mathbf{z}_{n-2,1,2}}{h_{r_3 d}(n-2)} h_{32}))] - \beta D(h_{r_4 d}(n-1)) (\sqrt{P_1} \bar{\mathbf{x}}_2^* h_{sr_4}^*(n-2) + \check{\mathbf{n}}_{42}^* \\ &\quad + (\frac{\mathbf{z}_{n-2,2,1}}{h_{r_1 d}(n-2)} h_{14})^* + (\psi(\frac{\mathbf{z}_{n-2,2,2}}{h_{r_3 d}(n-2)} h_{34})^*)) + \mathbf{w}_1\end{aligned}\quad (4.3.12)$$

$$\begin{aligned}\mathbf{z}_{n-1,2} &= \beta h_{r_2 d}(n-1) [\zeta(\sqrt{P_1} D(\bar{\mathbf{x}}_2 h_{sr_2}(n-2)) + \check{\mathbf{n}}_{22} + \frac{\mathbf{z}_{n-2,2,1}}{h_{r_1 d}(n-2)} h_{12} + \\ &\quad \psi(\frac{\mathbf{z}_{n-2,2,2}}{h_{r_3 d}(n-2)} h_{32}))] + \beta D(h_{r_4 d}(n-1)) (\sqrt{P_1} \bar{\mathbf{x}}_1^* h_{sr_4}^*(n-2) + \check{\mathbf{n}}_{41}^* \\ &\quad + (\frac{\mathbf{z}_{n-2,1,1}}{h_{r_1 d}(n-2)} h_{14})^* + (\psi(\frac{\mathbf{z}_{n-2,1,2}}{h_{r_3 d}(n-2)} h_{34})^*)) + \mathbf{w}_2\end{aligned}\quad (4.3.13)$$

From (4.3.12) and (4.3.13), the inter-relay interference is a recursive term in the received signal at the destination node. For example, (4.3.14), (4.3.15), (4.3.16) and (4.3.17) are IRI terms, which are functions only of the previous output values.

$$\beta h_{r_2 d}(n-1) \zeta(\frac{\mathbf{z}_{n-2,1,1}}{h_{r_1 d}(n-2)} h_{12} + \psi(\frac{\mathbf{z}_{n-2,1,2}}{h_{r_3 d}(n-2)} h_{32})) \quad (4.3.14)$$

$$\beta D(h_{r_4 d}(n-1)) (\frac{\mathbf{z}_{n-2,2,1}}{h_{r_1 d}(n-2)} h_{14} + \psi(\frac{\mathbf{z}_{n-2,2,2}}{h_{r_3 d}(n-2)} h_{34})^*) \quad (4.3.15)$$

$$\beta h_{r_2d}(n-1) \zeta \left(\frac{\mathbf{z}_{n-2,1,1}}{h_{r_1d}(n-2)} h_{12} + \psi \left(\frac{\mathbf{z}_{n-2,2,2}}{h_{r_3d}(n-2)} \right) h_{32} \right) \quad (4.3.16)$$

$$\beta D(h_{r_4d}(n-1)) \left(\frac{\mathbf{z}_{n-2,2,1}}{h_{r_1d}(n-2)} h_{14} + \psi \left(\frac{\mathbf{z}_{n-2,1,2}}{h_{r_3d}(n-2)} \right) h_{34} \right)^* \quad (4.3.17)$$

Therefore, these terms can be completely removed in order to cancel the IRI at the receiver, which are given by:

$$\begin{aligned} \mathbf{z}'_{n-1,1} &= \beta h_{r_2d}(n-1) [\zeta(\sqrt{P_1} D(\bar{\mathbf{x}}_1 h_{sr_2}(n-2)) + \check{\mathbf{n}}_{21})] - \beta D(h_{r_4d}(n-1)) \\ &\quad (\sqrt{P_1} \bar{\mathbf{x}}_2^* h_{sr_4}^*(n-2) + \check{\mathbf{n}}_{42}^*) + \mathbf{w}_1 \\ \mathbf{z}'_{n-1,2} &= \beta h_{r_2d}(n-1) [\zeta(\sqrt{P_1} D(\bar{\mathbf{x}}_2 h_{sr_2}(n-2)) + \check{\mathbf{n}}_{22})] + \beta D(h_{r_4d}(n-1)) \\ &\quad (\sqrt{P_1} \bar{\mathbf{x}}_1^* h_{sr_4}^*(n-2) + \check{\mathbf{n}}_{41}^*) + \mathbf{w}_2 \end{aligned} \quad (4.3.18)$$

As such, (4.3.18) has no IRI, with the desired signal and the noise. And the same method can be used to obtain the received signal at transmission step n at the destination node.

$$\begin{aligned} \mathbf{z}_{n,1} &= \beta h_{r_1d}(n) [\zeta(\sqrt{P_1} D(\bar{\mathbf{x}}_1 h_{sr_1}(n-1)) + \check{\mathbf{n}}_{11} + \frac{\mathbf{z}_{n-1,1,1}}{h_{r_2d}(n-1)} h_{21} + h_{41} \\ &\quad \psi \left(\frac{\mathbf{z}_{n-1,1,2}}{h_{r_4d}(n-1)} \right))] - \beta D(h_{r_3d}(n)) (\sqrt{P_1} \bar{\mathbf{x}}_2^* h_{sr_3}^*(n-1) + \check{\mathbf{n}}_{32}^* \\ &\quad + \left(\frac{\mathbf{z}_{n-1,2,1}}{h_{r_2d}(n-1)} h_{23} \right)^* + \left(\psi \left(\frac{\mathbf{z}_{n-1,2,2}}{h_{r_4d}(n-1)} \right) h_{43} \right)^*) + \mathbf{w}_1 \end{aligned} \quad (4.3.19)$$

$$\begin{aligned} \mathbf{z}_{n,2} &= \beta h_{r_1d}(n) [\zeta(\sqrt{P_1} D(\bar{\mathbf{x}}_2 h_{sr_1}(n-1)) + \check{\mathbf{n}}_{12} + \frac{\mathbf{z}_{n-1,2,1}}{h_{r_2d}(n-1)} h_{21} + h_{41} \\ &\quad \psi \left(\frac{\mathbf{z}_{n-1,2,2}}{h_{r_4d}(n-1)} \right))] + \beta D(h_{r_3d}(n)) (\sqrt{P_1} \bar{\mathbf{x}}_1^* h_{sr_3}^*(n-1) + \check{\mathbf{n}}_{31}^* \\ &\quad + \left(\frac{\mathbf{z}_{n-1,1,1}}{h_{r_2d}(n-1)} h_{23} \right)^* + \left(\psi \left(\frac{\mathbf{z}_{n-1,1,2}}{h_{r_4d}(n-1)} \right) h_{43} \right)^*) + \mathbf{w}_2 \end{aligned} \quad (4.3.20)$$

From (4.3.19) and (4.3.20), the IRI is a recursive term in the received signal at the destination node. For example, (4.3.21), (4.3.22), (4.3.23) and (4.3.24)

are IRI terms.

$$\beta h_{r_1d}(n) \zeta \left(\frac{\mathbf{z}_{n-1,1,1}}{h_{r_2d}(n-1)} h_{21} + \psi \left(\frac{\mathbf{z}_{n-1,1,2}}{h_{r_4d}(n-1)} \right) h_{41} \right) \quad (4.3.21)$$

$$\beta D(h_{r_3d}(n)) \left(\frac{\mathbf{z}_{n-1,2,1}}{h_{r_2d}(n-1)} h_{23} + \psi \left(\frac{\mathbf{z}_{n-1,2,2}}{h_{r_4d}(n-1)} \right) h_{43} \right)^* \quad (4.3.22)$$

$$\beta h_{r_1d}(n) \zeta \left(\frac{\mathbf{z}_{n-1,1,1}}{h_{r_2d}(n-1)} h_{21} + \psi \left(\frac{\mathbf{z}_{n-1,2,2}}{h_{r_4d}(n-1)} \right) h_{41} \right) \quad (4.3.23)$$

$$\beta D(h_{r_3d}(n)) \left(\frac{\mathbf{z}_{n-1,2,1}}{h_{r_2d}(n-1)} h_{23} + \psi \left(\frac{\mathbf{z}_{n-1,1,2}}{h_{r_4d}(n-1)} \right) h_{43} \right)^* \quad (4.3.24)$$

Therefore, these terms can be completely removed from (4.3.19) and (4.3.20) by using the same method, which are given by:

$$\begin{aligned} \mathbf{z}'_{n,1} &= \beta h_{r_1d}(n-1) [\zeta(\sqrt{P_1} D(\bar{\mathbf{x}}_1 h_{sr_1}(n-1)) + \check{\mathbf{n}}_{11})] - \beta D(h_{r_3d}(n)) (\sqrt{P_1} \\ &\quad \bar{\mathbf{x}}_2^* h_{sr_3}^*(n-1) + \check{\mathbf{n}}_{32}^*) + \mathbf{w}_1 \\ \mathbf{z}'_{n,2} &= \beta h_{r_1d}(n) [\zeta(\sqrt{P_1} D(\bar{\mathbf{x}}_2 h_{sr_1}(n-1)) + \check{\mathbf{n}}_{12})] + \beta D(h_{r_3d}(n-1)) (\sqrt{P_1} \\ &\quad \bar{\mathbf{x}}_1^* h_{sr_3}^*(n-1) + \check{\mathbf{n}}_{31}^*) + \mathbf{w}_2 \end{aligned} \quad (4.3.25)$$

Comparing (4.3.18) with (4.3.25), they have the same structure. However, according to the different offset transmission steps, the alternate channels are switched regularly. Therefore, the transmission symbols can be easily detected by the fast symbol-wise ML decoding.

4.3.3 Simulation Studies

In this section, the simulated performance of the asynchronous relay network will be shown by using the offset transmission with FIC and OFDM approaches. The performance is shown by the end-to-end BER using BPSK symbols. And $K = 64$ and $l_{CP} = 16$ are assumed. The delays τ_i $i \in (1, 2, 3, 4)$ are chosen randomly from 0 to 15 with the uniform distribution. The total power per symbol transmission is fixed as P .

Fig. 4.7 compares, firstly, the BER performance without FIC and with FIC. The advantage of using the FIC scheme is clear, the BER performance is significantly better than without FIC approach. In fact, without using FIC the scheme is unusable. The inter-relay interference considerably corrupts the transmission signal, thereby leading to the performance degradation. Secondly, the performance of Alamouti in an asynchronous two relay network without IRI is contrasted with that of the FIC Alamouti in an asynchronous four relay network with IRI. For the cooperative four relay network, if the FIC scheme is used to completely remove the inter-relay interference, the performance closely matches the Alamouti type scheme without IRI.

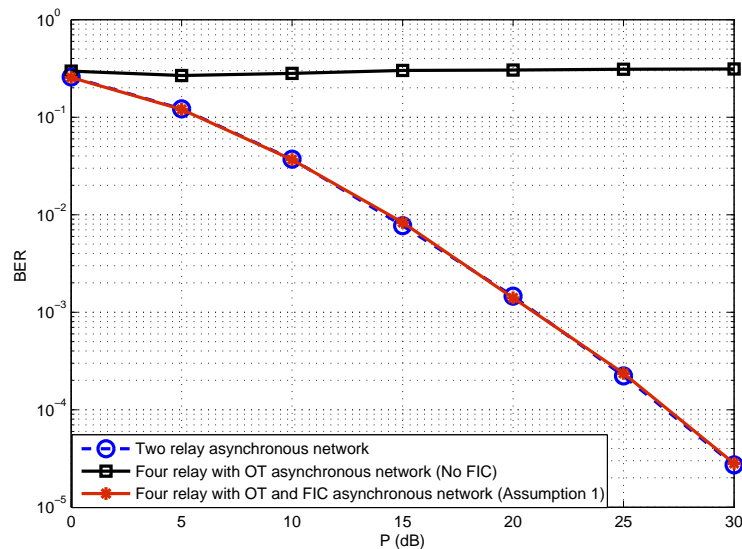


Figure 4.7. BER performance for no FIC and FIC approaches.

In Fig. 4.8, however, for the Alamouti type scheme with two relay networks, every transmission time slot is divided into two sub-slots. Therefore, the rate and bandwidth efficiency of this scheme is a half of the direct transmission. On the contrary, the proposed method uses the two group relay nodes in order to retain the successive transmission signal from the source node, so the full unity data rate can be obtained when the number of symbols is large.

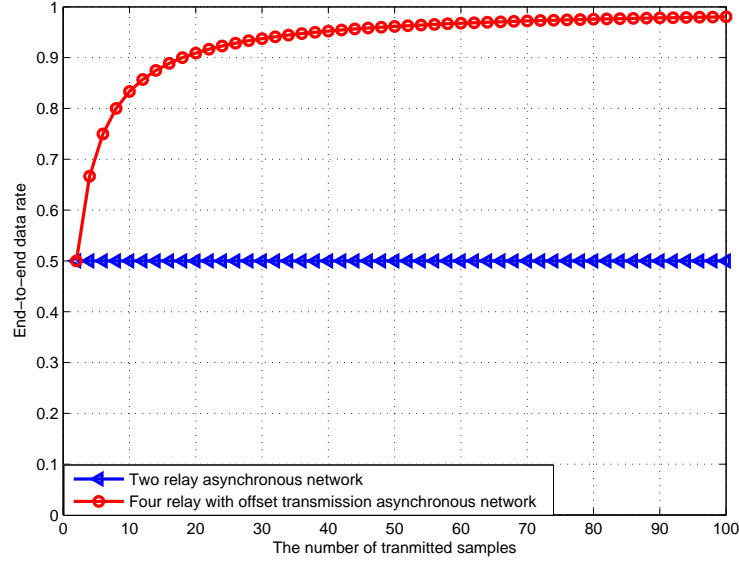


Figure 4.8. End-to-end transmission rate.

In the next simulation study the effect of relaxing Assumption 1 is considered. To model the effect that even with multiple antennas at the destination node there will be uncertainties in the values of $\mathbf{z}_{n-2,1,1}$, $\mathbf{z}_{n-2,1,2}$, $\mathbf{z}_{n-2,2,1}$ and $\mathbf{z}_{n-2,2,2}$ in (4.3.10), due for example to estimation errors in beamforming, the noise vectors is added to yield

$$\mathbf{z}_{n-1,1,1} = \beta\zeta(\mathbf{y}_{21})h_{r_2d}(n-1) + \mathbf{n}'_1 \quad \text{and} \quad \mathbf{z}_{n-1,1,2} = \beta D((-\mathbf{y}_{42}^*)h_{r_4d}(n-1)) + \mathbf{n}'_2$$

$$\mathbf{z}_{n-1,2,1} = \beta\zeta(\mathbf{y}_{22})h_{r_2d}(n-1) + \mathbf{n}'_1 \quad \text{and} \quad \mathbf{z}_{n-1,2,2} = \beta D(\mathbf{y}_{41}^*)h_{r_4d}(n-1) + \mathbf{n}'_2,$$

where all the elements of \mathbf{n}'_1 and \mathbf{n}'_2 are chosen to have noise powers at the relative levels of either -6 dB or -3 dB or 0 dB, and these three cases are denoted Assumption 2, Assumption 3 and Assumption 4. The degradation in BER is shown in Fig. 5, for example, at $\text{BER} = 10^{-3}$ the required transmit power increases from 21.5 dB to 22.5 dB and to 25 dB for the three cases.

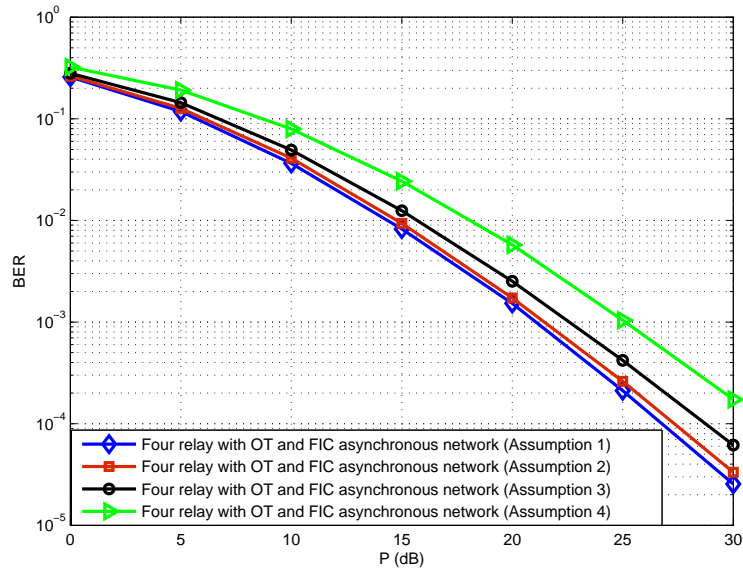


Figure 4.9. BER performance of the four relay with offset transmission and FIC and varying uncertainty in Assumption 1.

4.4 Summary

In this chapter, full diversity and improved end-to-end transmission rate can be achieved because an offset transmission with FIC scheme was used. Using offset transmission, the source can serially transmit data to the destination. However, the four-path relay scheme may suffer from IRI which is caused by the simultaneous transmission of the source and another group of relays. Therefore, the FIC scheme was used to fully remove these IRI terms. Then the offset transmission with FIC scheme was applied in cooperative network with asynchronism in the second/both stage(s). And a new OFDM and CP scheme was discussed to mitigate the timing error from the source to the relays and from the relays to the destination, which can avoid the CP removal at the relays. In the next chapter, multi-relay selection will be shown to decrease the outage probability.

OUTAGE PROBABILITY OF MULTI-RELAY SELECTION WITHOUT INTERFERENCE

In this chapter, firstly, the local measurements of the instantaneous channel conditions are used to select the best relay pair from a set of N available relays, which either come from the same cluster or different clusters, and then these best relays are used with the Alamouti code to improve the cooperative diversity and decrease the outage probability. This best relay pair selection scheme is shown to have robustness against feedback error in the relay selection and to outperform a scheme based on selecting only the best single relay. Secondly, the best four relays from a set of N available relays is chosen, by using local measurements of the instantaneous channel conditions, to further reduce the outage probability.

5.1 Introduction

In a cooperative relay network, many relays can help the source to transmit to the destination, however, sometimes some relays provide a poor channel quality which can affect the transmission quality to a certain extent [73]. Therefore, the use of relay selection schemes is attracting considerable attention to overcome this problem and preserve the potential diversity gains, [74], [75], [16], [76] and [77]. In [74], the authors derived simple expressions for outage probabilities for several DF cooperative diversity schemes with single relay selection. This method however requires high complexity at the relays and destination. In [75], exact outage and diversity performance expressions for the best relay selection are provided for a wide range of SNR regimes in the context of an AF transmission protocol. The work in [16] relies on using instantaneous end-to-end wireless channel conditions to obtain the best single relay for cooperative diversity. This work was extended in [76] to obtain outage-optimal opportunistic relaying in the context of selecting a single relay from a set of N available relays. They show that cooperative diversity gain is achieved even when certain relays remain inactive. However, using a single best relay is not always sufficient to satisfy the required outage probability at a destination node. Moreover, these works have not considered feedback error within the relay selection process, which means sometimes the best relay cannot be chosen because the wrong enable feedback information is received from the destination node. In the next section, the outage probability analysis of the best relay pair selection will be presented.

5.2 The Best Relay Pair Selection Without Interference

5.2.1 System Model

As is shown in Fig. 5.1, cooperative communication over Rayleigh flat-fading channels is considered. There is one source node and one destination node and many relay nodes, all equipped with single half-duplex antennas. Perfect channel state information is assumed to be known at the destination node, thereby avoiding considering the errors and associated reduction in outage probability performance which would be introduced when training data is used to extract such information [23] and [78]. In practice, the available relays might be clustered in physically different locations. Therefore, in the situation where the channel strengths might vary for the different relay clusters, i.e., Fig. 5.1(a) shows a scenario where N relay nodes and $N - 1$ relay nodes belong to different spatially separated clusters is considered, and Fig. 5.1(b) shows a case where N relay nodes come from the same cluster, respectively. This situation for Fig. 5.1(b) would be encountered in distributed space time code transmission when the target is to maximize spatial diversity between the paths, and the relays within each cluster are tightly packed so that selection from two different cluster locations is likely to be beneficial.

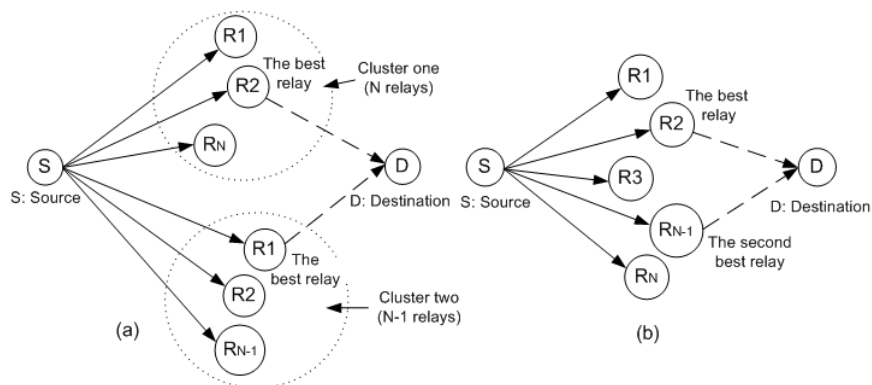


Figure 5.1. (a) shows the best relay pair selection from different clusters; (b) illustrates the best relay pair selection from the same cluster.

In the first hop, the source node transmits the signal x to the relays. The received signal at the i^{th} relay is given by

$$y_{sr_i} = \sqrt{E_s} h_{sr_i} x + n_{r_i}, \quad (5.2.1)$$

where E_s is the average energy per symbol, h_{sr_i} is the channel gain between the source and the i^{th} relay node, and n_{r_i} is the complex additive white Gaussian noise at the i^{th} relay node. In the second hop of cooperation, the i^{th} relay amplifies its received signal and forwards it to the destination through $h_{r_i d}$, which is the channel gain between the i^{th} relay node and the destination. The received signal at the destination node from the i^{th} relay is

$$y_{r_i d} = \sqrt{P_i} h_{r_i d} y_{sr_i} + n_d, \quad (5.2.2)$$

where n_d is the complex additive white Gaussian noise at the destination. The i^{th} relay gain denoted by $\sqrt{P_i}$ is calculated from $P_i = E_s / (E_s |h_{sr_i}|^2 + N_0)$, where N_0 is the noise variance [17]. Therefore, the instantaneous equivalent end-to-end SNR for the i^{th} relay can be written as

$$\gamma_{D_i} = \frac{\gamma_{sr_i} \gamma_{r_i d}}{1 + \gamma_{sr_i} + \gamma_{r_i d}}, \quad (5.2.3)$$

where $\gamma_{sr_i} = |h_{sr_i}|^2 E_s / N_0$ and $\gamma_{r_i d} = |h_{r_i d}|^2 E_s / N_0$ are the instantaneous SNR of the $S - R_i$ and $R_i - D$ links, respectively.

For the Rayleigh flat-fading channels, the probability density function (PDF) and the cumulative distribution function (CDF) of the SNR in the $u \in (sr_i, r_i d)$ links are given by

$$f_{\gamma_u}(\gamma) = \frac{1}{\tilde{\gamma}_u} e^{-\gamma/\tilde{\gamma}_u}, \quad (5.2.4)$$

$$F_{\gamma_u}(\gamma) = 1 - e^{-\gamma/\tilde{\gamma}_u}, \quad (5.2.5)$$

where $\bar{\gamma}_u$ denotes the mean SNR for all links. According to [79],

$$\gamma_i = \min(\gamma_{sr_i}, \gamma_{r_id}) > \frac{\gamma_{sr_i} \gamma_{r_id}}{1 + \gamma_{sr_i} + \gamma_{r_id}}. \quad (5.2.6)$$

Next, because the best pair relay selection scheme is used, the maximum ratio combiner (MRC) is employed at the destination node [79]. The practical implementation of the MRC may, however, incur a capacity penalty due to the need to adopt a time multiplexing approach to transmission between the relays and the destination node; however, this can be mitigated by adopting an orthogonal transmission scheme, i.e. distributed space-time coding. This section focuses on selection of two relays; however, that further improvement could be achieved by selecting three or even four relays, but thus may incur practical overheads such as increased complexity in synchronization. Therefore, the lower and upper bound for the equivalent SNR can be given as

$$\frac{1}{2} \sum_{i \in N_s} \gamma_i = \gamma_{low} \leq \gamma_D = \sum_{i \in N_s} \gamma_{D_i} < \gamma_{up} = \sum_{i \in N_s} \gamma_i, \quad (5.2.7)$$

where N_s denotes the set of relay indices for the relays chosen in the multi-relay selection scheme. The upper bound SNR is more suitable for analysis in the medium and high SNR ranges [79].

5.2.2 Outage Probability Analysis

In order to calculate the PDF and CDF for the end-to-end SNR, γ_{up} as given in (5.2.7), the first step is to obtain the moment generating function (MGF) of γ_{up} . In this section, firstly, the fixed relay case is considered and then the best relay pair selection schemes for cooperative systems are presented.

Fixed Relay

The MGF of γ_{up} can be obtained as

$$M_{\gamma_{up}}(s) = \prod_{i=1}^N M_{\gamma_i}(s), \quad (5.2.8)$$

where s is the Laplace transform complex variable. In order to obtain the MGF for the $S-R-D$ link, the CDF of $\gamma_i = \min(\gamma_{sr_i}, \gamma_{r_id})$ can be expressed as [80]

$$\begin{aligned} F_{\gamma_i}(\gamma) &= 1 - Pr(\gamma_{sr_i} > \gamma)Pr(\gamma_{r_id} > \gamma) \\ &= 1 - [1 - Pr(\gamma_{sr_i} \leq \gamma)][1 - Pr(\gamma_{r_id} \leq \gamma)] \\ &= 1 - [1 - F_{\gamma_{sr_i}}(\gamma)][1 - F_{\gamma_{r_id}}(\gamma)]. \end{aligned} \quad (5.2.9)$$

Substituting (5.2.5) with the appropriate index into (5.2.9) yields

$$F_{\gamma_i}(\gamma) = 1 - e^{-\gamma/\bar{\gamma}_{C_i}}, \quad (5.2.10)$$

where $\bar{\gamma}_{C_i} = \frac{\bar{\gamma}_{sr_i}\bar{\gamma}_{r_id}}{\bar{\gamma}_{sr_i} + \bar{\gamma}_{r_id}}$. Since independent and identically distributed (i.i.d.) Rayleigh fading relay channels are assumed, then $\bar{\gamma}_{sr_i} = \bar{\gamma}_{r_id} = \bar{\gamma}_0 = E_s/N_0$, and $\bar{\gamma}_{C_i} = \bar{\gamma}_C = 0.5\bar{\gamma}_0$. Therefore, the PDF of γ_i can be obtained by taking the derivative of the CDF (5.2.10) as

$$f_{\gamma_i}(\gamma) = \frac{1}{\bar{\gamma}_{C_i}} e^{-\gamma/\bar{\gamma}_{C_i}}. \quad (5.2.11)$$

Then using the definition of the MGF given by

$$M_r(s) = E[e^{-s\gamma}] = \int_0^{\infty} e^{-s\gamma} f_{\gamma}(\gamma) d\gamma, \quad (5.2.12)$$

the MGF of γ_i can be obtained as

$$M_{r_i}(s) = (1 + \bar{\gamma}_{C_i}s)^{-1}. \quad (5.2.13)$$

Finally, substituting (5.2.13) into (5.2.8), the expression for the MGF of the end-to-end SNR can be expressed as

$$M_{\gamma_{up}}(s) = \prod_{i=1}^N (1 + \bar{\gamma}_{C_i} s)^{-1} = (1 + 0.5\bar{\gamma}_0 s)^{-N}. \quad (5.2.14)$$

The following section will consider best relay pair selection from two spatially distinct clusters of relays.

Best Two Relay Pair Selection from Different Clusters

In this approach, one best relay is first selected from N available relays in cluster one, and then the other best single relay is selected from $N - 1$ available relays in cluster two, see Fig. 5.1(a). According to the relay selection scheme in [16], the general expression for determining the best relay from either cluster is

$$b^n = \arg \max_{i \in R^n} \{\gamma_i^n\}, \quad (5.2.15)$$

where $n = 1, 2$, $R^1 = \{1, 2, \dots, N\}$ and $R^2 = \{1, 2, \dots, N - 1\}$, γ_i^n is the instantaneous SNR for the relay i in cluster n . Therefore, the instantaneous SNR for the best two relays are obtained by

$$\gamma_{b^1} = \max_{i \in R^1} \{\gamma_i^1\} = \max_{i \in R^1} \{\min(\gamma_{sr_i}^1, \gamma_{r_i d}^1)\} \quad (5.2.16)$$

and

$$\gamma_{b^2} = \max_{i \in R^2} \{\gamma_i^2\} = \max_{i \in R^2} \{\min(\gamma_{sr_i}^2, \gamma_{r_i d}^2)\}. \quad (5.2.17)$$

Therefore, the CDF of γ_{b^1} and γ_{b^2} can be expressed as, respectively,

$$F_{\gamma_{b^1}}(\gamma) = [F_{\gamma_i^1}(\gamma)]^N = [1 - e^{-\gamma/\bar{\gamma}_C^1}]^N \quad (5.2.18)$$

$$F_{\gamma_{b^2}}(\gamma) = [F_{\gamma_i^2}(\gamma)]^{N-1} = [1 - e^{-\gamma/\bar{\gamma}_C^2}]^{N-1}. \quad (5.2.19)$$

Firstly, all relay links can be assumed to have the same average SNR, namely, $\bar{\gamma}_C^1 = \bar{\gamma}_C^2 = \bar{\gamma}_C$. Then the PDF of γ_{b1} and γ_{b2} can be obtained by using the derivative of the CDF, yielding

$$f_{\gamma_{b1}}(\gamma) = N f_{\gamma_i^1}(\gamma) [f_{\gamma_i^1}(\gamma)]^{N-1} = \frac{N}{\bar{\gamma}_C} e^{-\gamma/\bar{\gamma}_C} [1 - e^{-\gamma/\bar{\gamma}_C}]^{N-1} \quad (5.2.20)$$

and

$$f_{\gamma_{b2}}(\gamma) = (N-1) f_{\gamma_i^2}(\gamma) [f_{\gamma_i^2}(\gamma)]^{N-2} = \frac{N-1}{\bar{\gamma}_C} e^{-\gamma/\bar{\gamma}_C} [1 - e^{-\gamma/\bar{\gamma}_C}]^{N-2}. \quad (5.2.21)$$

Then substituting (5.2.20) and (5.2.21) into (5.2.12) and using the binomial expansion and after some manipulations the MGF of γ_{b1} and γ_{b2} can be obtained as

$$M_{\gamma_{b1}}(s) = \sum_{n=1}^N \binom{N}{n} \frac{n(-1)^{n-1}}{n + \bar{\gamma}_C s} \quad (5.2.22)$$

and

$$M_{\gamma_{b2}}(s) = \sum_{m=1}^{N-1} \binom{N-1}{m} \frac{m(-1)^{m-1}}{m + \bar{\gamma}_C s}, \quad (5.2.23)$$

where $\binom{N}{n} = N!/[n!(N-n)!]$ is the binomial coefficient. The expression for the MGF of γ_{up} for the end-to-end SNR can be obtained as

$$M_{\gamma_{up}}(s) = M_{\gamma_{b1}}(s) M_{\gamma_{b2}}(s) = \sum_{n=1}^N \sum_{m=1}^{N-1} \binom{N}{n} \binom{N-1}{m} \frac{nm(-1)^{n-1}(-1)^{m-1}}{(n + \bar{\gamma}_C s)(m + \bar{\gamma}_C s)}. \quad (5.2.24)$$

In order to find the PDF of γ_{up} , two cases have to be considered, one is $m = n$, the other one is $m \neq n$. When $m \neq n$, the MGF of the end-to-end

SNR is

$$M_{\gamma_{up}}^{m \neq n}(s) = \sum_{n=1}^N \sum_{m=1, m \neq n}^{N-1} \binom{N}{n} \binom{N-1}{m} \frac{nm(-1)^{n-1}(-1)^{m-1}}{(n + \bar{\gamma}_C s)(m + \bar{\gamma}_C s)} \quad (5.2.25)$$

Then the inverse Laplace transform is used to obtain the PDF in (5.2.26).

$$f_{\gamma_{up}}^{m \neq n}(\gamma) = L^{-1}\{M_{\gamma_{up}}^{m \neq n}(s)\} = \sum_{n=1}^N \sum_{m=1, m \neq n}^{N-1} \binom{N}{n} \binom{N-1}{m} \frac{nm(-1)^{n-1}(-1)^{m-1}}{\bar{\gamma}_C(m-n)} (e^{-\frac{n\gamma}{\bar{\gamma}_C}} - e^{-\frac{m\gamma}{\bar{\gamma}_C}}). \quad (5.2.26)$$

Then, the CDF of γ_{up} can be obtained by taking the integral of the PDF in (5.2.26) with respect to γ , yielding

$$F_{\gamma_{up}}^{m \neq n}(\gamma) = \sum_{n=1}^N \sum_{m=1, m \neq n}^{N-1} \binom{N}{n} \binom{N-1}{m} (-1)^{n-1}(-1)^{m-1} + \sum_{n=1}^N \sum_{m=1, m \neq n}^{N-1} \binom{N}{n} \binom{N-1}{m} (-1)^{n-1}(-1)^{m-1} \frac{nm}{\bar{\gamma}_C(m-n)} \left(\frac{\bar{\gamma}_C}{m} e^{-\frac{m\gamma}{\bar{\gamma}_C}} - \frac{\bar{\gamma}_C}{n} e^{-\frac{n\gamma}{\bar{\gamma}_C}} \right). \quad (5.2.27)$$

When $m = n$, the MGF of the end-to-end SNR is

$$M_{\gamma_{up}}^{m=n}(s) = \sum_{n=1}^{N-1} \binom{N}{n} \binom{N-1}{n} \frac{n^2(-1)^{2(n-1)}}{(n + \bar{\gamma}_C s)^2}. \quad (5.2.28)$$

Then we use the same method to obtain the PDF and CDF of γ_{up} , which are

$$f_{\gamma_{up}}^{m=n}(\gamma) = \sum_{n=1}^{N-1} \binom{N}{n} \binom{N-1}{n} \frac{n^2(-1)^{2(n-1)}\gamma}{\bar{\gamma}_C^2} e^{-\frac{n\gamma}{\bar{\gamma}_C}} \quad (5.2.29)$$

and

$$\begin{aligned}
F_{\gamma_{up}}^{m=n}(\gamma) &= \sum_{n=1}^{N-1} \binom{N}{n} \binom{N-1}{n} (-1)^{2(n-1)} e^{-\frac{n\gamma}{\bar{\gamma}_C} - \frac{\bar{\gamma}_C - n\gamma}{\bar{\gamma}_C}} \\
&+ \sum_{n=1}^{N-1} \binom{N}{n} \binom{N-1}{n} (-1)^{2(n-1)}. \tag{5.2.30}
\end{aligned}$$

Therefore, the total CDF of γ_{up} can be obtained by using (5.2.27) and (5.2.30),

$$\begin{aligned}
F_{\gamma_{up}}^{tol}(\gamma) &= 1 + \sum_{n=1}^{N-1} \binom{N}{n} \binom{N-1}{n} (-1)^{2(n-1)} e^{-\frac{n\gamma}{\bar{\gamma}_C} - \frac{\bar{\gamma}_C - n\gamma}{\bar{\gamma}_C}} \\
&+ \sum_{n=1}^N \sum_{m=1, m \neq n}^{N-1} \binom{N}{n} \binom{N-1}{m} \frac{nm(-1)^{n-1}(-1)^{m-1}}{\bar{\gamma}_C(m-n)} \\
&\left(\frac{\bar{\gamma}_C}{m} e^{-\frac{m\gamma}{\bar{\gamma}_C}} - \frac{\bar{\gamma}_C}{n} e^{-\frac{n\gamma}{\bar{\gamma}_C}} \right). \tag{5.2.31}
\end{aligned}$$

Secondly, in a practical environment, those two clusters have different distances and shadowing to the source and destination, namely, $\bar{\gamma}_C^1 \neq \bar{\gamma}_C^2$. Therefore, a different total CDF of γ_{up} by using (5.2.20) to (5.2.27) can be provided, which follows as

$$\begin{aligned}
F_{\gamma_{up}}^{tol}(\gamma) &= 1 + \sum_{n=1}^N \sum_{m=1}^{N-1} \binom{N}{n} \binom{N-1}{m} \frac{nm(-1)^{n-1}(-1)^{m-1}}{\bar{\gamma}_C^1 m - \bar{\gamma}_C^2 n} \left(\frac{\bar{\gamma}_C^2}{m} e^{-\frac{m\gamma}{\bar{\gamma}_C^2}} - \right. \\
&\left. \frac{\bar{\gamma}_C^1}{n} e^{-\frac{n\gamma}{\bar{\gamma}_C^1}} \right). \tag{5.2.32}
\end{aligned}$$

Next, the case when the relays are in a single cluster will be considered.

Best Two Relay Pair Selection from the Same Cluster

In this approach the best two relay pair nodes are selected from the N available relays in the same cluster, namely, select the maximum γ_{max} and the second largest γ_{max-1} from the N relays instantaneous SNR. Firstly, the selection of the maximum and the second largest is not independent, therefore, according to [52], the joint distribution of the two most maximum values can be obtained as

$$f(x, y) = N(N-1)F(y)^{N-2}f(x)f(y), \quad (5.2.33)$$

where $\gamma_{max} = x$ and $\gamma_{max-1} = y$, and $f(x) = 1/\bar{\gamma}_C e^{-x/\bar{\gamma}_C}$, $f(y) = 1/\bar{\gamma}_C e^{-y/\bar{\gamma}_C}$ and $F(y) = 1 - e^{-y/\bar{\gamma}_C}$. Therefore,

$$f(x, y) = \frac{N(N-1)}{\bar{\gamma}_C^2} [1 - e^{-y/\bar{\gamma}_C}]^{N-2} e^{-x/\bar{\gamma}_C} e^{-y/\bar{\gamma}_C}. \quad (5.2.34)$$

Then, $F_{\gamma_{up}}(\gamma)$ needs to be determined, which given that x and y are two non-negative values from N exponential random values with $x \geq y$, is calculated as

$$F_{\gamma_{up}}(\gamma) = \underbrace{\int_0^{\gamma/2} \int_0^x f(x, y) dy dx}_{I_1} + \underbrace{\int_{\gamma/2}^{\gamma} \int_0^{\gamma-x} f(x, y) dy dx}_{I_2}.$$

Using the PDF in (5.2.34), and after performing some manipulations,

$$I_1 = N(N-1) \sum_{n=0}^{N-2} \binom{N-2}{n} \frac{(-1)^n}{n+1} \left(\frac{n+1}{n+2} - e^{-\frac{\gamma}{2\bar{\gamma}_C}} + \frac{1}{n+2} e^{-\frac{(n+2)\gamma}{2\bar{\gamma}_C}} \right). \quad (5.2.35)$$

Next, we need to calculate I_2 , when n is equal to zero or not, yielding

$$I_2^{n=0} = N(N-1) \left\{ e^{-\frac{\gamma}{2\bar{\gamma}_C}} - \left(1 + \frac{\gamma}{2\bar{\gamma}_C}\right) e^{-\frac{\gamma}{\bar{\gamma}_C}} \right\} \quad (5.2.36)$$

and

$$I_2^{n \neq 0} = N(N-1) \sum_{n=1}^{N-2} \binom{N-2}{n} \frac{(-1)^n}{n+1} \left\{ e^{-\frac{\gamma}{2\bar{\gamma}_C}} - \left(1 + \frac{1}{n}\right) e^{-\frac{\gamma}{\bar{\gamma}_C}} + \frac{1}{n} e^{-\frac{(n+2)\gamma}{2\bar{\gamma}_C}} \right\}. \quad (5.2.37)$$

Therefore, substituting (5.2.35), (5.2.36) and (5.2.37),

$$\begin{aligned} F_{\gamma_{up}}^{tol}(\gamma) &= I_1 + I_2^{n=0} + I_2^{n \neq 0} \\ &= N(N-1) \left\{ \sum_{n=0}^{N-2} \binom{N-2}{n} \frac{(-1)^n}{n+1} \left(\frac{n+1}{n+2} - e^{-\frac{\gamma}{2\bar{\gamma}_C}} + \frac{1}{n+2} e^{-\frac{(n+2)\gamma}{2\bar{\gamma}_C}} \right) \right. \\ &\quad + \left(e^{-\frac{\gamma}{2\bar{\gamma}_C}} - \left(1 + \frac{\gamma}{2\bar{\gamma}_C}\right) e^{-\frac{\gamma}{\bar{\gamma}_C}} \right) + \sum_{n=1}^{N-2} \binom{N-2}{n} \frac{(-1)^n}{n+1} \left(e^{-\frac{\gamma}{2\bar{\gamma}_C}} \right. \\ &\quad \left. \left. - \left(1 + \frac{1}{n}\right) e^{-\frac{\gamma}{\bar{\gamma}_C}} + \frac{1}{n} e^{-\frac{(n+2)\gamma}{2\bar{\gamma}_C}} \right) \right\}. \end{aligned} \quad (5.2.38)$$

On the basis of (5.2.32) and (5.2.38), the desired outage probabilities can be evaluated.

Outage Probability

The outage probability is defined as when the average end-to-end SNR falls below a certain predefined threshold value, α . The outage probability can be expressed as

$$P_{out} = \int_0^{\alpha} f_{\gamma_b}(\gamma) d\gamma = F_{\gamma_{up}}(\alpha). \quad (5.2.39)$$

Therefore, using the CDF expression (5.2.31), the outage probability for the best relay pair selection from different clusters can be obtained as

$$\begin{aligned}
P_{out}^{tol} = & 1 + \sum_{n=1}^{N-1} \binom{N}{n} \binom{N-1}{n} (-1)^{2(n-1)} e^{-\frac{n\alpha}{\bar{\gamma}_C}} \frac{-\bar{\gamma}_C - n\alpha}{\bar{\gamma}_C} \\
& + \sum_{n=1}^N \sum_{m=1, m \neq n}^{N-1} \binom{N}{n} \binom{N-1}{m} \frac{nm(-1)^{n-1}(-1)^{m-1}}{\bar{\gamma}_C(m-n)} \quad (5.2.40) \\
& \left(\frac{\bar{\gamma}_C}{m} e^{-\frac{m\alpha}{\bar{\gamma}_C}} - \frac{\bar{\gamma}_C}{n} e^{-\frac{n\alpha}{\bar{\gamma}_C}} \right),
\end{aligned}$$

and when the available relays might be clustered in physically different locations, outage probability of the best relay pair selection from the different clusters can be obtained as

$$\begin{aligned}
P_{out}^{tol} = & 1 + \sum_{n=1}^N \sum_{m=1}^{N-1} \binom{N}{n} \binom{N-1}{m} \frac{nm(-1)^{n-1}(-1)^{m-1}}{\bar{\gamma}_C^1 m - \bar{\gamma}_C^2 n} \left(\frac{\bar{\gamma}_C^2}{m} e^{-\frac{m\alpha}{\bar{\gamma}_C^2}} \right. \\
& \left. - \frac{\bar{\gamma}_C^1}{n} e^{-\frac{n\alpha}{\bar{\gamma}_C^1}} \right). \quad (5.2.41)
\end{aligned}$$

Finally, the outage probability of the best relay pair selection from the same cluster can be expressed by using the CDF expression (5.2.38) as

$$\begin{aligned}
P_{out}^{tol} = & N(N-1) \left\{ \sum_{n=0}^{N-2} \binom{N-2}{n} \frac{(-1)^n}{n+1} \left(\frac{n+1}{n+2} - e^{-\frac{\alpha}{2\bar{\gamma}_C}} + \frac{1}{n+2} e^{-\frac{(n+2)\alpha}{2\bar{\gamma}_C}} \right) \right. \\
& + \sum_{n=1}^{N-2} \binom{N-2}{n} \frac{(-1)^n}{n+1} \left(e^{-\frac{\alpha}{2\bar{\gamma}_C}} - \left(1 + \frac{1}{n} \right) e^{-\frac{\alpha}{\bar{\gamma}_C}} + \frac{1}{n} e^{-\frac{(n+2)\alpha}{2\bar{\gamma}_C}} \right) \\
& \left. + \left(e^{-\frac{\alpha}{2\bar{\gamma}_C}} - \left(1 + \frac{\alpha}{2\bar{\gamma}_C} \right) e^{-\frac{\alpha}{\bar{\gamma}_C}} \right) \right\}. \quad (5.2.42)
\end{aligned}$$

These expressions can be used to study the performance of the best relay pair selection schemes.

5.2.3 Simulation Results

In this section, in order to verify the results obtained from the above mathematical expressions, there is no direct link between the source and the destination as path loss or shadowing is assumed to render it unusable. Outage probability performance of different relay selection schemes will be shown.

Fig. 5.2 shows comparison of the outage probability of the best two relay pair selection from the same cluster versus SNR. With the increase of the SNR, the theoretical results approximate gradually the simulation results based on (5.2.3). Therefore, this trend confirms the assumption in (5.2.7), which is the methods are more suitable for the medium and high SNR ranges.

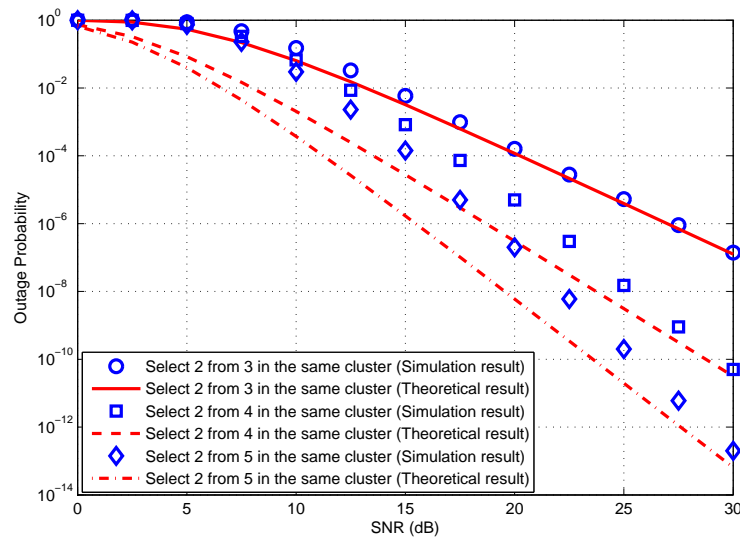


Figure 5.2. Comparison of the outage probability of the best relay pair selection from same cluster versus SNR, the theoretical results are shown in line style and the simulation results as points, where the threshold value α is 6 dB.

Fig. 5.3 shows the outage probability of the best two relay pair selection from different clusters based on the same SNR, which is 10 dB, in which the first cluster has N available relays and the second cluster has $N-1$ available relays, for different values of N and using the formula given in (5.2.40). It

can be seen that increasing the number of relays, N , decreases the outage probability, and hence when the number of relays is large, the outage event (no transmission) becomes less likely, for example, with the total number of available relays increasing from 3 to 9, the outage probability is significant decreased from almost 8% to 0.016%, when the threshold value α is 6 dB.

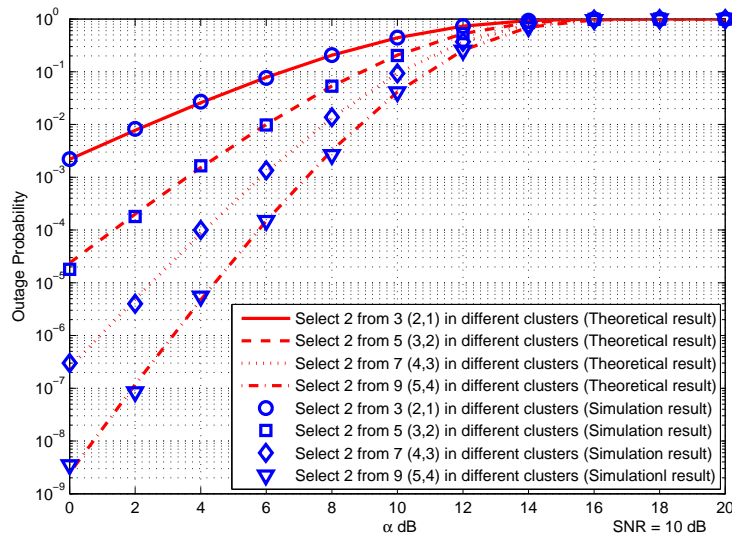


Figure 5.3. The outage probability of the best relay pair selection from different clusters based on the same SNR, the theoretical results are shown in line style and the simulation results as points.

For convenience in simulations, and in Fig. 5.4 and Fig. 5.5, the upper bound on (5.2.3) provided in (5.2.6) which explains why the theoretical and simulated results are essentially identical. On the other hand, Fig. 5.4 shows the outage probability of the best two relay pair selection from different clusters, in which the first cluster has N available relays, where SNR1 is 5 dB, and the second cluster has $N-1$ available relays, where SNR2 is 10 dB, for different values of N and using the formula given in (5.2.41). Obviously, because of the decrease of the SNR of cluster one, from 10 dB in Fig. 5.3 to 5 dB, the outage probability performance for each case is worse than that of Fig. 5.3.

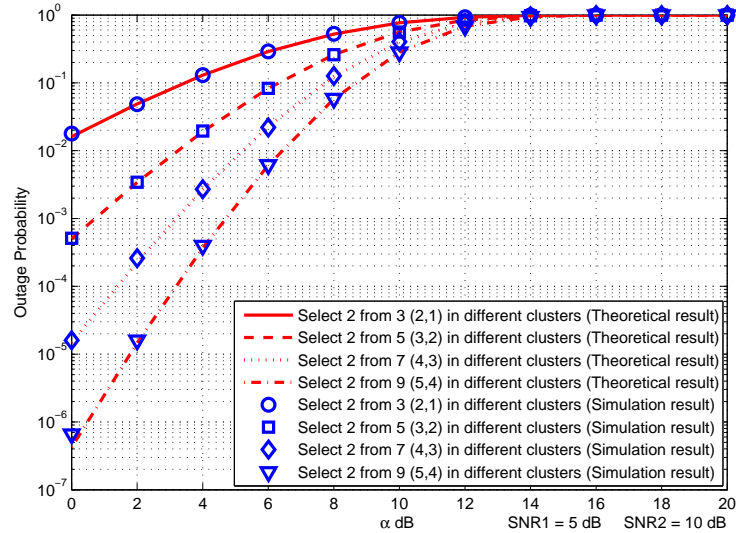


Figure 5.4. The outage probability of the best relay pair selection from different clusters based on different SNRs, the theoretical results are shown in line style and the simulation results as points.

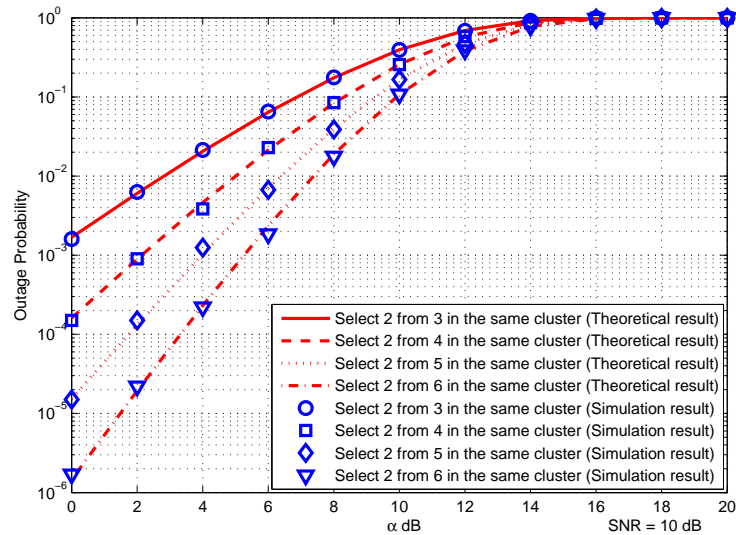


Figure 5.5. The outage probability of the best relay pair selection from the same cluster, the theoretical results are shown in line style and the simulation results as points.

Fig. 5.5 illustrates the best relay pair selection from N available relays in the same cluster to obtain the outage probability by using the equation given in (5.2.42). It can be seen that the theoretical results match extremely

well with the simulation results, and the outage probability reduces with increasing the number of available relays N , for example, when the threshold value α is 4 dB, the outage probability is decreased from almost 2% to 0.02%, with an increase in number of available relays from 3 to 6.

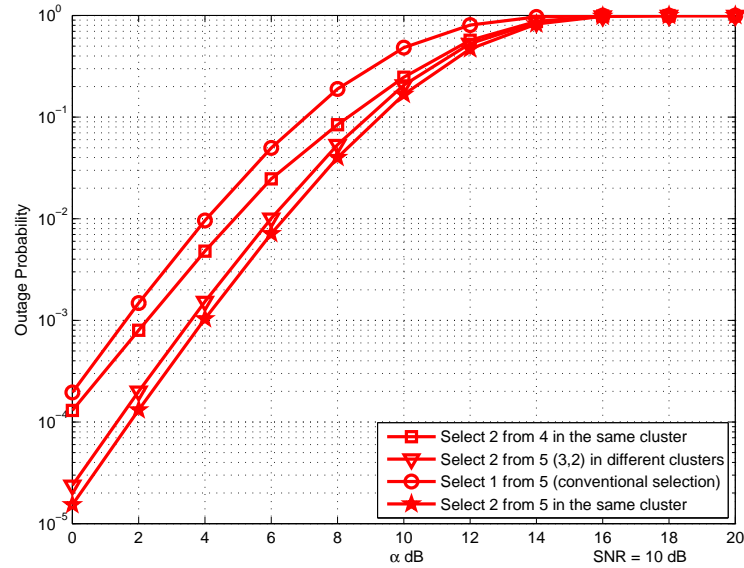


Figure 5.6. Comparison of the outage probability of different relay selection schemes.

Fig. 5.6 presents results for various relay selection methods. The top curve shows the outage probability performance for selecting only a single relay from five available relays. Next selecting a relay pair from a single cluster of four relays is considered so that the choice is made from C_4^2 possible pairs. In order to keep the number of possible pairs the same, the outage probability for selecting a pair is considered, namely, one from a cluster of three relays and the other one independently from a cluster of two relays, so that the number of possible pairs is $C_3^1 * C_2^1$. The curves clearly show that selecting from two clusters with five available relays has improved outage probability. For example at $\alpha = 4$ dB, the outage probability is decreased from almost 1% to 0.16%. The last curve is for the case of selecting two relays from five and yields the best outage probability, considerably improved upon

the first case of selecting a single relay from five. For the selection of one from five, it just uses a single relay to help the source to transmit the signal. This result confirms that pair selection provides more robust transmission than single relay selection. The next section will show even more benefit when there are errors in the feedback selection information from the destination to the relays.

5.2.4 Analysis of The Impact of Feedback Errors

The above studies have only considered perfect feedback of relay selection information. Therefore, the BER performance of the best relay pair selection from the same cluster, using DSTBC [9], is compared with the best single relay selection in the presence of feedback errors, when QPSK symbols are used in transmission. To simulate errors in the feedback of information from the destination, an error rate in the feedback is introduced. With an error rate of 0.1, for example, 10% of the selections are made in error, that is, rather than selecting the best relay, one of the other relays is chosen with equal probability of selection. As can be seen in Fig. 5.7, when the destination node transmits perfect channel feedback to the relays, i.e. an error rate of 0, the BER performance of the best single relay selection is worse than the best relay pair selection. Moreover, in the presence of errors in the channel feedback information, i.e. error rate over the range 0.1 to 0.5, the best relay pair selection outperforms the best single relay selection. These results illustrate clearly the increased robustness of the best relay pair selection scheme over the single relay selection scheme in the presence of moderate to severe feedback errors. For example at the SNR = 20 dB the BER for the single relay selection is reduced from almost 2×10^{-4} to 2.5×10^{-2} as the error rate changes from 0 to 0.5, whereas for the relay pair selection the BER changes from almost 6.5×10^{-5} only to 2.5×10^{-3} , confirming the improved robustness.

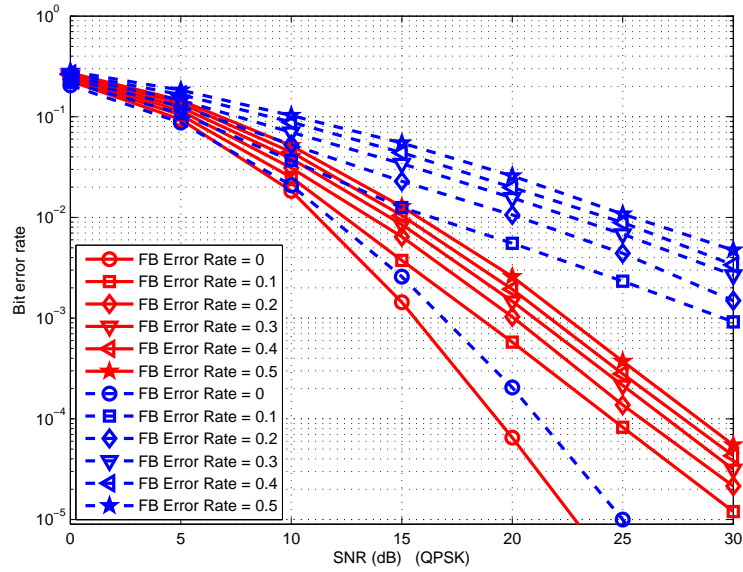


Figure 5.7. BER performance comparison of the best relay pair selection (solid line) from the same cluster with the best single relay selection (dashed line), with varying error in the feedback relay selection information from the destination.

In the next section, in order to reduce the outage probability, the best four relays selection without interference will be presented.

5.3 The Best Four Relays Selection Without Interference

5.3.1 System Model

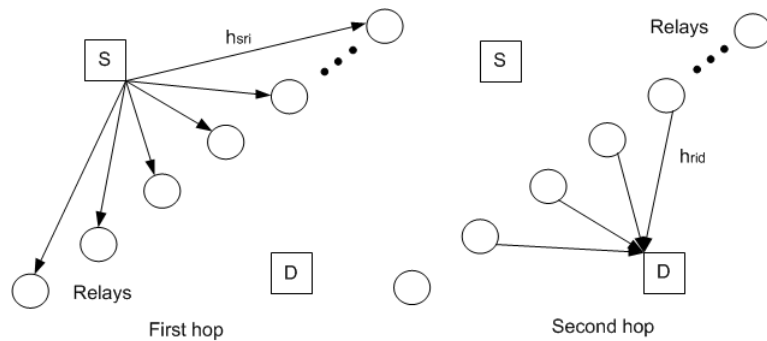


Figure 5.8. A half-duplex dual-hop best four relay selection system.

As is shown in Fig. 5.8, cooperative communication over Rayleigh flat-

fading channels is considered. There is one source node, one destination node and N available relay nodes, all equipped with single half-duplex antennas. Perfect channel state information is assumed to be known at the destination node.

Here the closed-loop quasi-orthogonal DSTBC with feedback scheme is used as in [81]. In the first hop, the source node transmits the signal $\mathbf{x} = [x_1 \ -x_2^* \ -x_3^* \ x_4]^T$ to the relays. The received signal at the i^{th} relay is given by

$$\mathbf{y}_{sr_i} = \sqrt{E_s} h_{sr_i} \mathbf{x} + \mathbf{n}_{r_i}, \quad (5.3.1)$$

where E_s is the average energy per symbol, h_{sr_i} is the channel gain between the source and the i^{th} relay node, and \mathbf{n}_{r_i} is the complex additive white Gaussian noise vector at the i^{th} relay node. In the second hop of cooperation, the i^{th} selected relay amplifies and forwards its received signal, which is designed to be a linear function of its received signal and its conjugate in (5.3.2), to the destination through $h_{r_i d}$, which is the channel gain between the i^{th} relay node and the destination. The received signal at the destination node from the i^{th} relay is (5.3.3)

$$\mathbf{t}_{r_i d} = \sqrt{P_i} (\mathbf{A}_i \mathbf{y}_{sr_i} + \mathbf{B}_i \mathbf{y}_{sr_i}^*), \quad (5.3.2)$$

$$\mathbf{y}_{r_i d} = h_{r_i d} \mathbf{t}_{r_i d} + \mathbf{n}_d. \quad (5.3.3)$$

According to [81], $\mathbf{A}_1 = \mathbf{I}_4$, $\mathbf{A}_2 = \mathbf{A}_3 = \mathbf{B}_1 = \mathbf{B}_4 = \mathbf{0}_4$,

$$\mathbf{A}_4 = \begin{bmatrix} 0 & 0 & 0 & 1 \\ 0 & 0 & -1 & 0 \\ 0 & -1 & 0 & 0 \\ 1 & 0 & 0 & 0 \end{bmatrix}, \mathbf{B}_2 = \begin{bmatrix} 0 & -1 & 0 & 0 \\ 1 & 0 & 0 & 0 \\ 0 & 0 & 0 & -1 \\ 0 & 0 & 1 & 0 \end{bmatrix}$$

$$\mathbf{B}_3 = \begin{bmatrix} 0 & 0 & -1 & 0 \\ 0 & 0 & 0 & -1 \\ 1 & 0 & 0 & 0 \\ 0 & 1 & 0 & 0 \end{bmatrix},$$

and \mathbf{n}_d is the complex additive white Gaussian noise vector at the destination. The i^{th} relay gain denoted by $\sqrt{P_i}$ is calculated from $P_i = E_s / (E_s |h_{sr_i}|^2 + N_0)$, where N_0 is the noise variance [17]. Finally, the maximum likelihood (ML) decoding can be used at the destination node.

Then, the instantaneous equivalent end-to-end signal-to-noise ratio (SNR) can be written as (5.3.4), because the MRC scheme is used at the destination. The practical implementation of the MRC may, however, incur a capacity penalty due to the need to adopt a time multiplexing approach to transmission between the relays and the destination node; therefore, this section adopt an orthogonal transmission scheme, namely, the best four relay selection with the closed-loop quasi-orthogonal DSTBC.

$$\gamma_D = \sum_{i \in N_s} \frac{\gamma_{sr_i} \gamma_{r_i d}}{1 + \gamma_{sr_i} + \gamma_{r_i d}}, \quad (5.3.4)$$

where N_s denotes the set of relay indices for the relays chosen in the multi-relay selection scheme. $\gamma_{sr_i} = |h_{sr_i}|^2 E_s / N_0$ and $\gamma_{r_i d} = |h_{r_i d}|^2 E_s / N_0$ are the instantaneous SNR of the $S - R_i$ and $R_i - D$ links, respectively.

For the Rayleigh fading channels, the PDF and the CDF of the SNR in the $u \in (sr_i, r_i d)$ links are given by

$$f_{\gamma_u}(\gamma) = \frac{1}{\bar{\gamma}_u} e^{-\gamma/\bar{\gamma}_u}, \quad (5.3.5)$$

$$F_{\gamma_u}(\gamma) = 1 - e^{-\gamma/\bar{\gamma}_u}, \quad (5.3.6)$$

where $\bar{\gamma}_u$ denotes the mean SNR for all links and $\gamma > 0$. According to [79],

$$\gamma_i = \min(\gamma_{sr_i}, \gamma_{r_id}) > \frac{\gamma_{sr_i} \gamma_{r_id}}{1 + \gamma_{sr_i} + \gamma_{r_id}}. \quad (5.3.7)$$

Therefore, the lower and upper bound for the equivalent SNR can be given as

$$\frac{1}{2} \sum_{i=1}^N \gamma_i = \gamma_{low} \leq \gamma_D < \gamma_{up} = \sum_{i=1}^N \gamma_i. \quad (5.3.8)$$

The upper bound SNR is more suitable for analysis in the medium and high SNR arrange.

And then the CDF of $\gamma_i = \min(\gamma_{sr_i}, \gamma_{r_id})$ can be expressed as [80]

$$\begin{aligned} F_{\gamma_i}(\gamma) &= 1 - Pr(\gamma_{sr_i} > \gamma) Pr(\gamma_{r_id} > \gamma) \\ &= 1 - [1 - F_{\gamma_{sr_i}}(\gamma)][1 - F_{\gamma_{r_id}}(\gamma)]. \end{aligned} \quad (5.3.9)$$

Substituting (5.3.6) with the appropriate index into (5.3.9) yields

$$F_{\gamma_i}(\gamma) = 1 - e^{-\gamma/\bar{\gamma}_{C_i}}, \quad (5.3.10)$$

where $\bar{\gamma}_{C_i} = \frac{\bar{\gamma}_{sr_i} \bar{\gamma}_{r_id}}{\bar{\gamma}_{sr_i} + \bar{\gamma}_{r_id}}$. Since i.i.d. Rayleigh fading relay channels are assumed, then $\bar{\gamma}_{sr_i} = \bar{\gamma}_{r_id} = \bar{\gamma}_0 = E_s/N_0$, and $\bar{\gamma}_{C_i} = \bar{\gamma}_C = 0.5\bar{\gamma}_0$. Therefore, the PDF of γ_i can be obtained by taking the derivative of the CDF (5.3.10)

as

$$f_{\gamma_i}(\gamma) = \frac{1}{\bar{\gamma}_{C_i}} e^{-\gamma/\bar{\gamma}_{C_i}}. \quad (5.3.11)$$

Next, the outage probability analysis will be considered for the best four relays selection scheme.

5.3.2 Outage Probability Analysis

In this approach the best four relay nodes are selected from N available relays, namely, the maximum γ_{max} , the second largest γ_{max-1} , the third largest γ_{max-2} and the fourth largest γ_{max-3} are selected from the N relays instantaneous SNR. Firstly, the selection of the L largest is not independent, therefore, according to [52], the joint distribution of the L most maximum values can be obtain as

$$f(x_1, x_2, \dots, x_L) = L! \binom{N}{L} [F(x_L)]^{N-L} \prod_{k=1}^L f(x_k), \quad (5.3.12)$$

where $x_1 \geq x_2 \geq \dots \geq x_L \geq x_{L+1} \geq \dots \geq x_N$ and $f(\cdot)$ and $F(\cdot)$ correspond to the PDF and CDF. Therefore, the joint PDF of the four largest selection can be expressed as

$$f(w, x, y, z) = N(N-1)(N-2)(N-3)[F(z)]^{N-4} f(w)f(x)f(y)f(z), \quad (5.3.13)$$

where $w = \gamma_{max}$, $x = \gamma_{max-1}$, $y = \gamma_{max-2}$, $z = \gamma_{max-3}$, and $F(z) = 1 - e^{-z/\bar{\gamma}_C}$ and $f(w) = 1/\bar{\gamma}_C e^{-w/\bar{\gamma}_C}$, $f(x) = 1/\bar{\gamma}_C e^{-x/\bar{\gamma}_C}$, $f(y) = 1/\bar{\gamma}_C e^{-y/\bar{\gamma}_C}$, $f(z) = 1/\bar{\gamma}_C e^{-z/\bar{\gamma}_C}$. Therefore,

$$f(w, x, y, z) = \frac{N(N-1)(N-2)(N-3)}{\bar{\gamma}_C^4} [1 - e^{-z/\bar{\gamma}_C}]^{N-4} e^{-w/\bar{\gamma}_C} e^{-x/\bar{\gamma}_C} e^{-y/\bar{\gamma}_C} e^{-z/\bar{\gamma}_C}. \quad (5.3.14)$$

Then the CDF $F_{\gamma_{up}}(\gamma)$ is calculated, where γ_{up} is the sum of w , x , y and z , which are identically distributed and formed as the ratios of exponential random variables. Therefore, the CDF is obtained by

$$F_{\gamma_{up}}(\gamma) = Pr\{w + x + y + z \leq \gamma\}. \quad (5.3.15)$$

Given that w, x, y and z are non-negative, with $w \geq x \geq y \geq z$. Finally,

$$F_{\gamma_{up}}(\gamma) = \int_0^{\frac{\gamma}{4}} \int_z^{\frac{\gamma-z}{3}} \int_y^{\frac{\gamma-z-y}{2}} \int_x^{\gamma-x-z-y} f(w, x, y, z) dw dx dy dz. \quad (5.3.16)$$

Using the PDF in (5.3.14), and after performing some manipulations,

$$\begin{aligned} F_{\gamma_{up}}(\gamma) = & \frac{N(N-1)(N-2)(N-3)}{\bar{\gamma}_C^3} \left\{ \frac{\bar{\gamma}_C^3}{24} - \left[\frac{\bar{\gamma}_C^3}{24} + \frac{\gamma \bar{\gamma}_C}{8} \left(\frac{\gamma + \bar{\gamma}_C}{3} \right) - \frac{\gamma^2 \bar{\gamma}_C}{48} + \right. \right. \\ & \left. \frac{\gamma^3}{144} \right] e^{-\frac{\gamma}{\bar{\gamma}_C}} + \sum_{n=1}^{N-4} \binom{N-4}{n} (-1)^n \left\{ \frac{\bar{\gamma}_C^3}{6(n+4)} - \left[\frac{\bar{\gamma}_C^3}{6(n+4)} - \frac{\bar{\gamma}_C^3}{6n} + \right. \right. \\ & \left. \frac{2\bar{\gamma}_C^3}{3n^2} - \frac{8\bar{\gamma}_C^3}{3n^3} \right] e^{-\frac{(n+4)\gamma}{4\bar{\gamma}_C}} + \left[\frac{2\bar{\gamma}_C^3}{3n^2} - \frac{\bar{\gamma}_C^2(\bar{\gamma}_C + \gamma)}{6n} - \frac{\gamma^2 \bar{\gamma}_C}{12n} + \frac{2\gamma \bar{\gamma}_C^2}{3n^2} - \right. \\ & \left. \left. \frac{8\bar{\gamma}_C^3}{3n^3} \right] e^{-\frac{\gamma}{\bar{\gamma}_C}} \right\} \end{aligned} \quad (5.3.17)$$

Therefore, the desired outage probabilities is calculated. The outage probability is defined as when the average end-to-end SNR falls below a certain predefined threshold value, α . The outage probability can be expressed as

$$P_{out} = \int_0^{\alpha} f_{\gamma_b}(\gamma) d\gamma = F_{\gamma_{up}}(\alpha). \quad (5.3.18)$$

The outage probability of the best four relays selection can be expressed by using the CDF expression (5.3.17) as

$$\begin{aligned} F_{\gamma_{up}}(\alpha) = & \frac{N(N-1)(N-2)(N-3)}{\bar{\gamma}_C^3} \left\{ \frac{\bar{\gamma}_C^3}{24} - \left[\frac{\bar{\gamma}_C^3}{24} + \frac{\alpha \bar{\gamma}_C}{8} \left(\frac{\alpha + \bar{\gamma}_C}{3} \right) - \frac{\alpha^2 \bar{\gamma}_C}{48} + \right. \right. \\ & \left. \frac{\alpha^3}{144} \right] e^{-\frac{\alpha}{\bar{\gamma}_C}} + \sum_{n=1}^{N-4} \binom{N-4}{n} (-1)^n \left\{ \frac{\bar{\gamma}_C^3}{6(n+4)} - \left[\frac{\bar{\gamma}_C^3}{6(n+4)} - \frac{\bar{\gamma}_C^3}{6n} + \right. \right. \\ & \left. \frac{2\bar{\gamma}_C^3}{3n^2} - \frac{8\bar{\gamma}_C^3}{3n^3} \right] e^{-\frac{(n+4)\alpha}{4\bar{\gamma}_C}} + \left[\frac{2\bar{\gamma}_C^3}{3n^2} - \frac{\bar{\gamma}_C^2(\bar{\gamma}_C + \alpha)}{6n} - \frac{\alpha^2 \bar{\gamma}_C}{12n} + \frac{2\alpha \bar{\gamma}_C^2}{3n^2} - \right. \\ & \left. \left. \frac{8\bar{\gamma}_C^3}{3n^3} \right] e^{-\frac{\alpha}{\bar{\gamma}_C}} \right\} \end{aligned} \quad (5.3.19)$$

5.3.3 Analysis of The Impact of Feedback Errors

In this section, the BER performance of the best four relays selection from a set of N available relays, i.e. $N = 6$, using DSTBC [81], is compared with the best single relay selection in the presence of feedback errors, when QPSK symbols are used in transmission.

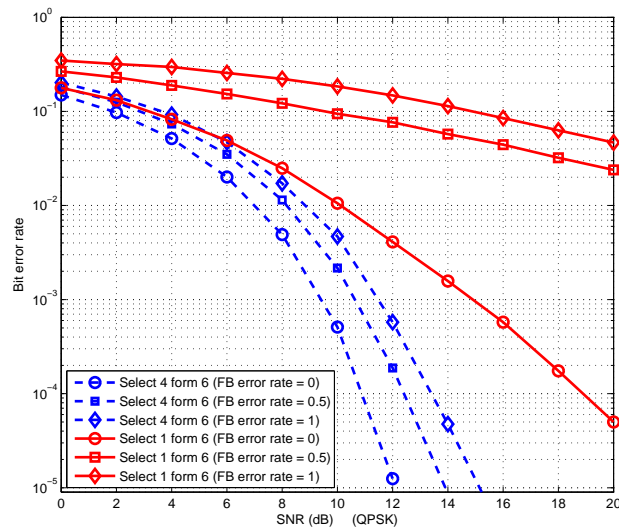


Figure 5.9. BER performance comparison of the best four relays selection (solid line) with the best single relay selection (dashed line), with varying error in the feedback relay selection information from the destination.

To simulate errors in the feedback of information from the destination we introduce an error rate in the feedback. With an error rate of 0.5, for example, 50% of the selections are made in error, that is, rather than selecting the best relay, one of the other relays is chosen with equal probability of selection. As can be seen in Fig. 5.9, when the destination node transmits perfect channel feedback to the relays, i.e. an error rate of 0, the BER performance of the best single relay selection is worse than the best four relays selection. Moreover, in the presence of errors in the channel feedback information, i.e. error rate over the range 0.5 to 1, the best four relays selection outperforms the best single relay selection. These results illustrate clearly the increased robustness of the best four relays selection scheme over the

single relay selection scheme in the presence of moderate to severe feedback errors. For example, at the $\text{SNR} = 12 \text{ dB}$, the BER for the single relay selection is reduced from almost 4×10^{-3} to 1.5×10^{-1} as the error rate changes from 0 to 1, whereas for the best four relays selection the BER changes from almost 1.25×10^{-5} only to 5.75×10^{-4} , confirming the improved robustness.

5.3.4 Outage Probability Analysis Verification

In this section, in order to verify the results obtained from the above mathematical expressions, all relay links can be assumed to have the same average SNR, and there is no direct link between the source and the destination as path loss or shadowing renders it unusable. The SNR $\bar{\gamma}_0 = 10 \text{ dB}$ is assumed.

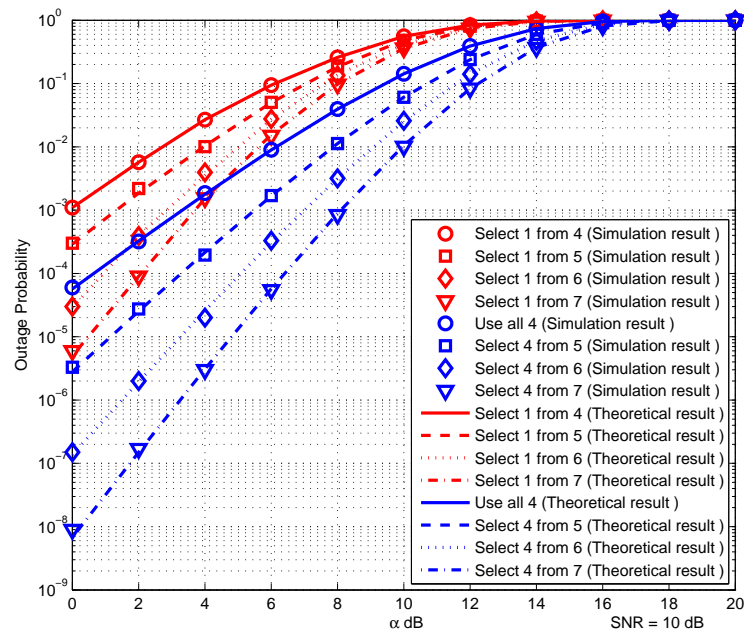


Figure 5.10. Comparison of the outage probability of the single relay selection and the best four relays selection schemes, the theoretical results are shown in line style and the simulation results as points.

Fig. 5.10 shows the comparison of the outage probability of the single relay selection and the best four relays selection schemes, using the formula given in (5.3.19). It can be seen that increasing the number of relays, N ,

decreases the outage probability, and hence when the number of relays is large, the outage event (no transmission) becomes less likely, for example, with the total number of available relays increasing from 4 to 7, the outage probability of a single relay selection is decreased from almost 9% to 1.5%, at the same time, the outage probability of the best four relays selection is decreased from almost 0.9% to 0.006%, when the threshold value α is 6 dB. This result confirms that pair selection provides more robust transmission than single relay selection, because for the single relay selection, it just uses a single relay to help the source to transmit the signal. Moreover, the curves show the analytical results and values found by simulations. A close match is observed between the two. In the next section, the multi-relay selection will be applied with interference at the relay nodes.

5.4 Summary

In this chapter, firstly, the local measurements of the instantaneous channel conditions were used to select the best relay pair from a set of N available relays, which either come from the same cluster or different clusters, and then these best relays were used with the Alamouti code to improve the diversity and decrease the outage probability. The best relay pair selection scheme was also shown to have robustness against feedback error and to outperform a scheme based on selecting only the best single relay. Secondly, in order to further reduce the outage probability, the best four relays were selected. In the next chapter, the outage probability analysis for two different multi-relay selection schemes will be introduced with inter-cluster interference for only the relay nodes, and then a more practical analysis will be discussed based on the inter-cluster interference for both the relay and the destination nodes.

OUTAGE PROBABILITY OF MULTI-RELAY SELECTION WITH INTERFERENCE

In this chapter, firstly, the outage probability analysis for two different multi-relay selection policies, which are asymptotical and semi-conventional policies to select the best multi-relays from a group of available relays in the same cluster by using local measurements of the instantaneous channel conditions are examined when inter-cluster interference is present only in the relay nodes. Secondly, a more practical analysis is discussed based on inter-cluster interference both at the relay nodes and the destination node. Furthermore, a new exact analytical expressions for the probability density function, and cumulative density function of the received signal-to-noise plus interference ratio (SINR) and closed form expressions for outage probability in the high SNR region over Rayleigh frequency flat fading channels are provided.

6.1 Introduction

Although AF has been studied extensively in the literature, little work has considered interference during the cooperation process. For example, in [77] a dedicated relay to forward the signal of one source to the destination is provided, whereas many relays and hops are used to help the source to transmit to the destination node in [44]. Multi-relay interference is however not considered in either work.

Furthermore, these relay selection criteria in [16, 75, 76] lack the flexibility to deal with the presence or absence of interference effects. In order to improve the practicality, in [82] the effects of multi-user interference are considered for relay nodes and a single relay selection scheme is used to overcome the effects of the interference, in the context of legacy networks. However, using a single best relay is not always sufficient to satisfy the required outage probability at a destination node.

Therefore, in this chapter, in order to overcome these shortcomings, firstly, the basic AF protocol [17] is considered when external out-of-cluster structural/unmanaged interference affects the cooperation process. However, to facilitate analysis, only interference at the relays is assumed and the effect of interference at the destination node is ignored, which matches the approach in [82]. Moreover, $\max(\min(\cdot, \cdot))$ type policies are used for relay selection. Secondly, two selection schemes will be focused upon to select two or four relays from a single group of relays. And new outage probability expressions will be derived for two or four relay selection and compared with the results for conventional best single relay selection. Finally, the BER performance of the best single relay selection scheme and the best two relay selection scheme will be examined by simulation, in the presence of errors in the feedback of relay selection information. In practice, this could be as simple as a single permission to transmit bit.

Finally, as considering interference only to be present at the relay nodes which is not practical; and as the max-min relay scheme does not yield a very accurate representation of end-to-end SINR, nor will any associated outage probability analysis be very accurate, in Section 6.3, an exact outage probability performance analysis in the presence of inter-cluster interference both at the relay and destination nodes in the high SNR region will be provided.

6.2 Multi-Relay Selection with Interference at the Relay

6.2.1 System Model

Fig. 6.1 shows two neighboring clusters of nodes denoted (C1, C2) as in [82]. The analysis of the effect of inter-cluster interference on the relays in cluster C1 is the focus. This cluster contains nodes linked by independent Rayleigh flat-fading quasi-static channels. Moreover, there is one source node and one destination node and many potential relay nodes grouped together, all equipped with single half-duplex antennas. Similar relay configurations have been studied in [46] and [45].

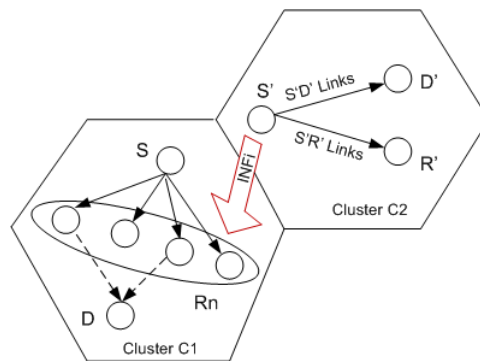


Figure 6.1. The system model. C1: cluster of interest, which contains a cooperative network which uses best two relay selection. S: source; D: Destination; Rn: potential relay group. C2: neighboring cluster, S': source; D': Destination. INFi: interference signal for the i^{th} relay ($S' \rightarrow Rn$).

For simplicity of exposition, there is no direct link between the source and the destination as path loss or shadowing is assumed to render it unusable and the neighboring cluster uses direct transmission from the source to a relay or the destination. In this protocol, the source broadcasts the signal to the relay nodes during the first hop, and during the second hop, the i^{th} selected relay, from the available group transmits the received signal to the destination node. Moreover, the interference which is generated by the neighboring cluster is assumed only to affect the relay node and is ignored at the destination node. Therefore, the system model can be developed as follows: the received signal at the i^{th} relay and the destination node are given by

$$y_{sr_i} = \sqrt{E_s}h_{sr_i}x + \sqrt{E_s}h_{s'r_i}x' + n_{r_i}, \quad (6.2.1)$$

$$y_{r_id} = \sqrt{P_i}h_{r_id}y_{sr_i} + n_d, \quad (6.2.2)$$

where x and x' are the source signals from the target and neighboring clusters, respectively, typically drawn from a prescribed finite constellation. E_s is the average energy per symbol; h_{sr_i} , $h_{s'r_i}$ and h_{r_id} are channel gains, which are the zero mean, independent, circularly-symmetric, complex Gaussian random variables with variances $\sigma_{sr_i}^2$, $\sigma_{s'r_i}^2$ and $\sigma_{r_id}^2$, between the source and the i^{th} relay node, between the neighboring source and the relay node and between the i^{th} relay node and the destination node; and the complex additive white Gaussian noise n_{r_i} and n_d are modeled as zero-mean mutually independent, circularly-symmetric, complex Gaussian random variables with variance N_0 at the i^{th} relay and the destination node, respectively. The i^{th} relay gain denoted by $\sqrt{P_i}$ is calculated from

$$P_i = E_s / (E_s|h_{sr_i}|^2 + E_s|h_{s'r_i}|^2 + N_0). \quad (6.2.3)$$

In this model, the source powers at the target and the neighboring cluster are

assumed to be the same. This model is representative of an ad-hoc network environment where there is no power control between adjacent clusters.

Next, because the two or four relay selection scheme is used, we assume that maximum ratio combining (MRC) is used at the destination [79]. The practical implementation of the MRC will, however, incur a capacity penalty due to the need to adopt a time multiplexing approach to transmission between the relays and the destination node; however, this can be mitigated by adopting an orthogonal transmission scheme, i.e. distributed space-time coding [44], which is available for two or four relays. Furthermore, increasing the number of selected relays will incur practical overheads such as increased complexity in synchronization. Therefore, this paper focuses on selection of two and four relays. Therefore, the instantaneous equivalent end-to-end signal-to-interference plus noise ratio (SINR) can be written as:

$$\gamma_D = \sum_{i \in N_s} \frac{P_i |h_{sr_i}|^2 |h_{r_i d}|^2}{P_i |h_{s'r_i}|^2 |h_{r_i d}|^2 + P_i |h_{r_i d}|^2 N_0 + N_0}, \quad (6.2.4)$$

where N_s denotes the set of two or four relay indices for the relays chosen in this relay selection scheme. Substituting (6.2.3) into (6.2.4), the end-to-end SINR is

$$\gamma_D = \sum_{i \in N_s} \frac{\gamma_{sr_i} \gamma_{r_i d}}{\gamma_{INFi} (\gamma_{r_i d} + 1) + \gamma_{sr_i} + \gamma_{r_i d} + 1}, \quad (6.2.5)$$

where $\gamma_{sr_i} = |h_{sr_i}|^2 E_s / N_0$ and $\gamma_{r_i d} = |h_{r_i d}|^2 E_s / N_0$ are the instantaneous SNRs of the source to i^{th} relay and i^{th} relay to destination links, respectively. And $\gamma_{INFi} = \gamma_{s'r_i} = |h_{s'r_i}|^2 E_s / N_0$ denotes the interference-to-noise ratio (INR) for the i^{th} relay as a result of the neighboring source. It is difficult to use (6.2.5) to find a closed form expression for the probability density function of γ_D , therefore, for high SNR, an asymptotic bound is provided as

$$\gamma_D \simeq \sum_{i \in N_s} \frac{\gamma_{sr_i}}{\gamma_{INFi}}, \quad (6.2.6)$$

which is the sum of the ratios between the SNR of the first hop and the INR of the interference, because when $SNR \rightarrow \infty$, then $\varepsilon(\gamma_{INFi})\varepsilon(\gamma_{r_id}) \gg \varepsilon(\gamma_{INFi}) + \varepsilon(\gamma_{sr_i}) + \varepsilon(\gamma_{r_id}) + 1$. In this case, the statistical description of the system is independent of the second hop.

For this asymptotic case, the PDF and CDF of each ratio in (6.2.6), which is between two exponential random variables [83], are given in closed form, as

$$f(\gamma) = \frac{L}{(L + \gamma)^2} \quad \text{and} \quad F(\gamma) = \frac{\gamma}{(L + \gamma)}, \quad (6.2.7)$$

where $f(\cdot)$ and $F(\cdot)$ denote the PDF and the CDF, respectively. The parameter $L = \frac{\varepsilon(\gamma_{sr_i})}{\varepsilon(\gamma_{INFi})} = \frac{\sigma_{sr_i}^2}{\sigma_{s'r_i}^2}$. Note that the parameter L controls the level of interference in the target and neighboring clusters.

Furthermore, considering interference at both the relays and the destination node is provided in Section 5.5. Two or four relay selection scheme assuming interference only at the relays will be implemented as in the following sections.

6.2.2 Two or four Relay Selection with Outage Probability Analysis

In order to introduce the two or four relay selection schemes, the conventional relay selection scheme will be firstly introduced.

Conventional relay selection

In [16] the conventional relay selection policy which is used in the ideal distributed implementation without interference is considered. It requires the instantaneous signal SNR between the links from the source to relay and the relay to the destination node to be known, and then a particular relay is selected to maximize the minimum between them; the relay selection scheme

can therefore be represented by

$$i_{con} = \arg \max_{i \in N} \min(\gamma_{sr_i}, \gamma_{r_id}), \quad (6.2.8)$$

where N represents the set of indices of all available relays.

The conventional relay selection policy offers the relay with the “best” end-to-end path between source and destination and provides diversity gain on the order of the number of the relays [76]. However, this relay selection criterion is only considered for environments without interference, and the best relay selection is not always sufficient to achieve the required outage probability at a destination node. Finally, when feedback error is present in the relay selection, the performance of the single relay selection scheme is significantly degraded, further discussion of which will be given in the simulation section. Therefore, to overcome these problems two and four relay selection schemes are proposed for use in interference configurations for legacy networks which are restricted to adopt a $\max(\min(\cdot, \cdot))$ type policy.

Asymptotic two and four relay selection

The first proposed two and four relay selection criterion is motivated by the simplified expression of the system. As has been seen in (6.2.6) the asymptotic behavior of the system converges to the sum of the ratios between source to relay and interference links. Therefore, a relay selection policy is to choose the best relay set which gives the maximum value of the ratio. Take the best two relay selection for example, the asymptotic selection policy can be obtained as

$$\mathbf{i}_{Asy} = \arg \max_{i \in N} \max_{i' \in N-1} \left(\frac{\gamma_{sr_i}}{\gamma_{INFi'}} \right), \quad (6.2.9)$$

where $\mathbf{i} = (i, i')$, i.e. a pair of relay indices, where i denotes the index of the relay with the best link in N , and i' is that of the best relay amongst the remaining $N-1$. In this approach the best two relay nodes are selected from

the N available relays in the group in the cluster, namely, select the relays with the maximum γ_{max} and the second largest γ_{max-1} from the N relays instantaneous SNRs. Using the theory of order statistics [52], the selection of the maximum and the second largest is not independent, therefore the joint distribution of the two most maximum values is obtained as

$$f(x, y) = N(N - 1)F(y)^{N-2}f(x)f(y), \quad (6.2.10)$$

where $\gamma_{max} = x$ and $\gamma_{max-1} = y$. Substituting (6.2.7) into (6.2.10),

$$f(x, y) = \frac{N(N - 1)L^2y^{N-2}}{(L + y)^N(L + x)^2}. \quad (6.2.11)$$

Then the CDF $F_{\gamma_{up}}^{Asy}(\gamma)$ is calculated, where γ_{up} is the sum of x and y , which are identically distributed and formed as the ratios of exponential random variables. Therefore, the CDF is obtained as

$$F_{\gamma_{up}}^{Asy}(\gamma) = Pr\{x + y \leq \gamma\}. \quad (6.2.12)$$

Given that x and y are non-negative, with $x \geq y$, then,

$$F_{\gamma_{up}}^{Asy}(\gamma) = \int_0^{\frac{\gamma}{2}} \int_y^{\gamma-y} f(x, y) dx dy. \quad (6.2.13)$$

Using the PDF in (6.2.11), and after performing some manipulations,

$$\begin{aligned} F_{\gamma_{up}}^{Asy}(\gamma) = & N(N - 1)L^2 \left\{ \frac{\left(\frac{\gamma}{2}\right)^{N-1} (LN + \frac{\gamma}{2})}{N(N - 1)L^2(L + \frac{\gamma}{2})^N} - \frac{\left(\frac{\gamma}{2}\right)^N}{(L + \frac{\gamma}{2})^N(L + \gamma)^2} \right. \\ & \left[\frac{2(L + \gamma)(L + \frac{\gamma}{2})}{L(N - 1)\gamma} + \frac{\left(\frac{L + \frac{\gamma}{2}}{L}\right)^N F_{2,1}(N, N; N + 1; -\frac{\gamma}{2L})}{N} \right. \\ & \left. \left. + \frac{\frac{\gamma}{2} \left(\frac{L + \frac{\gamma}{2}}{L}\right)^N F_1(N + 1; N, 1; N + 2; -\frac{\gamma}{2L}, \frac{\gamma}{2(L + \gamma)})}{LN + L + \gamma N + \gamma} \right] \right\}, \end{aligned} \quad (6.2.14)$$

where $F_{2,1}(a, b, c, z)$ is the first hypergeometric function, which can be calculated by using the Hypergeom Matlab function [84]. Furthermore, $F_1(a; b_1, b_2; c; x, y)$ is a formal extension of the Appell hypergeometric function of two variables, which can also be expressed by the simple integral in [85] as

$$F_1(a; b_1, b_2; c; x, y) = \frac{\Gamma(c)}{\Gamma(a)\Gamma(c-a)} \int_0^1 t^{a-1} (1-t)^{c-a-1} (1-xt)^{-b_1} (1-yt)^{-b_2} dt \quad \text{for } \Re(c) > \Re(a) > 0,$$

where $\Gamma(n) = (n-1)!$ is the Gamma function.

Therefore, the outage probability is defined as when the average end-to-end SNR falls below a certain predefined threshold value, α . The outage probability can be expressed as

$$P_{out} = \int_0^\alpha f_{\gamma_b}(\gamma) d\gamma = F_{\gamma_{up}}(\alpha). \quad (6.2.15)$$

The outage probability of the best two relay selection can be expressed by using the CDF expression (6.2.14).

Then a similar method can be used to obtain the outage probability for the best four relay selection as follows. The asymptotic selection policy can be obtained as

$$\mathbf{i}_{Asy} = \arg \max_{i \in N} \max_{i' \in N-1} \max_{i'' \in N-2} \max_{i''' \in N-3} \left(\frac{\gamma_{sr_i}}{\gamma_{INF_i}} \right), \quad (6.2.16)$$

where $\mathbf{i} = (i, i', i'', i''')$, i.e. four relay indices, in which i denotes the index of the relay with the best link in N ; i' is that of the best relay amongst the remaining $N-1$, and i'' is that of the best relay amongst the remaining $N-2$, and i''' is that of the best relay amongst the remaining $N-3$. The joint distribution of the four most maximum values is

$$f(w, x, y, z) = N(N-1)(N-2)(N-3)F(z)^{N-4}f(w)f(x)f(y)f(z), \quad (6.2.17)$$

where let $\gamma_{max} = w$, $\gamma_{max-1} = x$, $\gamma_{max-2} = y$ and $\gamma_{max-3} = z$. Substituting (6.2.7) into (6.2.17),

$$f(w, x, y, z) = \frac{N(N-1)(N-2)(N-3)L^4 z^{N-4}}{(L+z)^{N-2}(L+w)^2(L+x)^2(L+y)^2}. \quad (6.2.18)$$

Then the CDF $F_{\gamma_{up}}^{Asy}(\gamma)$ is calculated, and γ_{up} is formed as the sum of w , x , y and z random variables, which are identically distributed and ratios of exponential random variables. Therefore, the CDF is obtained by

$$F_{\gamma_{up}}^{Asy}(\gamma) = Pr\{w + x + y + z \leq \gamma\}. \quad (6.2.19)$$

Given that w , x , y and z are non-negative, with $w \geq x \geq y \geq z$, then,

$$F_{\gamma_{up}}^{Asy}(\gamma) = \int_0^{\frac{\gamma}{4}} \int_z^{\frac{\gamma-z}{3}} \int_y^{\frac{\gamma-z-y}{2}} \int_x^{\gamma-z-y-x} f(w, x, y, z) dw dx dy dz. \quad (6.2.20)$$

Substituting (6.2.18) into (6.2.20),

$$F_{\gamma_{up}}^{Asy}(\gamma) = \int_0^{\frac{\gamma}{4}} \int_z^{\frac{\gamma-z}{3}} \int_y^{\frac{\gamma-z-y}{2}} \int_x^{\gamma-z-y-x} \frac{N(N-1)(N-2)(N-3)L^4 z^{N-4}}{(L+z)^{N-2}(L+w)^2(L+x)^2(L+y)^2} dw dx dy dz. \quad (6.2.21)$$

Then, exploiting (6.2.21) as in (6.2.15), the outage probability can be evaluated, for example for the results in the simulation section the Mathematica software package [86] is used.

In this section the two or four relay selection approaches are considered as they are immediately applicable within a cooperative network, which exploits distributed space time coding [45] to improve the end-to-end performance, such as an Alamouti or Quasi-Orthogonal code, according to the number of selected relays. Furthermore, for this relay selection policy, it requires only the SNR of the links from source to relay nodes and the INR of the interference links which can be obtained by the relay nodes during the early

stage of transmission. In terms of the relay selection policy, moreover, the information describing the links between the relay and destination is not required at the destination node, therefore, this policy has a lower complexity than that of [76] and may save feedback set-up time.

Semi-conventional two and four relay selection

The semi-conventional two and four relay selection schemes are an extension of the conventional selection scheme and motivated by the expression of the general statistics (6.2.4). There are three advantages in the semi-conventional two and four relay selection scheme. Firstly, because this scheme is based on the conventional approach, it does not involve complex computational operations, and can be easily obtained from the conventional case without modifying the $\min(\cdot, \cdot)$ operation. Secondly, it is suitable for ad-hoc systems with mobility that dynamically and continuously change between interference and non-interference environments. Thirdly, the proposed scheme balances the gap between the conventional scheme and asymptotic case for the interference situation. Therefore, in this section, a simple ratio between the conventional $\min(\cdot, \cdot)$ operation and the interference term are considered, because it does not change the basic structural core of the system. In the following, the best two relays selection scheme becomes

$$\mathbf{i}_{Semi} = \arg \max_{i \in N} \max_{i' \in N-1} \left(\frac{\min(\gamma_{sr_i}, \gamma_{r_i d})}{\gamma_{INFi}} \right). \quad (6.2.22)$$

where $\mathbf{i} = (i, i')$, i.e. a pair of relay indices, where i denotes the index of the relay with the best link in N , and i' is that of the best relay amongst the remaining $N - 1$. Here, the outage behavior of the ratio $\frac{\gamma_{sr_i}}{\gamma_{INFi}}$ according to the semi-conventional scheme needs to be considered. In order to simplify the approximation of the corresponding outage bound as in [82], two cases will be considered.

In the first case, the value $\min(\gamma_{sr_i}, \gamma_{r_id}) = \gamma_{sr_i}$, which means the selected relay, the minimum between the two hops, is the link between source and relay. Therefore, the PDF and CDF are given in closed form and correspond to a ratio between the min operation and an exponential random variable, which are

$$f(\gamma) = \frac{2L}{(L+2\gamma)^2} \quad \text{and} \quad F(\gamma) = \frac{2\gamma}{L+2\gamma}, \quad (6.2.23)$$

where $f(\cdot)$ and $F(\cdot)$ denote the PDF and the CDF, respectively. Substituting (6.2.23) into (6.2.10),

$$f(x, y) = \frac{N(N-1)2^N L^2 y^{N-2}}{(L+2y)^N (L+2x)^2}. \quad (6.2.24)$$

Using the PDF in (6.2.24) and (6.2.13), and after performing some manipulations,

$$\begin{aligned} F'_{\gamma_{up}}(\gamma) = & N(N-1)2^N L^2 \left\{ \frac{(\frac{\gamma}{2})^{N-1} (LN + \gamma)}{2N(N-1)L^2(L+\gamma)^N} - \frac{(\frac{\gamma}{2})^N}{2(L+\gamma)^N(L+2\gamma)^2} \right. \\ & \left[\frac{2(L+2\gamma)(L+\gamma)}{L(N-1)\gamma} + \frac{2(\frac{L+\gamma}{L})^N F_{2,1}(N, N; N+1; -\frac{\gamma}{L})}{N} \right. \\ & \left. \left. + \frac{2\gamma(\frac{L+\gamma}{L})^N F_1(N+1; N, 1; N+2; -\frac{\gamma}{L}, \frac{\gamma}{L+2\gamma})}{(N+1)(L+2\gamma)} \right] \right\}, \end{aligned} \quad (6.2.25)$$

some definitions for which have already been shown in the last subsection.

In the second case, the value $\min(\gamma_{sr_i}, \gamma_{r_id}) = \gamma_{r_id}$, which means the minimum between the two hops of the selected relay is the link from relay to destination which is not considered in the ratio of interest. According to the assumption of [82], the conventional asymptotic relay selection can be used as an outage bound in this case. Therefore, based on the above two equiprobable cases, the semi-conventional end-to-end CDF is given as

$$F_{\gamma_{up}}^{Semi}(\gamma) = \frac{1}{2} F_{\gamma_{up}}^{Asy}(\gamma) + \frac{1}{2} F'_{\gamma_{up}}(\gamma), \quad (6.2.26)$$

where $F_{\gamma_{up}}^{Asy}(\gamma)$ and $F'_{\gamma_{up}}(\gamma)$ are denoted by (6.2.14) and (6.2.25), respectively. And the outage probability can be obtained by using (6.2.26).

Then a similar method is used to obtain the best four relays in the following processing. The semi-conventional selection policy can be obtained as

$$\mathbf{i}_{semi} = \arg \max_{i \in N} \max_{i' \in N-1} \max_{i'' \in N-2} \max_{i''' \in N-3} \left(\frac{\min(\gamma_{sr_i}, \gamma_{r_id})}{\gamma_{INF_i}} \right), \quad (6.2.27)$$

where $\mathbf{i} = (i, i', i'', i''')$, i.e. four relay indices, wherein i denotes the index of the relay with the best link in N ; i' is that of the best relay amongst the remaining $N - 1$, and i'' is that of the best relay amongst the remaining $N - 2$, and i''' is that of the best relay amongst the remaining $N - 3$. In the first case, the joint distribution of the four most maximum values can be obtained by substituting (6.2.23) into (6.2.17), yielding

$$f(w, x, y, z) = \frac{N(N-1)(N-2)(N-3)2^N L^4 z^{N-4}}{(L+2z)^{N-2}(L+2w)^2(L+2x)^2(L+2y)^2}. \quad (6.2.28)$$

Substituting (6.2.28) into (6.2.20), and after performing some manipulations,

$$F'_{\gamma_{up}}(\gamma) = \int_0^{\frac{\gamma}{4}} \int_z^{\frac{\gamma-z}{3}} \int_y^{\frac{\gamma-z-y}{2}} \int_x^{\gamma-z-y-x} \frac{N(N-1)(N-2)(N-3)2^N L^4 z^{N-4}}{(L+2z)^{N-2}(L+2w)^2(L+2x)^2(L+2y)^2} dw dx dy dz. \quad (6.2.29)$$

Therefore, the final end-to-end CDF can be obtained as

$$F_{\gamma_{up}}^{Semi}(\gamma) = \frac{1}{2} F_{\gamma_{up}}^{Asy}(\gamma) + \frac{1}{2} F'_{\gamma_{up}}(\gamma), \quad (6.2.30)$$

where $F_{\gamma_{up}}^{Asy}(\gamma)$ and $F'_{\gamma_{up}}(\gamma)$ are given by (6.2.21) and (6.2.29), respectively. And the outage probability can be evaluated by using (6.2.15) and (6.2.30), for example with the Mathematica software package [86].

6.2.3 Simulation results for outage probability analysis and impact of relay selection feedback errors

In this section, in order to verify the results obtained from the above mathematical expressions, the target source node and the neighboring source node use the same unity transmission power is assumed.

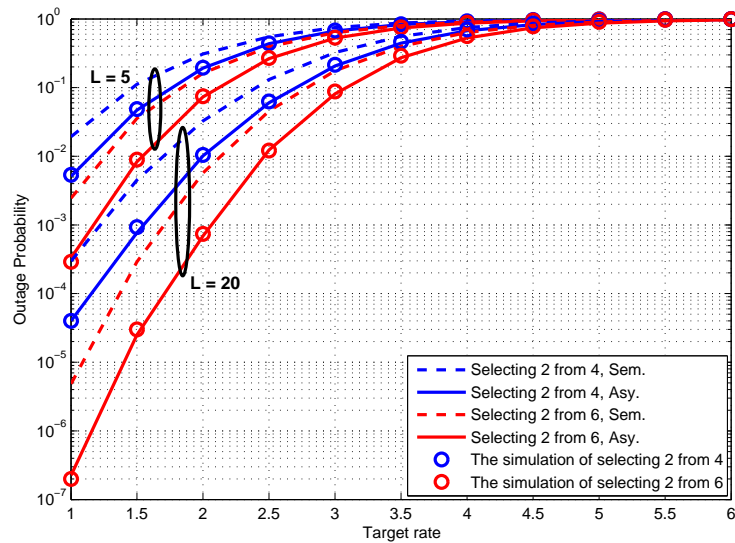


Figure 6.2. Comparison of the outage probability of the best two relay selection schemes, the theoretical results are shown in line style and the simulation results as points.

Fig. 6.2 shows the comparison of the outage probability of the best two relay selection schemes, where $L = 5$ and 20 . It can be seen that increasing the number of relays, N , decreases the outage probability, and hence when the number of relays is large, the outage event (no transmission) becomes less likely, for example, with the total number of available relays increasing from 4 to 6, the outage probability of the best two relay selection is decreased from almost 0.308 to 0.162 for the semi-conventional case; and from 0.192 to 0.073 for the asymptotic case when the target rate is 2 and $L = 5$. The outage performance of the asymptotic case closely matches the simulation results, when $\text{SNR} = 40$ dB. Moreover, with increased source-to-interference

power ratio, the performance in terms of outage probability is improved.

Fig. 6.3 shows the outage probability of the best four relay selection schemes, where $L = 5$ and 20. It can be seen that increasing the number of relays, decreases the outage probability, for example, with the total number of available relays increasing from 6 to 8, the outage probability of the best four relays selection is decreased from almost 0.013 to 0.0025 for the semi-conventional case; and from 0.0022 to 1.6×10^{-4} for the asymptotic case when the target rate is 1.5 and $L = 5$. With increased source-to-interference power ratio, the performance of outage probability again improves. Moreover, the asymptotic results match very well with the simulation results, when $\text{SNR} = 40$ dB.

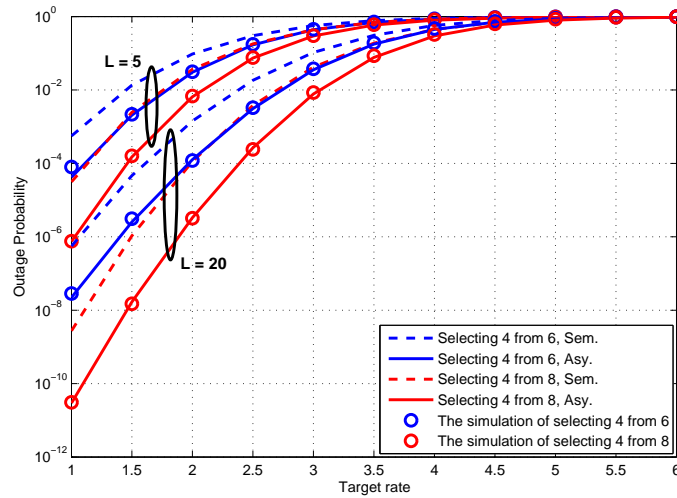


Figure 6.3. Comparison of the outage probability of the best four relay selection schemes, the theoretical results are shown in line style and the simulation results as points.

Fig. 6.4 shows the comparison of the outage probability of the single relay selection and the best two and four relay selection schemes, $\text{SNR} = 40$ dB and $L = 5$ or 10. Obviously, with increasing the number of selected relays, the outage probability decreases. For example, for the semi-conventional case, when the total number of available relays is 6, $L = 5$ and the target

rate is 1.5, the outage probability of a single relay, the best two relays and the best four relays selections are almost 0.1, 0.036 and 0.013, respectively. Furthermore, for the asymptotic case, when $N = 6$, $L = 10$ and the target rate is 1.5, the outage probability of the best relay, the best two relays and the best four relays selections are almost 0.0045, 5.59×10^{-4} and 9.01×10^{-5} , respectively. These results confirm that two and four relay selection schemes provide more robust transmission than single relay selection, because for the single relay selection, it just uses a single relay to help the source to transmit the signal. Therefore, a different number of relays can be selected to communicate with the source and destination node, according to the target outage probability. In the next section how the end-to-end BER performance of the relay selection schemes degrades is considered when there is error in selecting the particular relay(s) to use in transmission.

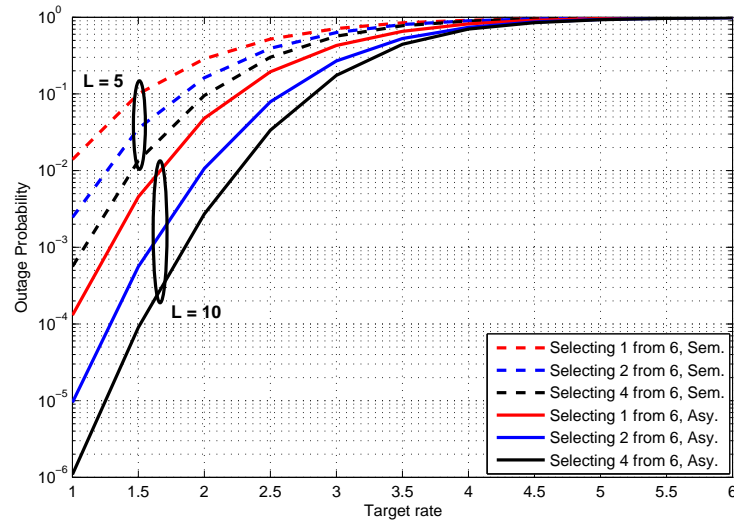


Figure 6.4. Comparison of the outage probability of the single relay selection and the best two and four relay selection schemes.

Next Fig. 6.5 will compare the BER performance of the best two relay selection from a group of N available relays, $N = 4$, with distributed Alamouti code with the best single relay selection in the presence of relay selection feedback errors, when QPSK symbols are used in transmission.

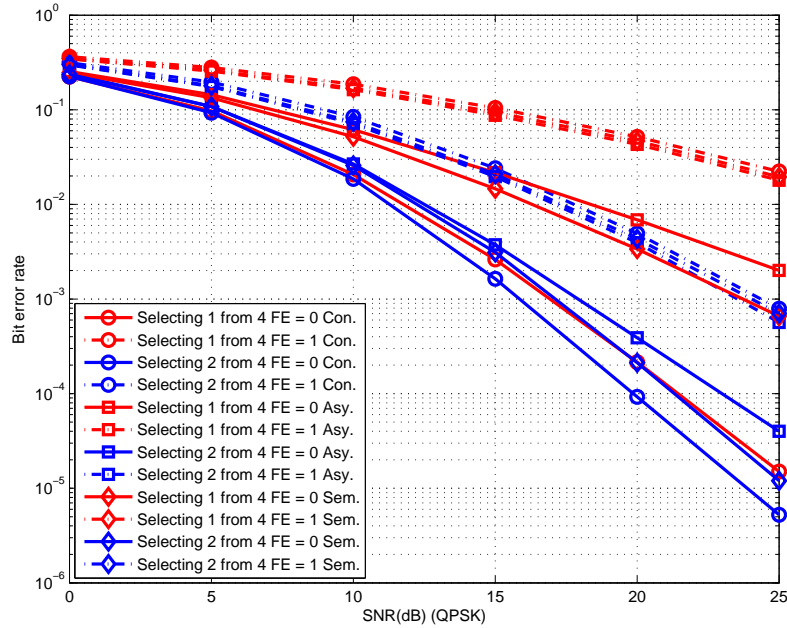


Figure 6.5. BER performance comparison of different best two relay selection schemes (blue line) with the different best single relay selection schemes (red line), with varying error in the feedback relay selection information from the destination.

The comparison between the best two relay selection and the single relay selection in a representative relay selection feedback error environment, and the signal-to-interference power ratio $L = 50$ is assumed. To simulate errors in the feedback of relay selection information from the destination an error rate in the feedback is introduced. An error rate of 0.5 corresponds to 50% of the selections being made in error; that is, rather than selecting the best relay, one of the other relays is chosen with equal probability of selection. As can be seen in Fig. 6.5, when perfect relay selection is made, i.e. an error rate of 0, the BER performance of the best single relay selection is worse than the best two relay selection for the three different relay selection schemes, which are denoted by circular, square and diamond dotted lines for the conventional, asymptotic and semi-conventional schemes, respectively. Moreover, in the presence of errors in the relay selection, i.e. error rate over the range 0 to 1, all of the different best two relays selection schemes

outperform that of the best single relay selection. These results illustrate clearly the increased robustness of the best two relay selection scheme over the single relay selection scheme in the presence of moderate to severe relay selection feedback errors. For example, for the conventional best two relay selection scheme, when the SNR is 20 dB, the BER for the conventional best two relay selection changes from almost 1×10^{-4} only to 4.9×10^{-3} as the error rate changes from 0 to 1, whereas the BER for the single relay selection is increased from almost 2.15×10^{-4} to 5.1×10^{-2} , confirming the improved robustness. In the next section, exact outage probability analysis for a cooperative AF relay network with relay selection in the presence of inter-cluster interference will be provided.

6.3 Relay Selection with Interference at Both the Relay and Destination

6.3.1 System Model

Fig. 6.6 shows a two clusters relay network where cluster one contains a source (S), a destination (D) and multiple relays ($R_i, i = 1 \dots N$) all equipped with single half-duplex antennas; and for simplicity of exposition, cluster two uses direct transmission from the source (S') to a relay (R') or the destination (D'). The coefficients $h_{sr_i}, h_{r_i d}, h_{s' r_i}$ and $h_{s' r'}$ are the instantaneous channels of the links between the source and the i^{th} relay node, the i^{th} relay node and the destination node, the cluster two source and the relay node and the cluster two source and the destination node; and the channel gains $g_j = |h_j|^2$ ($j = sr_i, r_i d, s' r_i, s' d$) are independent exponentially distributed random variables with mean values λ_j ($j = sr_i, r_i d, s' r_i, s' d$), and perfect channel information is assumed to be available at the relays and destination. The analysis of the effect of inter-cluster interference on the relays and destination in cluster one is considered which contains nodes linked by

independent Rayleigh flat-fading quasi-static channels and no direct link between the source and the destination as path loss or shadowing is assumed to render it unusable.

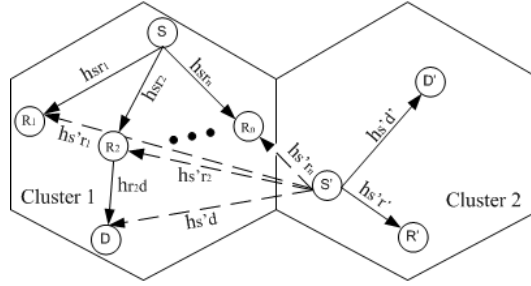


Figure 6.6. The cooperative transmission system model wherein the dashed lines denote the interference links and solid lines denote the selected transmission links, i.e. R_2 is selected for relaying to the destination.

In this model, similar to as in [82], the source powers at cluster one and cluster two are assumed to be the same. This model is representative of an ad-hoc network environment where there is no power control between adjacent clusters. Therefore, the source broadcasts the signal (x) to the relay nodes during the first hop, and during the second hop, the selected relay, i.e. R_2 , from the available group, transmits the received signal to the destination node. Moreover, the interference terms x' and x'' which are generated by the neighboring cluster two are assumed to affect the relay node at the first time slot and the destination node at the second time slot, respectively. Therefore, the system model can be developed as follows: the received signal at the i^{th} relay and the destination node are given by

$$y_{sr_i} = h_{sr_i}x + h_{s'r_i}x' + n_{r_i}, \quad (6.3.1)$$

$$y_{r_i d} = \sqrt{P_i}h_{r_i d}y_{sr_i} + h_{s'd}x'' + n_d, \quad (6.3.2)$$

where the complex additive white Gaussian noise terms n_{r_i} and n_d are modeled as zero-mean mutually independent, circularly-symmetric, complex

Gaussian random variables with variance N_0 at the i^{th} relay and the destination node, respectively. The i^{th} relay gain denoted by $\sqrt{P_i}$ is calculated from $P_i = 1/(|h_{sr_i}|^2 + |h_{s'r_i}|^2 + N_0)$.

Next, the instantaneous equivalent end-to-end SINR using the i^{th} relay can be written according to (6.3.2) as:

$$\gamma_{D_i} = \frac{P_i |h_{sr_i}|^2 |h_{r_i d}|^2}{P_i |h_{s'r_i}|^2 |h_{r_i d}|^2 + P_i |h_{r_i d}|^2 N_0 + |h_{s'd}|^2 + N_0}. \quad (6.3.3)$$

Then, the end-to-end SINR can be obtained as:

$$\gamma_{D_i} = \frac{\gamma_{sr_i} \gamma_{r_i d}}{\gamma_{sr_i} \gamma_{s'd} + \gamma_{r_i d} \gamma_{s'r_i} + \gamma_{s'r} \gamma_{s'r_i} + \gamma_{sr_i} + \gamma_{r_i d} + \gamma_{s'd} + \gamma_{s'r_i} + 1}, \quad (6.3.4)$$

where $\gamma_{sr_i} = g_{sr_i}/N_0$, $\gamma_{r_i d} = g_{r_i d}/N_0$, $\gamma_{s'r_i} = g_{s'r_i}/N_0$ and $\gamma_{s'd} = g_{s'd}/N_0$ are the instantaneous signal-to-noise ratios (SNRs) of the source to i^{th} relay, i^{th} relay to destination, cluster two source to i^{th} relay and to destination links, respectively.

In order to find a closed form expression for the probability density function of γ_{D_i} on the basis of (6.3.4), an asymptotic description in a high SNR range is obtained as

$$\gamma_{D_i} \simeq \frac{\gamma_{sr_i} \gamma_{r_i d}}{\gamma_{s'r_i} \gamma_{r_i d} + \gamma_{s'd} \gamma_{sr_i} + \gamma_{s'd} \gamma_{s'r_i}} = \frac{\gamma_i^0 \gamma_i^1}{\gamma_i^0 + \gamma_i^1 + 1}, \quad (6.3.5)$$

where the terms $\gamma_i^0 = \frac{g_{r_i d}}{g_{s'd}}$ and $\gamma_i^1 = \frac{g_{sr_i}}{g_{sr_i}}$; and when SNR is large, then $\varepsilon(\gamma_{s'r_i})\varepsilon(\gamma_{r_i d}) + \varepsilon(\gamma_{s'd})\varepsilon(\gamma_{sr_i}) + \varepsilon(\gamma_{s'd})\varepsilon(\gamma_{s'r_i}) \gg \varepsilon(\gamma_{sr_i}) + \varepsilon(\gamma_{r_i d}) + \varepsilon(\gamma_{s'd}) + \varepsilon(\gamma_{s'r_i}) + 1$, as in [82], where $\varepsilon(\cdot)$ represents the statistical expectation operator. In the next section, an exact method will be provided to obtain the CDF of the approximate overall SINR given by the right-hand side term in (6.3.5) and analyze the correspondence outage probability.

6.3.2 Relay Selection Scheme with Outage Probability Analysis

In this section, a relay selection approach will be used to choose the best individual relay node. Based on (6.3.5), γ_i^0 is an exponential random variable, which can be calculated based on $g_{r_i d}$. To facilitate analysis $g_{s' d}$ is replaced by its constant mean value is assumed, so that each γ_i^0 can be assumed independent, and γ_i^1 is the ratio between two exponential random variables, where $0 \leq \gamma_i^j \leq \infty$, $j \in (0, 1)$, and according to [83], can be written as $f_{\gamma_i^0}(\gamma) = \frac{1}{L_0} e^{-\frac{\gamma}{L_0}}$, $F_{\gamma_i^0}(\gamma) = 1 - e^{-\frac{\gamma}{L_0}}$, $f_{\gamma_i^1}(\gamma) = \frac{L_1}{(L_1 + \gamma)^2}$ and $F_{\gamma_i^1}(\gamma) = \frac{\gamma}{(L_1 + \gamma)}$, where $f(\cdot)$ and $F(\cdot)$ denote respectively the PDF and the CDF of the end-to-end SNR. The terms $L_0 = \frac{\lambda_{r_i d}}{\lambda_{s' d}}$ and $L_1 = \frac{\lambda_{s r_i}}{\lambda_{s' r_i}}$ are the mean channel gain ratios, which quantify path-loss and the shadowing effect.

Let $x = \gamma_i^0$ and $y = \gamma_i^1$ so that $f_{\gamma_i^0}(\gamma) = f_x(x) = \frac{1}{L_0} e^{-\frac{x}{L_0}}$ and $f_{\gamma_i^1}(\gamma) = f_y(y) = \frac{L_1}{(L_1 + y)^2}$, where $x > 0$ and $y > 0$, and exploiting independence, obtain

$$f_{xy}(x, y) = f_x(x)f_y(y) = \frac{L_1}{L_0} \frac{e^{-\frac{x}{L_0}}}{(L_1 + y)^2}. \quad (6.3.6)$$

Then, the CDF of $Z = \frac{xy}{x+y+1}$, where $Z = \gamma_{D_i}$, becomes

$$\begin{aligned} F_Z(z) &= P\left(\frac{xy}{x+y+1} \leq z\right) = P\left(x \leq \frac{yz+z}{y-z}\right) \\ &= \int_0^z \int_0^\infty f_{xy}(x, y) dx dy + \int_z^\infty \int_0^{\frac{yz+z}{y-z}} f_{xy}(x, y) dx dy, \end{aligned} \quad (6.3.7)$$

where $P(\cdot)$ denotes probability value. Therefore,

$$\begin{aligned} F_{\gamma_{D_i}}(\gamma) &= \int_0^\gamma \int_0^\infty f_{xy}(x, y) dx dy + \int_\gamma^\infty \int_0^{\frac{y\gamma+\gamma}{y-\gamma}} f_{xy}(x, y) dx dy \\ &= \frac{L_0}{L_1} \left(\int_0^\gamma \int_0^\infty \frac{e^{-\frac{x}{L_0}}}{(L_1 + y)^2} dx dy + \int_\gamma^\infty \int_0^{\frac{y\gamma+\gamma}{y-\gamma}} \frac{e^{-\frac{x}{L_0}}}{(L_1 + y)^2} dx dy \right) \\ &= 1 - \frac{L_1 e^{-\frac{\gamma}{L_0}}}{L_1 + \gamma} + \frac{L_1 \gamma (\gamma + 1) e^{\frac{(1-L_1)\gamma}{(L_1+\gamma)L_0}}}{L_0 (L_1 + \gamma)^2} \text{Ei}\left(1, \frac{\gamma(1+\gamma)}{L_0(L_1 + \gamma)}\right), \end{aligned} \quad (6.3.8)$$

where $\text{Ei}(a, b)$ represents the exponential integral, $\text{Ei}(a, b) = \int_1^\infty e^{-xb} x^{-a} dx$.

The best relay node is selected from the N available secondary relays. By using the theory of order statistics [52], the CDF of the end-to-end SINR of the secondary network γ_D corresponds to the selection of the largest γ_{D_i} from the N independent relays instantaneous SINRs in (6.3.5) with CDF which is given by (6.3.8), this is given by

$$F_{\gamma_D}(\gamma) = [F_{\gamma_{D_i}}(\gamma)]^N. \quad (6.3.9)$$

Furthermore, the outage probability is defined as when the average end-to-end SNR falls below a certain predefined threshold value, α . The outage probability can be expressed as

$$\begin{aligned} P_{out} &= \int_0^\alpha f_{\gamma_D}(\gamma) d\gamma = F_{\gamma_D}(\alpha) \\ &= \left[1 - \frac{L_1 e^{-\frac{\alpha}{L_0}}}{L_1 + \alpha} + \frac{L_1 \alpha (\alpha + 1) e^{\frac{(1-L_1)\alpha}{(L_1+\alpha)L_0}}}{L_0 (L_1 + \alpha)^2} \text{Ei}\left(1, \frac{\alpha(1+\alpha)}{L_0(L_1+\alpha)}\right) \right]^N. \end{aligned} \quad (6.3.10)$$

6.3.3 Outage Probability Analysis Verification

In this section, in order to verify the results obtained from the above mathematical expressions, it is supposed that $\varepsilon(\gamma_{sr_i}) = \varepsilon(\gamma_{r_i d}) = 40$ dB (symmetric hops for the secondary networks). However, this analysis can be extended straightforwardly to completely asymmetric configurations ($\varepsilon(\gamma_{sr_i}) \neq \varepsilon(\gamma_{r_i d})$).

Fig. 6.7 shows the outage probability of the best relay selection schemes versus the target rate, when $L_0 = 10$ and $L_1 = 10$. Firstly, it can be seen that increasing the number of relays, N , decreases the outage probability, i.e., with the total number of available relays increasing from 5 to 15, the outage probability of the best relay selection is decreased from almost 0.37 to 0.052 for the proposed scheme when the target rate is 1.5. Secondly, the theoretical outage performance of (6.3.10) matches very closely with the simulation

results. On the other hand, with the max-min selection scheme as commonly used by other researchers, where the CDF of γ_D is given approximately by $1 - \frac{L_1 e^{-\frac{\gamma}{L_0}}}{L_1 + \gamma}$ and can be derived as in [52], only a loose upper bound (smaller outage probability) is provided.

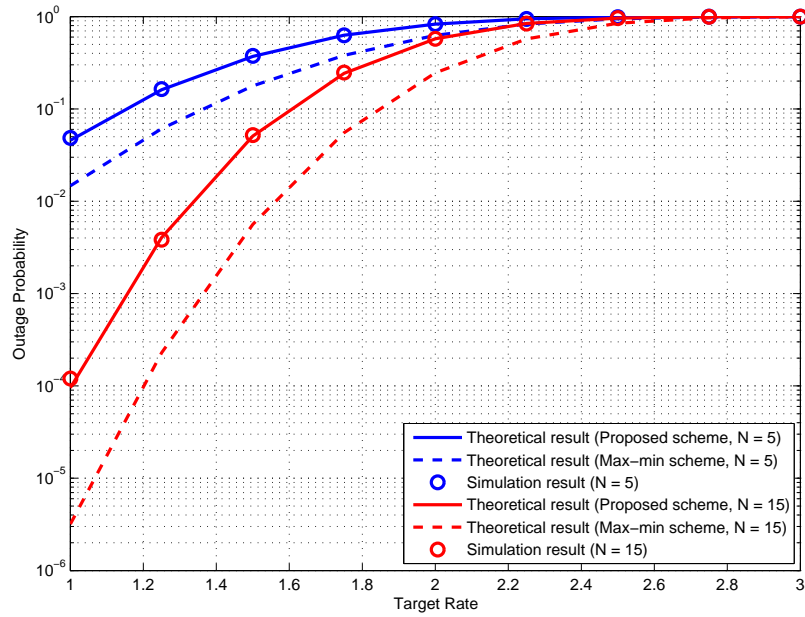


Figure 6.7. Comparison of the outage probability of the best relay selection schemes, the theoretical results are shown in line style and the simulation results as points.

6.4 Summary

This chapter has firstly examined two different selection schemes which are asymptotical and semi-conventional policies to select the best multi-relays from a group of available relays in the same cluster by using local measurements of the instantaneous channel conditions in the context of legacy systems which adopt $\max(\min(\cdot, \cdot))$ type policies. New analytical expressions for the PDF, and CDF of end-to-end SINR were derived together with near closed form expressions for outage probability over Rayleigh fading channels. Secondly, the best relay selection from a group of available relays by using local measurements of the instantaneous channel conditions in the context of cooperative systems which adopt a selection policy to maximize end-to-end SINR was provided, when inter-cluster interference was considered both at the relay nodes and the destination node. Moreover, a new exact closed form expression for outage probability in the high SNR region was provided. In the next chapter, outage probability analysis for a cognitive amplify and forward relay network with single and multi-relay selection will be introduced.

OUTAGE PROBABILITY OF MULTI-RELAY SELECTION IN COGNITIVE RELAY NETWORKS

This chapter evaluates the outage probability of a cognitive amplify and forward relay network with cooperation between certain secondary users, chosen by single and multi-relay (two and four) selection, based on the underlay approach, which requires adherence to an interference constraint on the primary user. The relay selection is performed either on the basis of a max-min strategy or one based on maximizing exactly the end-to-end SNR. To realize the relay selection schemes within the secondary networks, a predetermined threshold for the power of the received signal in the primary receiver is assumed. To assess the performance advantage of adding additional secondary relays, analytical expressions for the PDF, and CDF of the received SNR are derived. Closed form and near closed form expressions for outage probability over Rayleigh frequency flat fading channels are then obtained. In particular, lower and upper bound expressions for outage probability are presented and then a new exact expression for outage probability is provided. Finally, these analytical results are verified by numerical simulation.

7.1 Introduction

Cognitive radio (CR) is an efficient method to improve spectrum utilization by spectrum sharing between primary users and cognitive radio users (secondary users); that is the secondary user can be permitted to take advantage of the licensed band provided the data transmission of the primary users can be protected by using spectrum underlay, overlay and interweave approaches [30]. In the underlay approach, the secondary user is allowed to use the spectrum of the primary user (PU) so long as the interference from the secondary user is less than the interference level which the primary user can tolerate. Therefore, the transmission power of the secondary user is constrained not to exceed the interference threshold. In the overlay approach, the secondary user (SU) employs the same spectrum concurrently with the primary user while maintaining or improving the transmission of the primary user by applying sophisticated but generally computationally complex, signal processing and coding [30]. In the interweave approach, the secondary user utilizes the spectrum not currently being used by the primary user, known as a spectrum hole, identified by some form of spectrum sensing, however this is sensitive to issues such as the hidden terminal problem. As such, the underlay approach is more practical than others, and is the focus of this chapter.

A relay network can moreover be considered as an effective method to combat fading by exploiting spatial diversity [9], and as a way for two users with no or weak direct connection to attain a robust link. One or more relay nodes can be used to forward signals transmitted from the source node to the destination node. Inspired by cognitive radio and relay networks, cognitive relay networks have been investigated as a potential way to improve secondary user throughput using one of two schemes: cooperation between primary and secondary users [87], and cooperation between secondary users

[88–91].

For cooperation between secondary users, [88] analyzed the approximate outage performance in cognitive DF relay networks. Exact outage probability considering the spectrum sensing accuracy in cognitive relay networks was investigated in [89], and [90] proposed a distributed transmit power allocation scheme for multihop cognitive radio networks. Additionally, [91] investigated outage probability and diversity for cognitive DF relay networks with single relay selection. However, these works have only studied the DF relay scheme, and little prior work has considered multi-relay selection in cognitive AF relay networks.

Therefore, this chapter evaluates the performance of a cognitive AF relay network using single relay and multi-relay (two and four) selection to allow cooperation between secondary users according to the underlay approach and limit this study to four relay selection as practical distributed space-time block coding schemes are typically designed for no more than four relays [44]. Moreover, three types of outage probability analysis methods are provided, namely, ones based on well known lower and upper bounds and a new one using an exact analysis. The contributions of this chapter are to show that: 1) The outage probability for the secondary user is affected by two factors: the first factor is in the form of ratios of channel gains, i.e., in the secondary transmission, the ratio between the gain of the secondary source to chosen secondary relay channel, to the gain of the secondary source to the primary receiver channel, together with the ratio between the gain of the chosen secondary relay to secondary destination channel to the gain of the chosen secondary relay to the primary receiver channel; and the second factor is the interference threshold for the primary user; 2) multi-relay (two and four) selection according to these approaches can achieve low outage probability in the secondary user even when the power of the secondary source and relays is constrained; 3) a new exact outage probability analysis

is much more useful for end-to-end performance analysis than those based on the previous bounds.

7.2 System Model

Fig. 7.1 shows the cognitive relay network model. In this figure, SS , SR_i ($i \in (1, \dots, N)$), SD and PD represent a secondary source, N secondary relays, a secondary destination, and a primary destination, respectively. The operation of the secondary relays is assumed to be performed in a half duplex AF mode. SS broadcasts its signal to all SR_i in the first hop, and the selected SR_i (s) relay(s) their received signal(s) to SD in the second hop.

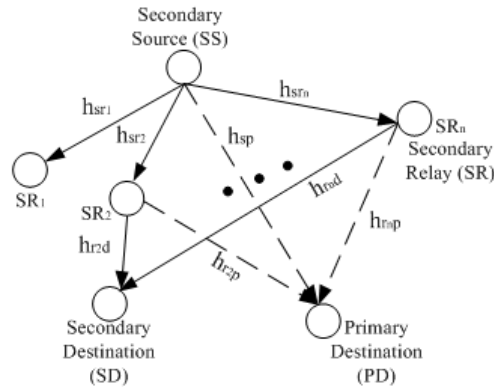


Figure 7.1. The cognitive relay network model wherein the dashed lines denote the interference links and the solid lines denote the selected transmission links, i.e., only SR_2 and SR_n are used for relaying to the secondary destination.

For simplicity of exposition, there is no direct link between the source and the destination as path loss or shadowing is assumed to render it unusable [92]. The coefficients h_{sp} , h_{sr_i} , $h_{r_i d}$ and $h_{r_i p}$ are the instantaneous channels of the links between SS and SP , SS and SR_i , SR_i and SD , and SR_i and SP , respectively. Statistically, the channel gains $g_j = |h_j|^2$ ($j = sp, sr_i, r_i d, r_i p$) are independent exponentially distributed random variables with mean values λ_j ($j = sp, sr_i, r_i d, r_i p$), and perfect channel information is assumed to

be available at the secondary relays and secondary destination.

In the underlay technique SS and SR_i can share the primary user's spectrum if the power of the received interference signal in PD from SS and SR_i satisfies a predetermined threshold defined by I_{th} . And because the multi-relay (two and four) selection scheme is used in this chapter, the limits on power for SS and SR_i are given by

$$g_{sp}P_{SS} \leq I_{th} \quad \text{and} \quad g_{r_i p}P_{SR_i} \leq \frac{I_{th}}{|N_s|}, \quad (7.2.1)$$

where $|N_s|$ denotes the cardinality of the set of relay indices for the selected relays; P_{SS} and P_{SR_i} are the transmission power of SS and SR_i , respectively. Therefore, the maximum transmission powers of SS and SR_i ¹ are equal to $\frac{I_{th}}{g_{sp}}$ and $\frac{I_{th}}{g_{r_i p}|N_s|}$, respectively. Using these powers, the received signal vector at SR_i is

$$\mathbf{y}_{sr_i} = h_{sr_i} \sqrt{\frac{I_{th}}{g_{sp}}} \mathbf{s} + \mathbf{n}_r, \quad (7.2.2)$$

where \mathbf{s} is a transmitted signal vector from SS , and \mathbf{n}_r is an AWGN vector with zero mean and σ_r^2 variance elements received in the SR_i node. The received signal vector at SD from the selected SR_i can be obtained as

$$\begin{aligned} \mathbf{y}_{r_i d} &= h_{r_i d} \sqrt{\frac{I_{th}}{g_{r_i p}|N_s|}} P_{R_i} \mathbf{y}_{sr_i} + \mathbf{n}_d \\ &= h_{r_i d} h_{sr_i} \sqrt{\frac{I_{th}^2}{g_{sp} g_{r_i p} |N_s|}} P_{R_i} \mathbf{s} + h_{r_i d} \sqrt{\frac{I_{th}}{g_{r_i p}|N_s|}} P_{R_i} \mathbf{n}_r + \mathbf{n}_d, \end{aligned} \quad (7.2.3)$$

where \mathbf{n}_d is an AWGN vector with zero mean and σ_d^2 variance elements received in the SD node, and P_{R_i} is the limited output amplify gain of SR_i which is defined in [93] as

$$P_{R_i}^2 = \frac{g_{sp}}{g_{sr_i} I_{th} + \sigma_r^2 g_{sp}}. \quad (7.2.4)$$

¹This design is for the worst case when the interference terms at the primary destination combine coherently.

Next, because the multi-relay selection scheme is used, the MRC is assumed to be used at the destination node [79]. The practical implementation of the MRC will, however, incur a capacity penalty due to the need to adopt a time multiplexing approach to transmission between the relays and the destination node; however, this can be mitigated by adopting an orthogonal transmission scheme, i.e. distributed space-time coding, which is available for two or four relays. Furthermore, increasing the number of selected relays will incur practical overheads such as increased complexity in synchronization. Therefore, this chapter focuses on selection of one relay and multi-relays (two and four). Then from (7.2.3) the overall instantaneous equivalent end-to-end SNR can be written as:

$$\gamma_{eq}^E = \sum_{i \in N_s} \frac{\gamma_i^0 \gamma_i^1}{\gamma_i^0 + \gamma_i^1 + 1}, \quad (7.2.5)$$

where N_s denotes the set of relay indices for the relays chosen in the single and multi-relay (two and four) selection schemes. The terms $\gamma_i^0 = \frac{g_{sr_i} I_{th}}{g_{sp} \sigma_r^2}$ and $\gamma_i^1 = \frac{g_{r_i d} I_{th}}{g_{r_i p} \sigma_d^2 |N_s|}$ are the SNRs of the first and second hop, respectively. In this chapter, three schemes to calculate the statistics (i.e., the PDF and CDF) of (7.2.5) will be provided. First two bounds on (7.2.5) by using the well known $\frac{1}{2} \min(\gamma_i^0, \gamma_i^1)$ (lower bounded) and $\min(\gamma_i^0, \gamma_i^1)$ (upper bounded) [79] are given, and note, as will be shown in the simulation section, that

$$\gamma_{eq}^{UB} = \sum_{i \in N_s} \min(\gamma_i^0, \gamma_i^1) > \gamma_{eq}^E \geq \sum_{i \in N_s} \frac{1}{2} \min(\gamma_i^0, \gamma_i^1) = \gamma_{eq}^{LB}. \quad (7.2.6)$$

And then a new and more accurate analysis for the statistics of (7.2.5) is provided. Therefore, in the next section, the PDF and CDF of (7.2.5) will be formed by using the two bounds in (7.2.6) and a direct exact calculation, respectively; and the outage probability of the cognitive AF relay network will be analyzed.

7.3 Relay Selection Scheme with Outage Probability Analysis

In this section, three types of outage probability analysis approaches will be presented for the best single or multi-relay (two and four) selection. Firstly, the PDF and CDF of the per hop SNR, wherein γ_i^0 is an exponential random variable, are calculated based on g_{sr_i} . To facilitate analysis g_{sp} is assumed to be replaced by its constant mean value, so that each γ_i^0 can be assumed independent, and γ_i^1 is the ratio between two exponential random variables, where $0 \leq \gamma_i^j \leq \infty$, $j \in (0, 1)$, and according to [83], can be written as

$$\begin{aligned} f_{\gamma_i^0}(\gamma) &= \frac{1}{L_0} e^{-\frac{\gamma}{L_0}} \quad \text{and} \quad F_{\gamma_i^0}(\gamma) = 1 - e^{-\frac{\gamma}{L_0}}, \\ f_{\gamma_i^1}(\gamma) &= \frac{L_1}{(L_1 + \gamma)^2} \quad \text{and} \quad F_{\gamma_i^1}(\gamma) = \frac{\gamma}{(L_1 + \gamma)}, \end{aligned} \quad (7.3.1)$$

where $f(\cdot)$ and $F(\cdot)$ denote the PDF and the CDF of the end-to-end SNR, respectively. The terms $L_0 = \phi_0 \frac{I_{th}}{\sigma_r^2}$ and $L_1 = \phi_1 \frac{I_{th}}{\sigma_d^2 |N_s|}$, where $\phi_0 = \frac{\lambda_{sr_i}}{\lambda_{sp}}$ and $\phi_1 = \frac{\lambda_{r_i d}}{\lambda_{r_i p}}$ are the mean channel gain ratios. Basically, the mean value of the channel gain incorporates the path-loss and the shadowing effect. Using these mean values does not necessarily imply that the relays are all at the same distance from the source and destination node, as one path could experience more shadowing but be closer to the source or destination node than another relay which has a better link.

7.3.1 The CDF and PDF of Lower Bound SNR

For the lower bound analysis, the CDF of $\gamma_{eq_i}^{LB} = \frac{1}{2} \min(\gamma_i^0, \gamma_i^1)$ can be expressed as [80]

$$F_{\gamma_{eq_i}^{LB}}(\gamma) = 1 - Pr(\gamma_i^0 > 2\gamma)Pr(\gamma_i^1 > 2\gamma) = 1 - [1 - F_{\gamma_i^0}(2\gamma)][1 - F_{\gamma_i^1}(2\gamma)]. \quad (7.3.2)$$

Therefore, substituting (7.3.1) into (7.3.2), the CDF of the $\gamma_{eq_i}^{LB}$ can be obtain as

$$F_{\gamma_{eq_i}^{LB}}(\gamma) = 1 - \frac{L_1 e^{-\frac{2\gamma}{L_0}}}{L_1 + 2\gamma}, \quad (7.3.3)$$

and the PDF of $\gamma_{eq_i}^{LB}$ can be obtained by taking the derivative of the CDF (7.3.3) as

$$f_{\gamma_{eq_i}^{LB}}(\gamma) = \frac{2L_1 e^{-\frac{2\gamma}{L_0}} (L_0 + L_1 + 2\gamma)}{L_0 (L_1 + 2\gamma)^2}. \quad (7.3.4)$$

7.3.2 The CDF and PDF of Upper Bound SNR

For the upper bound analysis, the CDF of $\gamma_{eq_i}^{UB} = \min(\gamma_i^0, \gamma_i^1)$ can be expressed as [80]

$$F_{\gamma_{eq_i}^{UB}}(\gamma) = 1 - Pr(\gamma_i^0 > \gamma) Pr(\gamma_i^1 > \gamma) = 1 - [1 - F_{\gamma_i^0}(\gamma)][1 - F_{\gamma_i^1}(\gamma)]. \quad (7.3.5)$$

Therefore, substituting (7.3.1) into (7.3.5), the CDF of the $\gamma_{eq_i}^{UB}$ can be obtain as

$$F_{\gamma_{eq_i}^{UB}}(\gamma) = 1 - \frac{L_1 e^{-\frac{\gamma}{L_0}}}{L_1 + \gamma}, \quad (7.3.6)$$

and the PDF of $\gamma_{eq_i}^{UB}$ can be obtained by taking the derivative of the CDF (7.3.6) as

$$f_{\gamma_{eq_i}^{UB}}(\gamma) = \frac{L_1 e^{-\frac{\gamma}{L_0}} (L_0 + L_1 + \gamma)}{L_0 (L_1 + \gamma)^2}. \quad (7.3.7)$$

7.3.3 The CDF and PDF of Exact SNR

Then, for the new exact outage probability analysis for relay selection the CDF and PDF of the end-to-end per hop SNR need to be obtained. Firstly, let $x = \gamma_i^0$ and $y = \gamma_i^1$ so that $f_{\gamma_i^0}(\gamma) = f_x(x) = \frac{1}{L_0} e^{-\frac{x}{L_0}}$ and $f_{\gamma_i^1}(\gamma) = f_y(y) = \frac{L_1}{(L_1 + y)^2}$, where $x > 0$ and $y > 0$, and exploiting independence, obtain

$$f_{xy}(x, y) = f_x(x) f_y(y) = \frac{L_1}{L_0} \frac{e^{-\frac{x}{L_0}}}{(L_1 + y)^2}. \quad (7.3.8)$$

Then, the CDF of $Z = \frac{xy}{x+y+1}$, where $Z = \gamma_{eq_i}^E$, becomes

$$\begin{aligned} F_Z(z) &= P\left(\frac{xy}{x+y+1} \leq z\right) = P\left(x \leq \frac{yz+z}{y-z}\right) \\ &= \int_0^z \int_0^\infty f_{xy}(x,y) dx dy + \int_z^\infty \int_0^{\frac{yz+z}{y-z}} f_{xy}(x,y) dx dy, \end{aligned} \quad (7.3.9)$$

where $P(\cdot)$ denotes probability value. Therefore,

$$\begin{aligned} F_{\gamma_{eq_i}^E}(\gamma) &= \int_0^\gamma \int_0^\infty f_{xy}(x,y) dx dy + \int_\gamma^\infty \int_0^{\frac{y\gamma+\gamma}{y-\gamma}} f_{xy}(x,y) dx dy \\ &= \frac{L_0}{L_1} \left(\int_0^\gamma \int_0^\infty \frac{e^{-\frac{x}{L_0}}}{(L_1+y)^2} dx dy + \int_\gamma^\infty \int_0^{\frac{y\gamma+\gamma}{y-\gamma}} \frac{e^{-\frac{x}{L_0}}}{(L_1+y)^2} dx dy \right) \\ &= 1 - \frac{L_1 e^{-\frac{\gamma}{L_0}}}{L_1 + \gamma} + \frac{L_1 \gamma (\gamma + 1) e^{\frac{(1-L_1)\gamma}{(L_1+\gamma)L_0}} \text{Ei}\left(1, \frac{\gamma(1+\gamma)}{L_0(L_1+\gamma)}\right)}{L_0(L_1 + \gamma)^2}, \end{aligned} \quad (7.3.10)$$

where $\text{Ei}(a,b)$ represents the exponential integral, namely $\text{Ei}(a,b) = \int_1^\infty e^{-bx} x^{-a} dx$. And the PDF of $\gamma_{eq_i}^E$ can be obtained by taking the derivative of the CDF (7.3.10) as

$$\begin{aligned} f_{\gamma_{eq_i}^E}(\gamma) &= \frac{L_1(L_1^2 - L_1 + L_1 L_0 + L_0 \gamma) e^{-\frac{\gamma}{L_0}}}{L_0(L_1 + \gamma)^3} \\ &\quad + \frac{[L_1^2(2\gamma + 1) - L_1 \gamma] e^{\frac{(1-L_1)\gamma}{(L_1+\gamma)L_0}} \text{Ei}\left(1, \frac{\gamma(1+\gamma)}{L_0(L_1+\gamma)}\right)}{L_0(L_1 + \gamma)^3} \\ &\quad + \frac{L_1^2 \gamma (\gamma + 1) (1 - L_1) e^{\frac{(1-L_1)\gamma}{(L_1+\gamma)L_0}} \text{Ei}\left(1, \frac{\gamma(1+\gamma)}{L_0(L_1+\gamma)}\right)}{L_0^2(L_1 + \gamma)^4}. \end{aligned} \quad (7.3.11)$$

7.3.4 Outage Probability Analysis

A. The best relay selection

The best relay node is selected as the one providing the highest end-to-end SNR from the N available secondary relays. By using the theory of order statistics [52], the CDF of γ_{eq}^{LB} , γ_{eq}^{UB} and γ_{eq}^E correspond to the selection of the largest $\gamma_{eq_i}^{LB}$, $\gamma_{eq_i}^{UB}$ and $\gamma_{eq_i}^E$ from the N independent relays instantaneous SNRs in the right and left side of (7.2.6) and (7.2.5), respectively, with a

statistic which is given by (7.3.3), (7.3.6) and (7.3.10). Therefore, the outage probability is defined as when the average end-to-end SNR falls below a certain predefined threshold value, α . The outage probability can be expressed as

$$P_{out}^{LB} = \int_0^\alpha f_{\gamma_{eq}^{LB}}(\gamma) d\gamma = F_{\gamma_{eq}^{LB}}(\alpha) = \left[F_{\gamma_{eq_i}^{LB}}(\gamma) \right]^N = \left[1 - \frac{L_1 e^{-\frac{2\alpha}{L_0}}}{L_1 + 2\alpha} \right]^N, \quad (7.3.12)$$

$$P_{out}^{UB} = \int_0^\alpha f_{\gamma_{eq}^{UB}}(\gamma) d\gamma = F_{\gamma_{eq}^{UB}}(\alpha) = \left[F_{\gamma_{eq_i}^{UB}}(\gamma) \right]^N = \left[1 - \frac{L_1 e^{-\frac{\alpha}{L_0}}}{L_1 + \alpha} \right]^N, \quad (7.3.13)$$

$$P_{out}^E = \int_0^\alpha f_{\gamma_{eq}^E}(\gamma) d\gamma = F_{\gamma_{eq}^E}(\alpha) = \left[F_{\gamma_{eq_i}^E}(\gamma) \right]^N \\ = \left[1 - \frac{L_1 e^{-\frac{\alpha}{L_0}}}{L_1 + \alpha} + \frac{L_1 \alpha (\alpha + 1) e^{\frac{(1-L_1)\alpha}{(L_1+\alpha)L_0}} \text{Ei}\left(1, \frac{\alpha(1+\alpha)}{L_0(L_1+\alpha)}\right)}{L_0(L_1 + \alpha)^2} \right]^N. \quad (7.3.14)$$

B. The best two relay selection

Then the best two relay nodes selection, namely, select the maximum and the second $\gamma_{eq_i}^{LB}$, $\gamma_{eq_i}^{UB}$ and $\gamma_{eq_i}^E$ from the N available secondary relays instantaneous SNRs in the right and left side of (7.2.6) and (7.2.5) are provided, respectively. According to [52], the selection of the maximum and the second largest is not independent, therefore the joint distribution of the two most maximum values can be obtained as

$$f^K(x_1, x_2) = N(N-1) \left[F_{\gamma_{eq_{x_2}}^K}(x_2) \right]^{N-2} f_{\gamma_{eq_{x_1}}^K}(x_1) f_{\gamma_{eq_{x_2}}^K}(x_2), \quad (7.3.15)$$

where $x_1 \geq x_2 \geq x_N \geq 0$, and $K \in (LB, UB \text{ and } E)$. Substituting (7.3.3) and (7.3.4), (7.3.6) and (7.3.7) and (7.3.10) and (7.3.11) into (7.3.15), re-

spectively, the three types of joint distribution can be obtained as

$$f^{LB}(x_1, x_2) = N(N-1) \left[1 - \frac{L_1 e^{-\frac{2x_2}{L_0}}}{L_1 + 2x_2} \right]^{N-2} \frac{L_1 e^{-\frac{2x_1}{L_0}} (L_0 + L_1 + 2x_1)}{L_0(L_1 + 2x_1)^2} \frac{L_1 e^{-\frac{2x_2}{L_0}} (L_0 + L_1 + 2x_2)}{L_0(L_1 + 2x_2)^2}, \quad (7.3.16)$$

$$f^{UB}(x_1, x_2) = N(N-1) \left[1 - \frac{L_1 e^{-\frac{x_2}{L_0}}}{L_1 + x_2} \right]^{N-2} \frac{L_1 e^{-\frac{x_1}{L_0}} (L_0 + L_1 + x_1)}{L_0(L_1 + x_1)^2} \frac{L_1 e^{-\frac{x_2}{L_0}} (L_0 + L_1 + x_2)}{L_0(L_1 + x_2)^2}, \quad (7.3.17)$$

$$f^E(x_1, x_2) = N(N-1) \left[\frac{L_1(L_1^2 - L_1 + L_1 L_0 + L_0 x_2) e^{-\frac{x_2}{L_0}}}{L_0(L_1 + x_2)^3} + \frac{[L_1^2(2x_2 + 1) - L_1 x_2] e^{\frac{(1-L_1)x_2}{(L_1+x_2)L_0}} \text{Ei}\left(1, \frac{x_2(1+x_2)}{L_0(L_1+x_2)}\right)}{L_0(L_1 + x_2)^3} + \frac{L_1^2 x_2 (x_2 + 1) (1 - L_1) e^{\frac{(1-L_1)x_2}{(L_1+x_2)L_0}} \text{Ei}\left(1, \frac{x_2(1+x_2)}{L_0(L_1+x_2)}\right)}{L_0^2 (L_1 + x_2)^4} \right] \left[\frac{L_1(L_1^2 - L_1 + L_1 L_0 + L_0 x_1) e^{-\frac{x_1}{L_0}}}{L_0(L_1 + x_1)^3} + \frac{[L_1^2(2x_1 + 1) - L_1 x_1] e^{\frac{(1-L_1)x_1}{(L_1+x_1)L_0}} \text{Ei}\left(1, \frac{x_1(1+x_1)}{L_0(L_1+x_1)}\right)}{L_0(L_1 + x_1)^3} + \frac{L_1^2 x_1 (x_1 + 1) (1 - L_1) e^{\frac{(1-L_1)x_1}{(L_1+x_1)L_0}} \text{Ei}\left(1, \frac{x_1(1+x_1)}{L_0(L_1+x_1)}\right)}{L_0^2 (L_1 + x_1)^4} \right] \left[1 - \frac{L_1 e^{-\frac{x_2}{L_0}}}{L_1 + x_2} + \frac{L_1 x_2 (x_2 + 1) e^{\frac{(1-L_1)x_2}{(L_1+x_2)L_0}} \text{Ei}\left(1, \frac{x_2(1+x_2)}{L_0(L_1+x_2)}\right)}{L_0(L_1 + x_2)^2} \right]^{N-2}. \quad (7.3.18)$$

Then the CDF of the random variable γ_{eq}^K is calculated, formed as the sum of the x_1 and x_2 random variables. Therefore, the three types of CDF can be obtained from

$$F_{\gamma_{eq}^K}(\gamma) = Pr\{x_1 + x_2 \leq \gamma\}. \quad (7.3.19)$$

Given that x_1 and x_2 are non-negative, with $x_1 \geq x_2$, then,

$$F_{\gamma_{eq}^K}(\gamma) = \int_0^{\frac{\gamma}{2}} \int_{x_2}^{\gamma-x_2} f^K(x_1, x_2) dx_1 dx_2. \quad (7.3.20)$$

Substituting (7.3.16), (7.3.17) and (7.3.18) into (7.3.20), respectively, and after performing some manipulations,

$$F_{\gamma_{eq}^{LB}}(\gamma) = N(N-1) \frac{2L_1^2}{L_0} \int_0^{\frac{\gamma}{2}} \left(1 - \frac{L_1 e^{-\frac{2x_2}{L_0}}}{L_1 + 2x_2} \right)^{N-2} \left[\frac{e^{-\frac{4x_2}{L_0}} (L_0 + L_1 + 2x_2)}{(L_1 + 2x_2)^3} - \frac{e^{-\frac{2\gamma}{L_0}} (L_0 + L_1 + 2x_2)}{(L_1 + 2x_2)^2 (L_1 + \gamma - 2x_2)} \right] dx_2, \quad (7.3.21)$$

$$F_{\gamma_{eq}^{UL}}(\gamma) = N(N-1) \frac{L_1^2}{L_0^2} \int_0^{\frac{\gamma}{2}} \left(1 - \frac{L_1 e^{-\frac{x_2}{L_0}}}{L_1 + x_2} \right)^{N-2} \left[\frac{e^{-\frac{2x_2}{L_0}} (L_0 + L_1 + x_2)}{(L_1 + x_2)^3} - \frac{e^{-\frac{\gamma}{L_0}} (L_0 + L_1 + x_2)}{(L_1 + x_2)^2 (L_1 + \gamma - x_2)} \right] dx_2, \quad (7.3.22)$$

$$F_{\gamma_{eq}^E}(\gamma) = N(N-1) \int_0^{\frac{\gamma}{2}} \left[\frac{L_1(L_1^2 - L_1 + L_1 L_0 + L_0 x_2) e^{-\frac{x_2}{L_0}}}{L_0(L_1 + x_2)^3} + \frac{[L_1^2(2x_2 + 1) - L_1 x_2] e^{\frac{(1-L_1)x_2}{(L_1+x_2)L_0}} \text{Ei}\left(1, \frac{x_2(1+x_2)}{L_0(L_1+x_2)}\right)}{L_0(L_1 + x_2)^3} + \frac{L_1^2 x_2(x_2 + 1)(1 - L_1) e^{\frac{(1-L_1)x_2}{(L_1+x_2)L_0}} \text{Ei}\left(1, \frac{x_2(1+x_2)}{L_0(L_1+x_2)}\right)}{L_0^2(L_1 + x_2)^4} \right] \left[\frac{L_1 e^{-\frac{x_2}{L_0}}}{L_1 + x_2} - \frac{L_1 x_2(x_2 + 1) e^{\frac{(1-L_1)x_2}{(L_1+x_2)L_0}} \text{Ei}\left(1, \frac{x_2(1+x_2)}{L_0(L_1+x_2)}\right)}{L_0(L_1 + x_2)^2} - \frac{L_1 e^{-\frac{\gamma-x_2}{L_0}}}{L_1 + \gamma - x_2} + \frac{L_1(\gamma - x_2)(\gamma - x_2 + 1) e^{\frac{(1-L_1)(\gamma-x_2)}{(L_1+\gamma-x_2)L_0}} \text{Ei}\left(1, \frac{(\gamma-x_2)(1+\gamma-x_2)}{L_0(L_1+\gamma-x_2)}\right)}{L_0(L_1 + \gamma - x_2)^2} \right]^{N-2} dx_2. \quad (7.3.23)$$

The outage probability can then be defined as the probability that the average end-to-end SNR falls below a certain predefined threshold value, α . The three types of outage probability can therefore be expressed as

$$P_{out}^K = \int_0^\alpha f_{\gamma_{eq}^K}(\gamma) d\gamma = F_{\gamma_{eq}^K}(\alpha). \quad (7.3.24)$$

C. The best four relay selection

The selection of the four largest SNRs is again not independent, therefore, according to [52], the joint distribution of the four most maximum values can be obtained as

$$f^K(x_1, x_2, x_3, x_4) = N(N-1)(N-2)(N-3) \left[F_{\gamma_{eq_{x_4}}^K}(x_4) \right]^{N-4} \prod_{i=1}^4 f_{\gamma_{eq_{x_i}}^K}(x_i), \quad (7.3.25)$$

where $x_1 \geq x_2 \geq x_3 \geq x_4 \geq 0$, $f(\cdot)$ and $F(\cdot)$ correspond to the PDF and CDF. Then the CDF of the random variable γ_{eq}^K is calculated, formed as the sum of the random variables from x_1, x_2 to x_4 , which are identically distributed exponential random variables. Therefore, the three types of CDF are obtained from

$$F_{\gamma_{eq}^K}(\gamma) = Pr\{x_1 + x_2 + x_3 + x_4 \leq \gamma\}. \quad (7.3.26)$$

and finally,

$$F_{\gamma_{eq}^K}(\gamma) = \int_0^{\frac{\gamma}{4}} \int_{x_4}^{\frac{\gamma-x_4}{3}} \int_{x_3}^{\frac{\gamma-x_4-x_3}{2}} \int_{x_2}^{\gamma-x_4-x_3-x_2} f^K(x_1, x_2, x_3, x_4) dx_1 dx_2 dx_3 dx_4. \quad (7.3.27)$$

Finally, (7.3.24) and (7.3.27) can be used to calculate the outage probability of the best four relay selection, based on the different CDF and PDF of the approximate overall end-to-end SNR, such as (7.3.3) and (7.3.4) for the lower

bound, (7.3.6) and (7.3.7) for the upper bound and (7.3.10) and (7.3.11) for the exact analysis. This result has been provided in Fig. 7.3 by using the Mathematica software package [86]. In the next section, these analytical results are verified by numerical simulations.

7.4 Outage Probability Analysis Verification

In this section, in order to verify the results obtained from the above mathematical expressions, the noise variances σ_r^2 and σ_d^2 are set to unity and $\lambda_{SR_i} = \lambda_{R_iD} = 40$ dB.

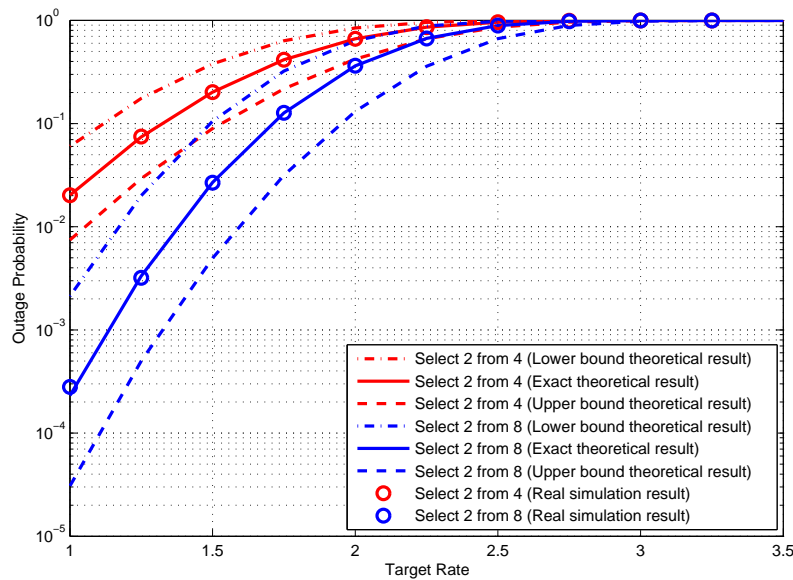


Figure 7.2. Comparison of the theoretical and simulated three types of outage probability analysis schemes for the best two relays selection ($\phi_0 = 5$, $\phi_1 = 10$ and $I_{th} = 2$).

Fig. 7.2 shows comparison of the theoretical and simulated three types of outage probability analysis schemes for the best two relays selection. That is, in this simulation, the predetermined threshold I_{th} in the primary receiver is assumed to be 2, and $\phi_0 = 5$ and $\phi_1 = 10$. From Fig. 7.2, the upper bound and lower bound can be confirmed, because the real simulation results are in between the lower and upper bound. Secondly, it can be seen that increasing

the number of relays, N , decreases the outage probability, and hence when the number of relays is large, the outage event (no transmission) becomes less likely, for example, with the total number of available secondary relays increasing from 4 to 8, the exact theoretical outage probability of the best relay selection is decreased from almost 0.2 to 0.027, when the target rate is 1.5.

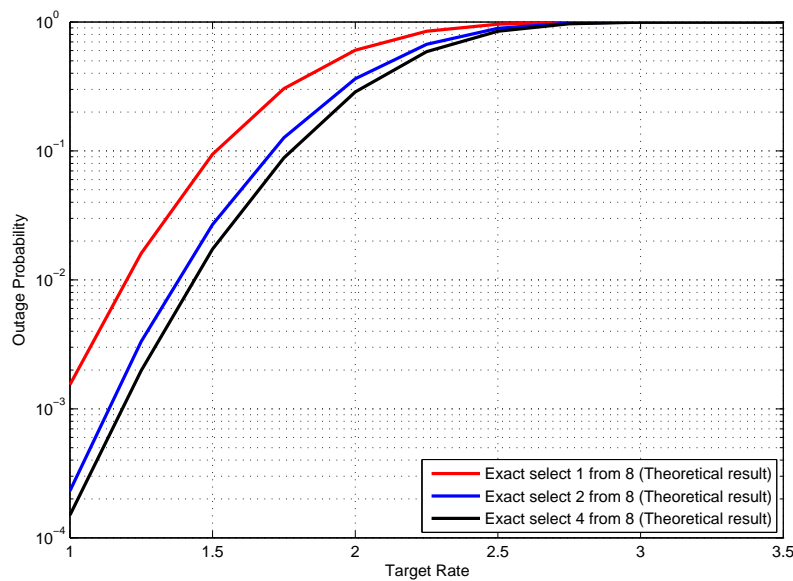


Figure 7.3. Comparison of the exact theoretical outage probability for the best relay selection and the best multi-relay selection ($\phi_0 = 5$, $\phi_1 = 10$ and $I_{th} = 2$).

Fig. 7.3 shows the comparison of the exact outage probability analysis for single relay and the two multi-relay selection schemes. To facilitate analysis, the predetermined threshold I_{th} in the primary receiver is assumed to be 2, $N = 8$ and $\phi_0 = 5$ and $\phi_1 = 10$. It is clearly seen that the exact outage probability is decreased when the number of selected relay is increased, for example, when the target rate is 1.5, the number of selected relays is raised from 1 to 2 and then 4, the exact outage probability is reduced from approximately 0.1 to 0.028 to 0.019, respectively. Therefore, when the predetermined threshold I_{th} in the primary receiver and the total number

of available selected relay N are restricted, more relays can be selected to communicate in order to provide sufficiently low outage probability for the secondary users.

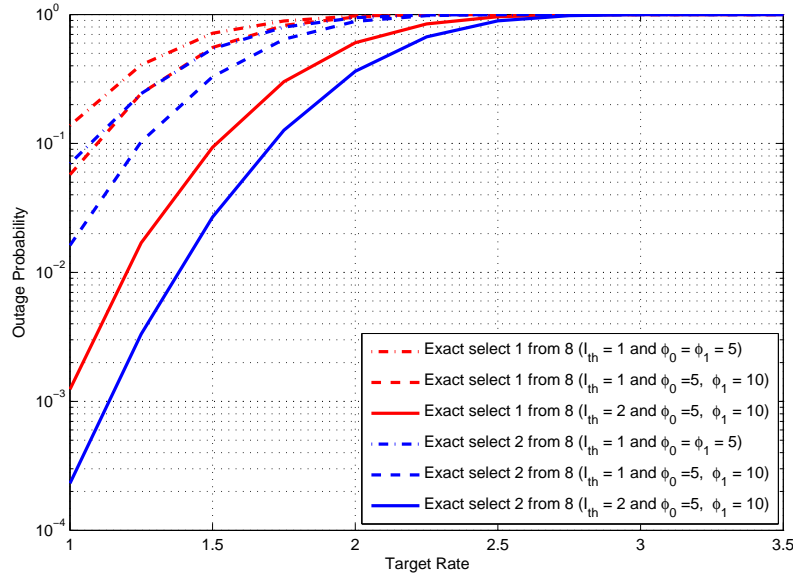


Figure 7.4. Comparison of the exact outage probability for a best single and best two relays selection for different thresholds I_{th} and mean channel gain ratios, ϕ_0 and ϕ_1 , $N = 8$.

Fig. 7.4 shows comparison of the exact theoretical outage probability of the single relay selection and the best two relays selection for the different thresholds I_{th} and mean channel gain ratios, ϕ_0 and ϕ_1 as in the figure legend. Firstly, there are the same trends for the outage probability for best single and best two relay selections. Therefore, taking the best two relays selection as an example. When $N = 8$, the target rate is 1.5, with increasing the mean channel gain ratios, the outage probability decreases, when the predetermined threshold is fixed, i.e., when the mean channel gain ratio ϕ_1 is increased from 5 to 10 and $\phi_0 = 5$ and $I_{th} = 1$, the outage probability of the best two relay selection is decreased from almost 0.55 to 0.31. Moreover, with increasing the predetermined threshold, the outage probability is decreased, when the mean channel gain ratio is fixed. For

example, when I_{th} is increased from 1 to 2 and $\phi_0 = 5$ and $\phi_1 = 10$, the outage probability of the best two relay selection is decreased from almost 0.31 to 0.026. These best relays could then be exploited for transmitting an orthogonal coding scheme such as [44] and thereby induce robustness to possible feedback errors in single relay selection schemes, which is confirmed in [94].

7.5 Summary

This chapter has examined three types of outage probability analysis strategies for a cognitive AF network with single or multi-relay (two and four) selection from the potential cooperative secondary relays based on the underlay approach, while adhering to an interference constraint on the primary user. New analytical expressions for the PDF, and CDF of end-to-end SNR were derived together with near closed form expressions for outage probability over Rayleigh fading channels. Numerical results were provided to show the advantage of the outage probability performance of the best multi-relay (two and four) selection in a cooperative communication system, i.e., more suitable relays can be selected to provide enough capacity for the secondary users when the predetermined threshold and the total number of available selected relays cannot be increased. Moreover, the theoretical values for the new exact outage probability match the simulated results can be confirmed. In the next chapter, the summary and conclusion to the thesis and possible future work will be provided.

SUMMARY, CONCLUSION AND FUTURE WORK

In this chapter, the contributions of this thesis and the conclusions that can be drawn from them are summarized. A discussion on possible future work is also included.

8.1 Summary and Conclusions

The research in this thesis has focused on two aspects of improving the performance of wireless cooperative networks. An offset transmission scheme with full interference cancellation and full inter-relay self interference cancellation schemes to improve the transmission rate and cancel interference from other relays have been presented. Multi-relay selection for cooperative AF type networks with and without inter-cluster interference has then been considered, in conventional and cognitive networks. Outage probability analysis was used for performance assessment. Considering the chapters in detail:

In Chapter 1, a general introduction to MIMO systems was provided including the basic concept, and characteristic advantages. Moreover, a brief introduction to cooperative networks was presented. Then, relay selection was presented for application in cooperative networks. In addition, a brief introduction to cognitive radio systems was provided highlighting the main

functions of cognitive radio and the features of cooperative cognitive networks. Finally, the outline of the thesis was briefly discussed.

In Chapter 2, an overview of the various methodologies in cooperative networks that are of interest in the thesis was presented. A brief introduction to distributed space-time coding schemes with orthogonal and quasi-orthogonal codes was given. A practically important method for distributed space-time coding, which does not need CSI at the receiver for decoding, which is differential space-time coding, was then discussed. This was followed by performance analysis of cooperative networks. One approach was pairwise error probability analysis, and the other was outage probability analysis. Finally, methods to achieve coding gain in transmission were considered. A simulation study was included to confirm the performance advantage of distributed transmission with and without outer coding.

In Chapter 3, unity end-to-end transmission rate was achieved through the offset transmission with FIC scheme. Using offset transmission, the source can serially transmit data to the destination. However, the four-path relay scheme suffered from IRI which was caused by the simultaneous transmission of the source and another group of relays. Therefore, the FIC scheme was used to remove fully these IRI terms. However, the FIC scheme was performed at the destination node, and so multiple antennas had to be used which maybe infeasible to achieve in practice. Therefore, an FSIC scheme was employed at the relay nodes within a four relay network and the pairwise error probability approach was used to analyze the cooperative diversity. This approach was shown to achieve the full available distributed diversity order, 3.5, without precoding and the end-to-end transmission rate to asymptotically approach unity when the number of samples is large.

In Chapter 4, an offset transmission with FIC scheme was applied in a cooperative network with asynchronism in the second/both stage(s). And a new OFDM with CP type transmission scheme was described to mitigate

the timing errors from the source to the relays and from the relays to the destination, and thereby avoid the CP removal at the relays. These approaches could not only closely match the Alamouti type scheme to achieve full diversity, but also provided unity transmission rate when the number of symbols is large.

In Chapter 5, the local measurements of the instantaneous channel conditions were used to select the best relay pair from the number of available relays, which either come from the same cluster or different clusters, and then these best relays were used with the Alamouti code to decrease the outage probability, i.e. when target SNR = 4 dB, the outage probability was decreased from almost 10^{-2} for the best relay selection to 10^{-3} for the best two relay selection. And the best relay pair selection scheme was also shown to have robustness to feedback error and outperform a scheme based on selecting only the best single relay. Secondly, in order to further reduce the outage probability to almost 2×10^{-4} , the best four relays were selected.

In Chapter 6, firstly, two different schemes which are asymptotical and semi-conventional policies to select the best multi-relays from a group of available relays in the same cluster were presented. These used local measurements of the instantaneous channel conditions in the context of legacy systems which adopt $\max(\min(\cdot, \cdot))$ type policies when inter-cluster interference is present only in the relay nodes. New analytical expressions for the PDF, and CDF of end-to-end SINR were derived together with near closed form expressions for outage probability over Rayleigh flat fading channels. Secondly, the best relay selection from a group of available relays by using local measurements of the instantaneous channel conditions in the context of cooperative systems which adopt a selection policy to maximize end-to-end SINR was provided. Inter-cluster interference was considered both at the relay nodes and the destination node. Moreover, a new exact closed form expression for outage probability in the high SNR region was provided.

In Chapter 7, three types of outage probability analysis strategies for a cognitive AF network with single or multi-relay (two and four) selection from the potential cooperative secondary relays based on the underlay approach, while adhering to an interference constraint on the primary user, were examined. New analytical expressions for the PDF, and CDF of end-to-end SNR were derived together with near closed form expressions for outage probability over Rayleigh fading channels. Numerical results were provided to show the advantage of the outage probability performance of the best multi-relay (two and four) selection in a cooperative communication system, i.e., more suitable relays can be selected to provide enough capacity for the secondary users when the predetermined threshold and the total number of available selected relays cannot be increased. For example, when the threshold value is 7 dB and $\phi_0 = 5$, $\phi_1 = 10$, $I_{th} = 2$, and the number of selected relays was increased from 1 to 4, the exact outage probability was decreased from almost 0.1 to 0.019. Moreover, the theoretical values for the new exact outage probability were confirmed by simulation.

In summary, in this thesis firstly the offset transmission scheme was provided to improve the end-to-end transmission rate, and the FIC or FSIC method was used to mitigate the inter-relay interference which is caused by the utilization of the offset transmission in synchronous and asynchronous systems. Secondly, the outage probability of the multi-relay selection scheme with and without interference in a cooperative AF network was investigated. Finally, the utilization of multi-relay selection was examined in cognitive AF relay networks, and a new exact outage probability analysis was confirmed.

8.2 Future Work

There are several directions in which the research presented in this thesis could be extended. The solutions presented in this thesis were for channels

which are assumed flat fading; but a wider class of fading channel conditions, modeled by for example the Nakagami-m distribution [95], could be considered. This fading distribution has gained much attention lately since the Nakagami-m distribution often gives the best fit to land-mobile and indoor mobile multipath propagation environments as well as scintillating ionospheric radio links [96].

Secondly, in Chapter 4, the robustness of the best multi-relay selection scheme in the presence of moderate to severe feedback errors is only confirmed by simulation results. In future work, a theoretical analysis should be considered. Furthermore, as only outage probability analysis of multi-relay selection was provided in Chapters 5, 6 and 7, there is opportunity for further diversity multiplexing tradeoff analysis to be performed.

Finally, wireless communication security is becoming a topical area of research and engineering [97] and [98]. In particular, physical layer security is becoming an important research area. The possibility of achieving perfect secrecy data transmission among the intended network nodes could be considered. As malicious nodes that eavesdrop the communication should not be able to obtain useful information [99–102]; how to use a multi-relay selection scheme to improve secrecy outage probability is a challenging problem that should be studied in the future.

A similar security issue also occurs in cognitive relay networks (CRN), where the PU enhances its performance through cooperation with SUs. In return, the cooperating SUs can gain opportunities for their own transmission. However, almost all the related works assume that SUs are trustworthy and well-behaved, which may not always be true in reality. There may exist some dishonest users, even malicious ones in the system, corrupting or disrupting the normal operation of the CRN. Consequently, the performance can therefore be compromised. Thus, this security issue also needs to be considered for emerging cognitive relay networks.

References

- [1] H. Bertoni, “Radio propagation for modern wireless systems,” *Prentice Hall, Upper Saddle River, NJ*, 1999.
- [2] J. Hamid, “Space-time coding theory and practice,” *Cambridge University Press*, 2005.
- [3] A. Paulraj, R. Nabar, and D. Gore, “Introduction to space-time wireless communications,” *Cambridge University Press*, 2003.
- [4] K. Fether, “Wireless digital communications,” *Father/Prentice Hall Digital and Personal Wireless Communication Series, Upper Saddle River, NJ*, 1995.
- [5] F. Khan, “LTE for 4G mobile broadband: air inter technologies and performance,” *Cambridge University Press*, 2009.
- [6] C. B. Chae, A. Forenza, R. W. Heath, M. R. Mckay, and L. B. Collings, “Adaptive MIMO transmission techniques for broadband wireless communication systems,” *IEEE Commun. Mag.*, vol. 48, no. 5, pp. 112–118, May 2010.
- [7] I. E. Telatar, “Capacity of multi-antenna Gaussian channels,” *European Trans. Tel.*, vol. 10, no. 6, pp. 585–595, Nov. 1999.
- [8] D. Tse and P. Viswanath, “Fundamentals of wireless communication,” *Cambridge University Press*, 2005.

-
- [9] J. N. Laneman and G. W. Wornell, "Distributed space-time-coded protocols for exploiting cooperative diversity in wireless networks," *IEEE Trans. Inf. Theory*, vol. 49, no. 10, pp. 2415–2425, Oct. 2003.
- [10] A. Nosratinia, T. E. Hunter, and A. Hedayat, "Cooperative communication in wireless networks," *IEEE Commun. Mag.*, vol. 42, pp. 74–80, Oct. 2004.
- [11] R. Pabst, B. H. Walke, D. C. Schultz, P. Herhold, H. Yanikomeroglu, S. Mukherjee, H. Viswanathan, M. Lott, W. Zirwas, M. Dohler, H. Aghvami, D. D. Falconer, and G. P. Fettweis, "Relay-based deployment concepts for wireless and mobile broadband radio," *IEEE Commun. Mag.*, vol. 42, pp. 80–89, Sep. 2004.
- [12] Y. Yang, H. Hu, J. Xu, and G. Mao, "Relay technologies for WiMAX and LTE-advanced mobile systems," *IEEE Commun. Mag.*, vol. 47, pp. 100–105, Oct. 2009.
- [13] K. Letaief and W. Zhang, "Cooperative communications for cognitive radio networks," *IEEE Commun. Mag.*, vol. 97, pp. 878–893, May 2009.
- [14] M. Dohler and Y. H. Li, "Cooperative communications: hardware, channel & PHY," *John Wiley Sons Ltd*, 2010.
- [15] J. N. Laneman, "Cooperative diversity in wireless networks: Algorithms and architectures," *Massachusetts Institute of Technology, Cambridge, MA, USA: PhD dissertation*, Aug. 2002.
- [16] A. Bletsas, A. Knisti, D. P. Reed, and A. Lippman, "A simple cooperative diversity method based on network path selection," *IEEE J. Sel. Areas Commun.*, vol. 24, no. 3, pp. 659–672, Mar. 2006.
- [17] J. N. Laneman, D. N. C. Tes, and G. W. Wornell, "Cooperative diversity

- in wireless networks: efficient protocols and outage behavior,” *IEEE Trans. Inf. Theory*, vol. 50, no. 12, pp. 3062–3080, Dec. 2004.
- [18] S. Ikki and M. H. Ahmed, “Performance analysis of dual-hop relaying communications over generalized Gamma fading channels,” in *Proc. of the IEEE Global Communications Conference, Washington, DC*, Nov. 2007.
- [19] Z. Yi and I. M. Kim, “Diversity order analysis of the decode-and-forward cooperative networks with relay selection,” *IEEE Trans. Wireless Commun.*, vol. 7, no. 5, pp. 1792–1799, May 2008.
- [20] T. Q. Duong and V. N. Q. Bao, “Performance analysis of selection decode-and-forward relay networks,” *IET Electronic Lett.*, vol. 44, no. 20, pp. 1206–1207, Sep. 2008.
- [21] C. K. Datsikas, N. C. Sgias, F. I. Lazarakis, and G. S. Tombras, “Outage analysis of decode-and-forward relaying over Nakagami-m fading channels,” *IEEE Signal Process. Lett.*, vol. 15, pp. 41–44, 2008.
- [22] M. O. Hasna and M. S. Alouini, “Harmonic mean and end-to-end performance of transmission system with relays,” *IEEE Trans. Commun.*, vol. 52, no. 1, pp. 130–135, Jan. 2004.
- [23] L. Sun and M. R. McKay, “Opportunistic relaying for MIMO wireless communication: Relay selection and capacity scaling laws,” *IEEE Trans. Wireless Commun.*, vol. 10, no. 6, pp. 1786–1797, June 2011.
- [24] I. Krikidis, J. S. Thompson, and S. McLaughlin, “Amplify-and-forward with partial relay selection,” *IEEE Commun. Lett.*, vol. 12, no. 4, pp. 235–237, Apr. 2008.
- [25] F. C. Commission, “Facilitating opportunities for flexible, efficient, and reliable spectrum use employing cognitive radio technologies,” *ET Docket*, no. 03-108, Mar. 2005.

- [26] B. Fette, "Cognitive radio technology," *Elsevier, Oxford, UK*, 2nd ed., 2009.
- [27] S. Haykin, "Cognitive radio: Brain-empowered wireless communications," *IEEE J. Sel. Areas Commun.*, vol. 23, no. 2, pp. 201–220, Feb. 2005.
- [28] C. Cordeiro, K. Challapali, and D. Birru, "IEEE 802.22: An introduction to the first wireless standard based on cognitive radios," *J. Commun.*, vol. 1, pp. 38–47, Apr. 2006.
- [29] C. R. Sevension, "In reply to comments of IEEE 802.18. 2004," [Online] Available: <http://ieee802.org/18>.
- [30] A. Goldsmith, S. A. Jafar, I. Maric, and S. Srinivasa, "Breaking spectrum gridlock with cognitive radios: an information theoretic perspective," *Proc. IEEE*, vol. 97, no. 5, pp. 894–914, May 2009.
- [31] W. Su, J. D. Matyjas, and S. N. Batalama, "Active cooperation between primary users and cognitive users in cognitive ad hoc networks," in *Proc. IEEE ICASSP, Dallas, USA*, 2010.
- [32] X. F. Tao, X. D. Xu, and Q. M. Cui, "An overview of cooperative communication," *IEEE Commun. Mag.*, vol. 50, no. 6, pp. 65–71, June 2012.
- [33] C. E. Shannon, "Two-way communication channels," in *Proc. 4th Berkeley Symp. Math. Stat. Prob*, pp. 611–644, 1961.
- [34] T. Cui, F. Gao, and C. Tellambura, "High-rate codes that are linear in space and time," *IEEE Trans. Commun.*, vol. 57, no. 10, pp. 2977–2987, Oct. 2009.
- [35] R. Vaze, K. T. Truong, S. Weber, and R. W. Heath, "Two-way transmission capacity of wireless ad-hoc networks," *IEEE Trans. Wireless Commun.*, vol. 11, no. 6, pp. 1966–1975, June 2011.

- [36] V. Tarokh, N. Seshadri, and A. R. Calderbank, "Space-time codes for high data rate wireless communication: Performance criterion and code construction," *IEEE Trans. Inf. Theory*, vol. 44, no. 2, pp. 744–765, Mar. 1998.
- [37] V. Tarokh, H. Jafarkhani, and A. R. Calderbank, "Space-time block codes from orthogonal designs," *IEEE Trans. Inf. Theory*, vol. 44, no. 2, pp. 1456–1467, July 1999.
- [38] A. Sendonaris, E. Erkip, and B. Aazhang, "User cooperation diversity—Part I: System description," *IEEE Trans. Wireless Commun.*, vol. 51, no. 11, pp. 1927–1938, Nov. 2003.
- [39] K. Azarian, H. E. Gamal, and P. Schniter, "On the achievable diversity-multiplexing tradeoff in half-duplex cooperative channels," *IEEE Trans. Inf. Theory*, vol. 51, no. 12, pp. 4152–4172, Dec. 2005.
- [40] R. U. Nabar, H. Bolcskei, and F. W. Kneubhler, "Fading relay channels: performance limits and space-time signal design," *IEEE J. Sel. Areas Commun.*, vol. 22, no. 6, pp. 1099–1109, Aug. 2004.
- [41] H. Muhaidat, M. Uysal, and R. Adve, "Pilot-symbol-assisted detection scheme for distributed orthogonal space-time coding," *IEEE Trans. Wireless Commun.*, vol. 8, no. 3, pp. 1057–1061, Mar. 2009.
- [42] G. S. Rajan and B. S. Rajan, "Leveraging coherent distributed space-time codes for noncoherent communication in relay networks via training," *IEEE Trans. Wireless Commun.*, vol. 8, no. 2, pp. 683–688, Feb. 2009.
- [43] B. Hassibi and B. M. Hochwald, "High-rate codes that are linear in space and time," *IEEE Trans. Inf. Theory*, vol. 48, no. 7, pp. 1804–1824, July 2002.
- [44] Y. Jing and B. Hassibi, "Distributed space-time coding in wireless relay

- networks,” *IEEE Trans. Wireless Commun.*, vol. 5, no. 12, pp. 3524–3536, Dec. 2006.
- [45] Y. Jing and H. Jafarkhani, “Using orthogonal and quasi-orthogonal designs in wireless relay networks,” *IEEE Trans. Inf. Theory*, vol. 53, no. 11, pp. 4106–4118, Nov. 2007.
- [46] S. M. Alamouti, “A simple transmitter diversity scheme for wireless communications,” *IEEE J. Sel. Areas Commun.*, vol. 16, no. 8, pp. 1451–1458, Oct. 1998.
- [47] H. Jafarkhani, “A quasi-orthogonal space-time block codes,” *IEEE Trans. Commun.*, vol. 49, no. 1, pp. 1–4, Jan. 2001.
- [48] H. Jafarkhani, “Space-time coding: theory and practice,” *Cambridge U.K.: Academic*, 2005.
- [49] Y. Jing and H. Jafarkhani, “Distributed differential space-time coding for wireless relay networks,” *IEEE Trans. Wireless Commun.*, vol. 56, no. 7, pp. 1092–1100, July 2008.
- [50] V. Tarokh and H. Jafarkhani, “A differential detection scheme for transmit diversity,” *IEEE J. Sel. Areas Commun.*, vol. 18, no. 7, pp. 1169–1174, July 2000.
- [51] J. G. Proakis, “Digital communication,” *4th ed. New York: McGrawhill, Inc.*, 2001.
- [52] N. Balakrishnan and A. C. Cohen, “Order statistics and inference: estimation methods,” *London : Academic Press*, 1991.
- [53] M. O. Damen, K. Abed-Meraim, and M. S. Lemdani, “Further results on the sphere decoder algorithm,” *in proc. IEEE ISIT, Washington, DC*, June 2001.

-
- [54] L. Ge, G. J. Chen, and J. A. Chambers, "Relay selection in distributed transmission based on the Golden code using ML and sphere decoding in wireless networks," *International Journal of Inf. Technology and Web Engineering in IGI Global Disseminator of Knowledge*, vol. 6, no. 4, 2011.
- [55] M. Evans, N. Hastings, and B. Peacock, "Statistical Distributions," *Wiley, 2nd ed.*, 1993.
- [56] A. J. Viterbi, "Error bounds for convolutional codes and an asymptotically optimum decoding algorithm," *IEEE Trans. Inf. Theory*, vol. 13, pp. 260–269, Apr. 1967.
- [57] G. D. Forney, "Burst error correcting codes for the classic bursty channel," *IEEE Trans. Commn. Tech.*, pp. 772–781, Oct. 1971.
- [58] J. L. Ramsey, "Realization of optimum interleavers," *IEEE Trans. Inf. Theory*, pp. 338–345, 1970.
- [59] G. L. Stuber, "Pinciples of mobile communication," *Kluwer Academic. second edition*, 2001.
- [60] B. Sklar, "Digital Communications-Fundamentals and Applications," *Prentice Hall*, 1988.
- [61] A. Goldsmith, "Wireless communications," *Cambridge University Press*, 2005.
- [62] C. Luo, Y. Gong, and F. Zheng, "Full interference cancellation for two-path cooperative communications," *Proc. IEEE WCNC., Budapest, Hungary*, 2009.
- [63] B. Hughes, "Differential space-time modulation," *IEEE Trans. Inf. Theory*, vol. 46, no. 7, pp. 2567–2578, Nov. 2000.

- [64] A. Y. Al-nahari, F. A. Abd El-Samie, and M. I. Dessouky, "Distributed space-time code for amplify-and-forward cooperative networks," in *Proc. 5th Future Information Technology, Busan, Korea*, June 2010.
- [65] G. Chen and J. A. Chambers, "Full interference cancellation for an asymptotically full rate cooperative four relay network," *IEEE International Conference on Inf. Theory and Inf. Security, Beijing, China*, Dec. 2010.
- [66] H. Wicaksana, S. H. Ting, C. K. Ho, W. H. Chin, and Y. L. Guan, "AF two-path half duplex relaying with inter-relay self interference cancellation: Diversity analysis and its improvement," *IEEE Trans. Wireless Commun.*, vol. 8, no. 9, pp. 4720–4729, Sep. 2009.
- [67] P. Herhold, E. Zimmermann, and G. Fettweis, "On performance of cooperative amplify-and-forward relay networks," in *Proc. International ITG Conf. Source Channel Coding (SCC'04), Erlangen, Germany*, 2004.
- [68] B. M. Hochwald and T. L. Marzetta, "Unitary space-time modulation for multiple-antenna communication in Rayleigh flat fading," *IEEE Trans. Inf. Theory*, vol. 46, pp. 543–564, Mar. 2000.
- [69] Y. Li and X. G. Xia, "Full diversity distributed space-time trellis codes for asynchronous cooperative communications," *Proc. IEEE Int. Symp. Information Theory (ISIT), Adelaide, Australia*, pp. 911–915, Sep. 2005.
- [70] Z. Li and X. Xia, "A simple Alamouti space time transmission scheme for asynchronous cooperative systems," *IEEE Signal Process. Lett.*, vol. 14, no. 11, pp. 804–807, Nov. 2007.
- [71] B. D. V. Veen and K. M. Buckley, "Beamforming: a versatile approach to spatial filtering," *IEEE ASSP Mag.*, vol. 5, no. 2, pp. 5–24, Apr. 1988.
- [72] Z. Li, X. G. Xia, and B. Li, "Achieving full diversity and fast ML decoding via simple analog network coding for asynchronous two-way relay

- networks,” *IEEE Trans. Commun.*, vol. 57, no. 12, pp. 3672–3681, Dec. 2009.
- [73] Z. Bali, W. Ajib, and H. Boujemaa, “Distributed relay selection strategy based on source-relay channel,” in *Proc. IEEE ICT, Doha, Qatar*, Apr. 2010.
- [74] K. Woradit, W. Suwansantisuk, H. Wymeersch, L. Wuttisittikulij, and M. Z. Win, “Outage behavior of cooperative diversity with relay selection,” in *Proc. IEEE Globecom, New Orleans, LA, USA*, 2008.
- [75] A. Adinoyi, Y. J. Fan, H. Yanikomeroglu, H. V. Poor, and F. Al-Shaalan, “Performance of selection relaying and cooperative diversity,” *IEEE Trans. Wireless Commun.*, vol. 12, no. 8, pp. 5790–5795, Dec. 2009.
- [76] A. Bletsas, H. Shin, and M. Z. Win, “Cooperative communications with outage-optimal opportunistic relaying,” *IEEE Trans. Wireless Commun.*, vol. 6, no. 9, pp. 3450–3460, Sep. 2007.
- [77] L. Lai, K. Liu, and H. E. Gamal, “The three-node wireless network: achievable rates and cooperation strategies,” *IEEE Trans. Inf. Theory*, vol. 52, no. 10, pp. 805–828, Mar. 2006.
- [78] S. Chen, W. Wang, and X. Zhang, “Performance analysis of multiuser diversity in cooperative multi-relay networks under Rayleigh-fading channels,” *IEEE Trans. Wireless Commun.*, vol. 8, no. 7, pp. 3415–3419, July 2009.
- [79] P. A. Anghel and M. Kaveh, “Exact symbol error probability of a cooperative network in a Rayleigh-fading environment,” *IEEE Trans. Wireless Commun.*, vol. 3, no. 5, pp. 1416–1421, Sep. 2004.
- [80] A. Papoulis, “Probability, random variables, and stochastic processes,” *McGraw-Hill*, 1991.

-
- [81] C. Toker, S. Lambotharan, and J. A. Chambers, "Closed-loop quasi-orthogonal STBCs and their performance in multipath fading environments and when combined with Turbo codes," *IEEE Trans. Wireless Commun.*, vol. 3, no. 6, pp. 1890–1896, Nov. 2004.
- [82] I. Krikidis, J. S. Thompson, S. McLaughlin, and N. Goertz, "Max-min relay selection for legacy amplify-and-forward systems with interference," *IEEE Trans. Wireless Commun.*, vol. 8, no. 6, pp. 3016–3027, June 2009.
- [83] S. Nadarajah and S. Kotz, "On the product and ratio of Gamma and Weibull random variables," *Econometric Theory, Cambridge University Press*, vol. 22, pp. 338–344, Feb. 2006.
- [84] A. Gilat and V. Subramaniam, "Numerical methods for engineers and scientists: An introduction with applications using Matlab," *John Wiley Sons Ltd*, 2011.
- [85] W. N. Bailey, "On the reducibility of Appell's function," *Quart. J. Math. Oxford*, pp. 291–292, 1934.
- [86] S. Wolfram, "The Mathematica Book," *Wolfram Media Press*, 5th ed., 2003.
- [87] O. Simeone, U. Spagnolini, and Y. Bar-Ness, "Stable throughput of cognitive radios with and without relaying capacity," *IEEE Trans. Commun.*, vol. 55, no. 12, pp. 493–497, May 2009.
- [88] K. Lee and A. Yener, "Outage performance of cognitive wireless relay networks," in *Proc. IEEE Globecom, New Orleans, LA, USA, San Francisco, USA*, Nov. 2006.
- [89] H. A. Suraweera, P. J. Smith, and N. A. Surobhi, "Exact outage probability of cooperative diversity with opportunistic spectrum access," in *Proc. IEEE ICC, Beijing, China*, May 2008.

- [90] J. Mietzner, L. Lampe, and R. Schober, "Distributed transmit power allocation for multihop cognitive radio systems," *IEEE Trans. Wireless Commun.*, vol. 8, no. 10, pp. 5287–5201, Oct. 2009.
- [91] J. Lee, H. Wang, J. Andrews, and D. Hong, "Outage probability of cognitive relay networks with interference constraints," *IEEE Trans. Wireless Commun.*, vol. 10, no. 2, pp. 390–395, Feb. 2011.
- [92] D. S. Michalopoulos and G. K. Karagianidis, "Performance analysis of single relay selection in Rayleigh fading," *IEEE Trans. Wireless Commun.*, vol. 7, no. 11, pp. 3718–3724, Oct. 2008.
- [93] J. N. Laneman and G. W. Wornell, "Energy efficient antenna sharing and relaying for wireless networks," *IEEE Wireless. Commun. and Networking conf. (WCNC), Chicago, USA*, vol. 49, no. 10, pp. 7–12, Oct. 2000.
- [94] G. J. Chen and J. A. Chambers, "Outage probability in distributed transmission based on best relay pair selection," *Accepted by IET Commun.*, June 2012.
- [95] M. Nakagami, "The m-distribution - a general formula of intensity distribution of rapid fading," *In W. C. Hoffman: Statistical Methods of Radio Wave Propagation*, Oxford, England, 1960.
- [96] M. K. Simon, J. K. Omura, R. A. Scholtz, and B. K. Levitt, "Spread spectrum communication handbook," *McGraw-Hill Inc, New York, revised edition*, 1994.
- [97] S. K. Miller, "Facing the challenge of wireless security," *Computer*, vol. 34, no. 7, pp. 16–18, July 2001.
- [98] W. A. Arbaugh, "Wirless security is different," *Computer*, vol. 36, no. 8, pp. 99–101, Aug. 2003.

-
- [99] Y. S. Shiu, S. Y. Chang, and H. C. Wu, "Physical layer security in wireless networks: a tutorial," *IEEE Trans. Wireless Commun.*, vol. 18, no. 2, pp. 66–74, Apr. 2011.
- [100] M. B. Shiu, J. Barros, and M. R. D. Rodrigues, "Wireless information-theoretic security," *IEEE Trans. Inf. Theory*, vol. 24, no. 3, pp. 339–348, June 1978.
- [101] I. Krikidis, J. S. Thompson, and S. McLaughlin, "Relay Selection for Secure Cooperative Networks with Jamming," *IEEE Trans. Commun.*, vol. 8, no. 10, pp. 5003–5010, Oct. 2009.
- [102] G. Chen, V. Dwyer, I. Krikidis, J. S. Thompson, S. McLaughlin, and J. A. Chambers, "Comment on 'relay selection for secure cooperative networks with jamming'," *IEEE Trans. Commun.*, vol. 11, no. 6, p. 2351, June 2012.